TUESDAY, JUNE 24, 1980

8:30 am - 9:45 am **2001 (A-B) COBO HALL**

FORMAL OPENING

WELCOME AND CALL TO ORDER. Howard J. Dworkin, M.D., Chairman, Local Arrangements Committee

WELCOME TO THE RENAISSANCE CITY. The Honorable Coleman A. Young, Mayor of Detroit

REMARKS. Leonard Rosenthall, M.D., Chairman, Scientific Program Committee

REMARKS. Leonard M. Freeman, M.D., President, Society of Nuclear Medicine

AWARDS. Merle K. Loken, M.D., Chairman, Awards Committee
Paul C. Aebersold Award to Michael J. Welch, Ph.D.

Berson-Yalow Award to Robert G. Hamilton, Ph.D., Rabia Hussain, Ph.D., Eric L. Ottensen, M.D., N. Franklin Atkinson, Jr., M.D.

Special Award to Captain William H. Briner for his efforts and skill in representing the Society of Nuclear Medicine

Distinguished Service Award to James L. Quinn, III, M.D. for his contributions to the establishment and practice of nuclear medicine (Awarded posthumously)

THE SECOND ANNUAL CHARLES DE HEVESY NUCLEAR MEDICINE PIONEER AWARD PRESENTATION honoring Merrill A. Bender, M.D., and Monte Blau, Ph.D. C. Craig Harris, M.S., lecturer

10:00-11:30 **Room 2040**

CLINICAL

HEART I

Session Chairman: Daniel Berman
Session Co-Chairman: Harvey J. Berger

COLD PRESSOR RADIONUCLIDE VENTRICULOGRAPHY. R.G. Kurtz, M.C. Besozzi, T.J. Brady, R.C. Kline, J.M. Clare, J.H. Thrall, B. Pitt, University of Michigan Medical Center, Ann Arbor, MI.

Cold pressor radionuclide ventriculography (CPRV) has recently been proposed as an alternative to exercise radionuclide ventriculography (ERV) for detecting patients with left ventricular dysfunction (LVD) and/or coronary artery disease (CAD). An abnormal response to CPRV has previously been defined as an $\geq$.03 decrease in left ventricular ejection fraction (EF) and an abnormal ERV response as a $\leq$.05 increase in EF from rest. To determine the relative sensitivity (S) and specificity (Sp) of CPRV and ERV, 59 patients with LVD and/or CAD and 7 with no CAD or LVD were studied. ERV detected 53 of 59 patients, S=90% and CPRV 57 of 59, S=97%, p=NS. In 33 of 59 the rest EF was normal (EF$\geq$.50) with new abnormalities detected by ERV in 27 of 33 S=82% and CPRV in 31 of 33, S=94%, p=NS. In 23 of the 59 the exercise response was adequate in that a pressure-rate product (PRP) of 250 was achieved. In this group ERV detected 22 of 23, S=96%, and CPRV 21 of 23, S=92%, p=NS. In 36 who failed to achieve adequate exercise levels, mean PRP=179, ERV detected 31, S=86% and CPRV 36, S=100%, p=NS. In the 7 without CAD or LVD, ERV was abnormal in 1, S p=86% but was equivocal in 3 due to inadequate exercise, and CPRV was abnormal in 1, Sp=86%, p=NS.

Thus, the S and Sp for ERV and CPRV are similar. However, CPRV has an advantage in patients who cannot achieve adequate exercise levels.

WHICH STRESS TEST SHOULD BE PERFORMED DURING TECHNETIUM-99m GATED CARDIAC BLOOD POOL SCINTIGRAPHY ($^{99}Tc^{m}$ GBPS) TO DETECT CORONARY ARTERY DISEASE (CAD)? D.A. Brennand-Roper, R.J. Wainwright, A.J.W. Hilson, M.N. Maisey, E. Sowton. Guy's Hospital, London, U.K.

95 normotensive patients (44 normals, 51 CAD) with normal or minimally impaired left ventricular function were studied using $^{99}Tc^{m}$ GBPS at rest and during different stress tests (dynamic supine exercise (DSE); isometric hand grip (IHG) and cold stimulation (CS) to evaluate their specificity and sensitivity. Abnormal criteria were taken as a fall in left ventricular ejection fraction (LVEF) of >8% or impaired regional wall movement (RWM).

1. Most normal patients had a significant increase in mean LVEF and preserved RWM with each intervention but false positive results were seen in 4% of patients with IHG, 5% patients with CS and 20% patients with DSE.

2. CAD patients had a significant fall in mean LVEF with CS but not with DSE or IHG.

3. 44/51 (86%) of individual CAD patients were detected by CS whereas only 16/25 (64%) patients and 13/22 (59%) patients were detected by IHG and DSE respectively.

It is concluded that CS in resting patients is more sensitive than IHG or DSE and is also more specific than DSE in the detection of CAD patients.

AN ACCURATE METHOD FOR THE DETECTION OF CORONARY HEART DISEASE (CHD) USING EQUILIBRIUM RADIONUCLIDE VENTRICULOGRAPHY (ERV) AND THE REGIONAL EJECTION FRACTION IMAGE (REFI) AT REST AND DURING HANDGRIP STRESS (HGS). J. Baron, H. Miller, S. Braun, R. Tardeman, and S. Liniado. Tel Aviv Medical Center, Israel.

Colour-coded REFIs (high resolution functional images) derived from ECG-gated ERVs, using a simple data processing system, were obtained in 72 patients undergoing coronary angiography (CA) at rest, during HGS, and after nitroglycerine (NTG) administration. The aim was to develop a method for CHD detection suitable for screening purposes and to compare the results with the CA results.

In 48/48 patients with CHD, the REFI showed a reduction at HGS reversed by NTG. 22/24 patients with normal CA showed unchanged REFI at HGS, i.e sensitivity 100%, specificity 92%. 23/48 (48%) CHD patients had a normal resting study. Stress-induced regional wall motion (RWM) reduction by the usual method of viewing ventricular border movement gave a sensitivity of 80% (38/48) and specificity of 96% (23/24). Using a stress-induced global E.F. reduction, a sensitivity of 60% (29/48) and specificity of 71% (17/24) was obtained.

Thus: 1) REFI is more sensitive than viewing border movement for the detection of RWM changes. 2) HGS is adequate for inducing RWM reduction in the presence of CHD. It does not induce angina nor produce movement artifacts. 3) When using HGS, global EF reduction is an inaccurate method for CHD detection. 4) The method is highly sensitive and specific for CHD and may prove valuable in the screening of asymptomatic high-risk groups.

NORMAL RESPONSES OF LEFT AND RIGHT VENTRICULAR EJECTION FRACTIONS DURING AEROBIC AND ANAEROBIC PHASES OF UPRIGHT AND SUPINE EXERCISE. J. Maddahi, N. Pantaleo, H. Brown, M. Freeman, S. Koerner, A. Waxman, and D. Berman. Cedars-Sinai Medical Center, Los Angeles, CA.

The development of anaerobic (An) metabolism during exericse (Ex) may alter global ventricular response to Ex.

This may be of clinical importance in patients with low An threshold (Th) due to deconditioning, valvular, and/or ischemic heart disease. To evaluate this effect, 13 normals (as proven by cardiac catheterization) were exercised in upright and supine positions past An Th to maximum (Max)Ex. Assessments were made at rest and during each stage of graded bicycle exercise. Left (L) and right (R) ventricular ejection fractions (VEF) were measured by multiple gated equilibrium scintigraphy with Tc-99m-RBC's. Additionally, tidal volume, minute ventilation (VE), oxygen consumption (VO_2), and carbon dioxide production (VCO_2) were calculated. The An Th was determined by noting the workload at which the ventilatory equivalent for oxygen (VE/VO_2) systematically rose, without an increase in the ventilatory equilivalent for carbon dioxide (VE/VCO_2).

	Ae# phase	An phase		Ae phase	An phase	
	Control	An Th	Max Ex	Control	An Th	Max Ex
LVEF	61±7	70±5+	76±4*	63±8	72±5+	76±4*
RVEF	49±6	60±6+	65±7*	46±7	56±6+	62±7*
HR^0	80±11	114±15+	154±16*	73±13	115±18+	142±18*
		UPRIGHT			SUPINE	

Ae#=aerobic; HR^0=heart rate; +p≤.01 vs. control; *p≤.01 vs. AnTh.

Thus, LVEF and RVEF increase during anaerobic as well as aerobic Ex; however, the rate of increase appears to be less during An phase.

EXERCISE RADIONUCLIDE VENTRICULOGRAPHY IN PATIENTS WITH PRIOR MYOCARDIAL INFARCTION. E.G. DePuey, R.E. Sonnemaker, E. Garcia, and J.A. Burdine. Baylor College of Medicine and St. Luke's Episcopal Hospital, Houston, TX.

In patients (pts) with prior myocardial infarction coronary ischemia is difficult to diagnose by treadmill exercise testing (TMT) due to existing ECG abnormalities. One hundred forty-three pts with chest pain and with ECG and historical evidence of prior infarction who were admitted for coronary angiography were studied at rest and during supine bicycle exercise with gated radionuclide ventriculography. Significant coronary stenosis (≥50%) was present angiographically outside of the infarct distribution in 94 pts (group I) but not in the other 49 (group II). All pts had resting wall motion (WM) abnormalities. The average resting ejection fraction (EF) in the two groups was 46.7 ±13.8% vs 48.4±12.8% (p>NS). The ventricular response to exercise was abnormal in 81% of group I pts and 69% of group II pts as manifested by a <5% increase in EF (average ΔEF=-2.6±7.8% vs 0.1±8.4%, p>.05). Existing WM abnormalities worsened in 29% of group I pts and 39% of group II pts. However, additional WM abnormalities developed in 26% of group I pts, but no pts in group II. The sensitivity and specificity of TMT in predicting additional coronary disease outside of the infarct distribution were poor (26% and 44%, respectively). Results were similar for pts with anterior and inferior infarcts. It is concluded that neither TMT, resting EF, the EF change with exercise, nor changes in WM of scarred myocardium is of value in differentiating these two groups of pts. However, the development of a new WM abnormality outside the infarct distribution is a highly specific albeit insensitive criterion of additional coronary stenosis.

EXERCISE RADIONUCLIDE VENTRICULOGRAPHY IN PATIENTS WITH CHEST PAIN AND NO PRIOR INFARCTION. E.G. DePuey, C. Sung, R.E. Sonnemaker, R.J. Hall, J.A. Burdine. Baylor College of Medicine and St. Luke's Episcopal Hospital, Houston, TX.

Previous studies to determine the accuracy of exercise radionuclide ventriculography (RNV) in diagnosing coronary artery disease (CAD) have been limited by small patient(pt) populations and inclusion of pts with prior infarcts. Two hundred seventeen pts with chest pain and no prior infarct were studied at rest and during supine bicycle exercise with RNV. A failure to increase ejection fraction by 5% (<5↑EF) and the development of wall motion abnormalities (ΔWM) were evaluated as criteria of coronary disease. Of these pts, 172 also underwent treadmill testing (TMT). All pts underwent coronary angiography, which demonstrated CAD (≥50% stenosis) in 141; in the remainder, diagnoses included mitral valve prolapse, pericarditis, non-occlusive coronary disease, left ventricular hypertrophy, and non-cardiac chest pain. The following diagnostic parameters were obtained:

	Sensitivity	Specificity	Accuracy
<5↑EF	74%	59%	67%
ΔWM	65%	88%	73%
<5↑EF or ΔWM	84%	54%	74%
TMT	50%	49%	50%

Since many pts were exercise-limited by symptoms or medications the accuracies were compared in pts subgrouped according to maximum heart rate-blood pressure products achieved during RNV. Whereas the accuracy of TMT decreased to 30% in 36 pts with rate-pressure products less than $1.5x10^4$, it was unchanged for RNV (76%). Thus RNV is superior to TMT as a screening test for CAD and maintains its accuracy in exercise-limited pts. However, <5↑EF and ΔWM may occur in pts with chest pain due to causes other than CAD.

WHAT IS THE NORMAL RANGE FOR LEFT AND RIGHT VENTRICULAR EJECTION FRACTION AT DIFFERENT LEVELS OF EXERCISE? FINDINGS OF SCINTIGRAPHIC VENTRICULOGRAPHY DURING GRADED ERGOMETRY IN 34 NORMALS. J. Maddahi, D. Berman, N. Pantaleo, M. Freeman, J. Prause, J. Forrester, H.J.C.Swan, and A.Waxman. Cedars-Sinai Medical Center, Los Angeles, CA.

Frequently patients (pts) with suspected cardiac or pulmonary disease do not achieve maximum (max) heart rate (HR) during exercise (Ex). Therefore, to interpret results of left (L) and right (R) ventricular ejection fractions (VEF) during submaximal Ex, a normal LVEF and RVEF range should be established for different levels of Ex. We have thus studied 34 normals (23 males and 11 females), with mean age of 47 (range 20-75) during graded stages of upright bicycle Ex. This group of normals included 15 with normal coronary arteries and 19 with <1% likelihood of coronary artery disease based on sequential Bayesian analysis of age, sex, symptom classification and results of multiple other noninvasive stress tests. LVEF and RVEF were determined by multiple gated equilibrium scintigraphy with Tc-99m-RBC's during each of 4-8 levels of Ex. The mean ±SD for EF's at different levels of HR are as follows:

HR	Control	80-89	90-99	100-109	110-119	120-129
LVEF	62±7	65±8	67±6	68±5	71±4	75±5
RVEF	48±5	51±9	55±8	51±6	58±	61±6

HR	130-139	140-149	150-159	160-169	170-179
LVEF	73±4	78±5	77±4	81±7	80±4
RVEF	58±9	60±8	61±7	66±10	65±5

Therefore, a normal range for LVEF and RVEF has been established for different levels of achieved HR during upright Ex. These data may help interpret EF values observed in pts with suspected disease who do not achieve max Ex level.

A STUDY OF VENTRICULAR FUNCTION IN VENTRICULAR SEPTAL DEFECTS AT REST AND AFTER EXERCISE
G. Jablonsky, MD; D. Feiglin, MD; D. Hilton, MD; P. McLaughlin, MD; FACC; B. Bar-Shlomo, MD; M. Druck, MD; J. Morch, MD; Toronto General Hospital Toronto, Ontario.

Little data is available on the effect of long-term volume overload on right and left ventricular function at rest and during exercise. We compared the right and left ventricular function of 23 patients (pts) with hemodynamically proven ventricular septal defects (VSD's) mean age 26.9 yrs with a range of 20-40 yrs) with 11 normal subjects (mean age 28 yrs with a range of 24-34 yrs) Of the 23 pts with VSD's, 11 had left to right shunt ratios of less than 2:1, 4 had Eisenmengers reaction and 8 had had surgical repair (mean interval from surgery was 16.8 yrs with a range of 9-20 yrs). All pts had supine gated nuclear angiograms at rest and during graded exercise to fatigue. Mean ejection fractions are as follows:

	N	2:1		Eisenmenger's		Post-Op	
	Rest	Rest	Ex	Rest	Ex	Rest	Ex
LV	67	79**	68	68*	54***54*	66	58*
RV	42	62**	44	45*	39 35*	38	40*

*not significant change rest→exercise
**p < .001 rest→exercise
***resting LVEF abnormal in Eisenmenger's vs. normal (p < .01)
We conclude: 1) resting ventricular function is normal in all groups except the Eisenmenger's 2) the response of both ventricles to exercise

is abnormal in all groups, 3) post-operative left and right ventricular function is abnormal at long-term follow-up.

UPRIGHT OR SUPINE - WHICH POSITION IS BETTER FOR EXERCISE SCINTIGRAPHIC VENTRICULOGRAPHY? M. Freeman, D. Berman, J. Maddahi, H. Staniloff, U. Elkayam, N. Pantaleo, A. Waxman, J. Forrester, and H.J.C. Swan. Cedars-Sinai Med.Ctr.,L.A.CA

Both upright (UPR) and supine (SUP) bicycle exercise (Ex) have been used with multiple gated equilibrium scintigraphy (MGES) for assessment of pts with coronary artery disease (CAD). To compare these modes of Ex we performed MGES in the 45° LAO view at rest and maximum (max) symptom limited UPR and SUP Ex in 33 pts: 22 pts with angiographic CAD (>50% stenosis) and 15 with normal coronary arteriograms (NCA). Segmental wall motion was assessed in 5 segments with a 5 point scoring system (3=normal, -1=dyskinesis). A total wall motion score (WMS) was assigned by summing the segmental scores. CAD was predicted if left ventricular (LV) ejection fraction (EF) did not rise by >10% or wall motion abnormality (WMA) developed during max Ex. Single (S) or multiple (M) vessel disease (VD) was predicted from the location of WMA. There was no significant (ns) difference between UPR and SUP Ex in max heart rate (HR) and systolic blood pressure (SBP) in NCA pts, but both max HR and SBP in the CAD pts were lower in SUP than in UPR Ex ($p<.05$). There was no difference between UPR and SUP positions for the means of LVEF, right ventricular (RV) EF or WMS in either the NCA or CAD pts at rest or during max Ex. The directional changes of LVEF, RVEF and WMS in UPR and SUP Ex were concordant in 34/37, 36/37, and 34/37 pts respectively. The predictions of NCA, SVD, or MVD by UPR and SUP Ex were concordant in 35/37 pts. LV volume increased both UPR and SUP from rest to max Ex in CAD pts, but only during UPR Ex in NCA pts. The increase in LV volume in CAD pts during SUP Ex may counterbalance lower SUP max HR-SBP product. These data suggest that UPR and SUP Ex are equally effective for assessment of pts with suspected CAD by MGES.

CORRELATION BETWEEN RADIONUCLIDE LEFT VENTRICULAR EJECTION FRACTION DURING ACUTE MYOCARDIAL INFARCTION AND CARDIAC DEATH OR CHF. K.P. Lyons, H.G. Olson, Veterans Administration Medical Center, Long Beach, CA.

Radionuclide left ventricular ejection fractions (LVEF) were measured acutely (2.6 ± 1.7 days) following documented acute myocardial infarction (AMI) in 151 patients. The results were correlated with cardiac death (CD) and subsequent congestive heart failure (CHF). In 124 of the 140 hospital survivors (89%), the LVEF was repeated at hospital discharge (HD) 14.1 ± 3.7 days post AMI. The average LVEF was 47 ± 15% acutely and 46% ± 15% at HD. At follow-up, 6.1 ± 3.6 months after AMI, 20 of the 151 patients had a cardiac death (13.2%), 11 during hospitalization and 9 after discharge. Twenty-nine of the 151 patients developed CHF (19.2%). Only one of 65 patients (1.5%) with a normal acute LVEF (≥50%) suffered a CD compared to 19 of 86 (22.1%) with an LVEF ≤49% ($P<0.001$). All of the patients who died during hospitalization had an abnormal LVEF ($P<0.01$). None of the patients with a normal LVEF went on to CHF versus 29 (33.7%) with an abnormal LVEF ($P<0.001$). Of the 124 patients studied at HD, 8 later had a CD (6.5%) and 26 developed CHF (21%). None of the patients with a normal LVEF at HD went on to CD or CHF versus 8 deaths (11%) and 26 CHF (36%), $P<0.02$ and $P<0.001$ respectively. Therefore: (1) During AMI, a normal LVEF is unassociated with in-hospital or late CD or with subsequent CHF. (2) A reduced LVEF during AMI correlates with a significantly increased risk for acute and remote CD and with CHF at follow-up. (3) The HD LVEF has equal prognostic value for risk of subsequent CD and CHF.

SCINTIGRAPHIC PARAMETERS OF INFARCT SIZE AND LONG TERM CLINICAL COURSE IN COMPLICATED MYOCARDIAL INFARCTION WITHOUT HEART FAILURE. J. Perez-Gonzalez, R. Dunn, E. Botvinick, Kanu Chatterjee, W. Parmley, T. Ports, University of California, San Francisco, CA.

Sixteen patients with acute infarction complicated by rhythm and conduction disturbances, but no heart failure underwent scintigraphic evaluation of left ventricular ejection fraction and infarct size within 4 days of admission. Infarct size was estimated as the area of largest Tc^{99m} pyrophosphate uptake (PYP), or area of largest Tl^{201} perfusion defect (Tl^{201}), and also as the percentage of left ventricular area affected by a perfusion defect (Tl^{201}%). Patients were followed for up to 31 months and their clinical course related to the acute scintigraphic findings. Eight patients had benign evolution and are asymptomatic (Group A). The remaining 8 patients (Group B) either died subsequently (7) or developed heart failure (1). Ejection fraction in Group A (53%±14.9) was not different from that of Group B (48%± 6.8%). However, infarct size parameters were significantly higher in Group B: PYP was 15±13.4 cm^2 in Group A compared to 34±24 cm^2 in Group B ($p<.05$); Tl^{201} was 16± 6.6 cm^2 in Group A compared to 32±11.1 in Group B ($p<.001$); and Tl^{201}% was 24%±11 in Group A and 45%±4.5 in Group B ($p<.002$). Patients whose myocardial infarction is complicated by rhythm and conduction disturbances may follow a benign or malignant course. The eventual development of either seems to be related to infarct size and could be predicted from scintigraphic indicators.

PROGNOSTIC SIGNIFICANCE OF RESTING ANTERIOR THALLIUM-201 DEFECTS IN PATIENTS WITH INFERIOR MYOCARDIAL INFARCTION R.S.Gibson, G.J.Taylor, D.D.Watson, G.A.Beller; University of Virginia, Charlottesville, VA.

Patients (pts) with inferior myocardial infarction (IMI) and associated left anterior descending (LAD) coronary artery disease (CAD) may be at increased risk for subsequent cardiac events (CE). To determine if Tl-201 scintigraphy after IMI can predict subsequent CE, 25 pts with enzymatic and ECG criteria for transmural IMI underwent serial imaging with computer quantitation at rest 7-35 days (mean 11.9) after hospital admission. All 25 pts had persistent inferior (INF) defects, whereas 13 (52%) also had anterior (ANT) defects consistent with LAD disease. Ten showed anterior wall rest redistribution and 3 had persistent ANT defects. Pts were divided into Group I (G-I) (INF and ANT defects) and Group II (G-II) (INF defects alone) and the number of CE recorded over an average 7.2 month follow-up (range 3-9 months). CE included sudden death (SD), reinfarction, angina and heart failure (CHF). Ten of 13 pts (77%) in G-I had 17 CE compared with 4/12 pts (33%) in G-II who had only 6 CE ($p<0.02$). Nine pts in G-I vs 3 in G-II developed angina ($p<0.03$). Although not statistically significant there was also an increased prevalence of SD (8% vs0%) and CHF (46% vs 25%) in G-I.

In conclusion, rest Tl-201 scintigraphy with computer quantitation is 1) highly sensitive for detection of transmural IMI even in the late hospital phase and 2) by detecting ANT wall hypoperfusion at rest, can identify those pts with IMI at high risk for subsequent cardiac events presumably due to LAD disease.

RELATION OF RIGHT VENTRICULAR (RV) EJECTION FRACTION TO PULMONARY ARTERY PRESSURE AND RIGHT ATRIAL PRESSURE IN AORTIC AND/OR MITRAL VALVE DISEASE G.G. Winzelberg, C.A. Boucher, R.D. Okada, K.A. McKusick, G.M. Pohost, H.W. Strauss, Massachusetts General Hospital,

Right-sided hemodynamic abnormalities resulting from left-sided valvular disease were compared to right ventricular (RV) systolic function in 43 patients with severe aortic and/or mitral disease. RV ejection fraction (EF) was derived from end-diastolic and end-systolic counts within the RV region of interest on gated first pass radionuclide angiography. Among 15 normal patients, the RVEF was 60±7% (mean ±1SD). RVEF was 2SD below normal in 14 (33%) of patients; peak pulmonary artery systolic pressure (PAP) was >50 mmHg in 29 (67%) of patients; and mean right atrial pressure (RAP) was elevated (>5 mmHg) in 26 (60%) of patients. RVEF was more frequently reduced with PAP >50 mmHg than <50, 45% vs. 7% ($p<.05$). A reduced RVEF occurred as often with normal as with elevated RAP, 41% vs. 31% (p NS). In conclusion: 1-Although RVEF reduction can be related to PAP, most patients with PAP >50 mmHg maintain a normal RVEF. 2-RVEF does not correlate closely with RAP. 3-Direct inferences about RVEF from PAP and RAP in patients with severe aortic and/or mitral disease should be made with caution.

BEAT TO BEAT ASSESSMENT OF LEFT VENTRICULAR PERFORMANCE IN ATRIAL FIBRILLATION DETERMINED WITH THE COMPUTERIZED NUCLEAR PROBE. J. Schneider, H. Berger, A. Gottschalk, and B. Zaret. Yale University, New Haven, Ct.

The irregular heart rhythm in atrial fibrillation (AF) results in non-uniform beat to beat ventricular performance. The effects of irregular AF on global left ventricular (LV) performance was assessed on a beat to beat basis in 8 patients (pts) using the computerized nuclear probe. This instrument has been interfaced to a multichannel recorder and provides a continuous simultaneous recording of relative LV volumes, background activity level, and ECG after Tc-99m blood pool labeling. LV ejection fraction (EF) determined with the probe in pts with normal sinus rhythm has been shown to be accurate and to correlate closely with camera studies (n=71, r=0.92), with a beat to beat variability of ±5.8% (EF units). In each AF pt, relative LV end-diastolic (ED) and stroke volumes (SV) and LVEF were determined in each of 50 consecutive beats. The mean LVEF (±2 SD), determined from these 50 beats, in individual pts ranged from 17±12% to 51±19%. In individual pts, 8 to 26% of beats resulted in an LVEF that exceeded the mean LVEF plus the previously noted variability. In these beats, the LVEF averaged 11% higher than the individual pt means. LVEF correlated with preceding cycle length (CL) and SV. A Starling effect (positive correlation of SV to ED) was evident in the 6 pts with mean LVEF >45% (r=0.54 to 0.81), but not in the 2 pts with LVEF <30% (r=0.04 and 0.31).

Thus, in AF, LVEF correlates with SV and CL, and a Starling effect is demonstrated for pts with near normal mean LVEF. At rest, LVEF underestimates the LV reserve for augmented performance. These data may impact upon the diagnostic utility of equilibrium ECG-gated techniques for assessment of LV function in AF.

BEAT TO BEAT ASSESSMENT OF LEFT VENTRICULAR PERFORMANCE USING A PORTABLE COMPUTERIZED NUCLEAR PROBE: VALIDATION, ANALYSIS OF VARIABILITY, AND INITIAL STUDY OF ECTOPY. H. Berger, R. Davies, W. Batsford, P. Hoffer, A. Gottschalk, and B. Zaret. Yale University, New Haven, Ct.

A computerized nuclear probe, interfaced to a multichannel chart recorder, was utilized for continuous simultaneous recording of a high temporal resolution relative left ventricular (LV) volume curve, background activity level, and ECG. After Tc-99m blood pool labeling, beat to beat relative end-diastolic volume and stroke volume, and LV ejection fraction (EF) were calculated in 10 consecutive sinus beats in 71 patients (pts). Mean LVEF by probe correlated well with LVEF obtained by first-pass radionuclide angiocardiography using a multicrystal camera (r=0.92). There was no difference in LVEF between probe and camera studies (mean±SEM: 53±3% vs 56±3%, pNS). Close agreement was demonstrated between initial and repeat analyses of the same data (n=58, r=0.97) and between initial and repeat probe studies (n=48, r=0.94). The overall variability of beat to beat LVEF averaged ±5.8% (EF units) and was not different in normal (nl) and abnl LVEF. As a demonstration of the technique's sensitivity to detect hemodynamic changes in single beats, the effects of induced ventricular (V) and atrial (A) premature beats (PB) were compared in 10 pts with nl LVEF. In 52 pairs of PB's in the same pts at identical coupling intervals, VPB's decreased LVEF significantly more than APB's compared to sinus beats (-30±3% vs -13±3%, p<0.01). Post-extrasystolic potentiation was similar whether the PB was from the V or A (+8±3% vs +5±3%, pNS).

Thus, LV performance can be determined accurately on a beat to beat basis with low variability. This radionuclide technique allows assessment of the hemodynamic consequences of spontaneous or induced cardiac arrhythmias.

LOW END-SYSTOLIC VOLUME AT REST - AN EXPLANATION FOR FAILURE OF INCREASE IN EJECTION FRACTION DURING EXERCISE IN NORMAL PATIENTS. M.D. Osbakken, D. Merrill, C.A. Boucher, R.D. Okada, H.W. Strauss, G.M. Pohost, Massachusetts General Hospital, Boston, MA

Twenty four patients were studied with supine rest (R) and exercise (ex) ventriculography. All patients had normal hemodynamics, left ventricular and coronary angiograms. Scan ejection fraction (EF) was derived by counts and scan end-diastolic index (EDV/Body surface area=EDVI) was determined by area length analysis. Stroke volume index (SVI) was EDVIxEF and end-systolic volume index (ESVI) was EDVI-SVI. 16 patients with ≥5% increase (↑) in EF with ex (Group A) were compared to 8 patients with <5% ↑EF with ex (Group B) (mean ± SEM; * $p<0.05$).

	Group A ≥5% ↑EF	Group B <5% ↑EF	p
EDVI Rest (cc/m^2)	43.3±3.7	34.8±4.8	-
EDVI Ex (cc/m^2)	47.4±4.1	37.1±1.6	-
ESVI Rest (cc/m^2)	17±1.9	10±1.6	*
ESVI Ex (cc/m^2)	13±2	11±1.1	-
%Δ ESVI (rest to ex)	↓ 25±5%	↑ 9±7%	*
SVI Rest (cc/m^2)	26±2.4	25±3.7	-
SVI Ex (cc/m^2)	35±3	26±3	-
%Δ SVI (rest to ex)	↑ 38±9%	↑ 7±4%	*
EF Rest	61±1.9	71±2.5	*
EF Ex	74±2.4	71±2.2	-

Age, sex, heart rate and systolic pressure at rest and ex did not differ in Group A vs Group B. The only significant difference at rest between the 2 groups is that Group B had a lower ESVI which did not decrease during ex. Because EDVI did not ↑ and ESVI did not ↓, EF did not ↑. This implies that there are a group of normal patients whose left ventricles are contracting maximally at rest. Thus, contractile function measured by EF can not be further augmented during ex.

CARDIAC BLOOD POOL ACTIVITY AFTER IN VIVO AND IN VITRO RED BLOOD CELL (RBC) LABELING. M.M. Graham and W.B. Nelp, Univ. of Washington, Seattle, WA

This study was done to compare the kinetics of Tc-99m precordial radioactivity following both in vivo and in vitro labeling of RBCs, since both methods are commonly used for studies of left ventricular function.

In 10 patients RBCs were labeled in vivo by injecting 12 mgm of pyrophosphate and 3.4 mg SnCl IV followed in 30 min by 20 mCi of Tc-99m. In 10 other patients RBCs were labeled in vitro after treatment with Sn (Brookhaven kit). Using a gamma camera and computer, time activity curves were recorded from the cardiac blood pool (CBP) and adjacent background (bkg) for 15 min after injecting Tc-99m.

With in vitro labeling, CBP activity fell 15% during 15 min(range 10-21%), but the CBP/bkg ratio remained constant (avg 3.5). In contrast, with in vivo labeling CBP activity fell 6% during the first 5 min, then slowly increased. Again CBP/bkg remained constant but at a lower value of 2.4 This suggests that with in vivo labeling the intravascular Tc-99m binds to RBC hemoglobin over several min. This allows Tc-99m to diffuse into the extracellular fluid (ECF) and then back into the plasma as Tc-99m is bound to RBCs. This is supported by the observed rate of transfer of Tc-99m from plasma to hemoglobin in intact RBCs in our lab where k= 0.46/min(T-1/2 1.5 min). Applying these hypotheses to a computer simulation of in vivo labeling using RBC, plasma and ECF compartments, whole blood activity curves similar to those observed in patients were produced. The steady fall of CBP activity with in vitro labeling is probably a combination of mixing, splenic uptake and elution of RBC label with renal excretion. The consistently higher CBP/bkg ratio with the in vitro label is easily perceptible on the final cardiac images.

THE INFLUENCE OF REGIONAL WALL MOTION ABNORMALITIES ON THE DETERMINATION OF THE EJECTION FRACTION USING FIRST PASS RADIONUCLIDE ANGIOCARDIOGRAPHY. M.L. Goris and J.H. McKillop, Stanford University School of Medicine, Stanford, CA.

The determination of left ventricular ejection fraction on the basis of count rates is based on the assumption that the tracer is well mixed within the ventricular cavity. In this paper we intend to investigate whether good mixing can be assumed to be present during the sampling interval in first pass nuclear angiocardiography (FPNA) in patients with low ejection fractions and regional wall motion abnormalities.

ECG gated blood pool studies (EGNA) at rest are used as a control. Except for the production of a 16 frame representative cycle, EGNA and FPNA are processed exactly in the same fashion, with automatic thresholding and region of interest selection. For FPNA the sampling interval is taken asymmetrically around the peak of LV activity.

Two groups of patients are considered. The first control group without coronary artery disease is composed of middle-aged volunteers and patients treated with adriamycin. The

second group is composed of middle-aged males following an infarction and who have localized wall motion abnormalities. Ejection fraction values are generally identical in the first group (average difference 1.6 ± 10.1) but not in the second group where smaller values are found in the lower range of EGNA (average difference -6.9 ± 9.3). Additionally 13/25 EGNA results from the second group fall below predicted value while none fall above, if the regression equation from the first group is used.

We conclude that mixing may be delayed in patients with localized wall motion abnormalities and low ejection fractions.

MEASUREMENT OF SYSTOLIC MYOCARDIAL THICKENING USING PLANAR IMAGING TECHNIQUES. J.H. Caldwell, D.L. Williams, G.D. Harp, K.L. Gould, G.W. Hamilton, VA Medical Center, Seattle, Wa.

Depressed systolic thickening of the myocardium (SMTh) is one of the earliest indicators of ischemia. The purpose of this study was to determine if SMTh can be measured using radionuclide (RN) techniques. Three 25 Kg dogs were chronically instrumented with a coronary flow probe and occluder, an ECHO crystal on the LV, and a left atrial (LA) catheter. On a study day, the myocardium was labeled by injection of Tc-99m MAA particles into the LA during dipyridamole induced maximal coronary blood flow (CBF). The dog was positioned in the equivalent of the LAO projection in front of a gamma camera with a high resolution collimator. Multiple gated acquisition images (each 200 K) were acquired during normal and reduced CBF along with simultaneous ECHO and CBF data. The raw images were processed through a low pass, low frequency linear filter and an interpolative background subtraction program. The computer then identified the endocardial and epicardial surfaces of the area of myocardium distal to the coronary occluder and calculated SMTh from each 40 msec image during the cardiac cycle.

For the 30 studies in the 3 dogs, SMTh by RN was 25.4±2.7% (mean±SEM) at baseline and decreased to 16.9±3.3% (p=.009) during stenosis (a decrease in CBF of 53±4.1%). Respective values for ECHO were 46.0±2.6% and 38.9±3.2% (p=.003). Although the percentage change of SMTh between baseline and stenosis was slightly but not significantly greater for RN than for ECHO (-32.9±16.1% vs. -15.9±5.8%; p=.18), the direction change correlated well (r=.50; SEE 7.43; y=1.38X -10.80; p=.005).

We conclude that it is possible to measure myocardial thickening by RN methods. The clinical usefulness of the technique must be defined.

10:00-11:30 **Room 2048**

CLINICAL

PEDIATRICS

Session Chairman: Letty G. Lutzker
Session Co-Chairman: Massoud Majd

97-RU-PARA-BUTYL-IDA (97-RU-BIDA) AS AN AGENT FOR DELAYED STUDIES OF THE BILIARY TRACT. E. Schachner, C. Gil, P. Som, N. Cicale, D.F. Sacker, H.L. Atkins, P.Richards, S. Treves, and G. Subramanian. Brookhaven National Laboratory, Upton, N.Y.

Early diagnosis of biliary atresia in the neonatal continues to be a query for the diagnostician. The physical properties of 131-I and 99m-Tc (131-I energy 340 keV, $T_{1/2}$ 8.04 days, relatively high radiation dose, and 99m-Tc, $T_{1/2}$ 6.4 hours) prevents their use in delayed imaging. 97-Ru on the other hand has excellent physical properties (Energy 216 keV, δ86%, $T_{1/2}$ 2.9 days) making it the isotope of choice. 99m-Tc-BIDA appears to have the highest hepatic uptake and the lowest rate of urinary excretion among the known hepatobiliary agents. Because of this fact, we labeled this agent with 97-Ru. BIDA was dissolved in normal saline (15 mg/ml) and the pH adjusted to 7.00. To this solution 97-$RuCl_3$ was added and the pH adjusted to 4.00. Then, this solution was heated for 30 min in a boiling water bath. After the compound was cooled at room temperature the final pH was raised to 7.00. Biodistribution in rats, as compared with 97-Ru-PIPIDA showed higher retention in the liver and slower excretion by the kidneys from 60 min on. Blood clearance in dogs showed similar rates for 99m-Tc-BIDA and 97-Ru-BIDA ($T_{1/2}$ 1.5 min for both). The scans in the dogs showed early visualization of the gall bladder (10 min) and its excretion through the intestinal tract. All these facts suggest that this radiopharmaceutical can be used for performing delayed studies of the biliary tract (e.g., 1-3 days) in cases where required(e.g., biliary atresia, neonatal hepatitis).

IMPROVEMENT OF RADIONUCLIDE LEFT TO RIGHT SHUNT QUANTITATION USING DECONVOLUTION ANALYSIS.
H.R.Ham,A.Dobbeleir,P.Viart,A.Piepsz and A.Lenaers.
St.Peter Hospital,Free University of Brussels, Belgium.

The purpose of this work was to evaluate whether deconvolution analysis improved shunt quantitation in clinical practice. Quantitative radionuclide angiocardiography(QRAC) was performed on 87 patients admitted for cardiac catheterization. The absence of a shunt was ascertained in 35 patients by selective cineangiography,intracardiac phonocardiography and/or contrast echography.Shunt quantitation was performed by QRAC without deconvolution (D),QRAC with D and oxymetry (OXY). Shunt quantitation was possible by QRAC with D in 83 patients and by QRAC without D in only 60 patients. Shunt quantitation was D was possible in all cases (21) with pro longed bolus and without D in only 11 cases. Shunt quantitation failed even after D in 4 cases with fragmented bolus. In patients without shunt the variance of the OXY determinations was greater than those of QRAC. The quantitative results of OXY and QRAC were correlated.The correlations were equally poor (r=.31 and .50).The greatest dicrepancy between OXY and QRAC values occurred in children under two years of age (decrease of the shunt due to crying?) and in atrial septal defect (poor reliability of OXY results).When these cases were discarded the correlation between OXY and QRAC without D remained poor (r=.58), while the correlation between OXY and QRAC with D improved (r=.84) which is highly satisfactory taking into account the errors bounded to each technique.
In conclusion, deconvolution analysis does improved the L-R shunt detection and quantitation and its clinical use is recommended.

ROUTINE DECONVOLUTION ANALYSIS OF PULMONARY TRANSIT CURVES IN PATIENTS WITH SUSPECTED LEFT-RIGHT CARDIAC SHUNTS. P.O. Alderson, K.H. Douglass, J.M. Roland, J.M. Links, P.M. Foard, G.P. Leitl, and H.N. Wagner, Jr. The Johns Hopkins Medical Institutions, Baltimore, MD.

We have shown in animal studies that deconvolution analysis (DCVA) allows accurate left-right (L-R) shunt quantitation by radionuclides, even when the injected bolus is prolonged. To investigate the clinical utility of DCVA, studies were performed in 17 children (ages 1-14, $\bar{x}$ = 6) and 3 adults with suspected L-R shunts, and in 54 consecutive controls (ages 3-82, $\bar{x}$=54) referred for LV function studies. The patients with suspected shunts had independent determinations of shunt size by oximetry. Tc-99m was injected at a slow, steady rate in peripheral veins, and monitored by a ROI over the superior vena cava. Shunt size was determined by applying the gamma variate method to deconvoluted and uncorrected pulmonary transit curves, and the results were compared. Only 5 of the 70 pts (7%) had injections which could not be deconvoluted. Shunt calculations were falsely positive ($\bar{x}$ QP:QS=1.34:1) in 18 controls prior to DCVA, but only 3 were abnormal after DCVA. Shunts were present by oximetry in 18 of the 20 patients. The correlation between oximetry and the gamma variate was poor (r = 0.52) prior to DCVA, but improved significantly (r = 0.95, p <.001) after DCVA. There were 2 false negatives in children with small shunts, but no false positives after DCVA. The results demonstrate that routine DCVA minimizes false-positives, provides accurate shunt quantitation and virtually eliminates the need to repeat studies because of an inadequate bolus injection.

COMPARISON BETWEEN ECHOCARDIOGRAPHIC AND NUCLEAR MEDICINE MEASUREMENTS OF LEFT VENTRICULAR EJECTION FRACTION IN CHILDREN AFTER REPAIR OF VENTRICULAR SEPTAL DEFECT. A.R. Siddiqui, R.A. Hurwitz, D.A. Girod, R.L. Caldwell, D.P. Moran. Indiana University School of Medicine, Indianapolis, IN.

Ejection fraction of left ventricle can be measured non-invasively using M-mode echocardiography and nuclear medicine techniques. Currently the most reliable method of measuring left ventricular ejection fraction is thought to be contrast ventriculography performed during cardiac catheterization. Although the assessment of ejection fraction utilizing the M-mode echocardiography has been quite reliable, its accuracy is questionable after open-heart surgery. Radionuclide assessment of left ventricular ejection fraction has been found to be very accurate in adults.

Left ventricular ejection fraction was obtained by all 3 methods in 17 children who had undergone repair of ventricular septal defect and often associated abnormalities. Radionuclide ejection fraction was obtained by multiple gated acquisition at equilibrium using Tc-99m labeled autologous red blood cells. The correlation between contrast and radionuclide studies was very good (r= .74), but poor between echocardiography and contrast studies (r= .35). All 4 patients with cardiomegaly and clinical evidence of poor left ventricular function were correctly identified by radionuclide study.

If the ejection fraction determined at cardiac catheterization in post-open heart surgery patient is taken to be the standard, it appears that radionuclide study is a very reliable substitute technique in evaluation of these patients, especially if compromised ventricular function is suspected.

RADIONUCLIDE "MILK" SCAN FOR DETECTION OF PULMONARY ASPIRATION IN INFANTS AND CHILDREN. R. Howman-Giles and M. Trochei. Royal Alexandra Hospital for Children, Sydney, Australia.

Recurrent bronchopulmonary infection, asthma, and apnoea may be associated with pulmonary aspiration (PA). This may occur as a result of incoordinate swallowing, gastro-esophageal reflux (GER) or tracheoesophageal fistula. The radionuclide method (RN) is a non-invasive physiological test which can detect PA directly even while the patient is asleep and assesses antireflux treatment. After fasting, 19 infants and children aged 1 month to 7.5 years (mean 11 months) were fed 500μCi of Tc99m sulphur colloid in milk. A dynamic swallow was collected for 1 frame/5 seconds until the pharynx was cleared. This was followed by unlabelled milk until sated and 1 minute frames for 60 minutes were collected on computer. Delayed images at 2 hours and 24 hours were performed. A second bottle of labelled milk was given for the last feed of the evening. Images were usually performed anteriorly in a supine position. However if the patient was having thickened feeds and/or upright feeding posture then the study was performed at 45^{o} upright recline using the appropriate labelled formula. Barium studies (Ba) were performed in 17 patients. Nine infants (47%) had positive RN scans for PA; 1 during swallowing; 6 at 2 hours and 2 the following morning. GER and PA was confirmed in 2 infants on Ba. Two infants who were on antireflux medications and posturing had negative scans. GER was confirmed in 15 patients by Ba and/or RN. RN is a valuable clinical non-invasive investigation to confirm PA in infants and children with recurrent pulmonary problems and to assess the results of therapy.

EVALUATION OF SPINAL FUSIONS BY BONE SCINTIGRAPHY: A PRELIMINARY REPORT. H.T. Harcke. St. Christopher's Hospital for Children, Philadelphia PA. M. Larkin and M. Clancy. Shriners Hospital for Crippled Children, Philadelphia PA.

Children who undergo spinal fusion for scoliosis may continue to show progression of their curve and/or experience pain following surgery. In certain cases this occurs as a result of defects in the fusion (pseudarthrosis). Bone scintigraphy would be helpful in the management of these patients if it could accurately identify the presence and location of pseudarthroses.

We have examined 30 children (age 12-17 yrs) experiencing pain and/or progression of scoliosis following spinal fusion. Scintigraphic examinations of the spine were performed using Tc-99m MDP. Thus far 15/30 have been re-explored and the operative findings correlated with the scintigraphic study.

We wish to report the following observations:
1) Bone graft material in general showed less tracer uptake than the spine.
2) Increased bone activity was commonly observed at the points where Harrington rod hooks were anchored.
3) 16 sites of pseudathrosis were associated with localized increases in uptake, 9 sites of pseudarthrosis were associated with normal uptake, and 5 sites of increased uptake were not associated with pseudarthrosis.
4) 7/15 children had more than one pseudarthrosis. The uptake varied from site to site.

This preliminary report suggests that bone imaging may be of limited clinical value in the localization of pseudarthroses.

BONE SCINTIGRAPHY IN UNCOMPLICATED AND TREATED SLIPPED CAPITAL FEMORAL EPIPHYSIS (SCFE). M.J. Gelfand and J.L. Strife. E.L. Saenger Radioisotope Laboratory and Division of Pediatric Radiology, University of Cincinnati and Children's Hospital, Cincinnati, OH.

Treatment of SCFE may be associated with avascular necrosis of the femoral head. In other cases, minimal SCFE may be difficult to confirm roentgenographically. Eight bone scintigraphic studies were performed in seven children with SCFE. Anterior and posterior routine pelvic images and anterior pinhole images were obtained 2 to 3 hours after intravenous injection of ^{99m}Tc diphosphonate.

Four children had more activity in the capital femoral metaphyseal growth center (CFMGC) of the affected side than on the contralateral side. Each had normal perfusion of both femoral heads. Two children known to have had manipulative reduction of the femoral head for SCFE had absent perfusion of the ipsilateral femoral head. In two children, after internal fixation of the femoral head three or more months prior to scintigraphy, activity in the ipsilateral CFMGC was similar to femoral head and neck activity. This indicated loss of the usual focal concentration of activity in the CFMGC that is normally present prior to epiphyseal closure.

Bone imaging is useful in the evaluation of femoral head perfusion in SCFE patients. Increased activity may be seen in the ipsilateral CFMGC as would be seen in a fracture; aiding, in some cases, in the confirmation of this lesion. The status of the CFMGC after internal fixation also may be evaluted.

SIMULTANEOUS SEPARATE GLOMERULAR FILTRATION RATE DETERMINATION -VALIDATION OF A METHOD. J.C. Leonard, E.L. Malone, W.K. Chu, E.W. Allen. Oklahoma Children's Memorial Hospital, Oklahoma City, Oklahoma

Several methods for determining GFR utilize Tc-99m Sn-DTPA, but only the method of Piepsz et al calculates the clearance of each kidney independently and to the best of our knowledge this algorithm has not been validated by others. Since each kidney contributes to the total GFR, comparing the sum of the individual GFRs should be equal to the GFR as determined by other established methods. This approach is necessary since selective ureteral catheterizations are infrequently performed in our patient population.

Our purpose is to validate Piepsz's algorithm and to further automate the technique on a clinical nuclear medicine unit with renal background and depth determinations as well as curve analysis and calculations being operator independent.

GFR as determined by creatinine clearance (cl) - 3 pts, Glofil cl - 3 pts, and serial plasma cl over a 3.5 hour period - 4 pts - was compared with the computer calculated GFR. Using a background ROI lateral to the kidney gave a correlation coefficient of 0.95, $p < .001$, in the ten patients studied. Using backgrounds inferior to the kidney gave a wider variation in results, presumably by not considering the contribution of splenic and hepatic activity to the renal curves.

The algorithm of Piepsz et al has been validated and can be used with minimal operator intervention. Wider clinical use is indicated.

THE EFFECT OF INTESTINAL HORMONES ON THE Tc-99m PERTECHNETATE (TcO4) IMAGING OF ECTOPIC GASTRIC MUCOSA IN EXPERIMENTAL MECKEL'S DIVERTICULUM. G.N. Sfakianakis, G.F. Anderson, D.R. King and E.T. Boles.
Children's Hospital, Columbus, Ohio.

Meckel's diverticula were created in 11 adult mongrel dogs by implanting full thickness vascularized patches of gastric wall onto Roux-en-Y loops of distal ileum. All animals had sequential camera imaging studies (every 10 min for 60 min) with computer acquisition (1 min frames for 60 min) following intravenous injection of 2mCi of TcO4. The scans were repeated following (1) subcutaneous injection of pentagastrin (6mg/kg)15 min prior to injection of TcO4, (2) pre-treatment with pentagastrin plus subsequent intravenous injection of glucagon (0.05 mg/kg) 10 min after the injection of TcO4, (3) glucagon alone. The surface area of gastric mucosa in the Meckel's was measured at necropsy.

By visual and computer analysis the following were observed: 1) Lesions as small as 0.95cm^2 visualized. 2) Pentagastrin alone accelerated accumulation of radioisotope in the stomach and ectopically in the Meckel's, but resulted in early visualization of duodenum. 3) Pentagastrin alone enhanced a "washout" phenomenon in the stomach and the Meckel's; i.e. rapid elution of activity. 4) Glucagon alone resulted in no early difference but prevented the early visualization of duodenum and enhanced the gastric activity later by preventing the "washout" phenomenon. 5) The combination of pentagastrin and glucagon enhanced radionuclide accumulation in the lesion, prevented the visualization of early activity in the duodenum, and eliminated the "washout" phenomenon.

The above findings indicate a potential role for glucagon in the diagnosis of ectopic gastric mucosa in humans.

Tc-99m-DIETHYL-IDA IMAGING IN CHILDHOOD HEPATOBILIARY DISEASE. R.Ohi, W.C.Klingensmith III, and J.R. Lilly. U. of Colorado Health Sciences Center, Denver, CO.

Thirty-three infants and children ranging in age from 2 months to 15 years were studied with Tc-99m- diethyl-IDA one to five times. Seventeen patients had biliary atresia, five had choledochal cyst, five had paucity of the intrahepatic ducts or Alagille's syndrome, three had neonatal hepatitis, two had alpha-1-antitrypsin deficiency, and one had congenital hepatic fibrosis. Five of the patients with biliary atresia were studied preoperatively. Four of these were studied before 3 months of age and demonstrated moderately good hepatocyte clearance in conjunction with no evidence of bile flow; the oldest patient (5½ months) had poor hepatocyte clearance without evidence of bile flow. In the 12 patients studied postoperatively, 2 patients without successful surgery showed decreasing hepatocyte clearance in serial studies. Of 10 patients with successful operations, hepatocyte clearance decreased in 5, stabilized in 2, and improved in 3. The 3 patients with neonatal hepatitis showed variable amounts of decrease in hepatocyte clearance with corresponding increases in transit time; intestinal activity was always demonstrated. All 5 patients with choledochal cyst were evaluated postoperatively; all showed good hepatocyte clearance and normal transit. In the 5 patients with paucity of intrahepatic bile ducts, the most striking finding was increased hepatobiliary transit time in the periphery of the right lobe and entire left lobe in 2 patients; central right lobe transit was normal. Of the 2 patients with alpha-1-antitrypsin deficiency, 1 had mistakenly had a Kasai procedure; the other showed normal clearance and mildly prolonged transit. The 1 patient with congenital hepatic fibrosis showed good clearance, several areas of focal intrahepatic ducts dilatation, and markedly prolonged transit. We tentatively conclude that Tc-99m-diethyl-IDA is useful in differentiating obstructive from nonobstructive cholestasis and in demonstating pathophysiology which may be helpful in evaluating infants and children with cholestatic disease.

CHILD ABUSE - ITS COMPLETE EVALUATION BY ONE RADIOPHARMACEUTICAL. D.L. Gilday, J.M. Ash, and M.D. Green. The Hospital for Sick Children, Toronto, Ont.

Although we have employed bone imaging for 7 years, as a screening procedure for the osseous evaluation of child abuse, it is only during the last year that we have performed cerebral blood flow images, kidney images and bone images with the same radiopharmaceutical to provide a 3 phase study.

The cerebral blood flow study has detected 1 SDH and continues to be a useful screening procedure. After it is completed the kidneys are serially imaged for 10 minutes. One partially obstructed kidney has been observed.

Two hours after injection a whole body bone scan is performed using a high resolution collimator. It has proved to be the most reliable tool for evaluating occult osseous trauma. We have observed one false negative study in comparison to x-ray and have successfully detected 8 lesions in children that were not seen by x-ray or suspected clinically.

Our hospital criterion for the diagnosis of child abuse by radiologic means is that the child has to have at least one unexplained fracture in the correct clinical setting. The bone scan has converted 8 children into the definite category from the suspicious one.

The 3 phase study is a simple and economical means of evaluating the vulnerable organs in the child suspected of having been abused. It has the added merit of reducing the potential radiation to the child by substituting the bone scan for a complete radiological survey except for the skull, where some fractures may be missed.

10:00-11:30 Room 2043

CLINICAL

LUNG

Session Chairman: Bruce R. Line
Session Co-Chairman: Ferrucio Fazio

EXPERIMENTAL EVALUATION OF PULMONARY PERFUSION IMAGING AND ARTERIOGRAPHY IN DIAGNOSIS OF PULMONARY EMBOLISM. N.P. Alazraki, D. Feigin, J. Bookstein, K. Seo, D. Motto, and J. Heaphy. Veterans Administration Medical Center, San Diego and University of California, San Diego, CA.

Accuracy of perfusion lung imaging was compared with subselective magnification pulmonary arteriography for identifying various sized experimental pulmonary emboli in dogs; we also correlated the scans and angiograms during resolution of emboli. Following baseline normal perfusion lung scans in 10 dogs, a catheter was placed into a 3-5 mm diameter pulmonary artery and arteriography with 3X magnification was performed. Autologous clots were injected unilaterally in 7 dogs and Ivalon non-resorbable fragments in 3 dogs. Arteriography was repeated 5 minutes after clot deposition, followed within 30 minutes by a perfusion lung scan. Both studies were repeated at 24 hours and at intervals up to 22 days post embolization, or until studies were normal.

Multiple occlusions involving arteries 1-2 mm in diameter were seen on magnification arteriograms and scans. As emboli lysed, rates of normalization of scan and angiogram varied, with excellent correlation between them. In Ivalon injected dogs, some discrepancies were noted. Early scan defects appeared larger than anticipated from the size of the occluded artery by angiogram. This disproportion suggested vascular spasm. As spasm cleared, although there was little change in the angiogram, striking regression of perfusion defects were seen on scan.

This study confirms the high sensitivity of lung scans to detect pulmonary emboli and suggests that vasospasm contributes to perfusion defects imaged by scan.

SCINTIGRAPHIC DETECTION OF PULMONARY EMBOLI IN PATIENTS WITH OBSTRUCTIVE PULMONARY DISEASE. P.O. Alderson, D.R. Biello, K.G. Sachariah, and B.A. Siegel, The Johns Hopkins Medical Institutions, Baltimore, MD., and Mallinckrodt Institute of Radiology, St. Louis, MO.

Obstructive pulmonary disease is frequently present in patients (pts) with suspected PE. The ability of Xe-133 ventilation:Tc-99m perfusion (V-P) imaging to diagnose PE in this setting was investigated by reviewing the studies of 83 pts with suspected PE. All V-P images showed zones

of abnormal washin or Xe-133 retention and multiple perfusion defects. Each pt had a posterior 3-5 min Xe-133 washin and prolonged Xe-133 washout imaging (60 sec images for 7-10 min) prior to perfusion. The perfusion scans included 4-6 views, 400-600K each, performed after injection of Tc-99m labeled particles. Each pt had a chest radiograph the same day and a pulmonary angiogram within 72 hrs. Scans were read without knowledge of the angiographic results. Xe-133 retention was graded as mild (0-3 min), moderate (4-6 min) or severe (7 min or greater) in each of six lung zones (upper, mid-, lower each lung). Angiographic evidence of PE was present in 23 of the 83 pts (28%). A low probability interpretation was made in 55 of the 60 pts (92%) without PE, and two were called nondiagnostic because of diffuse, moderate-severe Xe-133 retention. There were 3 false positive interpretations. A high probability reading was made in 19 of the 23 pts (83%) with PE. These 19 pts had 40 abnormal Xe-133 zones ($\leq$ 3 per pt), and 52% of zones showed mild retention. The 4 false negative studies each showed 3-4 abnormal Xe-133 zones, and 80% showed moderate or severe retention. Scintigraphic detection of PE is reliable when coexistent Xe-133 abnormalities are limited in their extent and severity.

COMPARISON OF KR-81m AND XE-133 VENTILATION IMAGING. T. R. Miller, H. H. Davis, J. I. Lee, D. R. Biello, A. G. Mattar, and B. A. Siegel. Mallinckrodt Institute of Radiology, St. Louis, MO.

Kr-81m has been proposed as an alternative to Xe-133 for ventilation imaging(V). We prospectively studied 64 patients(pts) with both agents and Tc-99m MAA(Tc) perfusion imaging(Q) to compare their effectiveness in diagnosing pulmonary embolism(PE). In each pt a Xe study was performed first consisting of posterior wash-in, equilibrium, and washout images. Then, the Tc was injected and alternating Tc-Kr images were obtained in 6 views. The Xe-Tc images and chest radiograph(CXR) were read independently of the Kr-Tc-CXR study by 3 observers. Four pts had pulmonary angiography(PA). The V-Q studies were interpreted as normal (N), or low(L), intermediate(I), or high(H) probability for PE.

Xe	N	L	I	H	N	L	I	L
Kr	N	L	I	H	L	N	L	H
No.	11	24	10	9	2	4	1	3
PA			1-	2+				1+

There were significant differences in 4 of the 64 pts (1I-L, 3L-H). The I-L difference was due to diffuse Xe retention but precise Kr matches in all areas of Q abnormality. Nine pts were H by Xe while those plus 3 more were H with Kr. In one (with + PA), the discrepancy was due to right middle and lower lobe overlap with Xe. In the other 2 (without PA), mild Xe retention was evident (V-Q match), but Kr was normal (V-Q mismatch), suggesting that either: 1)Xe is "too sensitive", or 2)Kr is "not sensitive enough." In conclusion, while Xe and Kr give essentially the same results in most pts, we found important differences in 3 of 12 pts with possible PE. A controlled prospective trial with PA is warranted before Kr is accepted for routine use.

EFFICACY OF KR-81M AND XE-127 IN EVALUATIONG NON-EMBOLIC PULMONARY DISEASE. H. Susskind, H.L.Atkins, A.G.Goldman, J.C.Acevedo, and P. Richards. Brookhaven National Laboratory, Upton, N.Y. 11973.

A clinical comparison was carried out to evaluate the use of Kr-81m and Xe-127 for determining lung ventilation defects in a group of 80 patients with a variety of non-embolic pulmonary diseases. Unlike Xe-133, Xe-127 is similar to Kr-81m in spatial resolution and tissue penetration, but differs markedly in half-life. The 13-sec half-life of Kr-81m results in images that reflect the distribution of regional lung ventilation, while precluding its equilibration in the lungs. The 36.4-d half-life of Xe-127, on the other hand, permits its equilibration, followed by its subsequent washout. 500,000-count Kr-81m ventilation images were obtained in each of four different positions - posterior, anterior, and right and left posterior oblique - and were interdigitated with Tc-99m MAA perfusion images. Both were compared with Xe-127 images in the posterior position obtained from the inspiration of the initial tracer bolus, after equilibration, and after 2 and 5 min of washout. In addition, the distribution of the two gases was compared on the basis of point-by-point computer analysis and display. The Xe data were clearly superior to those of Kr in 20 of the studies; in 10 of these, the Xe-127 was essential to the diagnosis, since the Kr images were normal. Kr-81m was superior to Xe-127 in 15 studies; in 1 of these it was essential to the diagnosis, since the Xe image was normal. However, Kr and Xe were equally useful in evaluating the remaining 45 studies (56%). Kr-81m was therefore essential to the diagnosis in only 1 study (1.2%) and superior to Xe-127 in only 15 studies (19%).

VALIDATION OF QUANTITATIVE NUCLEAR IMAGING FOR AEROSOL STUDIES OF THE LUNG. H. Itoh, G.C. Smaldone, D.L. Swift, P.O. Alderson, and H.N. Wagner, Jr. Kyoto University Hospital, Kyoto, Japan, and Johns Hopkins Medical Institutions, Baltimore, MD.

The purpose of the study was to evaluate the role of the gamma camera in determining pulmonary depositions of aerosols compared with other means: filtering and photometry.

Monodisperse sebacate aerosols labeled with technetium-99m human serum albumin (MMD 1 micron) were produced by a condensation technique and delivered to an anesthesized dog through a respiratory pump. A tyndallometer was placed before the tracheal tube to monitor inspiratory and expiratory aerosol concentrations. These signals were multiplied by aerosol flow, and the product was integrated with time to give the aerosol numbers going in and out of the dog. The radioaerosols deposited in the lung were stable with minimum clearance; thus the amount could be determined with the gamma camera after injecting radioactive microspheres at the end of the multiple exposure studies. Pulmonary depositions by the filter method were obtained by measuring the radioactivity in the filters which were placed in the inspiratory and expiratory lines.

Pulmonary deposition fractions determined by the different techniques agreed well, proving that scintillation imaging was useful for quantifying the aerosol depositions in the lung. Furthermore, the combined use of photometry and nuclear techniques would be useful especially in the case of the aerosols which are absorbed rapidly from the lung. The tyndallometer would provide an accurate measure of the total aerosols deposited within the lung, while the gamma camera would portray the distribution and regional clearance rates of the aerosols.

CLINICAL VENTILATION IMAGING WITH RADIOACTIVE INDIUM-113m. F. Fazio, P. Wollmer, J.P. Lavender and M.M. Barr. Hammersmith Hospital, London, U.K.

Deposition of small aerosols within the lungs takes place by: (a) sedimentation to lung periphery according to regional ventilation, and (b) impaction in large airways (central deposition). The latter can be substantial in patients with airflow obstruction, thus reducing usefulness of radioactive aerosols for ventilation imaging. As central deposition is mainly due to impaction of relatively large particles, a method has been proposed for removing the larger droplets from a polydispersed aerosol preparation (Hayes, M., Taplin, G.V., Chopra, S.K., et al, Radiology, 131: 256, 1979). We have implemented a modification of this method in clinical routine and compared it with regional ventilation as assessed with continuous inhalation of Kr-81m. Normal subjects, patients with pulmonary embolism and patients with variable degrees of airflow obstruction underwent the aerosol procedure immediately after a routine Kr-81m ventilation/Tc-99m perfusion lung scan. A solution of In-113m albumin was first nebulized, using a disposible device, in a large reservoir settling bag. Then the patient inhaled the aerosol from the bag during 5' of tidal breathing. This was followed by lung imaging on the gamma camera (equipped with a high energy collimator). The use of In-113m allows to perform a ventilation scan in multiple views (anterior, posterior, obliques) following the routine Tc-99m perfusion scan. Qualitative (image inspection) and quantitative (penetration index) comparison with Kr-81m scans indicates that this readily available aerosol technique provides ventilation images of good statistical quality and with relatively little central deposition, even in patients with severe airflow obstruction.

CORRELATION BETWEEN QUANTITATIVE RADIONUCLIDE LUNG STUDIES AND SPIROMETRY BEFORE AND AFTER A SURGICAL REMOVAL OF LUNG CARCINOMA. R. Gupta, U. Y. Ryo, J. Szidon, S. M. Pinsky. Michael Reese Hospital and University of Chicago, Chicago, Illinois.

As a part of pre-operative evaluations, a quantitative ventilation and perfusion study was performed in 21 patients with lung carcinoma(Ca). By dividing each lung into 3 equal regions of interest using a computer, quantitative values of ventilation and perfusion in the region of Ca were calculated in order to predict the reduction of lung function after surgical removal of the region. Pulmonary function study included spirometry and lung volumes and the values obtained after surgery were compared to the values predicted on the radionuclide studies.

The perfusion value in the lung with Ca was lower than that of ventilation value in 12 and equal or similar in 8 of 21 patients. In only one patient the perfusion value in the lung with Ca was significantly higher than that of ventilation value. Surgery was refused or regarded as too risky in 8 patients and post-operative spirometry data were available for correlation with radionuclide studies in 9 patients ; pneumonectomy 2, lobectomy 4, and segmental resection in 3 cases. Decrease in vital capacity and FEV_1 after the surgery averaged 18.4% and 13.5% while predicted reduction on ventilation and perfusion studies averaged 13.4% and 12.5% respectively. The most wide discrepancy between the predicted values and post-operative spirometry value was 20% observed in a patient who underwent radiation therapy after the operation.

Quantitative radionuclide lung study for the prediction of post-operative reduction in lung function is simple and reliable procedure and ventilation values appear to be slightly closer to the post-operative spirometry data.

COMPARATIVE EVALUATION OF LUNG SCAN IMAGES CORRECTED AND UNCORRECTED FOR RESPIRATORY MOVEMENT OF THE LUNGS. J.D. Massie, T.A. Powers, M. Kulkarni, R.D. Bowen, and J.J. Touya. VA Medical Center-Vanderbilt Univ., Nashville, TN.

A recent publication suggested that correcting for respiratory movement could improve the detection of perfusion defects by lung scan. This suggestion was based on results obtained in a PTE animal model imaged using a gated acquisition technique. We have evaluated the validity of such correction in humans. In 10 consecutive patients referred for lung scan, frozen inspiratory and expiratory images and conventional images were obtained successively. These images were independently rated on a scale of 1 to 4 for subjective quality by 4 well trained physicians and results statistically analyzed. Frozen inspiratory and expiratory images were obtained using the Gated Regional Spirometry (GRS) software slightly modified. After injection of 4 mCi of Tc-99m MAA, a posterior view of the lungs was acquired in frame mode, 64 x 64 matrix with a temporal resolution of 20 frames per respiratory cycle. A ROI on the lung bases was used to trigger the gate analysis program which selects and adds separately frames corresponding to the maximum inspiratory and expiratory efforts. To avoid the known difference between analog and digital images, conventional digital images were generated with 1000K and 100K counts. These four images were copied on a single film in random order. Frozen inspiratory images were ranked better than expiratory images, $p < .02$. Inspiratory images were also ranked better than 100K images but the difference was not statistically significant, $p > .10$. The 1000K image was the best, $p < .001$. Thus, the slight improvement obtained by correcting for lung movement is not worth the increased imaging time per view: 90 seconds versus 15 minutes.

ESTIMATION OF PULMONARY ^{11}C -CHLORPROMAZINE UPTAKE BY DUAL ISOTOPE RESIDUE DETECTION WITH A SCINTILLATION CAMERA. A. Syrota, F. Soussaline, M. Crouzel, and C. Kellershohn. S.H.F.J. Commissariat à l'Energie Atomique. ORSAY.

In order to investigate the lung endothelial cell function in man, we have developed a noninvasive method to measure the pulmonary Chlorpromazine uptake. Basic Amines such as Chlorpromazine and Imipramine bind to specific high affinity sites located on the membrane of the pulmonary endothelial cell. It has been demonstrated using isolated perfused rat lungs that the process is saturable and the molecules are not metabolized. The technique used was to inject intravenously a bolus containing a nonpermeating reference tracer ^{113m} In Transferrin and the test molecule ^{11}C -Chlorpromazine. Patients were positioned under a scintillation camera equipped with a specially designed collimator for 511 keV gamma rays. Data were recorded in two energy windows for 45 sec and at 2 and 4 mn for 20 seconds. Both ^{11}C Chlorpromazine and ^{113m} In Transferrin curves corresponding to the residue functions were plotted after selecting areas-of- interest in each lung. Correction was made of the in vivo Compton diffusion of ^{11}C in the ^{113m} In window using data recorded at 2 and 4 mn. Instantaneous uptake U(t) was calculated using an integral formula:

$$U(t) = \frac{q_t(t) - q_r(t)}{1 - q_r(t)}$$ where $q_t(t)$ and $q_r(t)$ were the normalized residue functions. 15 patients were studied, 7 normal and 8 with diffuse lung disease. In 6 patients Chlorpromazine ($0.2 mg.kg^{-1}$) was infused during 10 mn just before the tracer injection. Uptake showed a plateau of 80% in normal patients. Maximum uptake was variable in the other patients but a plateau was never observed. After infusion of Chlorpromazine in normal patients maximum uptake was similar but U (t) decreased in function of time.

10:00-11:30 **Room 3039**

RADIOPHARMACEUTICAL CHEMISTRY

STRUCTURE-ACTIVITY

Session Chairman: Michael Loberg
Session Co-Chairman: Raymond Counsell

IN VIVO EVALUATION OF COMPONENTS OF A TECHNETIUM HEDP RADIOPHARMACEUTICAL MIXTURE SEPARATED BY HIGH PERFORMANCE LIQUID CHROMATOGRAPHY. E. Deutsch, D. L. Ferguson, T. C. Pinkerton and W. R. Heineman. Department of Chemistry, University of Cincinnati, Cincinnati, OH.

Technetium radiopharmaceuticals are often complex mixtures rather than pure chemical compounds, and it is likely that the individual components of these mixtures have different in vivo distributions. If radiopharmaceutical mixtures can be separated into their individual components, these components can then be evaluated in vivo. Separated components may be capable of imaging organs that can be only poorly imaged, or not imaged at all, by the parental mixture. In addition, radiopharmaceutical preparative conditions can be modified to enhance the yield of those components with the most desirable in vivo properties, thus increasing the organ specificity of the entire mixture. As a first step in this process we have separated a Tc-99m labelled HEDP (1-hydroxyethylidene diphosphonate) radiopharmaceutical mixture (both with and without added Tc-99 carrier) into component fractions by high performance liquid chromatography (HPLC). Three separated components were evaluated in normal rats and shown to have significantly different biological distributions. Components containing technetium in a lower oxidation state (A) have a much superior distribution (in terms of imaging normal bone) than a component containing technetium in a higher oxidation state (B) (e.g., femur uptake for A and B are 2.28 ± 0.23 and 1.16 ± 0.06 %dose/g; kidney uptake for A and B are 0.22 ± 0.04 and 2.44 ± 0.15 %dose/g). It thus appears that HPLC separation of technetium radiopharmaceutical mixtures will be a valuable tool in the development of more efficacious imaging agents.

CARBON-11 LABELLED STEROIDS AS POTENTIAL RECEPTOR BINDING RADIOPHARMACEUTICALS. A. Feenstra, W. Vaalburg, D.A. Piers, S. Reiffers, M.G. Woldring, H. Doorenbos. University Hospital, Groningen, The Netherlands.

Steroids labelled with γ-emitting radionuclides are proposed as radiopharmaceuticals for the investigation of estrogen dependent tissues and malignancies. Because of its

potential for positron emission computed tomography we suggested previously carbon-11 as label. In many steroid hormones an ethynyl or methyl group can be introduced without destroying the hormonal activity or even with increasing hormonal action. In order to assess the utility of C-11 labelled 17α-ethynylestradiol and 11β-methoxy-17α-ethynylestradiol (moxestrol) as radiopharmaceuticals the 3H-labelled analogs were used to investigate the biodistribution in mature female rats. Both steroids showed a high specificity for estrogen receptor containing tissues. The blood clearance and uterus uptake were very rapid resulting in high uterus to blood ratio's within less than two half lives of carbon-11. In order to assess the lower limit of the specific activity needed for localisation of receptor containing tissues, loading dose effects were investigated. Moxestrol with specific activities of 77 Ci/mmol and 7 Ci/mmol showed 30 minutes after intravenous injection uterus to blood ratio's of 22.0 ± 6.9 and 19.0 ± 7.2 respectively. After administration of ethynylestradiol with a specific activity of 50 Ci/mmol this ratio was 9.6 ± 3.7.

From these data we conclude that both steroids are promising as radiopharmaceuticals for the investigation of estrogen receptor containing tissues. We labelled both compounds with the positron emitting carbon-11.

C-11-LABELED BRANCHED-CHAIN AMINES, POTENTIAL AGENTS FOR POSITRON TOMOGRAPHIC LUNG FUNCTION STUDIES. L.C. Washburn, T.T. Sun, B.L. Byrd, and R.L. Hayes. Medical and Health Sciences Division, Oak Ridge Associated Universities (ORAU), Oak Ridge, TN.

C-11-Labeled straight-chain primary aliphatic amines have been reported by Fowler et al (J. Pharmacol. Exp. Ther. 198:133-145, 1976) as potential agents for dynamic measurement of lung function. These amines were rapidly sequestered by the lung, with a maximum uptake at approximately 1 min after injection. However, the subsequent metabolic loss of radiolabel from the lung and other tissues was also rapid, thus making quantitative assessment of lung function by positron tomography impractical.

Using the C-14-labeled compounds, we have studied the effect of chain branching on the lung uptake and clearance of primary aliphatic amines in the rat. C-14-Labeled octylamine (OA), 2-methyloctylamine (MOA), and 2,2-dimethyloctylamine (DMOA) were synthesized from 1-chloroheptane, 2-chlorooctane, and 2-chloro-2-methyloctane, respectively, by nucleophilic displacement with C-14-labeled KCN followed by reduction with lithium aluminum hydride. MOA gave about twice the lung specificity at early times as OA, and in addition MOA was metabolized only about one-half as fast. DMOA had less lung uptake than the other two agents but showed virtually no metabolic loss of label. We conclude that C-11-labeled branched-chain amines may be better than the straight-chain analogs for positron tomographic lung function studies. (ORAU operates under contract number DE-AC05-76OR00033 with the U. S. Department of Energy, Office of Health and Environmental Research.)

pH SHIFT AGENTS FOR BRAIN IMAGING: STRUCTURE - BIODISTRIBUTION RELATIONSHIPS FOR Se-75 TERTIARY DIAMINES. H.F. Kung and M. Blau. State University of New York at Buffalo, Buffalo, N.Y.

We have recently described a new type of radiopharmaceutical, pH shift agents, which have high uptake and retention in brain (J.N.M. Feb. 1980). These are tertiary diamines which are neutral and lipid soluble at blood pH (7.4) and can freely cross the blood-brain barrier. Inside brain cells where the pH is low (7.0) they pick up H^+, become positively charged, and cannot diffuse out because they are no longer lipid soluble.

A series of Se-75 labeled tertiary diamines of the form $R_2N(CH_2)_nSe(CH_2)_nNR_2$ were synthesized. The brain uptake and wash-out curve was studied in rats as a function of the inherent lipid solubility and the change in lipid solubility with pH of each compound. Partition coefficient-pH profiles (n-octanol:buffer, at pH 6.0-8.0), pK's and lipid solubility of the neutral (basic) form were measured.

Compounds with high partition coefficients at blood pH had high initial brain uptake (∿3.0% at 2 min after i.v. injection). Compounds with low partition coefficients at intracellular pH had long brain retention times (up to several days). All of the compounds showed low plasma protein binding (% free >85%).

Using the Henderson-Hasselbalch equation the partition coefficient-pH profiles were calculated from the pK's and the inherent lipid solubility of each compound. These curves matched the experimental data closely. By changing the substitution groups on the N atoms and the distance between them, one can design agents with any desired partition coefficient-pH profile. Since this profile determines the biological behavior, it is possible to prepare agents with optimal uptake and wash-out curves.

A COMPARISON OF THE BIODISTRIBUTION OF 2-18-FDG and 3-18-FDG IN MICE, RATS AND DOGS. D.R. Elmaleh, K. Kearfott, M. M. Goodman, D. Varnum, R. Lade, R. Ackerman, H.W. Strauss and G.L. Brownell. Massachusetts General Hospital, Boston, MA.

To evaluate the usefulness of 3-18-FDG as compared to 2-18-FDG, we investigated the tissue distribution behavior of both agents in three animal species. The mice and rats were sacrificed at 1,5,30,60 and 120 min post i.v. injection and the tissue distribution in % dose per gram was assayed (see table). The dog distribution was obtained by quantitative imaging with the positron camera.

	2FDG Mice		3FDG Mice	
	5 min	60 min	5 min	60 min
Brain	5.70±1.07	4.56±1.95	3.54±0.71	1.64±0.27
Heart	20.5 ±5.4	21.5 ±8.30	7.32±0.77	10.1 ±1.70
Liver	2.78±0.54	0.81±0.36	3.83±0.82	2.26±0.48
Blood	3.14±0.46	0.46±0.15	5.70± .60	2.14±0.76

The arterial blood clearance and plasma analysis of 2-18-FDG and 3-18-FDG were determined. 2-18-FDG was found to clear the blood more rapidly than 3-18-FDG in all species. The blood curves for dogs with both agents were found to best fit three exponential components. The $t_{\frac{1}{2}}$ (min) for 2-18-FDG and 3-18-FDG were 1.01, 10.07, and 12.9; and 0.52, 2.75, and 140.8, respectively. The 3-18-FDG was found to behave differently in mice and rats. In dogs the three rate constants were determined from Sokoloffs' operational equation following the brain activity by 1 min single sweeps over a period of 2 hrs. for 2-18-FDG and 3-18-FDG.

STRUCTURAL AND MECHANISTIC STUDIES OF ADRENOMEDULLARY RADIOPHARMACEUTICALS. D.M. Wieland, L.E. Brown, M.C. Tobes, T.J. Mangner, W.H. Beierwaltes, and D.P. Swanson. University of Michigan Hospital, Ann Arbor, MI.

The neuron-blocking drug guanethidine accumulates in and displaces norepinephrine from adrenergic nerves. Aromatic analogs of guanethidine can be radioiodinated and evaluated as potential imaging agents for organs with rich adrenergic innervation. We report here: 1) a structure-distribution relationship (SDR) study of I-125-aralkylguanidines in dogs, 2) evidence for their sequestration in the storage vesicles of the adrenal (A.) medulla, 3) imaging of the dog and primate A. medullae with I-131- and I-123-meta-iodobenzyl-guanidine (m-IBG).

Eight I-125-labeled guanidines(I) were synthesized by radioiodide exchange in water at reflux. Radiochemical yields were 90-98%; specific activities ranged from 0.8-1.1 mCi/mg. Purity was confirmed by radio-HPLC.

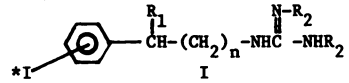

I

In the SDR study, all of the guanidines showed selective uptake in the A. medulla from 0.5-192 hours. However m-IBG (R_1,R_2=H,n=0) showed the highest uptake and target-to-nontarget concentration ratios.

Pretreatment of dogs with reserpine, a drug known to selectively block vesicular uptake, lowered the A. medulla uptake five-fold. Subcellular fractionation of the A. medullae revealed most of the radioactivity in the large granule fraction. Distinct images of the A. medullae of 3 dogs were obtained with I-123-m-IBG starting at 24 HR. Two rhesus monkeys gave similar images at 3-5 days with I-131-m-IBG.

STRUCTURE-DISTRIBUTION STUDY OF I-125-ω-IODOFATTY ACIDS. C.A. Otto, D.M. Wieland, L.E. Brown, and W.H. Beierwaltes. University of Michigan Hospital, Ann Arbor, MI.

The I-123-ω-iodofatty acids have two major drawbacks: 1) short myocardial T 1/2, 2) blood background. Both problems may be related to rapid β-oxidation of the fatty acids by the myocardium and other tissues. We report the synthesis and evaluation of various I-125-ω-iodofatty acids incorporating variations in chain length (I) and triple bond inclusion (II).

I = 125-$ICH_2(CH_2)nCOOH$(n = 6,9,14,20)

II = 125-$ICH_2(CH_2)_3$-C≡C-$(CH_2)_7COOH$

Compounds I were synthesized by a Li_2CuCl_4 catalyzed coupling of olefinic Grignards with ω-bromofatty acids followed by HBr addition and radioiodide displacement. Compound II was prepared by condensation of ω-bromooctanoic acid with the dilithio derivative of hexyn-6-ol followed by esterification, tosylation, iodide displacement and deesterification.

Compounds I were evaluated in rats with sacrifice 5, 10, 20 and 40 min after i.v. injection. At all time intervals reported, I (n=20) had significantly higher myocardial values than other I. Myocardial uptakes for I (n=20) and Tl-201 are similar. However high blood values for I (n=20) reduced heart/blood concentration ratios. The myocardial T 1/2 for I (n=20) was twice that of other I.

Compound II, a potential suicide inhibitor of enoyl-CoA-isomerase, showed similar extraction and myocardial T 1/2 as I (n=14). Blood values are slightly higher than comparable saturated fatty acids (0.19% kg dose/g vs 0.12%). Other potential allenic systems are under investigation as irreversible inhibitors of myocardial enzymes.

PARTIAL CHARACTERIZATION OF THE Tc-99m CYCLAM COMPLEX. W. A. Volkert, J. Simon, D. E. Troutner and R. A. Holmes. Department of Radiology and Chemistry, University of Missouri and Veterans Administration Hospital, Columbia, MO.

Macrocyclic amines rapidly complex Tc99m and exhibit excellent "in vivo" and "in vitro" stability. Following injection these complexes are rapidly cleared from the blood and are mainly excreted thru the kidneys. Since the objective of our research is to derivatize these ligands with hope of altering their biodistribution it is essential to understand the structuro-chemical features of these complexes. To date major emphasis has been directed to the investigation of the macrocyclic amine, cyclam (1, 4, 8, 11, tetracyclotetradecane), which was used to determine their chelating characteristics. Tc99m complexes of cyclam (Cyc) produced by Sn^{+2}, dithionite or Zr electrodes exhibited identical elution patterns from chromatographic columns, R_f values on TLC and migration distances during electrophoresis. This indicates that these reducing agents are not part of the final Tc-complex. Radiometric titrations of 3 x 10^{-4} M Tc-99 pertechnetate in 0.1 M Cyc at pH 11 using standardized Sn^{+2} solutions in an N_2 atmosphere showed that a 2 electron transfer is required to form Tc-Cyc indicating a +5 Tc oxidation state. A 1+ charge of the complex was estimated by comparing the migration distance of Tc-99-Cyc and Tc-99m-Cyc with Cyc complexes of known structure and charge made with Co^{+3} and Ni^{+2}. One likely form of Tc^{+5} complexed in basic aqueous media is a TcO_2^+ core that can form six coordinate Tc-complexes. If in fact the TcO_2^+ core is formed, we can conclude from our results that Tc forms a hexacoordinate complex with cyclam (eg. $[TcO_2(Cyc)]^+$).

SYNTHESIS AND TESTING OF LABELED GLYCOCONJUGATES AS CELL-SPECIFIC RECEPTOR RADIOPHARMACEUTICALS. D.R. Vera, K.A. Krohn, S.M. Steffen. University of California, Davis, CA.

Tc-99m-labeled neoglycoconjugates represent an important new class of radiopharmaceuticals that bind to cell surface receptors. Our initial experience has involved synthesis of neogalactoalbumin (NGA) and labeling it with technetium, resulting in a tracer which binds specifically to receptors on the hepatocyte membrane (HBP). This involves stepwise synthesis of acetobromo-α-D-galactose and its cyanomethyl derivative followed by the imidate, 2-imino-2-methoxyethyl-1-thiogalactoside (IME-thiogalactose). The IME reacts readily in mildly alkaline buffer with free amino groups of albumin and the resulting amidine bond is stable in dilute acid conditions used for Tc labeling. We use electrolysis to consistently achieve 95% labeling for Tc-99m-NGA. The resulting radiopharmaceutical purified by gel permeation chromatography is as stable as labeled native albumin. We have attached from 5 to 45 galactosyl residues. The HBP receptor binding affinity of NGA depends on the number of sugars attached to each albumin molecule and may be varied by as much as 10^4. A major concern for this compound was the possibility of aggregation which would convert it to a colloidal reticuloendothelial agent. The molecular weight distribution of Tc-99m-NGA was determined by BioGel P-300 chromatography. In all preparations the optical density and activity profiles matched and there was no activity or absorbance in the void volume or at the top of the column. Tc-NGA has features useful for cell-specific receptor-based imaging of the liver. It can be synthesized to produce the desired receptor affinity and labeling is rapid, efficient, and produces a ligand of high purity.
Supported by the American Cancer Society (Grant # RD-61).

Tc-99m(Sn)PYRIDOXYLIDENEPHENYLALANINE AND ITS LIPOPHILIC DERIVATIVES: AN APPROACH TO STRUCTURE/BIO-DISTRIBUTION RELATIONSHIP OF TECHNETIUM COMPLEXES. M. Kato-Azuma and M. Hazue. NIHON MEDI-PHYSICS CO., LTD. Takarazuka, JAPAN.

The objective of this investigation was to evaluate the structure/bio-distribution relationship of Tc-99m(Sn)pyridoxylidenephenylalanine derivatives, and to find a hepatobiliary imaging agent with rapid blood clearance, quick hepatobiliary transport and low urinary excretion. Phenylalanine derivatives with hydrophobic substituents on their aromatic ring were used as the amino acid constituents in the stannous preparations of Tc-99m pyridoxylideneaminates; they were o-F, m-F, p-F, p-Cl, o-methyl, p-methyl, m,m'-dimethyl and p-isopropyl-phenylalanine (all in DL form). The lipophilicity of the Tc-complexes was evaluated by the measurement of their n-octanol/buffer partition coefficient and their in vivo distribution was studied in rats.

The amount of urinary excretion correlated well with the global lipophilicity of the complex; the increase in lipophilicity diminished urinary excretion. The rate of blood clearance and hepatobiliary transport, on the other hand, reflected the structure of the complexes; the ortho-substituents were quite effective in accelerating blood clearance and hepatobiliary transport, and the opposite results were obtained with the para-substituents.

These results could be understood by considering the structure of the complexes. The para-substituents effectively increase the lipophilicity and hence reduce the urinary excretion; the ortho-substituents interfere with the rotation of the benzene ring and hence increase the rigidity of the complex's structure. The increase in rigidity of the structure would be effective in accelerating the blood clearance and the hepatobiliary transport of Tc-99m-(Sn)pyridoxylidenephenylalanine derivatives.

COMPLEXES OF TECHNETIUM WITH HYDROXYCARBOXYLIC ACIDS: d-GLUCONIC, d-GLUCOHEPTONIC, d-TARTARIC, AND CITRIC. C.D. Russell and A.G. Cash, University of Alabama and VA Medical Centers, Birmingham, AL.

Technetium complexes of several hydroxycarboxylic acids are used for medical imaging. To determine the oxidation state of technetium in these agents, we studied the reduction of Tc-99-pertechnetate in 0.1 M solutions of four hydroxycarboxylic acids, using polarography, coulometry, and amperometric titration with Sn(II). In gluconate, below pH 6, Tc(III) and Tc(V) complexes were identified with certainty, Tc(IV) questionably; at pH 6 to 10, Tc(IV) and Tc(V) were formed; above pH 10, Tc(III), Tc(IV), and Tc(V). In glucoheptonate, below pH 6, Tc(III) and Tc(V) were formed, and questionably Tc(IV); at pH 6 to 10, Tc(V); above pH 10, Tc(III), Tc(V), and probably Tc(IV). In tartrate, below pH 6, Tc(III), Tc(IV), and Tc(V) were formed; above pH 6, Tc(IV) and Tc(V). In citrate, below pH 10, Tc(III), Tc(IV), and Tc(V) were formed, above pH 10, Tc(IV) and Tc(V). For all four ligands the initial product of reduction by Sn(II) at pH 3 to 9 was Tc(V). In freshly prepared tin-labelled imaging agents of this class, the oxidation state is probably Tc(V). Lower stable oxidation states exist, attainable by using stronger reducing agents than tin; these may have altered imaging properties.

A STUDY OF STRUCTURAL REQUIREMENTS FOR POTENTIAL BONE LOCALIZING RADIOPHARMACEUTICALS. T.S.T. Wang, R.A. Fawwaz, E.G. Mojdehi and L.J. Johnson. College of Physicians & Surgeons, New York, NY.

Tc-99m labeled diphosphonates are commonly used bone imaging agents. This study was aimed at determining the effect of substitutions on phsophoryl groups and on the bridge carbon atom of MDP on bone localization.

Diisopropylmethylenediphosphonate, $CH_2(C_3H_7OPO_2N_a)_a$ (A); monobromomethylenediphosphonate, $BrCH(PO_3Na)_2$ (B); monohydroxymethylenediphosphonate, $HOCH(PO_3Na)_2$ (C); carbonyldiphosphonate, $CO(PO_3Na_2)$ (D); and dihydroxymethylenediphosphonate, $(HO)_2C(PO_3Na)_2$ (E) were synthesized. The purity of each compound was identified by tlc and elemental analyses. The chemical structure was confirmed by ir and nmr. Labeling of diphosphonates with Tc-99m pertechnetate was carried out with SN(II) as reducing agent. Labeling efficiencies were determined by ITLC.

Tissue distribution studies were done in rats at two hours after iv administration of tracer. Increasing bone localization was shown to occur in the order A<D<E<MDP<B<C. These results suggest that (1) compound A, the diphosphoryl ester of MDP, like MDP chelates with Tc-99m but exhibits lower bone localization than MDP. Thus the four hydroxy groups of the diphosphonate are equally essential for bone localization. (2) The mono substituted compounds (B) and (C) demonstrate higher bone concentration and faster blood clearance than MDP but the disubstituted compounds (D) and (E) are inferior to MDP with respect to these parameters. Thus the sterochemical structural conformation of diphosphonates is not as critical as the resonance hybrid contributing structures in bone localization.

AN EVALUATION OF FIVE NEW DIPHOSPHONATES FOR SKELETAL IMAGING. G. Subramanian, J. G. McAfee, T. Feld, E. Hofmann and C. Zapf. Upstate Medical Center, Syracuse, New York 13210.

3-amino 1-hydroxypropylidene 1, 1-diphosphonate (I), N,N dimethylamino N-diphosphonate (II), N-methylamino methylene diphosphonate (III), 1, N-methylamino 1,1-ethylidene diphosphonate (IV), and 1,1-ethylidene diphosphonate (V) were synthesized, analyzed and made into freeze dried kits with stannous chloride. All compounds were labeled with Tc-99m.

In New Zealand rabbits, bone lesion was induced by drilling two side-by-side 1/8" dia. burrholes in the tibia (J. Bone Joint Surg. 59A/213-217/1977). The subsequent formation of osteoid within the burrholes served as a good reproducible model of bone regeneration, less variable than fractures. One to two weeks later, biodistribution studies of the above compounds and Tc-99m-MDP were performed 2 and 3 hrs after I.V. injection. Sr-85 was also injected simultaneously as a biological standard. Samples were assayed from all major organs, normal bones and the tibial section containing the burrholes along with a precisely matched equivalent from the opposite limb.

The blood levels at 3 hrs were relatively high for compounds IV and I, similar for II, V and MDP and lowest for III. All diphosphonates localized well in the skeleton, but IV showed the lowest concentration whereas I & III had higher concentrations in the bone comparable to or slightly better than MDP. The abnormal/normal tibial ratios were the highest for I & II and lowest for IV. Only compounds I & III showed characteristics comparable to those of MDP and therefore may warrant clinical evaluation.

10:00-11:30 Room 3040

INSTRUMENTATION

EMISSION TOMOGRAPHY I

Session Chairman: L. Stephen Graham
Session Co-Chairman: Edward Hoffman

HEADTOME; A NEW HYBRID EMISSION TOMOGRAPH AND ITS APPLICATION FOR BRAIN STUDY. K. Uemura, I. Kanno, S. Miura, Y. Miura, Y. Kawata, S. Takahashi, K. Hirose and K. Koga. Research Institute for Brain and Blood Vessels, Akita and Shimadzu Seisakusho Ltd., JAPAN.

A high speed hybrid tomograph(Headtome) measuring single photon and positron emitters for brain study was developed and preliminary clinical results were reported.

The detector is made of 64 NaI Xtals of 16 x 28 x 70 mm arrayed on a ring of 42 cm diameter. Two collimator systems with axial shift mechanism for changing single photon and positron detection mode are set inside of the detector ring. Collimator system for single photon sampling consists of 64 sets of moving vanes which are set on each NaI Xtal and swing synchronously to and fro to see rapidly whole field of view(21 cm ϕ). Preliminary study of single photon images showed the resolution of 10 mm FWHM, and sensitivity for a 20 mm thick slice was 20 and 15 Kcps/μCi/ml for a 20 cm diameter cylindrical water phantom containing Tc-99m and Xe-133, respectively.

Clinical emission tomographic imaging of Tc-99m pertechnetate brain scan and 3-dimensional regional cerebral circulation study were carried out by HEADTOME. Tc-99m brain section images demonstrated better lesion contrast than that in standard brain scintigram. 3-dimensional imaging of regional cerebral circulation was studied by continuous intracarotid infusion of Kr-81m developed by F. Fazio. Distribution of decreased regional cerebral blood flow were imaged clearly in the patients with cerebral infarction. The fast sampling time of HEADTOME was also applicable to new method developed by I. Kanno and N.A. Lassen for non invasive 3-dimensional cerebral circulation study with Xe-133 inhalation.

A ROTARY POSITRON EMISSION TOMOGRAPH: "POSITOLOGICA". E.Tanaka, N.Nohara, T.Tomitani, M.Yamamoto, H.Murayama, Y. Suda, M.Endo, T.Iinuma, Y.Tateno, F.Shishido, K.Ishimatsu, K.Ueda, K.Takami. National Institute of Radiological Sciences, Chiba; Hitachi Medical Corp., Kashiwa; and Central Research Laboratory, Hitachi Ltd., Kokubunji; Japan.

A new positron ECT device for brain study has been constructed. The detector consists of 64 12x20x26 mm BGO crystals mounted on a circular gantry, controlled to rotate continuously at 60 rpm. The crystals are arranged in a 44 cm diameter circle, as determined by computer iteration to provide reasonable density uniformity for linear sampling with a 2 mm bin-width. The number of coincidence pairs per bin is 11.9 in average, with a minimum of 11, in a field of view of 23 cm in diameter. With this high detector redundancy, the reconstructed image is expected to be fairly insensitive to instabilities or misadjustment of detector gain.

In the coincidence logic system, 64 detector signals are divided into 8 groups, and the group coincidences are recorded. Coincidence signals are organized into a 12-bit address plus other flags, including a chance coincidence flag. All the signals from the rotating gantry are transmitted through a parallel 16-bit rotary photo-coupler to a computer interface. The coincidence data are finally arranged into 128 parallel projections. A rotational positron source assembly, containing several small Ge-68 sources, is mounted in the device for attenuation correction and detector calibration.

The device has a maximum field of view of 24 cm in diameter with a variable slice thickness of 1-2 cm. The spatial resolution is less than 9 mm FWHM in the central region and the sensitivity is about 17 kcps/μCi/ml for a 20 cm diameter water phantom for a 2 cm slice.

COMPARISON OF QUANTITATIVE TRANSAXIAL AND CORONAL POSITRON TOMOGRAPHY OF THE BRAIN. M.E. Phelps, J. Mazziotta, J. Miller, D.E. Kuhl. UCLA School of Medicine, Los Angeles, CA.

The compromizes between in-plane resolution, axial resolution, statistical noise, radiation dose and imaging time in computed tomography (CT) have resulted in ratios of plane thickness to in-plane resolution of 1 to 2 in emission CT and 4 to 10 in x-ray CT. The poorer resolution in slice thickness is accepted so that sufficient detection

efficiency is provided to meet the high statistical requirements of CT. However, optimum orientation of resolution depends upon the orientations, shapes and sizes of the structures under study. We have developed a way to directly record and reconstruct coronal tomographic sections with our whole body positron tomograph. The subject lays on his stomach with his chin resting in a foam rubber head holder such that the tomographic image plane is orthogonal to the orbital meatus and to the conventional transaxial image plane (i.e. orientation of coronal planes). Studies were carried out with (F-18) fluorodeoxyglucose (FDG) in normal volunteers in which tomographic images were taken at 1 cm intervals in both the transaxial and coronal directions throughout the entire intracranial compartment. The coronal images taken in this manner are of much higher quality than if they had been formed by reorganizing transaxial images using the method of Glenn et al. The coronal images show the best delineation of structures that have their smallest dimension primarily in the vertical direction while the transaxial approach is best for those structures where this is the case in transverse direction. The best approach therefore depends on the primary structures of interest.

Physical performances of an emission computed tomography system using a rotating conventional gamma camera. F. Soussaline, A.E. Todd-Pokropek, S. Zurowski, E. Huffer,* C. Raynaud, C. Kellershohn. Serv.Hosp.F.Joliot-Dépt de Biologie-CEA-ORSAY(France). *INFORMATEK SA ORSAY (France).

A flexible inexpensive system for single photon emission tomography seems highly desirable in a clinical environment. A standard GE 400 T maxicamera rotating on a ring stand, coupled to an INFORMATEK Simis 3 computer system has been studied and characterized by the measurement of some physical critical parameters. A total of 64 or 128 projections as 64 x 64 or 128 x 64 matrices are collected at regular positions. The reconstruction of any of the possible 64 adjacent transverse sections, which may be then sorted into coronal, sagittal and oblique sections, are obtained by filtered backprojection. Great care was taken to ensure the uniformity of the field of view, the position of the center and the choice of the energy window. Increasing angular sampling from 64 to 128 projections, as opposed to increasing spatial sampling, does not improve resolution. A considerable amplification of non-uniformity in tomographic planes has been observed, very dependent on the energy window selected. The spatial resolution of the system given by the FWHM of the line spread function was 15.5 mm in a 20 cm lucite phantom, and relatively independant over radial distance. The slice thickness was 19 mm (FWHM of the longitudinal response using a point source). The sensitivity was ≈5 cps/μCi for both a small (5 cc) and extented (1500 cc) uniform sources, enabling images of reasonable quality (of 0,5 M events/slice), to be obtained in 10 mn. Correction for Compton events by use of multiple energy windows, the choice of the filter and different methods of attenuation correction are being studied.

PRELIMINARY CLINICAL RESULTS OBTAINED IN EMISSION COMPUTED TOMOGRAPHY WITH A ROTATING CONVENTIONAL GAMMA-CAMERA. C.Raynaud, A.E. Todd-Pokropek, F. Soussaline, S. Zurowski, S. Ricard, and C. Kellershohn. Service Hospitalier Frédéric Joliot, Département de Biologie, CEA, Orsay, France.

A gamma tomography system(GT) comprising a GE 400 T gamma camera linked to an Informatek Simis 3 computer was used and results obtained in 40 patients are presented. In 25 brain tumors confirmed by X-ray computerized tomography(CT) or by surgery, the GT scans were clearly positive in 88% If only the 10 posterior fossa tumors are considered; GT scans were positive in all, while scintiscans were clearly positive in 3 and doubtfully positive in 5. In 10 patients highly suspected of liver tumor, the GT scans were positive while scintiscans were positive in 7 and doubtfully positive in 3. The 5 lung GT scans confirmed conventional scintiscans but did not add any information.

These initials results indicate that :
1) Excellent GT images can be obtained where the contrast tumor/tissue is about 2 times that in conventional scintiscans.
2) The reliability of the GT scans for detection of hot spots, as in brain tumor, seems excellent. It is unlikely however that such results, with rare exceptions, will be more accurate than those obtained with CT.
3) The usefulness of the method would seem much more evident in an organ such as the liver but a a long term follow-up is needed to confirm this impression.

RESULTS USING A NEW DYNAMIC COMPUTER-ASSISTED TOMOGRAPH TO STUDY BRAIN ISCHEMIA AND FUNCTION IN TRANSVERSE CROSS-SECTION. E.M. Stokely, E. Sveinsdottir, N.A. Lassen, and R.W. Parkey. Univ. Texas Health Science Center at Dallas, Texas.

A single-photon emission tomograph has been designed and built for regional studies of brain blood flow using either xenon-133 or xenon-127. The tomograph uses 4 arrays of 16 multislice detectors in each array to collect data from 3 simultaneous slices in 5 seconds using the intracarotid injection method. Three collimators were designed for the system: a high resolution dynamic collimator for the intracarotid injection modality with a 1.3-1.7 cm X 2.0 cm resolution (170,000 cps/μCi/cc, 3 slices, Tc-99m, 20 cm dia Phelps phantom), a high sensitivity collimator for inhalation delivery of xenon-133 with 1.8-2.4 cm X 2.5 cm resolution (357,000 cps/μCi/cc, 3 slices, Tc-99m, 20 cm dia phantom), and a high resolution collimator for static studies with 0.7-1.0 cm X 1.25 cm resolution, (35,000 cps/μCi/cc, Tc-99m). Only the high resolution dynamic collimator has been constructed thus far, and it has been used to perform studies on patients using both methods of xenon delivery. The injection method clearly reproduces the studies of Lassen et.al. demonstrating areas of increased blood perfusion in the brain in cross section following hand exercise. The inhalation modality has been used to demonstrate reduced perfusion in a patient who had a cystic tumor. The results using the inhalation modality for xenon-133 delivery suggests that brain ischemia can be studied in cross section using this tomographic imaging system.

QUANTITATIVE MYOCARDIAL FLOW-EXTRACTION DATA USING GATED ECT. T.F. Budinger, S.E. Derenzo, R.H. Huesman, L.G. Sherman, B.R. Moyer, and Y. Yano. Donner Laboratory, University of California, Berkeley, CA.

The use of emission computed tomography to measure physiological processes in vivo depends on the ability to measure tracer concentrations within well-defined volumes of tissue and the validity of the assumptions of the model. In ungated studies of the time dependences of Rb-82 concentration in ventricular blood A(t) departs radically from the expected blood clearance curve and reaches a steady level after 4 min. The most likely explanation was motion of myocardial tissue into the region of interest which was our estimate of the ventricular cavity. Studies using bolus injection of Rb-82 and the Donner 280-crystal tomograph gated over various portions of the cardiac cycle gave image data for 10 mm thick transverse sections taken for 15 sec to 30 sec intervals for 7 min after bolus (10 sec) injection of 20 to 150 mCi of Rb-82. Gating intervals were: from the R-wave for 70 msec; from the T-wave for 70 msec (end systole); and for the interval from 150 msec before the R-wave to the R-wave (end diastole). For the end diastole interval A(t) decreased as expected and was less than 3% of the peak value at 4 min. Using the ungated data, an error in the time integral of 11% was found for 3 min and of 59% for 6 min after injection. This error invalidates calculation of flow x extraction (FE) from the conservation of mass model: $FE = Q(\overline{T})/\int^{T} A(t)dt$ which assumes negligible washout and blood compartment concentration. Using gated studies FE varies with time in accordance with an expected clearance of $t_{\frac{1}{2}}$ = 30 min for Rb.

Errors in the myocardial concentration due to movement of adjacent tissues into the region of interest also argue for the need to gate.

RECENT DEVELOPMENTS IN SINGLE PHOTON EMISSION COMPUTED TOMOGRAPHY WITH A SMALL GERMANIUM CAMERA. DA Ortendahl, L Kaufman, W Rowan, R Herfkens and D Price, UCSF-RIL So. San Francisco, CA

Using the UCSF high purity germanium gamma-camera we have evaluated the use of germanium in single-photon ECT (1). The reconstruction algorithm for the current evaluation is simply a back projection of filtered projections using a ramp filter with no roll-off. The imaging characteristics of the HPGe camera allow the use of a weighted back projection algorithm to mitigate the loss of spatial resolution at depth. Improvements have recently been made in the depth correction algorithm; their effect on the 3-D images is compared to previous results (1). Using line sources a spatial resolution of 2-4mm at 10cm depth has been measured. Results of phantom studies will be shown. Head and kidney images of rats injected with Tc-99m MDP are presented. The potential for multiple radionuclide imaging is demonstrated with rats imaged simultaneously with Tl-201 and Tc-99m pyrophosphate for both normal and infarcted hearts. Measurement of the distribution of the down scattered Tc-99m allows the subtraction of its contribution from the Tl-201 image, thus reducing the background considerably. Germanium offers the potential for resolution in ECT significantly better than the 9 to 16mm FWHM available commercially and comparable with the alternative tomographic modalities.

1. Ortendahl DA, et al: High Resolution Single-Photon Emission Computed Tomography with a Small Germanium Camera. IEEE Trans. Nucl. Sci. NS-27 (In Press).

QUANTITATIVE CAPABILITIES OF A SINGLE PHOTON EMISSION TOMOGRAPHIC SCANNER. C.-M. Kirsch, R.E. Zimmerman, B.L. Holman, and R.J. English. Harvard Medical School, Boston, MA.

The quantitative capabilities of the Cleon 711 whole body scanner have been evaluated for Tc-99m, Tl-201 and Ga-67. This instrument obtains transaxial emission tomograms by means of a ring of 10 scanning collimated NaI detectors. All measurements were made using cylindrical plastic vials 2.5 by 5 cm, placed in a 20 by 35 cm cylinder filled with water. Using a figure of merit the pulse height analyzer setting has been optimized for a maximum signal to noise ratio. Line spread function and slice thickness were determined for Tc-99m, Tl-201 and Ga-67 by perpendicular and inclined pipettes in the cylinder. Regional sensitivity was measured by varying the position of the vials within the large phantom.

With the presently installed software the spatial resolution is 26 mm in air for all isotopes studied, 26 mm for Tc-99m and 28 mm for Tl-201 in water. The slice thickness is 38 mm for Tl-201 and 33 mm for Tc-99m in water. The regional sensitivity was found to be strongly dependent on the spatial distribution of the source and its physical location within the attentuating medium. This is due to the simple geometric attenuation correction presently available. When relative changes were measured within the phantom, the error between the true and measured change in activity was 4%.

This suggests that relative quantitative assessment of radionuclide distributions can be achieved under the condition that the source configuration is kept constant. Our results indicate that the attenuation correction algorithm requires improvement if absolute quantification is to be performed.

IMPROVING THE SPECIFICITY AND ACCURACY OF Tc-99m-IDA CHOLESCINTIGRAPHY WITH DELAYED VIEWS. H.S. Weissmann, L.A. Sugarman, J.D. Badia and L.M. Freeman. Montefiore Hospital and Medical Center, Bronx, NY.

The major diagnostic criterion in evaluating Tc-99m-IDA studies performed for acute cholecystitis(AC) is nonvisualization of the gallbladder(GB). Critical to the evaluation is the duration of the study. If the 296 patients studied for AC were only followed for 1 hour, the accuracy would have been 93% and specificity 87.7%. The lower specificity etc. is due to the fact that many cases of chronic cholecystitis(CC) may be associated with GB nonvisualization in the first hour. However, the great majority of these CC cases do exhibit GB visualization on delayed images (1-4 hrs). By obtaining such delayed views we identified 19 patients who had delayed GB visualization, including 2 with slow hepatic uptake and commensurately delayed biliary visualization secondary to hepatocellular disease and 17 with prompt hepatic uptake and visualization of the CBD and duodenum within the first hour. Of these 17, 14 had CC and not AC, while the remaining 3 had AC. Only 1 patient with persistent GB nonvisualization up to 4 hours had CC. Therefore, the delayed views reduced the false-positive rate from 9.9% to 0.6% and improved the accuracy for diagnosing AC to 97.6% and specificity to 99%. The delayed view is also important in improving the accuracy in other clinical situations. For example in post-cholecystectomy and bypass patients, even if the study appears entirely normal within the first hour, we routinely obtained delayed views because we have learned that a cystic duct remnant or bile leak may only be identified on the delayed views. Also in cases of cholestasis, visualization of obstructed intrahepatic biliary radicles or the common bile duct may only be observed on the delayed views.

THE HEPATIC PARENCHYMAL IMAGE IN HEPATOBILIARY SCINTIGRAPHY. M. L. Brown, J. E. Freitas, H. W. Wahner, Mayo Clinic and Mayo Foundation, Rochester, MN, William Beaumont Hospital, Royal Oak, MI.

Hepatobiliary scintigraphy with the Tc-99m iminodiacetic acid derivatives (IDA) has been shown to be useful in the workup of biliary diseases, especially for the diagnosis of acute cholecystitis. However, there has been little emphasis placed on the evaluation of the hepatic parenchymal images (HPI) that occur early in the imaging sequence. This study was undertaken to determine whether the HPI contained information similar to Tc-99m sulfur colloid images of the liver. A comparison was made in 50 patients between the IDA study and the SC examination obtained within seven days of each other. In 46 cases the number and position of lesions seen on the two studies were similar. This group included 17 cases of multifocal disease (15 metastatic disease and 2 polycystic disease), 22 unifocal lesions (5 intrahepatic gallbladders, 10 metastatic foci, 3 cysts, 2 hemangiomas, 1 normal biliary structures,and 1 pseudotumor) and 7 marginal defects (5 prominent gallbladder fossae and 2 metastatic foci). Of the four discordant images, one HPI was of poor technical quality and did not identify a metastatic focus, one appeared normal in a patient with cirrhosis with multiple filling defects on SC, and one did not identify the defect on SC that turned out to be prominent biliary structures. One cyst was seen on HPI and missed on SC. In addition to being very similar in lesion detection (47/50) the IDA scan also allowed more specificity in the later images in 13 cases. IDA will not be a replacement for SC scintigraphy because of the difficulty of doing multiple projections; however, critical evaluation of the HPI in IDA scintigraphy can provide important information on liver pathology.

2:00-3:30 Room 2040

CLINICAL

GI I

Session Chairman: E. Eikman
Session Co-Chairman: Heidi Weissman

ASYMPTOMATIC CYSTIC DUCT OBSTRUCTION IN CHRONIC CHOLECYSTITIS. J. E. Freitas and D. M. Fink-Bennett. William Beaumont Hospital, Royal Oak, MI.

Since gallbladder (GB) non-visualization during hepatobiliary imaging (HBI) appears diagnostic of acute cholecystitis (AC) in the setting of acute abdominal pain, 20 patients with chronic cholecystitis (CC) underwent HBI when they were pain-free to determine the prevalence of asymptomatic cystic duct obstruction, a potential cause of

false-positive HBI studies. All patients had CC diagnosed by clinical findings, oral cholecystography (OCG), and/or ultrasonography (US). All patients received 5 mCi of Tc-99m Iprofenin (PIPIDA) intravenously and serial 300K views were obtained for one hour. Eighteen patients had OCG with GB non-visualization present in 9, visualization of calculi in 7, and normal visualization in 2. Nineteen patients had US with calculi identified in all. Two of 20 patients demonstrated GB non-visualization yet common bile duct visualization during HBI. Non-visualization by OCG and multiple calculi by US were present in both. One of these 2 patients subsequently developed acute abdominal pain two weeks post-HBI with AC superimposed on CC found at operation. Five of the remaining 19 patients have had CC confirmed by elective cholecystectomy.

In this series, 10% (2/20) of CC patients (asymptomatic during HBI) demonstrated GB non-visualization during HBI compatible with chronic cystic duct obstruction. Since the prevalence of CC in patients who present with acute abdominal pain is approximately 35%, such chronic obstruction could induce a 3-4% false positive rate for HBI detection of acute cholecystitis.

EFFICACY OF HEPATOBILIARY IMAGING IN ACUTE ABDOMINAL PAIN. J. E. Freitas, D. M. Fink-Bennett, J. H. Thrall, and W. W. Resinger. William Beaumont Hospital, Royal Oak MI and University of Michigan Medical Center, Ann Arbor MI.

To assess the diagnostic efficacy of hepatobiliary imaging (HBI) in the rapid evaluation of acute abdominal pain, 26 patients underwent HBI following the intravenous injection of 5 mCi of Tc-99m Iprofenin (PIPIDA). All patients had acute abdominal pain of 72 hours or less. Prior to HBI, the referring physician completed Part I of the questionnaire indicating his differential diagnosis and his certainty of each diagnosis (expressed as a percentage). Immediately following HBI, the same physician completed Part II of the questionnaire indicating again his differential diagnosis and certainty based upon the HBI results. The HBI impact upon the physician's diagnostic certainty was expressed as a log likelihood ratio (LLR). A LLR of 0.0 represents no change in the physician's diagnostic certainty,while greater ratios represent progressively increasing efficacy. In these 26 patients, acute cholecystitis (AC) was the most likely diagnosis prior to HBI in 23; but post-HBI, AC was most likely in only 12. The mean LLR for this series was 1.41 ± 0.34 with 23 of 26 patients demonstrating a LLR greater than 0.0. In 16 of 24 patients, a LLR greater than 1.0 was obtained reflecting the considerable impact of HBI on the physician's diagnostic certainty. In 8 of 26 patients, HBI changed the physician's therapeutic decision.

Many imaging studies have utility, but their true value relates directly to their impact on the physician's diagnostic certainty (i.e. efficacy). HBI is efficacious in acute abdominal pain for it (1) considerably enhances the physician's diagnostic certainty, and (2) changes the therapeutic decision in many cases.

MULTICENTER TRIAL OF Tc99m DISOFENIN ([diisopropylphenylcarbamoylmethyl] iminodiacetic acid): A NEW HEPATOBILIARY AGENT FOR IMAGING JAUNDICED AND NON-JAUNDICED PATIENTS. A.Green, N.Rosenberg, M. Sheahan. New England Nuclear Corp., North Billerica, MA.

As it has been shown that Tc99m dimethyl -IDA loses utility as a hepatobiliary imaging agent with serum bilirubin levels greater than 5mg/dl, a new -IDA congener was evaluated in a multicenter trial. 23 normal volunteers at 5 institutions showed no adverse reactions or change in clinical laboratory studies after the administration of 0.75 -5.0 mCi Tc99m Disofenin (≤ 10 mg Disofenin). Blood levels at 30 minutes post-injection ranged from 2.9-13.8% and urinary excretion in the first 2 hours post-injection ranged from 3-18% of the injected dose. Images showed clear delineation of intrahepatic biliary ducts, gallbladder and extrahepatic ducts within 5-20 minutes after injection and intestinal activity within 25-60 minutes. Renal visualization either did not occur or was extremely faint. Using these criteria of normality, 97 patients were studied prospectively at 6 different institutions. There were no adverse reactions and all procedures were technically satisfactory. 20 of 21 patients with a final diagnosis of normal biliary system had a normal scan; a single patient with proteus sepsis but normal biliary tract showed delayed (120 minutes) intestinal transit. All 21 patients with cholelithiasis and partial or total obstruction showed delayed or no gallbladder visualization, delayed or absent intestinal visualization or dilated ducts. All 4 patients with acute cholecystitis without cholelithiasis showed no gallbladder visualization. Of 98 Tc99m Disofenin scans only 33 showed some renal visualization, all without interference with image interpretation. All but 1 of the 17 non-obstructed patients with elevated serum bilirubin levels ≥5mg/dl showed clear visualization of gut.

Tc-99m-DIISOPROPYL IMINODIACETIC ACID (DISIDA): THE BEST OVERALL CHOLESCINTIGRAPHIC RADIONUCLIDE FOR THE EVALUATION OF HEPATOBILIARY DISORDERS. H.S. Weissmann, J.D. Badia, T. Hall, L.A. Sugarman and L.M. Freeman. Montefiore Hospital and Medical Center, Bronx, NY.

Several iminodiacetic acid (IDA) analogs have been developed including HIDA (dimethyl), PIPIDA (paraisopropyl), BIDA (parabutyl) and DISIDA (diisopropyl). Our clinical experience with all four analogs suggests that DISIDA is the best overall agent to address the major clinical areas of suspected acute cholecystitis (AC) (as accurately as HIDA) and the differential diagnosis of cholestasis (as accurately as BIDA), as well as chronic cholecystitis (CC) and post-operative complications. We have studied 76 patients with DISIDA: 22 for suspected AC, 12 for CC, 24 for post-operative evaluation and 18 for cholestasis. We have found the accuracy of DISIDA for evaluating suspected AC to be comparable to HIDA. Also comparable to HIDA, it visualizes the normal common bile duct (CBD). Since we can visualize the CBD, we have also identified the same spectrum of cholescintigraphic patterns in CC that has been observed with HIDA, depending upon whether or not there is partial or complete obstruction of the cystic and/or CBD. It has also been as sensitive in detecting post-operative biliary leakage and obstruction, e.g. afferent loop syndrome. Most importantly, DISIDA has been extremely effective in distinguishing medical from surgical jaundice in 18 patients with the bilirubin ranging from 1.1 to 24.5 mg%. Therefore, at this time, DISIDA represents the single best "universal agent" to study all hepatobiliary problems where a radionulide imaging study is indicated.

CLINICAL COMPARISON OF Tc-99m-DIISOPROPYL-IDA AND Tc-99m-DIETHYL-IDA FOR EVALUATION OF THE HEPATOBILIARY SYSTEM. W.C.Klingensmith III, A.R. Fritzberg, V.M. Spitzer, and C.C. Kuni. U. of Colorado Health Sciences Center, Denver, CO

Animal studies indicate that the two best hepatobiliary imaging agents are Tc-99m-diisopropyl-IDA and Tc-99m-diethyl-IDA (Radiology 128:793,1978). We have conducted a clinical comparison between these two agents in 13 patients with a wide range of hepatobiliary function. Three patients had transient right upper quadrant pain of undetermined etiology; two patients each had alcoholic liver disease, primary biliary cirrhosis, and liver transplantation; one patient each had acute viral hepatitis, chronic active hepatitis, and abdominal trauma. The average time between studies was 1.4 days. Anterior and right lateral images were routinely acquired at 5,10,15,30,45, and 60 minutes; if intestinal activity was not present by 60 minutes; imaging was continued until it appeared or until 24 hours. In 5 patients 3 hour cumulative urine collections were obtained and in 4 patients rapid serial images following injection were obtained for quantification of relative extraction efficiency.

Tc-99m-diisopropyl-IDA tended to be superior to Tc-99m-diethyl-IDA in demonstrating: 1) liver parenchyma, 2) hepatic ducts, and 3) less renal activity ($p<0.05$ only for renal activity). In four of five patients Tc-99m-diisopropyl-IDA showed less renal excretion; but both agents demonstrated increasing renal excretion with increasing bilirubin levels. Tc-99m-diisopropyl-IDA had a 1.6x higher hepatocyte extraction efficiency than Tc-99m-diethyl-IDA. Our preliminary data suggests that there is a tendency for Tc-99m-diisopropyl-IDA to give better images of the hepatobiliary system although no large differences were detected.

CLINICAL COMPARISON OF Tc-99m-PARABUTYL-IDA AND Tc-DIETHYL-IDA FOR IMAGING THE HEPATOBILIARY SYSTEM: W.C.Klingensmith III, A.R. Fritzberg, C.C.Kuni, and J.R. Lilly. U. of Colorado Health Sciences Center, Denver, CO.

Animal and preliminary patient data suggests that Tc-99m-parabutyl-IDA might be superior to Tc-99m-diethyl-IDA in imaging the hepatobiliary system in patients with high blood bilirubin levels (Radiology 128:793, 1978). A direct clinical comparison between these two agents was made in 14 patients. The total serum bilirubin range was 1.2 to 50.6 mg/dl (mean = 13.3). The average time between studies was 2.0 days. Anterior and right lateral images were acquired at 5, 10, 15, 30, 45, and 60 minutes; if intestinal activity was not present at 60 minutes, imaging was continued until it appeared or until 24 hours. Visual evaluation of all 14 paired studies showed Tc-99m-parabutyl-IDA to be superior ($p<0.05$) in maximum liver to background ratio (5-60 min) and least renal activity; Tc-99m-diethyl-IDA was superior ($p<0.05$) in liver to background ratio at 5 minutes. There was a tendency ($p>0.05$) for Tc-99m-diethyl-IDA to demonstrate the intrahepatic ducts better and to show an earlier intestinal arrival time. In the 8 patients who showed evidence of biliary excretion, both agents demonstrated excretion in 6, only Tc-99m-diethyl-IDA in 1 (bilirubin: 17.1 mg/dl), and only Tc-99m-parabutyl-IDA in 1 (bilirubin: 50 mg/dl). We tentatively conclude that, in general, Tc-99m-parabutyl should be used as a secondary agent, even in patients with markedly elevated bilirubins. However, in certain situations, in which biliary tract visualization is unlikely and detection of intestinal activity is critical, e.g. biliary atresia, Tc-99m-parabutyl-IDA might serve as the primary agent.

TECHNETIUM-99m HIDA HEPATIC LOBAR DISTRIBUTION AND RETENTION RATIOS IN THE DETECTION OF INTRAHEPATIC CALCULI. S.H. Yeh, O.K. Liu, P.F. Chiu, and M.J. Huang. Veterans General Hospital, Taipei, Taiwan

Sequential scintiphotography with Tc-99m PG has been used for detecting liver stones (J Nucl Med 18: 635, 1977). However, it is qualitative and tedious. An alternative method which is simple and quantitative is described below.

Data were acquired in the hepatic region for one min at 5 and 40 min after I.V. injection of Tc-99m HIDA with the patient in the same position. A computer routine was used to calculate: (A) right and left lobar distribution ratio (R/L) with correction for the relative lobar thickness by dividing the ratio of the count rates of the right and left lobes at 40 min by that at 5 min; and (B) individual lobar retention ratio (RRR for right, RRL for left) at 40 min. Nine patients strongly suspicious of intrahepatic stones were studied. R/L, RRR and RRL were also determined in 36 normal individuals. The mean ratio ± 1 S.D. was 0.96 ± 0.14 for R/L, 0.55 ± 0.17 for RRR, and 0.57 ± 0.18 for RRL.

In all 9 proven patients, 4 had unilobar and 5 had bilobate liver stones. Retention ratios of all 14 affected lobes increased greatly from 1.00 to 2.92. All 4 unilobar cases had normal retention ratios (range 0.71-0.86) in the unaffected lobes. R/L's were outside the normal range in all 4 unilobar cases (R/L's = 0.30, 0.32, 0.41, 3 left; R/L = 1.61, 1 right). Although R/L's were within normal range in 2 of 5 bilobate cases, individual R/L's ratios still reflected the main side of involvement compatible with RRR and RRL.

Initial results indicate that R/L, RRR and RRL are useful parameters easily obtained for detecting intrahepatic lithiasis. Thus this new technique may replace sequential scintiphotography for screening this disease.

2:00-3:30 Room 2043

CLINICAL

BONE I

Session Chairman: Richard Holmes
Session Co-Chairman: Ignac Fogelman

QUANTITATIVE BONE IMAGING OF PATIENTS WITH CARCINOMA OF THE PROSTATE. J.G. Hardy, M.L. Wastie, and A.E. Kulatilake. Queen's Medical Centre, Nottingham, U.K.

Quantitative bone imaging has been employed to monitor the response to estrogen and estramustine phosphate therapy of patients with bone metastases from carcinoma of the prostate. The technique devised avoids the need to compare the uptake into metastases with that into apparently normal bone, since many patients had widespread metastatic involvement. Following intravenous injection of 10mCi Tc-99m methylene diphosphonate, imaging was undertaken using a large field gamma camera and the data recorded by computer. By imaging an external standard the uptake into a selected site (ROI) was quantified and expressed as a "standardized count" (SC) using the equation,

$$SC = \frac{\text{count rate from ROI}}{\text{count rate from standard}} \times \frac{\% \text{ dose in standard}}{\text{area of ROI}} \times 10^3$$

Follow-up studies were undertaken at 3 monthly intervals for periods of up to 15 months. Of the 81 patients investigated 40 (49%) had bone metastases. Prior to treatment the "standardized counts" from regions of interest over the lower thoracic and lumbar vertebrae of patients without bone metastases were 10.70 ± 2.88 (32 patients) and 9.77 ± 2.74 (34 patients), respectively. There were slight reductions in the average values following therapy but these were not statistically significant ($p>0.4$ for all follow-up times). Variable responses have been observed in the uptake of the radiopharmaceutical into metastatic bone; in some cases there have been increasing "standardized counts" whilst in others the values have decreased or remained constant. A decrease in uptake may represent an improvement. Quantitative bone imaging is playing an important role in the management of patients with carcinoma of the prostate.

BONE SCANS IN STEROID-TREATED PATIENTS WITH SYSTEMIC LUPUS ERYTHEMATOSOUS (SLE). J.J. Conklin, J. Denseraux, P.O. Alderson, T.M. Zizic, D.S. Hungerford, and H.N. Wagner, Jr. The Johns Hopkins Medical Institutions, Baltimore, MD.

Patients with SLE are particularly susceptible to ischemic necrosis of bone (INB) when they are treated with steroids. A prospective study of bone scanning for detection of INB was performed in 36 such patients (97% females, age range 16-63). Since the hips, knees and shoulders are usually affected by INB in SLE, 300 K converging collimator images of these joints were obtained on film and in digital format 2-3 hrs after injection of 20 mCi of Tc-99m methylene diphosphonate. All patients had joint radiographs, and 12 had intraosseous pressure (IOP) determinations in the marrow space of affected joints (n=37) for independent assessment of INB. Scans showed abnormally increased joint activity in 28 of the 36 patients. A total of 95 joints showed abnormalities, 19% were in hips, 35% in knees and 46% in shoulders. Nineteen of 31 joints with elevated IOP had abnormal scans (sensitivity = 61%), and scans were abnormal in 3 of 6 joints with normal pressures (specificity = 50%). Thus, the positive predictive value of the scans compared to IOP was 86% (19/22). Scans were significantly more sensitive than radiographs for detecting early INB. Ten of 31 joints with abnormal IOP were detected only by scan, but only 3 showed abnormal radiographs with normal scans. Fifteen of the 19 joints with abnormal IOP and abnormal scans were painful. The results confirm the high frequency of INB in patients with SLE who are treated with steroids, and demonstrate that bone scans are more sensitive than skeletal radiographs for early detection of INB.

Tc-99m MDP IMAGING AS AN EARLY TEST FOR FEMORAL HEAD OSTEONECROSIS. D.A. Weber, G. Bauer, L.I. Hansson, L. Ceder, L. Darte, L. Stigsson and N. Egund. Lund University Hospital, Lund, Sweden and University of Rochester School of Medicine and Dentistry, Rochester, NY.

A prospective study of hip fracture patients was made to evaluate the use of bone imaging as an early indicator of femoral head osteonecrosis and other healing complications. A series of 25 patients was imaged with Tc-99m MDP within 3½ wk of fracture and nailing; repeat studies were scheduled at 4, 8, 12, 24 and 36 mo. Early perfusion

phase and later bone deposition images of the hips were recorded. Repeat radiographs and a review of clinical symptoms were obtained at each scheduled visit; tetracycline deposition was evaluated in 13/25 patients. Eleven additional patients with various hip problems were imaged 2 mo to 3 yr after fracture.

Major and partial Tc-99m MDP filling defects suggesting sites of osteonecrosis, as well as normal or enhanced Tc-99m MDP deposition in the femoral head characterized the images within 3½ wk of fracture. Marked variations in the healing process were demonstrated; some defects revascularized and showed bone remodelling at 4 mo whereas others showed no change at 1 yr or more after fracture. Radiographic changes in the femoral head were seen infrequently. Imaging studies of the acute and early stages of fracture healing (0-12 mo) show Tc-99m MDP to be a sensitive test for changes in bone vasculature and remodelling. Correlation of these and subsequent changes with femoral head pathology and fracture resolution will define the predictive accuracy and usefulness of this procedure.

THE INFLUENCE OF PERMEABILITY ON UPTAKE OF BONE IMAGING AGENTS. M.A. King, D.J. Lanteigne and S.C. Marks, the University of Massachusetts Medical School, Worcester, MA, J. Brand, the University of Rochester Medical School, Rochester, NY.

It has recently been established that the 99m-Tc labeled phosphates and phosphonates are less permeable than the earlier bone imaging agents; therefore, increased local permeability may be an important factor in the localization of 99m-Tc labeled agents in some pathological states. We conducted two tests of this hypothesis. In the first, the sterile inflammatory reaction one day post a single exposure of 1800R to the hind leg of rabbits was used as the model for inducing changes in vascular permeability. Alterations in the relative initial clearance of 99m-Tc MDP and 85-Sr, as well as relative clearance of 113-Sn microspheres (relative blood perfusion), were determined in sacrificed rabbits.

In the second part, the thickness of the layer of cells covering bone surfaces (permeability of the "bone membrane barrier") was studied in vitro. Intact and lightly scraped neonate rat calvaria were incubated at 37°C in Tris buffered isotonic salt solution at pH 7.4 with 99m-Tc MDP and 85-Sr. As verified histologically, the scraping simulated an increase in permeability by removing much of the periosteum. That cell viability was not important in the uptake process was determined by comparing the uptake of calvaria which were heat treated (70°C for 20 min), or repeatedly frozen in liquid nitrogen, against that of controls.

The results of these studies confirm the higher permeability of 85-Sr and indicate that an increase in local permeability can result in significant increases in local uptake of 99m-Tc labeled bone imaging agents.

SCINTIGRAPHIC EVALUATION OF PARATHYROID-INDUCED BONE DISEASE IN CHRONIC DIALYSIS PATIENTS. R.W. Myers, E. Dresin, B.M. Morse, R.B. Doud, R.L. Rasmussen, and J.M. Price. Herrick Memorial Hospital, Berkeley, CA.

To evaluate the role of the Tc-99m total body bone scan (BS) in assessing hemodialysis associated skeletal disease, serum alkaline phosphatase and parathyroid hormone levels (PTH) were compared to the independently and quantitatively graded radiographic parathyroid bone series (PBS) and the BS at 48 comparable times in 41 patients. BS scores of 0 to 10 represented subjectively low to high bone/background ratios in multiple areas when compared to matched controls with normal renal function. Each PBS was graded 0 to 10 for none to extreme findings of parathyroid bone disease.

BS scores were correlated with PTH ($r = .64$, $p < .001$) as were PBS scores ($r = .61$, $p < .001$). When PTH > 2500IU (normal < 600IU) were considered indicative of significant bone disease, the BS score was increased at least one grade over normal in 21 of 24 studies (sensitivity = 88%). Conversely, 18 of 24 studies with PTH < 2500IU had low-grade BS scores (specificity = 75%). Findings for PBS when compared to PTH > or < 2500IU were: sensitivity = 54% (13 of 24 studies) and specificity = 58% (14 of 24 studies). Alkaline phosphatase levels were not significantly correlated with BS, PBS or PTH.

BS determination of bone-soft tissue ratio is a relatively sensitive indicator of significant hyperparathyroidism in chronic hemodialysis patients and offers improved accuracy for that isolated purpose when compared to standard radiographic modalities or other routine laboratory data.

DEMONSTRATION OF INTRA-ARTICULAR DEPOT CORTICOSTEROID EFFECT ON SYNOVIAL PERMEABILITY IN OSTEOARTHRITIS. M.J. Eymontt, G.V. Gordon, H.R. Schumacher, J.R. Hansell. University of Pennsylvania and VA Hospital, Philadelphia, PA.

Intra-articular injections of corticosteroids have been widely used to treat painful knee effusions in osteoarthritis but their mode of action in this "noninflammatory" condition has not been examined. Thirteen patients with osteoarthritis and painful effusions had one knee injected with normal saline, triamcinolone hexacetonide 20 mg or prednisolone tebuate 20 mg. Fifteen mCi of Tc-99m albumin were given intravenously prior to, 24 hours, one week, and two weeks after the injection of the depot corticosteroid or saline. One ml samples of whole blood and synovial fluid were obtained 30 minutes after the administration of radiolabeled albumin, counted and a blood to synovial fluid count rate ratio determined. A synovial fluid WBC and differential were also determined.

Seven of ten patients injected with corticosteroids improved clinically concomitant with an increase in the blood to synovial fluid count rate ratio at 24 hours to two weeks despite a rise in the synovial fluid WBC in some. Two patients had no clinical response and no change in this same ratio despite a synovial fluid WBC rise in one of them. All three patients injected with saline had no clinical improvement or change in the ratio, though one had a modest rise in the synovial fluid WBC.

These data suggest that in addition to causing increases in synovial fluid WBC, presumably from post-injection microcrystalline-induced synovitis, corticosteroids may have a separate effect altering the permeability of the synovium. Also, decreases in pain and knee swelling correlate better with vascular permeability, as assessed by the count ratio, than with synovial fluid WBC.

DYSPROSIUM-165 FERRIC HYDROXIDE MACROAGGREGATES - A THERAPEUTIC AGENT FOR RADIATION SYNOVECTOMY. M.A. Davis, D.J. Hnatowich, R.W. Atcher, S. Shortkroff, W.D. Bloomer, and C.B. Sledge. Harvard Medical School, Boston, MA. and University of Massachusetts Medical Center, Worcester, MA.

Radiation synovectomy in which Y-90 and Au-198 colloidal particles are injected into the synovial sac in patients with rheumatoid arthritis has not achieved widespread use because of unfavorable dosimetry due to leakage from the joint and translocation to the lymph nodes. Dysprosium-165 ($T_{½}$ = 2.32 hr, β^- 1.3 MeV maximum, soft tissue penetration = 5.7 mm) coprecipitated on ferric hydroxide macroaggregates (Dy-FHMA) has been used to ablate the synovium. Compared to previously used agents, the short half-life and larger particle size (0.5-5 μm) yield less leakage and subsequently decrease radiation exposure to nontarget tissue. Our previous studies of the agent in arthritic rabbits have shown leakage from the joint to be less than one percent, primarily to the liver, compared to values reported for Y-90 (6%) or Au-198 (4%). Recently, tracer doses of Dy-FHMA have been administered to two patients and leakage from the knee assessed by serial blood samples and bremsstrahlung imaging. The results of these studies, showing minimal leakage, encouraged a therapeutic trial in which 150 mCi of Dy-FHMA was administered to these patients, delivering a dose of 5,000 rads to the synovium. Leakage assessed in the same manner was 1-3% at 20 hours to the liver with a radiation dose estimated at 3-6 rads. Results show the agent may provide significant improvement over the previous agents. Assessment of therapeutic efficacy is continuing with Tc-99m pertechnetate synovial scintigraphy using both conventional cameras and single photon emission computed tomography.

2:00-3:30 Room 3037

CLINICAL

NEUROLOGY

Session Chairman: Abass Alavi
Session Co-Chairman: Harold L. Atkins

EMISSION COMPUTED TOMOGRAPHY OF F-18 FLUORODEOXYGLUCOSE AND N-13 AMMONIA IN PARTIAL EPILEPSY. D.E. Kuhl, J. Engel, Jr., and M.E. Phelps. UCLA School of Medicine, Los Angeles, CA.

Seventeen patients with partial epilepsy had EEG monitoring concurrent with cerebral emission computed tomography (ECT) after F-18 fluorodeoxyglucose and N-13 ammonia were given intravenously as indicators of local cerebral glucose utilization (LCMRglc) and relative perfusion, respectively. In 12 of 15 patients who had unilateral or focal electrical abnormalities, interictal F-18 fluorodeoxyglucose scan patterns clearly showed localized regions of decreased (20-50%) LCMRglc, which correlated anatomically with the eventual EEG localization. These hypometabolic zones appeared normal on x-ray computed tomography in all but three patients and were unchanged on scans repeated on different days. In 5 of 6 patients who underwent temporal lobectomy, the interictal F-18 fluorodeoxyglucose scan correctly detected the pathologically confirmed lesion as a hypometabolic zone, and removal of the lesion site resulted in marked clinical improvement. In contrast, the ictal F-18 fluorodeoxyglucose scan patterns clearly showed foci of increased (82-130%) LCMRglc which correlated temporally and anatomically with ictal EEG spike foci and were within the zones of interictal hypometabolism (3 studies in 2 patients). N-13 ammonia distributions paralleled F-18 fluorodeoxyglucose increases and decreases in abnormal zones, but N-13 ammonia differences were of lesser magnitude. We conclude that the interictal F-18 fluorodeoxyglucose-ECT scan is useful now in aiding localization of the dysfunctional cerebral zone most likely to be responsible for seizures in patients considered for temporal lobectomy. With further development, ECT may help in categorizing better the various forms of the disorder and in elucidating the basic mechanisms of epilepsy in man.

DETERMINATION OF CEREBRAL METABOLISM IN SENILE DEMENTIA USING F-18-DEOXYGLUCOSE AND POSITRON EMISSION TOMOGRAPHY. A.Alavi, S.Ferris, A.Wolf, M. Reivich, T.Farkas, R.Dann, D.Christman, R.R.MacGregor, J.Fowler. Hospital of the Univeristy of Pennsylvania, Philadelphia, PA and Brookhaven National Laboratory, Upton, NY

Using the technique described by Ketty and Schmidt, other investigators have shown diminished total cerebral metabolism in dementia. With the introduction of F-18-deoxyglucose and positron emission tomography it has become possible to map regional cerebral metabolism in the human brain. In this report we describe our preliminary data in 8 young and 4 elderly normal controls, and 6 patients who were diagnosed as having senile dementia by psychometric testing. The mean ages were: young control 23 years (18-28), elderly control 72 years (60-86) and dementia patients 72 years (64-78). Moderate to severe atrophy and ventricular dilatation were noted on the CT scan in all dementia patients. The elderly controls showed mild to moderate atrophy. The metabolic rates were significantly lower (50% or more) in elderly controls compared with the young subjects, consistent with atrophy on CT. The patients with dementia showed values 20-30% below that of elderly controls. The most striking difference was seen in the frontal lobes. Generally there was a good correlation between the metabolic rates and CT-psychometric ranking. Although the young normal subjects showed symmetry on their metabolic scans, both old controls and dementia patients showed significant asymmetry with the right hemisphere more active in the majority. These data indicate that this technique probably will be useful in the evaluation of patients with senile dementia. Another possible application of this technique will be in the evaluation of the effects of drugs and other therapeutic approaches.

TOMOGRAPHIC MAPPING OF THE METABOLIC CHANGES IN THE VISUAL CORTEX DURING VISUAL STIMULATION OF VOLUNTEERS AND PATIENTS WITH VISUAL DEFICITS. M.E. Phelps, D.E. Kuhl, and J.C. Mazziotta. UCLA School of Medicine, Los Angeles, CA.

Positron computed tomography (PCT), F-18 fluorodeoxyglucose and an extension of Sokoloff et als model provide an in vivo method that now allows the study of local metabolic function of the human brain. We have previously measured all of the rate constants and validated the precision (±4% s.d.) for the measurement of the local (~1.5cm^2) cerebral metabolic rate for glucose (LCMRGlc) in man. In 9 volunteers, LCMRGlc was measured in the primary (area 17) and associative (areas 18 & 19) visual cortex during eyes closed and open to an oscillating checker board pattern. This visual evoked metabolic response (VEMR) generally showed good correlation to EEG visual evoked potential (VEP). However, there were clearly instances when the two were not correlated, e.g., high VEP with low VEMR: equal VEP with one-and two eye stimulation, whereas the VEMR from the two eye stimulations equaled 1.5 times the one eye value. Patients (5) with homonymous hemianopsia and structurally intact visual cortex by x-ray CT, clearly showed metabolic deficits (20-40% below normal) in the contralateral visual cortex consistant with their field cuts, exhibited high LCMRGlc in the functioning visual cortex, and generally the impaired visual cortex showed no or low metabolic responses to visual stimulation. Variable LCMRGlc patterns of the visual cortex were found in patients with acquired and congenital blindness or with visual aura. The ratio of LCMRGlc of left to right visual cortex was 1.03±0.04 for one eye stimulation (normal two eye stimulation 1.02±0.04), confirming that man has a 50% left-right crossing of the visual system. This technique provides an exciting new tool for investigation of local cerebral function in man.

RESPONSE TO AUDITORY STIMULATION AS MAPPED BY POSITRON EMISSION TOMOGRAPHY (PET) AND F-18-DEOXYGLUCOSE (FDG). A. Alavi, W.Rintelmann, M.Reivich, J.Greenberg, D. Christman, J.Fowler, A.Stein, R.R. MacGregor, A.Wolf. Hospital of the University of Pennsylvania, Philadelphia, PA and Brookhaven National Laboratory, Upton, NY

We have performed auditory studies using FDG and PET. Sixteen normal right-handed subjects (7 controls and 9 stimulated) are included. In 4 of the controls the ears were exposed to ambient noise while in 3 the ears were covered by silent earphones, thus attenuating the ambient noise. The subjects stimulated were divided into two groups: a group of 6 subjects listened to connected discourse in English in one ear (3 to the right and 3 to the left) and the other ear was covered by a silent earphone. Three other subjects listened to unfamiliar (Hungarian) connected discourse through one ear while the other ear was covered (2 to the right and 1 to the left). Both groups were asked to attend to the stimuli and were checked for this either during or at the completion of the study. The control group displayed symmetric activity in both temporal lobes with a variation not exceeding 3-4%. In all subjects stimulated with the English story there was significant asymmetry in metabolic activity, with the right temporal lobe showing more uptake. In 3 subjects stimulated with the Hungarian story, there was more activity in the ipsilateral temporal lobe to the ear stimulated. Two subjects showed greater activity in the right and 1 in the left hemisphere. Our findings suggest that when subjects attend to connected discourse (either meaningful or non-meaningful), the right temporal lobe displays greater activity than the left, irrespective of ear stimulated.

SENSITIVITY ANALYSIS OF THE FLUORODEOXYGLUCOSE (FDG) METHOD FOR THE MEASUREMENT OF LOCAL CEREBRAL METABOLIC RATE OF GLUCOSE (MR). S. Huang, M. Phelps, E. Hoffman, and D. Kuhl. UCLA School of Medicine, Los Angeles, Ca. 90024

FDG method for measuring MR assumes the use of average normal values of 4 kinetic rate constants (k's) of FDG transport gives accurate MR. Sensitivity of method to errors in assumed values was investigated to assess accuracy of FDG method. When true MR is in normal range, error sensitivity to k's was evaluated analytically and found to be related to standard deviation (SD) of k's. SD of k's in 13

normal subjects was found to be about 30%. Corresponding SD of estimated MR was found to be about 11%, if measurement was 40 to 120 min after FDG injection. For MR's differ greatly from normal range, error sensitivity to k's was investigated by computer simulation of FDG transport model. Wide ranges of errors in k's that correspond to more than 3-fold changes in MR were studied. It was found that if measurement was 60 min after FDG injeciton, error in estimated MR was less than 0.2 (true MR - normal MR), with overestimation for high MR and underestimation for low MR. Computer simulation was also used to investigate cases in which MR changes during time interval between FDG injection and measurement. Estimated MR was found to be weighted average of MR in interval with larger weights for MR of early time. For example, if MR changes from 14 to 7mg/min/100gm at 20 min, estimated MR at 60 min would be 11mg/min/100gm. As time for first MR is lengthened, estimated MR becomes closer to MR of early time. This result is useful in interpreting MR measurements involving stimulation and intervention studies. It is concluded that FDG method must be applied with care to obtain accurate MR measurements.

TRANSVERSE SECTION MEASUREMENTS OF OXYGEN UTILIZATION IN THE BRAIN OF MAN. N.M. Alpert, R.H. Ackerman, J.A. Correia, S. Finklestein, F.S. Buonanno, G.L. Brownell and J.Taveras. Massachusetts General Hospital, Boston, MA.

We are currently evaluating a method for measuring regional cerebral oxygen utilization rate ($CMRO_2$) in man using transverse section imaging during continuous inhalation of ^{15}O-CO_2 and-O_2. The method follows the theoretical principles described by Subramanyam et al (J. Nucl. Med. 19:48-53, 1978). Transverse section data were obtained with the MGH positron camera, yielding the tissue concentrations of ^{15}O-H_2O during separate measurements with ^{15}O-O_2 and ^{15}O-CO_2. Arterial samples were drawn to determine the concentrations of ^{15}O in whole blood, plasma and hemoglobin. Cerebral blood flow (CBF) images were computed as $CBF=\lambda \cdot C_W/(C_A - p^{-1}C_W)$, where λ is the ^{15}O decay constant, p is the partition coefficient and C_A, C_W are the arterial and tissue ^{15}O-concentrations during inhalation of ^{15}O-CO_2. The local cerebral extraction fraction (E) of O_2 was computed as $E=C_A C_T (C_W C)^{-1} - C_p C^{-1}$, where C_T is the ^{15}O tissue concentration during inhalation of ^{15}O-O_2, and C_p, C are the ^{15}O plasma and hemoglobin concentrations, respectively. $CMRO_2$ was determined as $E \cdot CBF \cdot \bar{C}$, where $\bar{C}$ is the arterial O_2-content. Studies have been carried out in 4 normal subjects and 16 patients. In normal subjects $CMRO_2$ was usually highest in the calcarine cortex, 3-6ml/100g/min, and was lowest in the centrum semiovale, 1.5-2.5cm/100g/min. In patients with stroke $CMRO_2$ was dramatically reduced (less than 50% of normal) in areas of focal infarction. These results though preliminary demonstrate the feasibility of measuring $CMRO_2$ in well-defined regions of the brain in normal and abnormal subjects.

TRANSVERSE SECTION MEASUREMENTS OF CEREBRAL BLOOD FLOW IN MAN. N.M. Alpert, J.A. Correia, R.H. Ackerman, S. Finklestein, F.S. Buonanno, G.L. Brownell and J.M. Taveras. Massachusetts General Hospital, Boston, MA.

We are currently evaluating a method of measuring local cerebral blood flow (CBF) in transverse section using the continuous inhalation of $C^{15}O_2$(1). To quantitate the data it is necessary to know the concentration of ^{15}O-H_2O in arterial blood (C_A) and the cerebral tissues (C_T) as well as the local H_2O partition coefficient, p. Tissue concentrations were measured in transverse sections of 2.8cm thickness with a resolution of 1.5cm FWHM using the MGH Positron Camera. Arterial samples were drawn to determine C_A. A partition coefficient of 0.94 was used. A CBF image was computed using the relation (1) $CBF=\lambda C_T/(C_A - p^{-1}C_T)$, where λ is the ^{15}O decay constant. Statistical error in CBF increases with CBF and was typically ∿6% at CBF=30 and 25% at CBF=100.

A total of 22 subjects have been studied.

In 4 normal subjects CBF (in cc/100g/min) varied from 30-45 in the centrum semiovale, 60-100 in frontotemporal cortex and 80-120 in the occipital cortex. In 4 patients with stroke CBF was depressed to values of 10-20 in the area of the infarct. In 3 patients with glioblastoma CBF was ∿15 at the tumor site, and depressed throughout both hemispheres.

These data indicate that the method provides physiologically reasonable quantitative CBF results in well defined regions of normal and abnormal brain tissue.

(1) Subramanyam et al. J. Nucl. Med. 19, 48-53 (1978)

REGIONAL CEREBRAL BLOOD FLOW MEASUREMENTS IN PATIENTS WITH TRANSIENT ISCHEMIC ATTACKS AND STROKE: A CRITICAL COMPARISON OF XENON AND TECHNETIUM TECHNIQUES. A. Waxman, E. Siegel, M. Brachman, D. Tanasescu, D. Berman, L. Mamanna, K. Newcomer, D. Chapman, H.J.C. Swan, and H. Rose. Cedars-Sinai Medical Center, Los Angeles, CA.

The evaluation of regional cerebral blood flow (RCBF) using Xe-133, until recently, was considered an invasive technique. The purpose of this study was to evaluate a noninvasive inhalation modality in the assessment of regional cerebral flow.

Ninety-four patients were included in this study. There were 20 normal pts, 32 pts with transient ischemic attacks, and 42 pts with cerebral infarction. All pts underwent a xenon study using a Marshaw cerebral blood flow system. In addition, Anger camera technetium flow and/or scans were performed. When possible the results were correlated with computed tomography. Absolute values for fast compartment flow, mean flow, and initial slope index were determined for the xenon study. A measurement was considered abnormal if it was greater than 2 standard deviations below the mean value for the normal population. Results are summarized in the following table:

	TIA (Positive)		Infarction (Positive)	
Xe-133	31/32	(97%)	41/42	(98%)
Tc99m Flow	7/28	(25%)	20/39	(51%)
Tc99m Scan	0/6	0	12/19	(63%)
CT	0/7	0	8/16	(50%)

Importantly, normal RCBF studies were found in 19/20 normal patients. We conclude that the xenon inhalation technique for RCBF is a highly sensitive indicator of cerebral vascular disease with sensitivities far in excess of the technetium flow, technetium scan, or computed tomography studies.

UPTAKE OF N-13 BY BRAIN TUMORS FOLLOWING ADMINISTRATION OF N-13 L-GLUTAMATE. R.E. Reiman, R.S. Benua, A.S. Gelbard, J. Allen, J.J. Vomero and J.S. Laughlin. Memorial Sloan-Kettering Cancer Center, New York, NY.

N-13 sodium L-glutamate was used an an imaging agent in 7 pediatric patients with malignant brain tumors and in 3 normal subjects. Imaging was performed using a quantitative digital rectilinear scanner beginning 5 min after i.v. injection. Uptake of N-13 by the brains of the normal subjects was minimal. Greatly increased concentration of N-13 was observed in primitive neuroectodermal tumor (PNET) and medulloblastoma. The uptake of N-13 by embryonal pineal carcinoma and pineoblastoma was lower but still permitted tumor detection. Dysgerminoma and anaplastic glioma concentrated N-13 minimally. In general, the tumor visualization with glutamate was comparable to that with Tc-99m pertechnetate, except that the contrast (tumor-to-normal brain) was much higher for one case of PNET (7.1 versus 2.3 for pertechnetate) and slightly higher for medulloblastoma (2.4 versus 1.8). We conclude that N-13 glutamate, like Tc-99m pertechnetate, does not cross the normal blood-brain barrier and that N-13 activity readily localizes in certain tumors. The higher contrast seen in medulloblastoma and PNET may be due in part to the more rapid blood clearance of N-13; however, the large discrepancy in N-13 and Tc-99m uptake in the latter tumor raises the possibility that altered or enhanced tumor metabolism as well as a blood-brain barrier defect may affect the tumor uptake of N-13.

SINGLE-PASS BRAIN UPTAKE AND WASHOUT OF I-123 N-ISOPROPYL-p-IODOAMPHETAMINE AND ITS BINDING TO BRAIN CORTICAL SYNAPTOSOMES. H. S. Winchell, W. D. Horst, L. Braun, W. H. Oldendorf. Medi-Physics, Inc. Emeryville, CA; Brentwood VA Hospital, Los Angeles, CA.

Previous work demonstrated rapid brain uptake and prolonged brain retention of I-123 N-isopropyl-p-iodoamphetamine in rats, dogs and monkey. Present work is

addressed to evaluation of its kinetics employing serial BUI measurements following intracarotid injection of the agent in rats (method of Oldendorf, et al.) and amine uptake and release in rat brain cortical synaptosomes (method of coyle and Snyder and method of Horst, et al.). BUI measurements were: 5 sec, 124±13; 1 min, 182±12; 2 min, 257±27; 3 min, 423±48; and 4 min, 580±88. These results correspond to a single-pass extraction efficiency of 100%/pass and a washout-$t_{\frac{1}{2}}$ of ≈183 sec. This compares to washout-$t_{\frac{1}{2}}$ for water of 68 sec, antipyrine 93 sec, and nicotine 171 sec. The agent inhibited norepinephrine uptake in synaptosomes equally as well as d-amphetamine, but was far more potent than d-amphetamine in inhibiting synaptosomal uptake of serotonin. The agent was comparable to d-amphetamine in causing release of norepinephrine and serotonin from synaptosomes, but was somewhat more effective than d-amphetamine in causing release of dopamine. The results suggest that initial distribution of the agent in the brain can be used to measure regional brain perfusion and that it interacts with brain amine binding sites similar to, but not identical with, that seen with d-amphetamine, indicating a possible application in study of brain amine metabolism.

INDIUM-111 PLATELET SCANNING IN CAROTID ARTERY ATHEROSCLEROSIS. R.L. Lantieri, D. Guthaner, J. Baumert, F. Conley, M.L. Goris, and D. A. Goodwin. Veterans Administration Medical Center and Stanford University Medical Center, Stanford, CA.

Indium-111 labeled autologous platelets were used to scan the neck in 24 patients, 21 suspected of having significant carotid vessel disease. There were 23 males and 1 female with average age 64 years (range 51-80). Most were under evaluation for transient ischemic attacks; one had a recurrent stroke, and 8, neck bruits, 2 asymptomatically.

85 ml venous blood was obtained in 15 ml acid citrate dextrose solution and platelets seperated using differential centrifugation. 2.5 mCi In-111 oxine was used for labeling. 0.5 mCi dosage was injected with labeled platelets resuspended in platelet poor plasma. Imaging was performed at 1, 2, and 20 hrs over anterior neck using medium energy collimation and obtaining 50-100K counts in 10 min. Computer acquisition in 10 studies were processed using interpolative background subtraction and in 6, time-activity curve analysis.

17 patients had carotid arteriography and 10 thromboendarterectomy on 12 carotid vessels. 7 plaques were grossly ulcerated. Platelet scanning was found a useful adjunct to carotid arteriography in detecting functionally significant carotid lesions. All lesions actively aggregating platelets (ulceration) were detected except 1 in a patient with bilateral ulcerations. Background subtracted computer processing was essential for increased sensitivity while time-activity curve analysis was useful in evaluating false positives secondary to vessel volume asymmetry. Ulcerated lesions revealed increased uptake with time; scan and arteriography identified 7/7 ulcerations.

2:00-3:30 **Room 3039**

RADIOPHARMACEUTICAL CHEMISTRY

GALLIUM

Session Chairman: David A. Goodwin
Session Co-Chairman: Gopal Subramanian

ROLE OF SYNERGISTIC LIGAND BINDING IN THE GALLIUM-TRANSFERRIN COMPLEX. J.F. Harwig, M. Raiszadeh, and W. Wolf. Radiopharmacy Program, University of Southern California, Los Angeles, CA.

Transferrin (Tr) has been identified as the blood constituent responsible for the binding of tracer level gallium-67 and for its transport to and introduction at the site of tumor. Despite this key role of Tr in the ultimate deposition of Ga within the tumor tissue, little is known about the nature of the Ga-Tr complex. We have investigated the involvement of ternary ligands in the binding of Ga at the metal binding sites of Tr.

Ga-67 citrate was incubated with human Tr, 2.5 mg/ml, at 37° C and pH 7.4 in CO_2-free saline or a 0.005 M solution of the sodium salts of citrate, oxalate, bicarbonate or MOPS buffer. At various times aliquots were taken for Sephadex G-50 gel filtration using the respective salt solution as eluent. Binding was essentially instantaneous, reaching its maximum level within 1 min. With saline, citrate and MOPS binding efficiency was only 5 - 15%, while with bicarbonate and oxalate greater than 90% binding was achieved. The incubations were repeated with C-14 labeled anions and the chromatographic eluates were monitored for UV absorbance and for Ga-67 and C-14 radioactivity. In the case of bicarbonate and oxalate the Ga-67 and C-14 activity eluted with the protein fraction, while with citrate the protein fraction contained very little Ga-67 and no C-14. There was no binding of C-14 bicarbonate or oxalate to Tr in the absence of Ga.

This study demonstrates the fundamental role and importance of synergistic anion binding in the chemistry of the Ga-Tr complex and thus in understanding the manner in which this complex is involved in tumor localization of Ga.

DEMONSTRATION OF GALLIUM-67 BOUND TO MOUSE TRANSFERRIN IN LYSATES OF EMT-6 SARCOMA CELLS HARVESTED FROM BALB/c MICE AFTER PRIOR INTRAVENOUS INJECTION OF ^{67}GA-CITRATE. S.M. Larson, Z. Grunbaum, and J.S. Rasey. Seattle Veterans Administration Medical Center and University of Washington School of Medicine, Seattle, Wa.

Previous studies have shown that EMT-6 sarcoma (BALB/c mice) contains cell associated transferrin receptors when grown in vitro as a tissue monolayer, or in vivo as a solid subcutaneous tumor. This receptor serves in vitro as a common transport pathway for both ^{67}Ga and ^{59}Fe uptake. We now report that ^{67}Ga labelled to mouse transferrin (mTf) was present in hypotonic extracts of EMT-6 cells harvested from solid subcutaneous tumors of BALB/c mice after intravenous injection of ^{67}Ga-citrate. Five week old, female BALB/c mice (Simonsen) received SQ injection of $2x10^5$ EMT-6 cells, and 12-15 days later solid tumors of 100mg average size developed. 80μCi ^{67}Ga-citrate (Mediphysics) were injected intravenously, and 1 hour later 100 μl blood per mouse was drawn by retro-orbital puncture. After sacrifice, 10 tumors were dissected free of fat and subcutaneous tissue, washed 3 times in 0.2M iced sucrose solution, minced, passed through a fine wire screen, and homogenized in a hypotonic solution of 1mM PMSF in distilled water, 10 parts water to 1 part cells. After centrifugation to remove stromal elements, tumor cell lysate was compared to ^{67}Ga-labelled mouse serum with respect to immunodiffusion patterns on Ouchterlony Agar plates, using antibodies against mTf, whole serum and IgG. The only serum protein that was present in appreciable concentration in tumor cell lysate was mTf, and the presence of ^{67}Ga-mTf was not due to contamination by mouse serum. We believe these data support the hypothesis that ^{67}Ga is concentrated by EMT-6 sarcoma in the form of ^{67}Ga-mTf, after intravenous administration of ^{67}Ga-citrate.

MECHANISM OF GALLIUM-67 UPTAKE BY TUMORS: SIMILARITIES OF GALLIUM AND IRON METABOLISM. J.S. Rasey, S.M. Larson and N.J. Nelson, Department of Radiation Oncology, University of Washington and VA Hospital, Seattle, WA.

Tumor cell iron and gallium uptake have been compared. The transferrin (Tf) receptor hypothesis for gallium-67 uptake by the in vivo-in vitro EMT-6 mouse sarcoma proposes that gallium-67 binds to Tf and this complex binds to a cell surface Tf receptor. After incorporation of the receptor-metal-Tf complex, Ga-67 binds to intracellular acceptor molecule(s). Because Tf is an iron transport protein, it was suggested that Fe-59 would be concentrated by tumor cells in vitro in the presence of Tf and also that stable (ferric) iron could compete with gallium at some or all steps outlined in the Tf receptor hypothesis.

EMT-6 cells in vitro were incubated with Fe-59 citrate, Ga-67 citrate, and varying amounts of Tf. In some experiments stable ferric citrate was added with the radioactive tracers. In other experiments cells were either preloaded with stable ferric citrate prior to addition of

tracers or post-incubated with the stable iron compound after labelling. Tumor cells concentrate Fe-59 as well as Ga-67 in the presence of Tf. Sephacryl S-200 column chromatography of tumor cell lysates after labelling shows that both metals bind to similar molecular weight proteins within the cell. Co-incubation of cells with Fe-59, Ga-67, and stable ferric citrate reduces uptake of both labels. Preincubation of cells with ferric citrate slightly reduces gallium uptake while post-incubation with stable iron does not accelerate Ga-67 removal from the cell. We conclude that tumor cell gallium and iron metabolism are similar. Principal competition occurs at the initial step, binding of metal to Tf. Ferric iron may partially saturate gallium acceptor molecules inside the cell.

TIME-RELATED GA-67-CITRATE CONCENTRATION IN TUMOR AND ABSCESS AND THE EFFECT OF DESFERRIOXAMINE (DFO). Z.H. Oster, P. Som, D.F. Sacker and H.L. Atkins. Brookhaven National Laboratory, Upton, NY and SUNY at Stonybrook, NY

The optimal administration time of DFO after Ga-67 injection for improving the target/non-target ratio were studied in mice with EMT-6 sarcoma and spontaneous Adeno Ca, rabbits with Adeno Ca and rats with turpentine abscesses. Ga-67 given IV was followed by 50mg/Kg DFO IV in experimental animals and same volume of saline in the controls. Tissue distribution studies were done at fixed intervals. When DFO is given 2 to 24 hrs after Ga-67, blood levels decrease by 52-92%. DFO given 4-5 hrs after Ga-67 decrease mice tumor activity 43-55%, rabbit tumor activity 16%, and only 7% in the abscesses. At 24 hrs after Ga-67, the washout from both tumor and abscesses was less (5-15%), and tumor/blood ratios in DFO treated animals increased (EMT-6 Sa from 1.8 to 10.73; mouse Adeno Ca from 1.95 to 3.49; abscesses from 3.11 to 12.50). Ga-67 concentration in rat abscesses was highest 2 hrs post injection (0.8%/g), decreased 5 hrs (0.45%/g) and was unchanged for 24 hrs. Mice tumors had a much higher Ga-67 concentration than abscesses (4.65-7.60%/g vs 0.8%/g), and their concentration decreased with time (35% at 24 hrs). Similar decreases were seen in all organs examined except the liver. In the liver the activity remained constant and DFO had no effect.

In conclusion, 1) this data supports the hypothesis of different mechanisms of Ga-67 uptake in tumor and abscess, 2) Ga-67 binding in the liver differs from that in other organs and could be related to ferritin, and 3) it seems that the optimal administration time of DFO is 24 hrs after Ga-67 injection.

THE INFLUENCE OF pH AND OTHER FACTORS ON Ga-67 BINDING TO HUMAN TRANSFERRIN (TF), HUMAN POLYMORPHONUCLEAR LEUKOCYTES (PMNs) AND BACTERIA (B). R. Weiner, P. Hoffer, M. Thakur, P. Soloway and R. Root. Yale University, New Haven, CT.

TF, PMNs and B are components presumably important in the accumulation of Ga-67 in abscesses. We have examined the affect of a variety of conditions on the uptake of Ga-67 by these components.

The influence of pH on Ga-67-TF association was studied using equilibrium dialysis. At lower pH closer to acidic character of abscess fluid, the quantity of Ga-67 bound to TF decreased markedly to only 5% at pH 6. Isolated PMNs were suspended in Hank's balance salt solution (HBSS) adjusted to pH's between 6.2-7.4. The cells incubated with Ga-67 citrate, washed free of non-bound Ga-67 and the bound activity measured. At pH 6.16 the PMN bound Ga-67 was reduced to 50% of control (pH 7.35). An incubation temperature increase from 37°C to 39°C to parallel the febrile state increase, did not significantly increase cell bound Ga-67. Salmonella typhimurium (St) and Shigella boydeii (Sb) were grown overnight in media and media with reduced iron content to assess the affect of hypoferremia, which usually accompanies bacterial infections. The bacteria were suspended in HBSS, incubated with Ga-67 citrate, washed free of unbound Ga-67 and the bound activity measured. There was no significant difference in Ga-67 uptake between organisms grown in normal vs "iron starved" conditions. However, St, the siderophore producing bacteria, bound significantly more Ga-67 than did the non-siderophore producing, Sb under both conditions.

Thus, the data suggest TF in the acidic millieu of an abscess could deliver more "free" Ga-67 while the PMN could bind less. In addition, B are probably a more significant factor in Ga-67 localization.

SIDEROPHORE MEDIATED MECHANISM OF GALLIUM UPTAKE DEMONSTRATED IN MICRO-ORGANISMS. T. Emery, Utah University, Department of Chemistry, Logan, UT, and P.B. Hoffer, Yale University, Section of Nuclear Medicine, New Haven, CT.

Direct uptake of Ga-67 citrate has been observed in micro-organisms (1) but the exact mechanism of uptake is not known. Since gallium binds avidly to siderophores (S) and these iron chelating agents facilitate transport of iron into micro-organisms, we have explored the possibility that Ga-67 uptake in micro-organisms is also facilitated by S.

Desferriferrichrome, an S, was labeled with either Ga-67 or Fe-59 and incubated with the fungus Ustilago Spaerogena. The rate of uptake with either label was identical and almost quantitative by 90 minutes. Uptake of the S with either radionuclide was inhibited by 1 mM sodium azide.

Gallium-67 citrate was also added directly to actively growing cultures of U. Spaerogena and the extent of uptake and identity of binding molecules determined. Preparation and identification procedures included centrifugation, washing, subsequent cell disruption by heat, extraction with benzyl alcohol and electrophoresis and paper chromatography.

These experiments revealed 96% uptake of Ga-67 in 1 hour and demonstration that virtually all of the Ga-67 is bound to S.

Additional experiments revealed that once S is labeled with Ga-67 it cannot be reutilized or released from the cell but that Ga-67 can be transferred from one intracellular S to another. Also, excess gallium can displace iron from S.

These studies support the concept that Ga-67 acts in biologic systems as an analog of the ferric ion. They also demonstrate an S mediated pathway of uptake for gallium in micro-organisms.

1. Menon, S., Wagner, H.N., Jr., Tsan, M-F, JNM.19:44, 1978

THE SOURCE OF GALLIUM-67 IN GASTROINTESTINAL CONTENTS. D.C. Chen, U. Scheffel, E.E. Camargo, M.F. Tsan. The Johns Hopkins Medical Institutions, Baltimore, MD.

The source of Ga-67 in gastrointestinal(GI) contents was studied in rats. To prevent loss of fecal Ga-67, the anus was sutured before IV injection of Ga-67 citrate (5μCi/100 g B.W.). Secretion of Ga-67 into the content of the GI tract was rapid; 2.9%, 6% and 9.1% of the injected dose was secreted at 1, 6 and 24 hr post-injection(PI) respectively. In contrast, the Ga-67 in the GI tissues remained relatively constant throughout this period. Feeding had no effect on Ga-67 secretion into the GI tract. Analysis of Ga-67 contents in various parts of the GI tract revealed that up to 6 hr PI more than 54% was in the small intestine; whereas, at 24 hr, 60% was in the colon. This suggests that part of Ga-67 in the colon comes from the upper GI tract. To localize the source of fecal Ga-67, ligations were also made at the gastroduodenal(GD) junction and terminal ileum before IV injection of Ga-67. At 6 hr PI, 80% of Ga-67 in the GI contents was in the small intestine. Ligation of the common bile duct reduced Ga-67 contents in the GI tract by 20%. To further quantitate the amount of Ga-67 secreted via the bile, duodenal loops were created by ligation at the GD junction and 10 cm from it to collect the bile. Collection of bile was verified using Tc-99m HIDA. From Ga-67 in the duodenal loops of rats with and without their common bile duct tied, we found that 1.3% of the injected dose was secreted via the bile in 6 hr. The results suggest that the majority of fecal Ga-67 comes from small intestine(60%), with bile(20%), colon(10%), esophagus and stomach(10%) contributing a smaller fraction.

ROLE OF $FeCl_3$ In Ga-67 UPTAKE BY HeLa S3 IN VITRO. A. Muranaka, Y. Ito, T. Kaji, N. Otsuka, K. Nagai, and I. Narabayashi. Kawasaki Medical School, Kurashiki, Japan.

Keeping the role of transferrin in mind, this study was undertaken to elucidate the effect of $FeCl_3$(Fe) on Ga uptake by HeLa S3. Concentration of Ga-67 added to medium was 1 μCi/ml and uptake was measured 24 hrs later. In addition, the effect of Fe on Ga-binding to serum as well

as the correlation between Ga and Fe was studied using equilibrium dialysis with cellulose membrane. When 0.01~0.1 mM of Fe was added to Eagle's MEM medium(MEM) only, and MEM containing 1~10 % normal human serum or 1 % fetal calf serum(FCS), Ga uptake was markedly increased. However, Fe did not affect Ga uptake in 10 % FCS-MEM. The effect of Fe was changed by differences of serum-species and the concentration of sera in the medium. There was noted a marked binding of Ga to serum by the dialysis. Activity of Ga retained inside the cellulose bag was below 1 % in the serum-free MEM. But, when 0.01 or 0.1 mM Fe was added, the activity retained inside the bag was 6.5 and 35.2 % respectively. This is supposedly due to formation of polymer complex of Ga and Fe in MEM. Even in the presence of serum, the activity retained in the bag was independent of the concentration of serum and was nearly the same as that without serum. Comparing Ga uptake in MEM only under several situations such as a) Ga only, b) simultaneous administration of Ga and 0.1 mM Fe, and c) administration of Ga-Fe complex(retained in the bag), the values were 1.1, 15.5, 33.5 % dose/10^6 cells respectively. It is obvious that the effect of administration of Ga-Fe complex on uptake was marked. The contribution of Ga-Fe complex in Ga uptake was confirmed, being irrespective of mediation of transferrin.

EFFECT OF MEMBRANE ACTIVE DRUGS ON IN-111 LABELED HUMAN POLYMORPHONUCLEAR LEUKOCYTES (IN-PMN). M.L. Thakur, L. Walsh, B.L. Zaret, and A. Gottschalk. Yale University, New Haven, CT

The combination of 1 μM procainamide (P) and radiation (>600 rads) treatment has been shown to increase lethality in mammalian cells. Our interest in using In-PMN in imaging inflammation in acute myocardial infarction in man, lead us to investigate the possible modulation in In-PMN function treated with lidocaine (L) and (P). PMN were isolated by a modified method of Boyum from 30 ml of blood from healthy humans. 7-8 million In-PMN (5.8 ± 0.2 K rad/PMN) were incubated with approximate clinical blood levels of L (0.022 μM) and P (0.03 μM) for 0.5, 1 and 3 hrs, and 3 hrs respectively. A much higher concentration of L (0.11 μM) was used in two other groups. In one In-PMN were incubated for 2 hrs, labeled and further incubated for 1 hr (T PMN). In-PMN untreated with L or P served as reference (R) and PMN unexposed to either In-111 or L and P as control (C). Chemotaxis of T, R and C stimulated with Na-caseinate was measured by penetration of the leading front into a 1.2 μ filter in a Boyden chamber. Adherence of T and R was measured on a nylon wool column. Chemotaxis and adherence of In-PMN exposed to 0.022 μM L and 0.03 μM P for up to 3 hrs remained unaltered. The 3 hr exposure to 0.11 μM L reduced chemotaxis to 79.7 ± 4.8%, ($P<0.005$) and 82.1 ± 6.2% ($P<0.005$) of R and C respectively and adherence to 82.2 ± 25% ($P<0.25$) of R. The pre and post incubation with 0.11 μM L also reduced chemotaxis to 86 ± 4.8%, ($P<0.005$) of C.

Data thus far indicate L and P at approximate clinical concentrations do not alter In-PMN function but may be toxic at higher doses.

2:00-3:30 **Room 3035**

RADIOASSAY

HEMATOLOGY & ONCOLOGY

Session Chairman: Stanley Goldsmith
Session Co-Chairman: Avir Kagan

RADIOIMMUNOASSAY OF ß THROMBOGLOBULIN (ßTG) AND PLATELET FACTOR 4 (PF4) IN PATIENTS WITH THROMBOSIS. R.Dudczak, K.Lechner, M.Pichler, K.Kletter, H.Frischauf. First Department of Internal Medicine, Univ.Vienna, Austria

To determine the usefullness of ßTG and PF4 as markers for the in vitro diagnosis of thrombosis we evaluated ßTG and PF4 by radioimmunoassay kits (Amersham, Abbot Lab., respectively) in 50 normals and in patients with deep vein thrombosis (DVT, n=43), pulmonary embolism (PE, n=11), amaurosis fugax (AF, n=32), chronic peripheral arterial disease (CHAD, n=11), coronary artery disease (CAD, n=11), diabetes mellitus (DM, n=11), and artificial heart valves (AHV, n=31).

In normals the plasma levels of ßTG and PF4 were $\bar{x}$ ± SD: 43.7 ± 15.6 ng/ml and 6.8 ± 3.5 ng/ml respectively, and rose with increasing age. Significantly elevated plasma levels of ßTG and PF4 were found in all patients with recent onset of DVT and PE ($\bar{x}$+SD: ßTG ng/ml: 113.9+42.7; 100±10.4 respectively; PF4 ng/ml: 21.7±5.9; resp. 19.4±1.2). Raised plasma levels of ßTG and PF4 were also found in patients with a history of DVT, but also in patients with CHAD, CAD, AF, AHV, DM. There was a positive correlation between ßTG and PF4 in normals as well as in patients ($r=0.8449$).

In conclusion, ßTG as well as PF4 can be used as sensitive markers of increased in vivo platelet activation. The clinical value of theses tests in the diagnosis of thrombosis appears limited since unspecific elevated plasma levels of ßTG and PF4 are also found in patients without recent thrombosis. However its high sensitivity for in vivo platelet activation could make it of potential value as predictive marker of a high risk group for thrombosis.

PLATELET FACTOR 4(PF4) RADIOASSAY AND CLINICAL SIGNIFICANCE, Fuad S. Ashkar, Albert V. Heal, Andrea Soricelli, Mukbil Hourani and Aldo Serafini, Nuclear Medicine, University of Miami, Jackson Memorial Hospital, Miami, Fla.

PF4 is a small molicular weight protein that is secreted from the α-granules of platelets when the cells undergo the release reaction, after contact with subendothelial tissue.

PF4 is quantitated by a classical competitive Radioassay utilizing I^{125} labeled and unlabeled PF4, specific PF4 antiserum and ammonium sulfate separation system.

Special multiple sampling venipunctures are performed, where two sequential samples are drawn in standard EDTA vacutainers and incubated in a crushed ice water bath for 30 minutes. Centrifugation at 2500 x g at 2-4°C for 20 minutes follows. Then the top 0.5 ml of plasma is aspirated and assayed from the second sample only.

Normal subjects and patients with cardiovascular disease and diabetes mellitus were studied. The data showed that there was no statistical difference in PF4 values between age groups, or males and females. Normal Values are <10ng/ml.

Significant increases in PF4 values were found in patients with active cardiovascular diseases, suggesting platelet abnormal aggregation or subenothelial tissue contact and activation.

CLINICAL SIGNIFICANCE OF SERUM VITAMIN B_{12} (B_{12}) MEASURED BY RADIOASSAYS USING PURE INTRINSIC FACTOR (IF). I.W. Chen, E.B. Silberstein, M. Sperling, E. Barnes, and H.R. Maxon. Eugene L. Saenger Radioisotope Laboratory, Univ. of Cincinnati, Cincinnati, OH.

It has been reported that analogs of B_{12} can interfere in B_{12} radioassays which use crude IF containing R-protein and that patients with true B_{12} deficiency could be misdiagnosed. Serum samples from 53 patients [15 were subsequently confirmed to have pernicious anemia (PA)] and 42 healthy volunteers were assayed using crude IF (measured B_{12} + B_{12} analogs), pure IF (measured B_{12} only), and a mixture of crude IF + R-protein blocking agent (block IF) (probably measured B_{12} only). Values obtained by pure IF and block IF agreed well ($r=0.9587$, slope 1.24, Y-intercept -100, n=84) suggesting that blocking of binding B_{12} analogs to R-protein was complete in the latter radioassay. Results obtained with pure IF were compared with those obtained with crude IF. The mean B_{12} levels in 42 healthy subjects (499 ± 23 pg/ml, mean ± 1 SEM was significantly higher using crude IF than those obtained with pure IF (408 ± 29 pg/ml, $p<0.05$). Normal ranges were: deficient <100 borderline 100-180, normal 180-900 pg/ml for pure IF assay and <180, 180-250, 250-1000 pg/ml respectively for crude IF

assay. B_{12} levels by pure IF assay were abnormally low in all 15 patients with PA (<100 pg/ml) while those by crude IF assay were normal in 7 of 15 (>250 pg/ml, mean=308 pg/ml). Of 38 patients who were subsequently shown not to have PA, 12 were in the borderline region by pure IF assay but 11 of these 12 were normal by crude IF assay.

Our data confirm previous reports that B_{12} deficiency can be diagnosed more accurately by measuring serum B_{12} levels with use of either pure IF or crude intrinsic factor + R-protein blocking agent.

RELIABILITY OF DUAL ISOTOPE SCHILLING TEST FOR THE DIAGNOSIS OF PERNICIOUS ANEMIA OR MALABSORPTION SYNDROME. **Y.C. Choy, E.E. Kim, P.A. Domstad, F.H. DeLand. University of Kentucky and V A Medical Centers, Lexington, KY.**

To evaluate the dual isotope Schilling test for the diagnosis of pernicious anemia (PA) or malabsorption syndrome (MAS), 65 studies were selected for correlation with the clinical diagnosis. Criteria for PA included MCV>100, serum B_{12}<100ng/L, megaloblastic marrow, achlorhydria, reticulocytes>5% on B_{12} therapy, atrophic gastritis, and elevated serum antibodies to parietal cells or intrinsic factor (IF). Criteria for MAS included decreased serum B_{12}, folate and carotene; increased fecal fat, abnormal D-xylose absorption, abnormal radiographic and biopsy findings. Co-58 cyanocobalamin and Co-57 cyanocobalamin bound to IF were given orally to fasting patients: 1 mg of nonradioactive B_{12} was injected i.m. within 2 hr. Aliquots of 24 hr urine samples were counted; if the excretion of Co-58 was less than 7% with Co-57/Co-58 ratio greater than 1.7 the test indicated PA; a ratio less than 1.7 indicated MAS. Disorders in the MAS group were nontropical sprue (1), pancreatic insufficiency (2), regional enteritis (1), gluten sensitive enteropathy (2), hypothroidism (2), and idiopathic steatorrhea (4). The dual isotope Schilling test correctly diagnosed PA in 10 of 12 patients, and MAS in 8 of 12. In 2 cases with false negative Schilling tests for PA: excretion was borderline but enhanced by IF 1.2x-1.4x. One patient with steatorrhea had a positive test for PA but other diagnostic criteria suggested MAS. Sensitivity, specificity, and accuracy of the dual isotope Schilling test were 83, 98, 94% for PA, and 67, 90, 86% for MAS respectively. This study confirms the reliability of the dual isotope Schilling test for the diagnosis of PA and MAS.

Myoglobinemia in Sickle Cell Crises. *P.A. Bardfeld, E.F. Roth,Jr., S.J. Goldsmith, E. Radel, J.C. Williams, Mount Sinai School of Medicine and the Montefiore-NCB Affiliation, New York City.*

Muscle pains and tenderness are common events in painful crises associated with Sickle Cell Anemia. This study was undertaken to assess the degree of muscle damage occurring during vaso-occlusive crises and to determine if a sensitive indicator of myoglobinemia might serve as a useful, objective measure of sickle crises. Blood was obtained from non-uremic homozygous patients for Hb S in both steady state and during painful crises for which they sought medical attention. Myoglobin in plasma was assayed using a Nuclear Medical Systems, Inc. RIA kit. The following myoglobin levels were obtained (in nanograms per ml):

	n	*Mean*	*±S.D.*	*Range*	*P*
No crisis	*17*	*7.4*	*10.1*	*0-24*	
					<0.001
Crisis	*30*	*53.8*	*67.6*	*0-260*	

In this study which included both adults and children, 14 of 30 patients had plasma myoglobin levels of 30 ng/ml or greater during crises. The remainder had levels within two S.D. of the steady state mean which was not different from that found in normal subjects. The myoglobinemia was not correlated with either plasma alpha-hydroxybutyrate dehydrogenase or CPK levels which were measured enzymatically in the same samples. Although estimation of myoglobinemia is not an infallible test of crises, it may aid in diagnosis and the results suggest the need to evaluate muscle tissue during the course of this disease.

SERUM FERRITIN LEVELS IN MAN WITH SPECIAL REGARD TO AGE-DEPENDING CHANGES. J. Spitz, G. Spitz-Scherholz, H.J. Pusch Kliniken der Landeshauptstadt Wiesbaden, 62 Wiesbaden, BRD

In 498 persons, divided into four groups, serum ferritin, serum iron, hemoglobin, red blood cells, hematocrit, total iron binding capacity, percent saturation, medium cell volume, medium cell hemoglobin and medium cell hemoglobin concentration was estimated.
The geometric mean serum ferritin values were significantly different for each group: I group (healthy young women, 16-30 years) 36 ng/ml; II group (healthy young men, 20-30 years) 83 ng/ml; III group (female patients, 60-80 years) 123 ng/ml; IV group (male patients, 60-80 years) 170 ng/ml.

There was no correlation of any clinical significance found between serum ferritin and the other parameters of peripheral blood. 35% of the healthy young women showed serum ferritin values under 30 ng/ml, thus indicating empty iron stores without any sign of iron deficiency anemia in periphal blood.
In contrast to this, the two groups of patients over 60 years showed even higher serum ferritin values than healthy young men, whereas the plasma iron content was essentially lower (111 µg/dl for young men against 67 µg/dl for old patients). Consequently we found a positive correlation of serum ferritin with age ($r = 0.52$) and a negative one of serum iron with age ($r = -0.62$).
The reason for these diverging tendencies is to be seen in the growing incidence of chronical disorders of the organism in later years of life, blocking the use of storage iron and causing cell damage to the liver.

Therefore, high normal or elevated serum ferritin values in elder people cannot exclude iron deficiency.

THE VALUE OF RADIOIMMUNOASSAY FOR PROSTATIC ACID PHOSPHATASE IN DISEASE OF THE PROSTATE. J.J. Steinbach, W.E. Farnsworth, M.J. Gonder, and R. Cartagena. Veterans Administration Medical Center, Buffalo, NY.

The diagnostic value of three new radioimmunoassay (RIA) kits for prostatic acid phosphatase (Smith, Kline & French, New England Nuclear and Mallinckrodt) was examined. One hundred twenty two patient samples were analyzed: 21 - without prostatic disease; 45 - with benign prostatic hypertrophy; 56 with carcinoma of prostate (14 - Stage I-II; 21 - Stage III; 21 - Stage IV). The diagnosis of prostate disease was confirmed by histological examination. Statistical analysis was based upon: a) determination of mean ± SD, followed by calculation of specificity, sensitivity and predictability of each kit for the entire sample; b) arbitrarily selecting a desired specificity level followed by determination of the sensitivity of each method. The normal value obtained for each kit:

	NEN	SKF	MAL
Nonprostatic disease	4.4 ± 1.2	0.71 ± 5.5	1.8 ± .33

The overall sensitivity of the tested kits ranged from 30-40% for the entire sample. When, however, only Stage IV carcinoma of prostate was considered, the sensitivity improved to a range of 43-62%. When specificity was arbitrarily set at 100% the obtained overall sensitivity was only in the range of 34-41%. However, when Stage IV cancer of prostate only was used, this range improved to 45-62%.

The examined RIA kits appear to perform best when patients with Stage IV cancer of the prostate are examined. In the general sample examined, they appear to have low sensitivity and specificity.

A COMPARISON OF ENZYME AND RADIOIMMUNOASSAY FOR PROSTATIC ACID PHOSPHATASE IN THE DIAGNOSIS OF PROSTATIC CANCER. L. Reese, P. Uksik, F. Taylor, St. Joseph's Hospital and University of Western Ontario, London, Ontario, Canada.

Serum from 222 controls, 64 patients with benign prostatic hypertrophy (BPH), 49 with cancer of the bladder (CB), 38 with cancer of the prostate (CP) and 10 females had determination of Prostatic Acid Phosphatase (PAP) levels by the Babson enzyme assay and by radioimmunoassay (RIA) using kits from New England Nuclear (NEN) in all samples and Serono in the 38 CP, 27 BPH, 11 CB and 30 controls. The serum was aliquoted prior to acidification.

The results of the 3 assays were retrospectively analyzed using all available clinical data. The CP

patients were staged - 7 A's, 8 B's, 5 C's, 6 D's and 12 on hormones.

The controls had PAP values of 1.86 ± .47 I.U./L for the enzymatic assay, 2.84 ± 1.05 ng/ml for NEN and 1.38 ± 0.76 ng/ml for Serono. CB were in the same range and BPH 2.16 ± 0.61 I.U./L for the enzymatic, 3.09 ± 1.2 ng/ml for NEN and 1.70 ± 1.19 ng/ml for Serono. Using our upper level of normal for the enzymatic of 3 I.U./L, 8 ng/ml for NEN and 4 ng/ml for Serono none of the Stage A or those on hormones were positive. Of the B's 37%, 80% of the C's and 67% of the D's were positive by enzyme and NEN. Serono was positive in 50% of B's, 80% of C's and 83% of D's. This gave an overall sensitivity of 55% for enzymatic and NEN and 65% for Serono with 100% specificity for NEN, 93% for Serono and only 44% for the enzyme assay.

The RIA is more sensitive and very much more specific. Claims that it should be used for screening purposes to detect Stage A disease are not warranted.

COMBINED STUDY OF RADIONUCLIDE LIVER IMAGING, ULTRASOUND AND RADIOIMMUNOASSAYS FOR ALPHA$_1$-FETOPROTEIN AND CARCINOEMBRYONIC ANTIGEN IN THE DETECTION OF FOCAL HEPATIC LESIONS. T. Aburano, K. Kuwajima, A. Tada, K. Ichiyanagi, N. Tonami and K. Hisada. Kanazawa University Hospital, Kanazawa, Japan.

Combined study of radionuclide (RN) liver imaging, ultrasound (US) and radioimmunoassays (RIA) for alpha$_1$-fetoprotein (AFP) and carcinoembryonic antigen (CEA) was undertaken to increase the detection rate of focal lesions in the liver. RN liver imaging with Tc-99m-colloid was performed as a screening procedure in the detection of focal hepatic lesions, and RIA for AFP and CEA were routinely performed as an adjunct to RN liver scan. US was mainly used to evaluate the equivocal liver scan. Only discrete focal defects in the liver were taken as a positive scan. Tc-99m-colloid scan could not detect any discrete focal defects in 43 out of 214 patients (20%) with focal hepatic lesion. In 11 out of 43 with false negative scan, US could reveal focal hepatic lesions, and most of these patients were associated with equivocal RN scan. All of the remaining 32 with false negative scan were associated with single or multiple small lesions less than 2 cm in a diameter. In these 32 patients, two showed the persistently increased levels of AFP, which were strongly suspicious of the presence of hepatoma. And eight showed the increased levels of CEA combined with simple hepatomegaly or high alkaline phosphatase activity, strongly suspicious of the presence of metastatic liver cancer.

The overall detection rate of focal hepatic lesions by the combined study of RN imaging, US and RIA for AFP and CEA was 90%, and proved to be significantly higher, compared to that of 80% by RN imaging alone.

2:00-3:30 Room 3040

INSTRUMENTATION

EMISSION TOMOGRAPHY II

Session Chairman: Jim Sorenson
Session Co-Chairman: Dennis Kirch

INVITED SPEAKER

Dennis L. Kirch, Denver, CO
REVIEW OF 7-PINHOLE COLLIMATOR CONCEPT.

COMPARISON OF SEVEN PINHOLE & ROTATING SLANT TOMOGRAPHY OF A CARDIAC PHANTOM. S.C. Gottschalk, K.A. Smith, R.H. Wake. Technicare Corporation, Solon, OH.

Three dimensional tomographic reconstructions from planar views with an Anger gamma camera using a Seven Pinhole (7PH) and Rotating Slant Hole (RSH) collimators are described. The z-axis resolution after reconstruction is shown to be 50% better than the backprojected PSF. Iowa cardiac phantom studies in a water bath with Th-201 in the myocardial cavity, water in the ventricular cavity, and a simulated 90 degree anterior myocardial defect are described. Defect activity was varied from 0% to 75% of the myocardial activity. Reconstructions are demonstrated to be linear and qualitatively correct. The relation between defect activity and reconstructed activity is illustrated. Defect propagation for 7PH is significantly worse than for RSH collimators. Scatter from water was a major limitation to quantitative reconstructions at small phantom-collimator distances, with PSF contributing more at larger distances. 7PH collimator sensitivity drop off with depth made it more sensitive to statistics. 7PH collimator has the most severe partial view artifacts. Advantages and disadvantages of both collimators from physical points of view are summarized.

MOTIVATION FOR THE ROTATING SLANT HOLE APPROACH TO SCINTILLATION CAMERA TOMOGRAPHY. D.W. Shosa, J.W. O'Connell, and R.S. Hattner. University of California, San Francisco, San Francisco, California.

Results of an earlier investigation concerned with the evaluation of rotating slant hole technology with small field-of-view scintillation cameras (25 cm diameter) were presented at the Western Regional Meeting (1979). The present investigation extends consideration to larger cameras (38 and 53 cm diameters) with particular emphasis on the prospects of multiple-view systems. The analysis includes evaluation of tradeoffs among the variables of sensitivity, spatial resolution and perspective angle. It also gives due consideration to the important problem of camera positioning. We find that, in most cases, rotating slant hole systems can be designed which will yield comparable spatial resolution, comparable or superior sensitivity and superior perspective angle relative to seven pinhole designs. In addition, rotating slant hole systems are typically easier to position than pinhole systems. There are also advantages with respect to the finer angular sampling which is available, with respect to a simpler treatment of attenuation correction in the reconstruction algorithm and with respect to the effective use of the central as opposed to the peripheral response of the detector.

CARDIAC TOMOGRAPHY USING A ROTATING SLANT HOLE COLLIMATOR AND A PORTABLE CAMERA. D. Pavel, E. Byrom, C. Meyer-Pavel, R. Balon

Univ. of Illinois Med. Center, Chicago, Illinois

The collimator fits a portable camera head, has parallel holes of 3 cm length, slanted by 25°, and rotates in 6 positions, for 6 views 60° apart, around the axis of a 40° LAO projection. The reconstruction is based on a least squares iterative algorithm. An optimization of the acquisition and processing for Tl-201 was attempted based on phantom studies and on 21 clinical studies. Acquisition: for a usual dose, 3 to 5 min/view were adequate, yielding 90,000 325,000 cts/view. Processing: a standard processing of 12 planes, of 1.3 cm thickness, starting at 1 cm from the collimator surface was used in all cases. Varying the number of planes from 12 to 8 does not change the quality of the image. With 6 planes the resolution was slightly degraded. Varying the slice thickness to 1 cm decreased the sharpness of the reconstruction slightly. No false (+) or false (-) results were obtained as compared to the routine views and to the clinical and laboratory data. Phantoms: the small and large lesion in the Tl-201 phantom were clearly defined and their depth precisely estimated. The addition of background activity (of relative intensity comparable to that in the field of view of clinical studies) had only minimal effect on the reconstruction. In the Au-195 stacked ring phantom the smallest lesion (0.6 cm thick) was

very sharply delineated. Advantages: easy and rapid positioning; markedly enlarged LV can be imaged; 3 of the 6 acquired images closely resemble the standard analog views and can be used as such; reconstruction starts at face of collimator; very good resolution; enables tomography at bedside.

A MULTISEGMENTAL SLANT HOLE TOMOGRAPHIC COLLIMATOR (MUST): A NEW TOMOGRAPHIC GAMMA CAMERA SYSTEM. W. Chang, S.L. Lin, R.E. Henkin, and B.C. Salo. Loyola Univ. Med. Center, Maywood, IL.

Interest in slant hole collimators for emission tomography is growing. To maximally utilize the crystal area of a 10" camera, a four-quadrant rotatable slant hole collimator was built. Each quadrant covers a 90° pie-shaped area. The collimator is constructed using square hole technology with each quadrant slanted 25° toward the central axis. The collimator resolution measured on a 1/4" crystal camera at 140 kev is 9 mm FWHM at 10 cm depth in a scattering medium. The sensitivity is 30% higher than a standard HR collimator for each quadrant. This results in a 3-fold increase in sensitivity for cardiac imaging vs an HR collimator.

When rotated, an ellipsoid-like common volume is generated along the central axis. 16 tomograms are reconstructed in the common volume with 7 mm spacing. Clock phantom measurements demonstrate each slice to be evenly spaced and at the predicted depth. In this system, planar FWHM of 0.9, 1.1 and 1.3 cm and depth FWHM of 2.5, 2.9 and 3.6 cm are achieved at planes which are 8.8, 12.6, and 16.5 cm respectively from the collimator face for 140 kev photons. Longitudinal tomograms are reconstructed using one 45° collimator rotation. 201-Thallium tomographic patient studies demonstrate less distortion than the corresponding 7 pinhole tomograms.

The greatly increased sensitivity and minimal distortion introduced by the collimator makes high quality tomograms feasible in multiple projections. A greater angle can be employed on an LFOV and field size thus expanded for tomography of organs other than the heart.

CHAMBER VOLUME DETERMINATION USING A 4-QUADRANT SLANT HOLE TOMOGRAPHIC SYSTEM. W. Chang, R.E. Henkin, S.L. Lin, and B.C. Salo. Loyola Univ. Med. Center, Maywood, IL.

A number of attempts have been made to estimate left ventricular volume from Nuclear Medicine studies. The methods to date have generally employed geometric assumptions which were often inaccurate, especially in patients with ventricular dilatation. We have developed a tomographic system utilizing a 4-quadrant slant hole collimator. Evenly spaced tomographic planes have been generated by this system. The depth of each plane is precisely known.

Volume determinations have been made on left ventricular volume phantoms ranging in size from 46 to 198 cc utilizing the stationary 4-quadrant collimator. The volume estimation algorithm, developed in this laboratory, was applied to the tomographic images reconstructed from the phantoms in the system described above. The correlation between actual and determined volume was excellent with an $r = 0.96$. The algorithm represents an edge search-summation routine which estimates the area of the left ventricle for each tomographic plane.

Patient studies are currently under way documenting the accuracy of the method in the clinical environment.

The absence of distortion, combined with the excellent planar resolutions ranging from .9 to 1.3 cm FWHM and depth resolutions from 2.5 to 3.6 cm in the volume of interest (a 10x15 cm ellipsoid), results in a simple clinical method for volume determination which should be applicable to normal and abnormal left ventricles. These determinations are feasible from standard gated blood pool images.

IN-VIVO SIMULATION OF THALLIUM-201 MYOCARDIAL SCINTIGRAPHY BY SEVEN PINHOLE EMISSION TOMOGRAPHY. D.L. Williams, J.L. Ritchie, G.D. Harp, J.H. Caldwell, and G.W. Hamilton. VA Medical Center, Seattle, WA.

The imaging characteristics of seven pinhole cardiac emission tomography and planar LAO imaging were compared using a multi-chamber heart phantom (University of Iowa design) under simulated in-vivo conditions for Tl-201. For both imaging modalities, the phantom was suspended in a 20 l cylindrical lucite tank such that the distance between the tank's exterior surface and the apex was 4.4 cm and the distance to the mid-plane of a 3 cm long, 24 cc defect containing only water was 10 cm. All other myocardial wall chambers (1 cm thick) contained the same concentration of activity. The left ventricular chamber's activity concentration was 5% relative to the walls. Activity was added to the tank such that the myocardial-to-background ratio by planar imaging was 2:1 for the walls containing thallium. Thus, the relative distribution of activity concentrations approximated that reported for planar myocardial imaging.

The minimum observed ratio of defect-to-normal-wall in 16 reconstructed planes was 0.54, not zero as expected. Seven pinhole tomography did not accurately quantitate the defect. In addition, the presence of the defect was observed in all reconstructed planes distal to those which geometrically intersected it, and in most proximal planes. However, defect-to-normal-wall contrast was significantly better than by background subtracting (50%) and smoothing the planar LAO image. Seven pinhole emission tomography does not appear to offer quantitative tomography for myocardial scintigraphy, but may be useful clinically when compared to planar imaging, due to its ability to achieve higher image contrast.

PERFORMANCE CHARACTERISTICS OF SEVEN-PINHOLE TOMOGRAPHY. V.A. Brookeman. Guy's Hospital, London, UK.

An evaluation of some performance characteristics of a seven-pinhole emission tomography system using a wide-field gamma camera was made for three different pinhole diameters and two software packages. Vertical resolution was determined centrally and 2 or 5 cm off-center in X and in Y directions, at 8, 10, and 13 cm from the tomo-collimator face, with forward- and back-scatter material present. Vertical FWHM values given in the table below are the mean of all values at any one depth. Two hollow 5 and 10 cm cubes uniformly filled with Tc-99m solution were imaged to assess the tomosystem's ability to reproduce uniform volume sources. The horizontal response showed some decrease in the cubes' centers on all reconstructed planes, this artefact decreasing on increasingly distant planes. This central dip in horizontal count profiles ranged from about 4 to 56% of the side maximum counts, depending also on the software employed. The response in a vertical direction first increased from about 93% of the maximum response, which occured about the cubes' centers, then fell with increasing distance to about 57% of maximum. These results indicate potential artefacts in clinical seven-pinhole tomographic imaging and problems in quantitation.

Dist. from coll. face (cm) \ Pinhole Diam. (mm)	Vertical FWHM (cm) Co-57 4.5	Co-57 5.5	Co-57 7.5	Au-195 4.4	Au-195 5.5	Au-195 7.5
8	1.4	1.6	2.0	1.7	1.8	2.1
10	2.2	2.4	2.9			
13	2.5	2.7	3.2	3.0	3.2	3.7

VARIABLE ANGLE SLANT HOLE COLLIMATOR. R. Moore, N. Alpert, J. Lazewatsky, H. Strauss. Massachusetts General Hospital, Boston, MA.

A variable slant angle parallel hole (VASH) collimator which fits a standard Anger camera was constructed from a stack of 200 precisely photoetched tungsten plates, each 1.25 mm thick, with 1.25 mm holes and septae of .30 mm thickness. Collimator plate registration is controlled by aligning the stack against a set of six knife edges controlled by a parallelogram array. The slant hole effect is achieved by moving the parallelogram holder to shear the stack of plates thus forming inclined channels. The FWHM

was measured using a Tc-99m point source with the collimator unsheared (photons entering perpendicular to the crystal surface) as 1.8 mm @ the surface and 12 mm @ 7.5 cm from the collimator face. With the collimator sheared to 20° (photons entering the crystal at 70°) the resolution was 1.68 mm and 10 mm FWHM, respectively. The impreved resolution agrees with the expected theorhetical gain due to channel lengthening. The VASH sensitivity was compared to an all purpose collimator: unsheared 48% and at 20°, 36%.

Clinical use of this collimator could improve image resolution by decreasing imaging distance, additionally, the combination of rotation with collimator angulation would enhance planar tomography resolution.

4:00-5:30 Room 2048

CLINICAL

ENDOCRINE

Session Chairman: Milton Gross
Session Co-Chairman: John Freitas

DEXAMETHASONE SUPPRESSION (DS) I-131-IODOMETHYLNORCHOLESTEROL (NP-59) ADRENAL UPTAKE IS A MEASURE OF 17-KETOSTEROID (17-KS) EXCRETION IN HYPERANDROGENISM. M. Gross, T. Valk, D. Swanson, J. Freitas, M. Woodbury, D. Schteingart, and W. Beierwaltes, University of Michigan Medical Center, Ann Arbor, Michigan.

The degree to which adrenal uptake of NP-59 reflects the pathophysiologic process in patients with hyperandrogenism has not been established. To assess this relationship, the DS adrenal uptake of NP-59 was correlated with plasma testesterone levels (T) and 24 hr urinary 17-KS excretion in fifteen patients with adrenal hyperandrogenism. All patients received 4 mg of dexamethasone daily commencing one week prior to I.V. NP-59 (1 mCi) and continued throughout the study. Posterior and left lateral images were obtained 3 and 5 days post-tracer injection. Adrenal % dose uptakes (%DU) were performed with a semioperator independent computer algorithm. Patients were separted into bilateral (BV) and unilateral visualization (UV) groups. Correlation coefficients (r) were generated comparing total (right + left) %DU with T and 17-KS excretion (Table).

		17-KS		T	
Scan Pattern	(n)	r	p	r	p
Bilateral	(11)	0.86	<.001	.42	ns
Unilateral	(4)	0.99	<.001	.36	ns

Mean DS 17-KS and T were 8.2±1.2 mg/24° and 0.9±.12 ng/ml in BV and 13.1±5.0 mg/24° and 2.03±.99 ng/ml in UV, respectively. Mean %DU was 0.35±.04 and 0.34±.11 in BV and UV, respectively. There was a positive correlation of 17-KS with %DU in both the BV and UV groups. No correlation was seen with T and %DU. Thus, NP-59 adrenal %DU reflects the biochemical abnormality and the degree of adrenal cortical dysfunction in patients with androgen excess while under dexamethasone suppression.

THE RELATIONSHIP OF ^{131}I-6β-IODOMETHYLNORCHOLESTEROL (NP-59) ADRENAL UPTAKE TO PLASMA LIPIDS IN CUSHING'S SYNDROME. T. Valk, M. Gross, J. Freitas, D. Swanson, D. Schteingart and W. Beierwaltes, University of Michigan Medical Center, Ann Arbor, Michigan.

To assess the importance of the endogenous lipid pool on ^{131}I-6β-iodomethylnorcholesterol (NP-59) adrenal gland uptake, plasma cholesterol (C) and triglyceride (TG) levels were correlated with NP-59 adrenal uptake in 14 patients with Cushing's Syndrome (CS). Eight patients with pituitary dependent CS and 6 patients with pituitary independent CS (4 with ACTH-independent CS--2 adrenal adenomas and 2 bilateral nodular hyperplasias, and 2 with ectopic ACTH CS) were evaluated with posterior and left lateral adrenal images obtained from 5 to 7 days after NP-59 (1 mCi) administration. Percent dose uptakes (%DU) (right + left) were calculated using a semioperator independent computer algorithm. Coefficients of correlation (r) were calculated comparing plasma C and TG with %DU. The mean %DU was 0.50±.07 and 1.18±0.24 in pituitary dependent CS and pituitary independent CS, respectively ($p < .05$). Plasma C was negatively correlated with %DU ($r = -0.78$, $p < .01$) in pituitary dependent CS and not correlated with %DU in pituitary independent CS. TG did not correlate with %DU in either of the groups examined.

In conclusion: (1) %DU may distinguish pituitary dependent CS from pituitary independent CS, (2) plasma C is inversely correlated with NP-59 %DU in pituitary dependent CS, (3) NP-59 %DU in pituitary independent CS is not affected by the level of plasma C reflecting the marked elevation of ACTH in ectopic ACTH CS or the primary adrenal cortical disease in adrenal adenoma or bilateral nodular hyperplasia, and (4) elevated plasma C (>400-500 mg/dl) may limit the usefulness of adrenal scintigraphy in CS.

ADRENAL IMAGING WITH I-123-LABELED-IODOMETHYL-19-NORCHOLESTEROL. F. Shishido, Y. Tateno, T.Ido, T. Irie, K. Suzuki, K. Fukushi, R. Iwata, M.Kojima, M. Maeda, T. Ito, and H. Ogawa. National Institute of Radiological Sciences, Kyushu Univ. and Daiichi Radioisotope Lab. Chiba, Fukuoka, and Tokyo, Japan.

I-123-labeled-6β-iodomethyl-19-norcholesterol (I-123-NCL), which was synthesized after Kojima et al, was utilized for the imaging of adrenal glands. Adrenal images of six cases were obtained by intravenous administrations of 2.6 mCi - 6.7 mCi I-123-NCL. Scanning was performed 1, 2 and 3 days after I-123-NCL administration using MaxiCamera II (GE) and Gammaview RC-1C-1635LD (Hitachi) attached low energy paralel and conversing collimator.

Four of six cases were visualized in 1 day after administration of about 5 mCi I-123-NCL and the optimal scans were obtained at 2 days after injection in these cases. The dose of 2.6 mCi I-123-NCL did not give satisfactory scans in a patient with cancer of the bladder.

It was found that the dose of 5 mCi was sufficient for the adrenal imaging and the optimal scans were obtained at 2 days after the intravenous administration of I-123-NCL. The image qualities were superior to that of I-131-NCL. The estimate absorbed dose of I-123-NCL was less than that of I-131-NCL.

These results suggested I-123-NCL was an excellent adrenal imaging agent for a clinical examination.

RESULTS OF QUANTITATIVE ADRENAL IMAGING IN 62 CASES USING Se-75 SELENOCHOLESTEROL. B. Shapiro, K.E. Britton and L.A. Hawkins. University of Michigan Medical Center, Ann Arbor, MI. and St. Bartholomew's Hospital, London, U.K.

The adrenals of 61 patients with suspected adrenal cortical disease and one normal volunteer were imaged with 6βmethyl Se-75 selenomethyl-19-norcholestrol-5-(10)-en-3β--ol. A dose of 250 μCi was administered and imaging performed at 3 and 6 days in 19 cases studied by rectillinear scanning and at 7 and 16 days in 43 cases studied by gamma camera. In the latter adrenal depth was determined from lateral renal scans, and in 10 cases by single photon emission tomography. Adrenal uptake was quantified from stored static images by computer.

Mean uptake in normal adrenals was 0.17% (range 0.07-0.30%). Mean uptake in Conn's adenoma was 0.47% (8) and bilateral hyperplasia 0.33% (14). Diagnostic accuracy in 22 cases of Conn's Syndrome was 77%. Mean uptake in adenomas causing Cusing's Syndrome was 0.93% (5), pituitary dependent hyperplasia 0.58% (12), ectopic ACTH syndrome 0.69% (7), congenital hyperplasia 3.61% (1), adrenal carcinoma 0.008% (3). Localization of postadrenalectomy remnants was achieved in all three cases studied. Diagnostic accuracy in 32 cases of Cushing's Syndrome was 87.5%.

The technique was found to be a reliable noninvasive procedure in investigation of adrenocortical disease. The radiopharmaceutical may be superior to I-131 cholesterol derivatives in that; higher uptake in normal adrenals was observed; long effective half-life permits imaging when background activity is low; the spectrum of Se-75 is better suited to gamma camera imaging; the thyroid need not be blocked; and storage at room temperature for up to 6 weeks is possible.

IMAGING OF THYROID NEOPLASMS HAVING TSH RECEPTOR. K.Kusakabe,T.Yamasaki,S.Kurihara and H.Akiba. Dept. of Radiology, Tokyo Women's Medical college, Tokyo, Japan.

In this study, TSH was labeled with iodine-131 and used for imaging of thyroid neoplasms having TSH receptor. The bovine TSH was labeled with I-131 according to the method of Chloramin T. Images were obtained at 30 min,1,3,6 and 24 hr after administration of 100 to 200 Ci of I-131 TSH using rectilinear scanner. In order to detect the allergic reaction to bovine TSH, the anti TSH antibody in the patient's serum was measured before injection of radioiodinated TSH using the method of radioimmunoassay. Seven patients with thyroid neoplasms were studied by the scintigraphy with I-131 TSH. Four sites of thyroid cancer including lymphnode metastases and 6 sites of thyroid adenoma including 4 sites of hyperfunctioning adenoma were evaluated. Out of four sites of hyperfunctioning adenoma, two showed remarkable tumor uptake of I-131 TSH in the scans but two did not show any uptake compared with Na I-131 scans. In two patients out of three with thyroid cancer, uptake of radioiodinated TSH in lymphnode metastases was found on I-131 TSH scans. The animal studies were also performed using I-125 TSH and H-3 TSH. No inorganic iodin could be detected in rat thyroid following injection of I-125 TSH by the paper chromatography. No uptake of H-3 TSH could be found in other organs except the thyroid gland in rat. Normal thyroidal uptake of H-3 TSH was 2.7% of injected dose. These findings suggest that I-131 TSH was bound to the TSH receptor of the thyroid neoplasms and normal thyroid tissue. This approach may offer considerable potential for the estimation of TSH receptor levels in thyroid neoplasms for therapeutic purposes.

INADEQUACY OF MODERATE DOSE OF I-131 FOR ABLATION OF THYROID REMNANTS FOLLOWING SURGERY FOR DIFFERENTIATED THYROID CARCINOMA (DTC). A.R. Siddiqui, J. Edmondson, H.N. Wellman, H.M. Park, R. Schnute, and C.C. Johnston. Indiana University School of Medicine, Indianapolis, IN.

Treatment for DTC includes total or near-total thyroidectomy and post-operative ablation of the remaining thyroid tissue with I-131. The usual ablative dose of I-131 ranges from 100 to 200 mCi. The feasibility of using a smaller dose, 29.9 mCi, was evaluated, since it is the maximum that can be given to out patients.

Twenty-one sequential patients (pts) with DTC were evaluated following total or near-total thyroidectomy. Approximately 6 weeks after surgery, each pt was given thyroid stimulating hormone intramuscularly on three consecutive days followed by 29.9 mCi of I-131 on the third day. Neck and chest scans were performed 24 and 48 hours after radioiodine. Follow up scans were performed at 9-15 month intervals. These scans were done using 3 mCi of I-131 with the pts off l-thyroxine for 6 weeks and off triiodothyroxine for at least 1 week.

Nineteen out of the 21 pts showed residual thyroid tissue on the initial scan following surgery. Two pts accumulated radioiodine in the tissue outside the thyroid bed as well and were given conventional doses of I-131. Ten of the remaining 17 pts had serial studies, only one of which showed complete ablation of residual tissue. Eight had persistent activity in thyroid bed and one presented with lymph node metastasis.

Our findings indicate that total or near-total thyroidectomy rarely removes all thyroid tissue and an "out patient" dose of I-131 (29.9 mCi) is not adequate for ablation of post-operative thyroid remnant.

OPTIMIZATION OF I-131 SCAN DOSE IN PATIENTS WITH THYROID CANCER. A. Waxman, L. Ramanna, N. Chapman, M. Brachman, D. Tanasescu, D. Berman, B. Catz, G. Braunstein. Cedars-Sinai Medical Center, Los Angeles, California

I-131 has been used in the evaluation of thyroid cancer for the detection of metastases as well as residual primary disease. The purpose of this paper was to compare the sensitivity of a 2 mCi initial scan dose to higher scan doses in detecting residual iodine avid tissue.

Twenty-two patients were included in this study. Fourteen received an initial scan dose of 2 mCi of I-131 and were rescanned within one week with 10 mCi. All studies were done 3-5 days following I-131 using rectilinear technique.

The results for the 14 patients undergoing the 2 and 10 mCi scan protocol are summarized in the following table:

	2 mCi-10 mCi-	2 mCi< 10 mCi	2 mCi= 10 mCi	2 mCi+ 10 mCi+	2 mCi- 10 mCi+
Patient #	4	4	0	1	5
Sites	5	5	0	1	9

On the basis of the 2 mCi study 10 patients were thought to be free of disease with no residual activity demonstrated in the neck or chest area. A rescan within one week using 10 mCi of I-131 showed 6 of these patients to be positive with an abnormality demonstrated in the neck or chest region. A site by site analysis showed 10 additional sites detected in this patient population using the 10 mCi scan dose, which were not detected with 2 mCi. The 30 mCi scan dose was felt to be superior to the 2 mCi scan in 3 of 6 patients studied. A comparison of 10 mCi with 100 mCi was performed in 7 patients with the 100 mCi scan rated superior in 3 of the 7 cases.

We conclude that a 2 mCi I-131 scan dose is inadequate for the determination of residual activity in patients undergoing ablation for thyroid cancer.

I-131 WHOLE BODY SURVEYS: TOMOGRAPHIC VS. GAMMA CAMERA IMAGING. P. Kirchner, T. Brown, N. Bidani, C. Armstrong, B. Brunsden, and L. DeGroot. The University of Chicago, Chicago, IL.

Post-thyroidectomy whole-body imaging for residual thyroid tissue and functioning thyroid metastases is still frequently done with rectilinear scanners since appropriate gamma camera collimators are often not available. Imaging techniques vary widely; minimum detectable activity is rarely defined for any depth in the body. A recent failure to detect residual neck activity (0.5-1.0% uptake) with rectilinear scanning prompted a comparison of I-131 imaging with a dual 5" rectilinear scanner (ON-84), gamma camera (PG-IV), and multiplane tomoscanner (Pho/Con).

Phantom studies assessed detectability of 5uCi I-131 (0.5% usual dose) as function of distance from collimator or focal plane and resolution of point sources separated in xy and z. The ON-84 did not detect 5uCi at 6cm above and 9cm below the 5" focal plane and showed poor resolution even at the focal plane. Both PG-IV and Pho/Con detected 5uCi over 19cm depth but the Pho/Con resolution was clearly superior. Clinical studies evaluated blind by 3 reviewers compared Pho/Con with multiple camera images obtained on the same day in each of 30 patients (total of 70 benign and 9 metastatic foci of activity). Neither instrument found any foci which were altogether missed by the other. Scanning time and ease-of-interpretation were comparable, but image information content was better with the Pho/Con because of better 3-dimensional localization.

Both Pho/Con and gamma camera images are more reliable than rectilinear images for detecting and resolving clinically important small foci of I-131. Use of a reference source with each clinical study is recommended to establish a lower level of detectable activity for each study.

A VALUABLE SCINTIGRAPHIC SIGN FOR THE DIAGNOSIS OF THYROID CYST: THE "RIM SIGN." M.D. Okerlund, J. Sommers, T.Grell O. Clark, L. Kaufman, and R. Filly. University of California Medical Center, San Francisco, California.

14 of 16 consecutive thyroid cysts were found to have a unique positive diagnostic sign on 2 or more of the modalities of (1)rectilinear scan with 123-iodide (2) scintillation camera photograph with 5-10mCi Technetium 99m pertechnetate, or (3)fluorescent excitation scan with 241-americium. All cysts were subsequently proven by at least 2 of the techniques of ultrasonography, needle aspiration, or surgery. The "rim sign" consists of a single centrally nonfunctioning thyroid nodule with a thin rim of surrounding functioning thyroid tissue apparent on both the anterior, and (in the case of the scintillation camera) confirmed by appropriate oblique projection. A statistical study was then made to evaluate the possible significance of the rim sign and comparison made with 84 consecutive solid nodules imaged and removed surgically. Analysis yielded 14 true positives, 2 false positives, 0 false negatives, and 84 true negatives. This data indicates a diagnostic sensitivity of 87.5%, a specificity of 97.6%, and an accuracy of 96% for the "rim sign" in

this series. The predictive value using Bayes' Theorem was 90.1% assuming a 16% prevalence of cystic nodules found in this series, which closely approximates data from a number of clinics. The "rim sign" is a useful, sensitive, specific and accurate sign for the presence of thyroid cyst. This sign is of possible importance since almost all thyroid cysts are benign, and further helps to select patients for ultrasonography and either avoidance of early operation or consideration instead of needle aspiration as a management strategy.

CLINICAL IMPORTANCE OF THE "INDETERMINATE" NODULE IN THYROID IMAGING: THE COMMONEST CAUSE OF THE "FALSE NEGATIVE THYROID IMAGING STUDY. M.D.Okerlund, J. Sommers, T. Grell, M.Galante, T. Hunt, and O. Clark. University of California Medical Center, San Francisco, California.

7% of 1100 consecutive thyroid imaging studies (I-123 scintigrams plus Tc-99m pertechnetate pinhole pictures) had "indeterminate" nodules: no change in gland outline and no evidence of nodule size or location without marking despite palpatory findings present. If indeterminate on scan, subsequent gamma camera picture showed these to be clearly cold in 69%, functioning in 13%,and indeterminate in 18%. To study the possible significance of these, surgical findings were determined and compared with 100 nodules initially clearly cold by the same techniques.

Histology Image:	"Cold"	Indeterminate By scan	By scan and camera
Adenoma	34(34%)	39(50%)	6(42.9%)
Carcinoma	19(19%)	9(12%)	1(7.1%)
Cyst	17(17%)	1(1%)	1(7.1%)
Involution	12(12%)	11(14%)	3(21.4%)
Nodular goiter	9(9%)	12(15%)	2(14.3%)
Thyroiditis	9(9%)	6(8%)	1(7.1%)

Indeterminate thyroid nodules were almost all solid and mostly tumors. Anatomically, most were anterior with underlying normal thyroid, or posterior with overlying tissue. Since physical examination provided the only initial indication of the nodule's presence, this emphasizes the need for correlation of images with findings. No I-123/Tc-99m discordant images were found in this series and no truly "warm nodule." Indeterminate nodules have the same diverse etiologies and significance as clearly cold nodules, and should not be confused with the very rare "warm" lesion, the latter not seen in 1100 cases.

AN ACCURATE MEASUREMENT OF DIMENSIONS AND MASS OF THYROID GLAND USING A COMPUTER AND A GAMMA CAMERA. A. Jansen, M. Eklem & G. T. Krishnamurthy. VA Medical Center & UOHSC, Portland, Oregon.

Over the years, the measurements of the thyroid mass for calculating I-131 therapy doses have been obtained using images from a rectilinear scanner. At present, gamma cameras are replacing scanners as the instrument of choice for imaging. This investigation was undertaken to develop a technique for the measurement of thyroid mass using images from a gamma camera interfaced to a computer, and to compare the results with those obtained using a scanner image.

In 6 patients the thyroid images were obtained 20-30 minutes after the injection of 5-10 mCi of Tc-99m pertechnetate. A high resolution (HR) focussing and HR parallel hole collimators were used with the scanner and camera respectively. An image of a phantom of known dimensions was included as a reference with the thyroid images obtained with the camera-computer. On the scans the area was measured with a planimeter after outlining the gland boundary manually. An automatic edge detection program set to a threshold was used to determine the gland boundary on camera images. The gland area was measured by noting the number of pixels flagged in the gland vs. the standard.The mass was obtained by using the following formula: Thyroid mass = area x average length of lobes x 0.321.

The mass determined from the gamma camera images showed high correlation ($r=0.97$) ($p < 0.002$) with the mass obtained from the scans. It is concluded that the dimensions & mass of the thyroid can be determined accurately using a gamma camera and a computer.

THE NORMAL RAIU IN THE MADISON, WISCONSIN AREA. L.M. Lieberman, S.J. Gatley, and B. Pastakia. The University of Wisconsin Hospital, Madison, WI.

The present trend throughout the US of the 24 hr RAIU by the thyroid gland is unclear. Several reports have suggested a decrease in the RAIU while others have indicated a possible rise, reversing a trend known to have occurred before 1967. Since the 24 hr RAIU continues to be an important parameter of thyroid function, it is important that the normal range be known for each geographical area.

We have performed 6 and 24 hr RAIU tests with I-123 on a group of 61 normal subjects aged 18-61 years living in or near Madison. Forty-five women and 14 men were determined to be euthyroid by completing a questionnaire asking for any history of thyroid or kidney disease and whether they were taking any medications. Serum T3, T4, and FTI tests were done, and the concentration of stable iodine in a random urine sample was determined. Fifty to 100 µCi of I-123 were given orally and the RAIU test performed in accordance with IAEA specifications.

The mean urinary iodide excretion was 683 ± 84.5 µg/l corresponding to approximately 800 µg/24 hr somewhat higher than reported by other workers. We attribute this to a high dietary intake of iodide in our area probably due to an average iodide concentration of 384 µg/g found in six samples of commercially baked bread sold in and near Madison.

The 6 hr RAIU (mean ± SD) was 8.2 ± 3.8% (range = 1.8-19.6%) and the 24 hr RAIU 15.5 ± 5.7% (range = 2.0-33.5%), which is lower than that reported for normal subjects in Minneapolis (1975) 20.5%, and in Chicago (1971) 20.0%, but higher than that in LaCrosse, WI (1971) 12.1%.

THE ROLE OF Tc-99m PERTECHNETATE UPTAKE IN PATIENTS WITH THYROID DISEASE. M.S. Sucupira, E.E. Camargo, E.L. Nickoloff, P.O. Alderson, and H.N. Wagner, Jr. The Johns Hopkins Medical Institutions, Baltimore, MD.

To investigate the usefulness of the 20 min Tc-99m pertechnetate uptake test, the records of 159 consecutive patients (pts) were reviewed. Of these, 95 pts (77 females, 18 males; 10-78 years) who met the criteria of having at least one year follow-up or a confirmed diagnosis by biopsy or surgery were included in our study. In these pts, the Tc-99m pertechnetate uptake was compared to hormonal values (T3 resin uptake T4 RIA, T-index) obtained at the time of the uptake, and the clinical diagnosis one year later. All patients received an intravenous injection of 5 mCi of Tc-99m pertechnetate. Imaging was performed using a pinhole collimator and a scintillation camera interfaced to a dedicated computer. Regions of interest for the thyroid and the background were used to calculate the 20 min Tc-99m pertechnetate uptake as percent injected dose. Uptakes and hormonal values were confirmatory in 81% of pts (1 hypo-, 8 hyper-, 68 euthyroid) and discordant in 15 pts (16%): in 4 pts with high hormonal values the uptake was normal, 2 had Graves' disease in remission and 2 had toxic nodular goiter; in 10 pts with normal hormonal values, the uptake was low in 4 due to exogenous iodide or T4, and high in 6, 3 with persistent hyperthyroidism and 3 with Hashimoto's disease; in one pt with low hormonal values the high uptake provided evidence of persistent hyperthyroidism while on therapy. In 3 pts (3%) the uptake was misleading when the clinical diagnoses were reviewed one year later. The Tc-99m pertechnetate uptake is a useful adjunct to measurement of hormonal levels in pts with suspected thyroid disease.

4:00-5:30 **Room 2043**

CLINICAL

ONCOLOGY I

Session Chairman: Steven Pinsky
Session Co-Chairman: Robert Henkin

UPTAKE OF Ga-67 IN IRRADIATED TUMORS - IS Ga-67 A TRUE INDICATOR OF TISSUE RESPONSE TO IRRADIATION? R. Hardoff,

D. Front, G. Yoselevski, Y. Ben-Arieh. Rambam Hospital and Technion Faculty of Medicine, Haifa, Israel.

Ga-67 is extensively used for evaluation of patients after radiotherapy. It has not been shown, however, that the fact that most Ga-67 scans become negative after radiotherapy means that irradiated tumors regress and disappear. Radiotherapy may supress some mechanism of Ga-67 uptake while the tumor remains viable. The present study was undertaken in order to correlate Ga-67 uptake and tissue response to irradiation in a tumor model. Methyl cholantren induced fibrosacroma in C57B female mice was used. Uptake in viable tumors (n=30) and in viable and non viable parts of tumors containing necrosis (n=7) was determined as percent of injected dose per gram tissue. Percent uptake in viable tumors was 9.6±1.4 and in non viable parts 2.5±0.5. Other tumors (n=19) were locally irradiated using 57Kv X-rays at a rate of 200 rads/minute; 3000 rads were delivered to the tumor while the rest of the body of the mouse was shielded. Fourteen days later uptake of Ga-67 and histology of the tumors were assessed. Three groups of response were found. Group A (n=4), where more than half of the tumor remained viable and uptake was 10±0.4; Group B (n=11), where half or less of the tumor was viable and uptake was 5.2±1.5; Group C (n=4), where the greater part or all of the tumor underwent fibrosis and necrosis and Ga-67 uptake was 2.3±0.6. Uptake in blood, liver, bone and muscle was essentially the same in animals with and without irradiation. A good correlation was thus found between Ga-67 uptake and the amount of viable tissue left in the tumor after local irradiation.

GALLIUM-67 IN HILAR AND MEDIASTINAL STAGING OF PRIMARY LUNG CARCINOMAS. R. Neumann, M. Merino, P. Hoffer, H. Stern, A. Toole, and A. Gottschalk. Yale University, New Haven, CT.

Gallium-67 imaging for detection of hilar and mediastinal lymph node metastases from primary lung carcinomas has been advocated by several authors. Based on these studies, a procedure was proposed in which mediastinoscopy could be avoided in patients whose primary lung carcinomas concentrated gallium with no abnormal gallium concentration in the hilum or mediastinum. Our study was undertaken to determine the sensitivity and specificity of this gallium procedure in our clinic.

In our prospective series 47 individuals had preoperative gallium studies. 9-10 milliCuries of Ga-67 citrate was injected and images obtained at 48 to 72 hours using both a Searle Pho/Con tomographic instrument and a Searle LFOV camera with multipeak spectroscopy. Each image was independently scored for abnormal gallium concentration in the thorax and mediastinum by two experienced observers without knowledge of the clinical stage of disease. As in the method described in previous reports we grouped the hilar and mediastinal zones for final determination of sensitivity and specificity. The accuracy of each study was determined by site-by-site analysis of tissue diagnoses from the surgical specimens.

Thirty-eight studies were included in the final analysis after exclusion of small cell (oat cell) carcinomas and non-primary lung tumors. Our sensitivity for gallium detecting the primary tumor was 91%. For detection of hilar or mediastinal metastases the sensitivity was 55%, specificity 63%, and accuracy 60%. Thus we have been unable to confirm the very favorable results reported by others in detecting metastatic disease in hilar and mediastinal nodes from primary lung carcinomas.

GALLIUM-67 CITRATE (Ga-67) IMAGING, HISTOLOGIC SUBTYPES, AND SURVIVAL IN HISTIOCYTIC LYMPHOMA. J. E. Freitas, M. L. Brown+, E. G. Bernacki, R. H. Nishiyama* and B. Schnitzer*. William Beaumont Hospital, Royal Oak, MI, *University of Michigan Medical Center, Ann Arbor, MI, and +Mayo Clinic, Rochester, MN.

To assess the relationship of Ga-67 lesion detection rate, histologic subtype and survival, the medical records, Ga-67 scans, and tissue histology of 57 patients with biopsy-proven histiocytic lymphoma were reviewed. All patients fulfilled the following criteria: 1) Pathologic tissue was available for histologic subclassification. 2) 48-72 hour scan obtained after intravenous injection of 3-5 mCi of Ga-67, and 3) a minimum follow-up of 1.5 years. The 57 patients were divided into 5 histologic subtypes: large cell non-cleaved (LNC), large cell cleaved (LC), mixed (M), pleomorphic (P), and blastic (B). Each group underwent site-by-site GA-67 lesion detection analysis compared to disease extent based on pathologic, surgical, radiographic, and clinical criteria. Patient survival was determined by medical record review and patient contact. All patients were treated by standardized protocol based on staging.

Because of its small size (2 patients) and paucity of positive sites (4), the B group was excluded from analysis. Site-by-site Ga-67 sensitivity pre-treatment was 67% (total series), 80% (LNC), 40% (LC), 66% (M), and 72% (P) respectively. Two year survival was 56% (total series), 52% (LNC), 75% (LC), 83% (M) and 33% (P) respectively. Ga-67 sensitivity for LNC and P versus LC was significant ($P < 0.01$) by X-2 tests as was survival of M versus P($P < 0.01$).

Histologic subclassification of histiocytic lymphoma has value for it can predict differences in survival and Ga-67 site-by-site lesion detection.

RADIOLABELLED ORNITHINE AS A MARKER OF CANCER. M.M. Webber, D.C. Buffkin, A.D. Schwabe, G. J-F. Juillard, L.R. Bennett, and R.C. Verma. UCLA School of Medicine, Los Angeles, CA.

Ornithine is an ubiquitous amino acid, the metabolism of which appears to be closely associated with the process of growth. The metabolism of L-(1-C-14)ornithine monohydrochloride was studied in patients with histologically proven diagnoses of cancer and in normal volunteers in order to preliminarily assess the efficacy of utilizing radiolabelled ornithine as a marker of cancer.

Following the i.v. injection of 8 uCi C-14 ornithine, the decarboxylation of ornithine was monitored for a 2.5 hour period utilizing the vibrating reed electrometer-ionization chamber model of Tolbert, as modified by Davidson and Schwabe. Thirteen normal subjects ranged from 7.3-33.3% of the administered dose being recovered, displaying a mean of 14.16% and a S.D. of ±6.48%. Ten patients, tested before initiation of therapy, ranged from 18.2-32.1%, displayed a mean of 23.02% with a S.D. of ±4.52%. Application of the t-test indicates a confidence level >99.5% that a significant difference exists between the means. Sensitivity of this test is 100%, while specificity is 92.3%. Re-testing of two normal volunteers showed little or no change in ornithine metabolism over a 2-5 month period. Results from testing three cancer patients before and after therapy correlate well with the clinical response.

Our observations suggest that in normal individuals ornithine metabolism proceeds quite slowly. In the patient with neoplasia, however, the higher utilization suggests that altered ornithine utilization may be a very sensitive test for malignancy.

POSITRON IMAGING FEASIBILITY STUDIES: I. SELECTIVE TUMOR CONCENTRATION OF ^{3}H-THYMIDINE, ^{3}H-URIDINE, AND ^{14}C-2-DEOXY-GLUCOSE. S.M. Larson, Z. Grunbaum, and J.S. Rasey. Seattle Veterans Administration Medical Center and University of Washington, Seattle, Wa.

Accelerated glycolysis and nucleic acid synthesis may be exploited to provide improved tumor imaging based on positron emission tomography. Som et al found active concentration of ^{18}F-2-fluoro-deoxyglucose by a spontaneous dog seminoma and several mouse tumors after intravenous injection of the radiotracer (J. Nucl. Med. 20:662, 1979). We have extended these studies to a well characterized animal tumor model, the EMT-6 sarcoma, and have evaluated in addition the tumor uptake of nucleic acid precursors. Animals with solid EMT-6 tumors ranging from 50-200 mg were selected for study. Ten animals per group received intravenous injections of one of the following tracers: 2-deoxy-D[]-^{14}C]-glucose (sp.ac.=54 mCi/mM), 10 µCi per mouse; [5-^{3}H]-uridine (sp.ac.=29.7 Ci/mM) or [methyl-^{3}H]-thymidine (sp.ac. =2 Ci/mM), 25 µCi per mouse. Animals were sacrificed at 1 hr after injection. The amount of radioactivity in blood, liver, kidney, muscle and tumor was determined after combustion of the tissues. To another group of 6 tumor bearing mice, 2.0 µCi ^{67}Ga-citrate was injected. These animals were sacrificed at 48 hrs because previous work had

shown that ^{67}Ga tumor-to-blood ratios reached a stable maximum at this time. For the ^{3}H and ^{14}C-labeled substrates, absolute uptakes in tumor and tumor-to-blood ratios were as high at 1 hr after intravenous injection as comparable maximum values achieved for ^{67}Ga-citrate at 48 hrs after intravenous injection. Thus, positron labeled analogues of thymidine, uridine and 2-deoxyglucose should be useful radiopharmaceuticals for tumor imaging by positron emission tomography.

CUTANEOUS LYMPHOSCINTIGRAPHY: EVALUATION OF LYMPHATIC DRAINAGE PATTERNS IN TRUNCAL MELANOMA. R.C. Kline, M.J. Tuscan, D.P. Swanson, J.H. Thrall, J.E. Niederhuber, University of Michigan Medical Center, Ann Arbor, MI.

Truncal melanoma, which accounts for 25% of all melanoma, has a poor prognosis. Most authorities advocate wide local excision of the primary with lymph node dissection of the at-risk axilla or groin. Drainage has conventionally been predicted on the basis of proximity to the midline and "Sappey's line", which runs 2 cm above the umbilicus circumferentially to the spinous process of L2 or L3. Lesions within 2.5 cms of either line are considered to have bidirectional drainage. The usefulness of this anatomic approximation is limited, however, by the high variability of lymphatic drainage.

In order to delineate actual lymphatic drainage from the primary site, cutaneous lymphoscintigraphy was performed in 26 patients with truncal melanoma. All had had punch, incisional, or simple excisional biopsy before study. 4 mCi of Tc-99m sulfur colloid (24 patients) or Tc-99m antimony sulfide colloid (2 patients) were injected intradermally at multiple sites around the lesion. Scintigrams were obtained 4 and 24 hours post injection.

Findings on scan were consistent with anatomical predictions in 11/26 (42%) patients. In 5/26 (19%) patients the scintigram showed drainage to fewer regions than predicted anatomically. In 10/26 (38%) patients colloid drainage was found in more regions than predicted anatomically.

Cutaneous lymphoscintigraphy is valuable in the preoperative evaluation of patients with truncal melanoma. Furthermore, the technique should prove of use in patients not undergoing dissection, since at-risk sites can be identified and followed closely.

BRONCHOSCOPIC TUMOR DETECTION USING A MINIATURE RADIATION DETECTOR AND COBALT-57 BLEOMYCIN. J.M. Woolfenden, W.S. Nevin, H.B. Barber, and D.J. Donahue. University of Arizona Health Sciences Center, Tucson, AZ.

A 2.4x10 mm sodium iodide detector has been constructed and used with a tumor-seeking tracer during fiberoptic bronchoscopy. The goals are to locate small tumors, particularly submucosal ones, and to find the source of malignant cytology. Standard external imaging is performed 24 hours after intravenous injection of 1 mCi Co-57 bleomycin; bronchoscopy is then done. The detector, coupled to an external photomultiplier tube by a flexible fiberoptic light guide, is passed through the bronchoscope channel, and counts are taken at standard sites throughout the bronchial tree. Thirteen patients have been studied and have pathological confirmation of tumor; 1 had 2 tumors. Of the 14 tumors identified, 7 were identified by the detector, 7 were visible to the bronchoscopist, and 8 were evident on radiograph; 3 were not identified by any of these methods. The detector located 3 submucosal tumors; 1 tumor, in a patient with positive sputum cytology, was found only by the detector. The smallest tumor found by the detector was 6x6 mm; a 3x3 mm tumor in the same patient was missed. There has been 1 apparently false-positive detector reading.

These preliminary results suggest that detector sensitivity for tumor detection is similar to that of bronchoscopy and chest radiography, and that bronchoscopically invisible submucosal tumors and occult sources of malignant cytology can be found in some patients. Further studies are in progress to assess minimum detectable tumor size and to define further the sensitivity and specificity of the technique.

Tl-201 SCINTIGRAPHY IN POST-OPERATIVE PATIENTS WITH THYROID CANCER — A COMPARATIVE STUDY OF ^{131}I. N. Tonami, K. Hisada, T. Aburano and H. Seto. Kanazawa University School of Medicine and Toyama College of Medicine and Pharmacy, Kanazawa and Toyama, Japan.

We have reported that ^{201}Tl was strongly concentrated in primary lesions of thyroid cancer and also concentrated in metastatic lesions in patients with untreated thyroid cancer. These observations implied that ^{201}Tl might be a suitable radiopharmaceutical to survey affected lesions in post-operative patients as well and we performed ^{201}Tl scintigraphy to visualize malignant lesions in 30 post-operative patients with thyroid cancer. The results were compared with those of ^{131}I and/or ^{99m}Tc pertechnetate scintigraphy. Out of 9 patients having malignant lesions among 16 patients without normal thyroid tissue, ^{201}Tl concentration was observed in 7 patients, while ^{131}I concentration was observed in only 3 patients. There was no case which showed a positive concentration of ^{131}I and a negative concentration of ^{201}Tl. Tl-201 concentration was seen in all of 6 focal lesions in 6 patients and metastatic lung lesions in one patient. Metastatic lymph nodes were visualized by ^{201}Tl in two of 4 patients. On the other hand, ^{131}I concentration was seen in 2 of 6 focal lesions in 6 patients and metastatic lung lesions in one patient. Metastatic lymph nodes were visualized by ^{131}I in one of 4 patients. All of 5 patients having malignant lesions among 14 patients with remaining normal thyroid tissue showed positive concentrations of ^{201}Tl. ^{201}Tl scintigraphy can be performed without any preparations and our results indicate that ^{201}Tl scintigraphy might be a useful procedure to depict residual and recurrent lesions regardless of the presence of normal thyroid tissue.

BREMSSTRAHLUNG IMAGING OF INTRAPERITONEAL P-32 DISTRIBUTIONS. D.C. Sullivan, C.C. Harris, J.L. Currie, W.T. Creasman, R.H. Wilkinson, Jr., and F. Bagne. Duke University Medical Center, Durham, NC

With the introduction of chromic phosphate P-32 suspension for intracavitary therapy, the distribution of the P-32 material has been inferred from the distribution of some Tc-99m-labeled agent such as sulfur colloid. It has been generally accepted that bremsstrahlung imaging of the beta-emitting P-32 would be unsatisfactory. We have imaged intraperitoneal P-32 in 14 patients, 7 of whom received a bolus injection, and 7 of whom received a premixed 500 ml infusion. A large-field gamma camera with a high-energy collimator and an energy window of 100-450 keV was used. Images of sufficient resolution to evaluate distribution have been obtained from time of infusion to 7 weeks post-infusion. Immediately following instillation of a well-mixed suspension (in 500 ml of normal saline), the P-32 distributions show movement, with position changes, to dependent regions of the peritoneal cavity. Later P-32 images show fixed patterns which change little with time. Small focal concentrations appear within 3-24 hours; these may represent activity in mesenteric lymph nodes. We have further determined that 1. chromic phosphate P-32 particles will not necessarily be suspended in liquid volumes unless mixed and stirred, 2. particles will settle out of undisturbed suspensions, and 3. there is insignificant sticking of particles to glass or plastic surfaces even after several hours suspension in normal saline. For these reasons we now premix chromic phosphate P-32 suspension with 500 ml of saline in the hope of obtaining better intraperitoneal dispersion.

4:00-5:30 Room 3037

CLINICAL

PERIPHERAL VASCULAR

Session Chairman: Michael Siegel
Session Co-Chairman: Milo M. Webber

TOURNIQUET PRESSURE (TP) AND RADIONUCLIDE VENOGRAPHY (RNV). R.C. Verma, J. Sabbe, D. Ayers, C. Rowe, and J. Eisenman. *

In a previous study of RNVs with graduated TP in non-thrombophlebitic subjects, we had shown that: a) calf deep veins (DV) were visualized in 19/20 of subjects without above-ankle tourniquet (AAT), b) in 20%, flow through DV was occluded at pressures which did not affect SV flow, c) no correlation existed between SV occlusive pressure and systolic, diastolic or mean brachial or popliteal BP and d) at TP >50 mmHg, flow through previously nonvisualized DVs was demonstrated upon release of TP. The above study was extended to compare results of graduated BP cuff TP (BPT) with manual rubber tubing (RTT) AAT and above-knee tourniquet (AKT).

Changes in venous flow produced by a lightly tied RTT were equivalent to those resulting from cuff TP of under 50 mmHg and occluded just 3/15 of the SVs. The tightly tied RTT significantly diminished flow through SV and led to sluggish flow through DV and as with the cuff, on release, flow through previously nonvisualized DV was demonstrated. Moreover, a tight AKT contributed more to diminishing flow through SV (without affecting DV flow) than tightening the AAT or an additional AAT. It might be that the difference in depth of the DV compared to the SV in the ankle is not as great as in the thigh; hence, beyond a critical pressure, flow through both DV and SV is occluded.

Based upon the above comprehensive study,it is recommended that: a) ideally most patients for RNV be studied without tourniquets, b) if DV are not or poorly visualized, tight RTT above ankle and knee must be employed to occlude flow through SV and direct it through DV and c) flow must also be imaged during release of TP because some DVs in calf and thigh are visualized in this phase only.

*Olive View Section, UCLA School of Medicine, Los Angeles.

FIBRINOPEPTIDE A (FPA) IN PATIENTS WITH SUSPECTED AND DOCUMENTED VENOUS THROMBOSIS. G.L. DeNardo, S.J. DeNardo and A.W. Rose. University of California Davis Medical Center, Sacramento, CA. Supported in part by American Cancer Society Grant #PDT 94B.

FPA is a peptide specifically cleaved from fibrinogen by thrombin during the course of fibrin production. Therefore, it should be elevated in all disorders associated with fibrin deposition, and specifically venous thrombosis. Because its $T_{\frac{1}{2}}$ is 2-3 minutes, elevated FPA levels reflect currently active disease.

Presence or absence of venous thrombosis was determined by contrast venography, I-125-fibrinogen uptake test and/or I-123-fibrinogen scintigraphy. FPA levels were measured on 51 samples from 50 patients with suspected or documented venous thrombosis. FPA radioimmunoassay was performed by incubating the supernatant (after ethanol precipitation of plasma fibrinogen) with FPA antiserum and I-125-desaminotyrosyl-FPA. After separation, the bound FPA fraction was compared to a standard curve. The range of FPA for normal control subjects was <0.2-2.7 ng/ml (mean=1.5 ng/ml) and for normal women on contraceptive drugs, 3.4-4.4 ng/ml (mean=3.9 ng/ml). The range of FPA in documented venous thrombosis was 1.5-41 ng/ml, whereas the range was <0.2-3.4 ng/ml in patients with suspected venous thrombosis subsequently proven not present. 95% of patients with documented venous thrombosis had elevated FPA levels including 4 patients treated with anticoagulants, but the latter had only mildly elevated FPA levels. FPA levels dramatically decreased when patients with venous thrombosis were treated with heparin.

Although non-specific, FPA radioimmunoassay appears useful in the diagnosis and treatment of venous thrombosis.

FUNCTIONAL ALTERATIONS OF MUSCLE PERFUSION IN TYPE II MUSCLE ATROPHY: DEMONSTRATION BY LOWER EXTREMITY PERFUSION SCANS. **P.A. Domstad, Y.C. Choy, E.E. Kim, and F.H. DeLand. University of Kentucky Medical Center, Lexington, KY.**

Significant progress in the clinical assessment of peripheral vascular disease has resulted from the use of radionuclide scans to evaluate alterations of blood flow through small vessels. Not widely recognized is that functional changes in muscle perfusion can cause abnormal tracer distribution in these perfusion scans despite a demonstrated lack of vascular degenerative changes or vasculitis. Two patients with Type II muscle atrophy and normal vessels on muscle biopsy were examined in whom abnormal lower extremity perfusion scans were obtained after the administration of Tc-99m labeled human albumin microspheres directly into the femoral arteries. The pathophysiologic mechanism underlying the altered perfusion pattern may be similar to that causing the bone scan changes seen in Sudeck's atrophy. These case studies illustrate the use of this technique for delineating muscle groups affected by a myopathic process. Muscle perfusion scans can be used as an aid in selecting biopsy sites and may provide a means of following the response to therapy.

COMPARISON OF I-125 FIBRINOGEN UPTAKE TESTING (FUT) AND CONTRAST VENOGRAPHY IN THE DETECTION OF DEEP VEIN THROMBOSIS (DVT) IN PATIENTS WITH HIP SURGERY OR FRACTURE. L.S.Malmud, N.D.Charkes, P.T.Makler, Jr., J.Reilley, S.Levin. Temple University Hospital, Philadelphia, PA.

Venous thrombo-embolic disease is the most frequent complication of hip fracture or surgery. Previous studies have suggested varying degrees of sensitivity for the FUT. The purpose of this study was to determine the sensitivity and specificity of the FUT compared to venography in 143 consecutive patients treated with low dose heparin and undergoing both procedures. The FUTs were performed using either Abbott or Amersham Fibrinogen. Contrast venography was routinely performed on the 8th day of the FUT or earlier if the FUT was abnormal. Compared to venography, the sensitivity of the FUT over-all was 87.3% and the specificity 86.3% with a predicted value of 83.3% ($p<.001$). For hip fracture, the over-all sensitivity was 90.9%, specificity 87.5%, with an over-all accuracy of 88.9% ($p<.01$). In patients undergoing hip replacement, the sensitivity was 88.6%, specificity 87.0%, and over-all accuracy 87.6% ($p<.01$). The FUT became abnormal within 3 days in approximately 60% of the patients who had abnormal tests.

Forty % of patients with fractured hip developed DVT. After negative venography 16 patients developed positive FUTs in the same leg which had undergone venography. Four of those 16 had repeat venography, demonstrating new thrombi in 50%, or 5% of the total studied by contrast venography.

The I-125 FUT is a clinically useful, sensitve diagnostic technique in patients at high risk for developing deep venous thrombosis. These data suggest that the FUT should be a routine study in patients with hip fracture in whom low dose heparin is not effective in preventing DVT.

THALLIUM-201 VENOGRAPHY. E.B. Silberstein, P.J. Robbins. The University of Cincinnati Medical Center and FDA Nuclear Medicine Laboratory, Cincinnati, OH.

Serendipitous visualization of a consistent linear structure in the arm and shoulder of patients having thallium myocardial scintigraphy led to the investigation of this phenomenon in 20 patients, 17 of whom were having stress thallium-201 myocardial scintigraphy with 3 injected at rest. It was found that the upper arm structure was visualized only on the side of injection, persisted for at least 40 minutes post-injection, and was never seen on the contralateral side. The phenomenon occurred whether the injection was made directly into the median cubital vein, through 0.9% NaCl or 5% dextrose in water. Important asymmetries were seen in patients with thrombophlebitis receiving bipedal injections.

To demonstrate that the structures visualized with thallium-201 were veins Sprague-Dawley rats were injected with the radionuclide in one femoral vein. Then the iliac vein proximal to the injection site and the contralateral iliac vein were carefully excised and washed for counting and comparison with whole blood thallium-201 counts. In rats there was a significant ($p<0.05$) increase in iliac vein counts on the injected side as compared to the contralateral side and to intra-cardiac blood counts.

The animal and human data indicate thallium uptake on or into veins on the ipsilateral side of injection. Experiments are underway to determine if this is by active transport and to further correlate thallium with contrast venography in patients.

PROGNOSTIC EVALUATION OF ISCHEMIC ULCERS: Tl-201 PERFUSION DATA VERSUS DOPPLER ULTRASOUND. M.E. Siegel, C.A. Stewart, P. Kwong and I. Sakimura. LAC-USC Medical Center and Rancho Los Amigos Hospital, Los Angeles, CA

The purpose of this paper is to present a technique for non invasively and objectively determining the relative perfusion of ischemic ulcers using Tl-201 and comparing its prognostic ability with that of doppler ultrasound.

Twenty nine ulcers were studied in 26 patients. All patients had a perfusion scan using 1.5 mCi of Tl-201 and in 27 ulcers of 23 of the patients standard doppler ultrasound evaluation of the lower extremities was performed. Objectively the Tl-201 distribution is quantitated via point counting over the ulcer and surrounding area from which the degree of hyperemia of the ulcer is determined. Established doppler criteria of at least 0.35 for non diabetics and 0.45 for diabetics was used to predict ulcer healing ability. The previously reported ratio of greater than 1.5:1 for the degree of hyperemia as suggested by Tl-201 was used as the criteria for ulcer healing.

Using the above criteria Tl-201 perfusion data correctly predicted healing potential in 20 of 23 healed ulcers. Doppler alone predicted only 14 of 21 of the eventually healed ulcers with a true negative rate of 82% versus a 95% rate for the Tl-201. Doppler predicted non healing in 3/6 ulcers with a true positive rate of 30% while Tl-201 predicted 5/6 with a true positive rate of 62%.

The study suggests the Tl-201 perfusion scan data is a useful non invasive test for determining ulcer healing potential and may be more sensitive and specific than doppler ultrasound.

201-THALLIUM EXERCISE SCINTIGRAPHY OF LEG MUSCLE - USEFUL FOR EVALUATION OF PERIPHERAL VASCULAR DISEASE? I.B. Tyson, E.W. Bough, E.J. Gandsman and D. North
The Miriam Hospital and Brown University, Providence, R.I.

Adjunctive leg muscle images were obtained in 22 patients undergoing Tl^{201} myocardial scintigraphy after upright bicycle exercise. All patients received 1.5 to 2.0 mCi of Tl^{201} intravenously one minute prior to termination of exercise and were imaged with a large field gamma camera and low energy all-purpose collimator. Scintigrams (125,000 counts) of the thigh or calf muscles were obtained immediately after exercise (Ex) and redistribution (Redis) cardiac imaging and stored in a minicomputer. Of 16 patients with no known peripheral vascular disease, 8 underwent anterior thigh scintigraphy and 8 posterior calf scintigraphy. From selected regions of interest over both the lateral and medial muscle groups of the thighs or calves, left to right (L/R) ratios were calculated from the Ex and Redis images. The L/R ratios ($\bar{m} \pm sd$), including both medial and lateral groups, for calf and thigh scintigrams were:

	L/R ratio		
Scintigrams	Ex	Redis	p (paired t test)
thighs	0.99 ± .05	1.01 ± .07	NS
calves	1.03 ± .07	1.03 ± .09	NS

Leg scintigrams (2 of calves, 4 of thighs) were also obtained in 6 patients with suspected peripheral vascular disease either from past history or current symptoms. For all 6 patients, the Ex L/R ratio for at least one muscle group fell outside a range of mean ± 2sd. In 3 of these patients the L/R ratio had returned to within 1sd of the mean in the Redis image.

It is concluded that Tl^{201} leg scintigraphy may have potential for use in evaluation of peripheral vascular disease.

THE REDISTRIBUTION RELATIONSHIP BETWEEN THE REST AND DELAYED Tl-201 PERIPHERAL PERFUSION SCAN. M.E. Siegel and C.A. Stewart. LAC/USC Medical Center, Los Angeles, CA.

The purpose of this study is to define the relationship between the state of perfusion represented by the delayed Tl-201 exercise perfusion study and the resting study.

To maximize the change between rest and stress perfusion studies, 10 patients with no known peripheral vascular disease were utilized. In addition, 5 patients with peripheral vascular disease were also studied. Each patient received a 1.5 mCi dose of Tl-201 during physiologic stress and scans, and point counting of the thighs, knees, calves, and ankles were obtained immediately and hourly up to 6 hours post injection. The point counting data was used to quantify the distribution of perfusion between muscle masses and between muscular and non-muscular regions. One week later, at rest, the patients received a second dose, and scans and point counting were repeated.

Subjectively reviewing the rest, stress, and delayed stress scans, there was some indication in the abnormals and less indication in the normals of redistribution from the stress to the rest pattern. Objectively, there were significant differences in the delayed stress perfusion ratios compared to those of the rest studies. Reviewing the graphed perfusion ratios, there appeared to be a tendency to return to the resting levels in both normals and abnormals, but not reaching these levels during the period of observation.

Using the reasonable time frame of this study, the delayed stress scan does not equal the distribution of perfusion at rest, yet, the changes which occur may be adequate for clinical utility.

MEASUREMENT OF LIMB BLOOD FLOW AT EXERCISE - A NEW TECHNIQUE. J.J. Steinbach, D. Pendergast, P. Cerretelli, M. Blau, and R. Wicks. Veterans Administration Medical Center and The State University of New York at Buffalo, Buffalo, NY.

Present physiological measurements of muscle blood flow at exercise are complicated by the physical nature of NaI scintillation detectors. A new technique using a small (10 gm wt) CdTe semiconductor detector is described.

Following intramuscular injection of 70-80 μCi of Xe-133 in saline (0.1-0.2 ml), measurements of blood flow are obtained at rest and at various workloads. The technique was initially validated by comparing the values obtained by the Xe-133 clearance with those obtained by the intra-arterial microsphere technique in treadmill trained dogs. There was good relative correlation between the two methods ($p=0.85$). However, the values obtained by the Xe-133 clearance were lower by a factor of two.

Blood flow measurements of the deltoid, biceps, and brachioradial muscles were done on 4 volunteers using arm cranking exercise at various workloads. Blood flow of the gastrocnemius and vastus lateralis muscles were done on 6 and 8 volunteers respectively using a bicycle ergometer. Muscle blood flow (ml/g/min) at various workloads (rest - 175 watts) was:

	Rest	50	75	125	175
Biceps	.04-.06	.35-.4	.45-.5	.45-.5	
Gastrocn.	.02-.03	.1 -.18	.18-.3	.2 -.3	.2-.3

The method appears to be exceptionally suited for physiological measurements of blood flow in the exercising muscle. The high increase in blood flow at low workloads suggests that it will also be useful in patients with low exercise tolerance.

INDIUM-111 PLATELET IMAGING FOR THE IN-VIVO DETECTION OF THROMBI IN ABDOMINAL ANEURYSMS AND PSEUDO-ANEURYSMS AND FOR EVALUATION OF PLATELET ACTIVE DRUGS. J.L. Ritchie, J.R. Stratton, B. Thiele, L.A. Harker, and G.W. Hamilton. Seattle V.A. Medical Center and University of Washington School of Medicine, Seattle, Wa.

Gamma camera imaging of In-111-oxine labeled platelets (PLT) may detect abnormal PLT deposition in humans and assess platelet active drugs in vivo. We studied 15 pts on no platelet drugs who were at risk for thrombi from abdominal aortic aneurysm (AAA) (12 pts), pseudoaneurysms at vascular graft anastamotic sites (2 pts), or femoral aneurysms (1 pt), as defined by ultrasound or angiography. Five pts were restudied after 7-10 days of ASA (325 mg tid) plus dipyridamole (DP) (75 mg tid), and 2 pts after 7 days of sulfinpyrazone (200 mg qid). Imaging was performed at 2 amd 24 hrs after autologous PLT labeling. Abnormal PLT deposition was defined as activity which increased over time as blood pool activity decreased. Both anterior analog images and computer profiles were used.

At baseline, 11 pts had positive studies and 4 pts had negative studies; the 4 negative studies were all pts with AAA. No pt had decreased PLT deposition on ASA and DP. Both pts studied on sulfinpyrazone had decreased PLT deposition. Abnormal PLT deposition was seen in 1 pt after Dacron graft insertion for AAA throughout the graft. In 1

case, thrombus removed at surgery had 3.5 times In-111 activity in the endothelium vs. the outer half. By electron microscopy, PLT were present in only the endothelial half.

This large vessel example demonstrates the efficacy of PLT imaging for identifying thrombi and for assessing in vivo antithrombotic drug effect and thrombogenicity of prosthetic materials.

4:00-5:30 Room 3039

RADIOPHARMACEUTICAL CHEMISTRY

TUMOR

Session Chairman: Raymond L. Hayes
Session Co-Chairman: Max Lin

A COMPARISON OF RADIOPHARMACEUTICALS FOR LYMPHOSCINTIGRAPHY. B.M. Gallagher, M.L. Delano, R. Watt, L.L. Camin. Radiopharmaceutical Research, NEN Corp., N. Billerica, MA

The clinical application of radiocolloids for planning radiation therapy and the delineation of drainage pathways may provide a reliable and convenient agent for the management of patients with malignant disease. Although several reports exist on the use of selected radiocolloids for lymphoscintigraphic studies, relatively little comparative data are available on the absorption, lymphatic sequestration and overall biokinetics of these agents in the same animal model. This study compared these parameters for colloidal gold-198 (Au-198) and Tc-99m labeled Sb_2S_3, phytate, $(SnOH)_2$, microaggregated albumin (μAA), minimicroaggregated albumin (mμAA) and human serum albumin (HSA) in a rat model. The absorption from the footpad following subcutaneous administration showed that HSA > mμAA > Sb_2S_3 > Au-198 ≅ phytate > μAA > $Sn(OH)_2$. The biokinetics and absolute uptake by popliteal and lumbar nodes showed that mμAA ≅ Sb_2S_3 ≥ Au-198 > phytate > μAA > HSA ≅ $Sn(OH)_2$. Both Sb_2S_3 and mμAA had an excellent lymphatic uptake, with mostly liver and spleen background for Sb_2S_3 and less liver and higher kidneys for mμAA. The blood activity for Sb_2S_3 was greater than for mμAA and the overall biological clearance was slower for Sb_2S_3. Excellent images of the parasternal lymph nodes in rabbits could be obtained with mμAA following subcostal injection. The results of these studies suggest mμAA to be an excellent lymphoscintigraphic agent because of a high absorption from the injection site, excellent lymph node uptake, a rapid metabolism and biological clearance, all of which reduce the radiation burden to the patient and lastly, the ease of preparation for use within minutes after reconstitution with generator eluate.

TISSUE DISTRIBUTION STUDIES OF 17β (16α I-125) IODOESTRADIOL IN RATS BEARING MAMMARY ADENOCARCINOMA. W.J. Shaughnessy, S.J. Gatley, T.J. Simpkin, and L.M. Lieberman. The University of Wisconsin Hospital, Madison, WI

A radioiodinated analog of estradiol, 17β (16α I-125) iodoestradiol (I-125 E2) has been synthesized by Hochberg (Science 205:1188-1191) who presented evidence to suggest that the compound concentrates in rat uteri in vivo. We have investigated I-125 E2 in female Fischer rats bearing 13762 mammary adenocarcinoma (Mason Research Institute).

Groups of three animals were injected intravenously with 2 μCi each and killed at intervals of 0.25, 1, 2, 4 and 8 hr. Eighteen tissues were sampled and examined for radioactivity. The transplanted mammary adenocarcinoma concentrated I-125 maximally at 0.25 hr, being 0.25% dose/g, decreasing to 0.1%/g at 1 and 2 hr and 0.04%/g at 8 hr. The highest tumor/blood ratio was 2.3 at 4 hr.

The uterus showed 0.87% dose/g concentration at 0.25 and 1 hr, reducing to 0.5%/g at 4 hr and 0.18%/g at 8 hr. The tissue with the highest concentration at 0.25 hr was the adrenal gland showing 2.6% dose/g. Adrenal/blood ratio was maximal at 0.25 hr (16.6) while uterus/blood ratio was maximal at 4 hr (14.3).

Our findings confirm those of Hochberg, suggesting that I-125 E2 binds to estrogen receptors in the uterus. The relatively high uptake of I-125 in the adrenal gland at 0.25 hr warrants further investigation. A potential estradiol adrenal imaging agent labeled with I-123 would be highly desirable as suggested by Sturman et al. (J Nucl Med 16:77-79) who showed tritiated estradiol uptake in the dog adrenal to be maximal 3-7 min post injection at 0.31% dose/g.

I-131 DNase, A POTENTIAL TUMOR IMAGING AGENT. S.N. Reske, K. Vyska, K. Reske+, L.E. Feinendegen. Institute of Medicine Nuclear Research Center, Jülich, +Institute for Immunology, University Mainz, FR Germany.

DNase binds specifically and strongly to actin at a molar ratio of 1:1. Actin, a major component of the cytosceleton in eucaryotic cells, underlies the cell membrane as a network of microfilaments. Radioactively labelled DNase may therefore serve as indicator for intracellular actin in tissues where the cell membrane is damaged. Commercially available pancreatic DNase I was labelled with I-131 by the chloramine-T method. For tissue-distribution studies 1.5 μCi I-131-DNase (ID) was injected i.v. in 10 female NMRI mice bearing a transplanted sarcoma 180, a tumor known to develop a rather large central necrotic area. Organs were assayed for radioactivity 1 and 3.5 hr p.i. in a well scintillation counter. In addition 15 μCi ID was injected i.v. in 5 sarcoma 180 bearing NMRI mice for whole body imaging. The scans were taken between 10 minutes and 3.5 hrs p.i. with a γ-camera equipped with a pinhole collimator in p.a. projection. ID is accumulated in the tumor tissue (1.5 - 2.0 % dose/g tissue). The ratio of the radio-activity in the tumor to the surrounding muscle tissue was 3-5:1. Whole body scintigrams 3.5 hrs p.i. showed a significant accumulation of radioactivity in tumor, thyroid and stomach. In experiments with fluorescamine-labelled ID this compound is mainly associated with morphologically altered cells in tumor tissue 3.5 hrs p.i. The results obtained so far indicate that ID might provide a potential tumor imaging agent.

COMPARISON OF TUMOR AND ABSCESS UPTAKE OF In-111 BLEOMYCIN ANALOGUES WITH Co-57 BLEOMYCINS IN BALB/c MICE. J.E. Baumert*, C.I.Diamanti*, D.A.Goodwin*, L.H.DeRiemer**, and C.F.Meares**. *Veterans Administration Medical Center, Palo Alto, California and **Department of Chemistry, University of California, Davis, California.

Co-57 Bleomycin, a sensitive tumor-imaging compound, has an undesirable physical half-life (270 days). We have modified the Co-59 (stable) chelate of bleomycin A-2 with EDTA and Benzyl EDTA. The resulting bleomycin analogues, BLEDTA and Benzyl BLEDTA, can be labeled with In-111 Cl_3 ($T_{1/2}$ - 2.8 days). This study employs a new mouse model to compare tumor and abscess uptake of In-111 BLEDTA and In-111 Benzyl BLEDTA with Co-57 Bleomycin A-2, Co-57 Bleomycin A-2DM, Ga-67 citrate, and In-111 Cl_3. Each mouse had a KHJJ tumor in one flank and a sterile abscess in the other. Tumor, abscess and organ samples were obtained 24 hr after each compound was injected.

The Co-57 Bleomycins had the lowest tumor uptakes. They were significantly less ($p<0.001$) than the In-111 Bleomycin analogues and much less than Ga-67 citrate and In-111 Cl_3. However, the tumor/blood ratios were much higher ($p<0.001$) than the In-111 Bleomycin analogues, Ga-67 citrate and In-111 Cl_3. The tumor/RE system (liver, spleen, BM) ratios were equally favorable for Co-57 Bleomycin A-2DM and In-111 Benzyl BLEDTA. Both were more than 7X as high as those found with Ga-67 citrate and In-111 Cl_3. The tumor/abscess ratios were the highest in the Co-57 Bleomycins (3:1) and lowest in the In-111 Bleomycin analogues (1.2:1).

We conclude; (a) The Co-57 Bleomycins have the highest target-to-non-target ratios and are the most specific for tumor, (b) The In-111 Bleomycin analogues have similar target-to-non-target ratios and are the least specific for tumor, and (c) Ga-67 citrate and In-111 Cl_3 have the lowest target-to-non-target ratios in the reticuloendothelial system.

IN VIVO RECEPTOR BINDING OF RADIOLABELED ESTROGENS, R.E. Gibson, A. Mazaitis, B. Francis, R. Patt, W.C. Eckelman, R.C. Reba and H. O'Brien. George Washington Univeristy Medical Center, Washington, D.C. and Los Alamos Scientific Laboratories, Los Alamos, N.M.

Three radiohalogenated derivatives and two tritium labeled estrogens with a range of affinity constants were evaluated as radioindicators for estrogen receptors. These receptor binding radiotracers may be useful in the detection of estrogen dependent malignancy. In vitro receptor assays using immature rat uterus showed that the radiolabeled estrogens had receptor affinities ranging from 10^7 M^{-1} to $2x10^9 M^{-1}$. All concentrated in the uterus of the immature rat; however, based on in vivo displacement studies using excess estradiol, only H-3 estradiol (E), Br-77 bromoethynylestradiol (BEE), and Br-77 bromoethynyl, 11-methoxy estradiol (BEME) showed estrogen receptor binding. I-125 iodohexestrol showed a reported high affinity constant in vitro but nonspecific binding competed effectively with receptor binding in vivo. When the displacement study was carried out in vivo with thyroxine receptor binding was detected. No receptor binding was detected with the antiestrogen CI 625. These results agree qualitatively with a bimolecular model which predicted uterus to blood (U/B) ratios of >1 for all compounds except the antiestrogen. As the model predicts, specific activity plays an important role in the U/B ratio. BEE which had a specific activity of <10 C/mmol had a lower U/B ratio than E which had a specific activity of 100 C/mmol. Further experiments using E at various specific activities confirmed these results. The BEE and BEME are both stable in vitro and in vivo to debromination. Two of the gamma emitting estrogen derivatives BEE and BEME should be useful as probes for estrogen dependent malignancy.

SYNTHESIS OF ^{203}Hg-ESTRADIOL AND ITS BINDING TO MAMMARY TUMORS. J. Shani[1], L.M. Lieberman[2], M. Cais[3], Y. Josephi[3] and M. Shimoni[3]. [1]Department of Pharmacology, The Hebrew University Medical School, Jerusalem, Israel; [2]Department of Radiology (NM), University of Wisconsin Hospitals, Madison, Wisconsin, USA and [3]Department of Chemistry, Technion - Israel Institute of Technology, Haifa, Israel.

Studies on the antigenicity of metallohaptens in metalloimmunoassays (M.Cais et al., Nature, 270:534,1977) indicated that immunorecognition by appropriate anti-estrogen antisera for mercurated estrogens was retained to a reasonable degree despite the stereoelectronic effects of the substituent (M. Cais, Y.Josephi and M.Shimoni, to be published). Similarly, recent glycerol gradient experiments (M.R.Sherman, M.Shimoni F.B.Tuazon and M.Cais, to be published) demonstrated that, along with a high level of non-specific binding, there was a distinct specific binding of mercurated estradiol by estrogen receptors in human breast tumor cytosols. In view of these observations, the γ-emitters ^{203}Hg-2-chloromercuri-estradiol-17β and ^{203}Hg-4-chloromercuri-estradiol-17β were prepared as potential radiopharmaceuticals for selective detection of estrogen-receptor-containing mammary adenocarcinoma, and as a model substrates for similar studies with other metallohaptens. The mercurated estradiols were injected iv into either Sprague-Dawley female rats bearing spontaneous mammary tumors or into Fisher rats transplanted with 13762 mammary adenocarcinoma.The rats were decapitated 1h-4d after the injection and 15 major and endocrine organs were sampled and counted. With blood clearance phases of $T_{½}$ 1.4 and 8 days, binding of the labelled drugs to the mammary tumors was significantly different from the binding to the healthy mammary glands. While the organ/blood ratio for the healthy organs was ∿1, a ratio of 4 (2d post-injection) and 10 (4d post-injection) was obtained for the mammary tumors.

TECHNETIUM-99M TETRASULFOPHTHALOCYANINE AS A POTENTIAL TUMOR SCANNING AGENT. J. Rousseau, D. Autenrieth, and J.E. van Lier. University of Sherbrooke Medical Center, Sherbrooke, Que., Canada.

Phthalocyanine and porphyne derivatives have previously been shown to accumulate in malignant tissue. With the aim of developing a tumor scanning agent we have labeled tetrasulfophthalocyanine (TSPc) with Tc-99m and studied its tissue distribution in healthy and tumor bearing animals.

TSPc-Tc-99m and TSPc-Tc-99 were prepared either by condensation of sulfophthalic acid in the presence of pertechnetate and reducing agent or by direct labeling of TSPc with reduced pertechnetate. Reaction products were purified by ion exchange chromatography and analysed by UV-spectroscopy and ITLC. The in vivo distribution of the purified Tc-99m labeled product was studied in female rabbits and in Fisher 344/CRBL female rats bearing the 13762 mammary adenocarcinoma. The activity distribution in the animals was followed by scintillation scanning. In some instances animals were sacrificed and the individual organs counted.

Scanning experiments in rats bearing a 5 mm nonvascularized tumor in the thigh clearly revealed selective tumor uptake of Tc-99m (tumor/muscle ratio 4:1). The stability of the labeled complex was evident from the absence of activity in the stomach, thyroid and salivary glands of rabbits. The organ distribution however showed an accumulation and fixation of the tracer in renal and hepatic tissue. This may result from the presence of polimeric products in the Tc-99m-TSPc preparation. Studies on Tc-99m-TSPc samples obtained after further chromatographic purification on Sephadex G-25 are in progress.

COMPARISON OF TUMOR LOCALIZING PROPERTIES OF COBALT-57 BLEOMYCIN AND FOUR ANALOGUES: BLEOMYCINIC ACID, PHLEOMYCIN, PEPLEOMYCIN AND TALLYSOMYCIN. J.N. Hall, J.M. Woolfenden, L.S. Rothman and J.D. Douros. University of Arizona Health Sciences Center, Tucson, AZ and National Cancer Institute, Bethesda, MD.

The purpose of this study was to compare bleomycin and other bleomycin-type antibiotics as radiolabeled tumor-seeking agents. Bleomycin and 4 analogues labeled with Co-57 were examined for biological distribution in an established bleomycin-sensitive tumor model, the Ridgway osteogenic sarcoma, transferred by subcutaneous passage in AKD2-F1 mice. Radiolabeling was checked by thin layer chromatography using methanol : 10% ammonium acetate (1:1) as the solvent. Biological distribution studies were performed at 4 and 24 hours after intravenous administration. The following table shows the tumor-to-muscle and tumor-to-blood ratios obtained (average of 5 or more animals):

	4 Hours		24 Hours	
	T/M	T/B	T/M	T/B
Bleomycin	24.6	49.2	29.5	35.9
Pepleomycin	21.4	23.0	61.1	65.4
Bleomycinic Acid	17.9	108.3	41.9	57.8
Tallysomycin	8.8	14.7	25.1	15.9
Phleomycin	13.0	18.2	15.7	47.0

Absolute tumor uptake of the tracer was highest for bleomycin, followed in descending order by pepleomycin, tallysomycin, phleomycin, and bleomycinic acid. Pepleomycin, and possibly also bleomycinic acid, may be superior to bleomycin for tumor localization on the basis of high tumor-to-non-tumor ratios. Studies of pepleomycin in other tumor models are in progress.

F-18-2 and 3-FLUORODEOXY-D-GLUCOSE AS POTENTIAL DIAGNOSTIC TRACERS FOR TUMORS. M.M. Goodman, D.R. Elmaleh, L. Merk, R. Lade, K. Kearfott, D. Varnum, S. Kopiwoda, G.L. Brownell and H.W. Strauss, Mass. General Hospital, Boston, MA

Tumors are known to consume and metabolize extra amounts of glucose for their growth. To determine if this high metabolism rate could be used for tumor localization we studied the biodistribution of two glucose analogs; F-18-2-fluoro-2-deoxy-D-glucose (2-18-FDG) and 3-fluoro-3-deoxy-D-glucose (3-18-FDG) in rats implanted with RT-9 and RT-24 (glioma tumor model). Following IV injection animals were sacrificed at 5, 30 and 60 mins in groups of 6 (see table).

	2-18-FDG				3-18-FDG			
Tissue	30 min		60 min		30 min		60 min	
	M	± SE	M	± SE	M	± SE	M	± SE
Tumor	3.25	.18	2.86	.02	1.83	.18	2.60	.08
Blood	.68	.03	.37	.05	1.96	.02	1.56	.01
Heart	13.70	.51	4.07	1.80	3.02	.05	2.41	.04
Brain	4.05	.12	3.74	.23	1.52	.04	1.21	.36
Liver	.84	.03	.53	.05	1.54	.04	1.21	.01

The uptake at 1 hr in % dose per gram in tumor was similar for both agents 2.86±.02 for 2-18-FDG and 2.60 ± .08 for 3-18-FDG. The clearance of 3-18-FDG from blood is slower than 2-18-FDG which makes the tumor to blood ratio with 2-18-FDG more favorable. However, both agents are potential agents for tumor detection when used with positron tomography techniques.

4:00-5:30 Room 3040

INSTRUMENTATION

COMPUTER TOMOGRAPHY

Session Chairman: John Erickson
Session Co-Chairman: David Pickens

NON-UNIFORMITY AND ARTIFACT CREATION IN EMISSION TOMOGRAPHY
A. Todd-Pokropek*, S. Zurowski** and F. Soussaline**
UCH London UK* Dept de Biologie CEA Orsay France**

All tomographic reconstruction algorithms assume that the values measured on projections are constantly proportional to line integrals through the object to be reconstructed. In emission tomography, one common cause of failure is a result of attenuation. Two other types of failure, considered here, are caused by non-uniformity and spatial distortion of the 'detector'. These have been studied initially by simulation, the results confirmed by practical measurements with a GE 400 T rotating camera tomograph.

For a given area of changed (non-uniform) sensitivity of the detector, a ring artifact is created in the tomogram of amplitude proportional to 1/the distance from the central axis of the detector. Thus very large artifacts can occur along the axis of rotation. These artifacts are also inversely proportional to the size of the area of modified sensitivity. This can be explained by comparing the Fourier transform of 'artifacts' and the object. Uniformity correction is thus normally essential.

As spatial sampling along the projection is increased, a large increase in noise occurs in the gamma tomograms,for constant total counts. This seems to be due in part to the presence of coloured noise created by the data collection system, and seemingly due to differential non-linearity. This has been simulated, and has been found to be a function of total coloured noise power, and not especially to noise at the sampling frequency. This could be improved by using better ADCs. Integral non-linearity (spatial distortion)has been studied, but in realistically noisy situations is not troublesome. Thus several sources of error exist, which are barely noticable in conventional imaging, but which, because of the properties of the tomographic reconstruction, can create severe artifacts and increase in noise in tomograms.

NOISE PROPAGATION PROPERTIES OF THE ECAT POSITRON SCANNER.
F. Soussaline, S. Houle, D. Plummer and A. Todd-Pokropek.
Service Hospitalier Frederic Joliot, Orsay, France.

In positron emission computed tomography, an important statistical limitation is that due to the propagation, during reconstruction, of the random fluctuations arising from the Poissonian distribution of the photon emission from the source. The statistical precision of the ECAT positron scanner (EC&G Ortec) has been investigated in terms of the ratio of the root-mean-square (RMS) uncertainty in the value of a given image pixel over its expected mean value.

Budinger et al (J Comp Assist Tomog 1: 131, 1977) have proposed a relation for this ratio:

$$\frac{RMS}{mean} = K \cdot N^{-1/2} \cdot b^{3/4}$$

where N is the total number of detected counts and b the number of image cells in the object. The constant K is dependent on the reconstruction filter and has been calculated for each of the filters of the ECAT system. At the center of a 20-cm diameter cylinder of uniform activity, the following values for K and for the FWHM d were obtained: 1) high resolution filter: K=0.68 and d=1.57cm; 2) medium resolution filter: K=0.37 and d=1.68cm; 3) low resolution filter: K=0.20 and d=1.92cm; and 4) normal filter: K=0.94 and d=1.46cm. These values are in excellent agreement with those obtained both by actual measurement of cylindrical phantoms and by computer simulation.

CUBIC SPLINE FOR DESIGN OF RECONSTRUCTION FILTERS IN EMISSION COMPUTED TOMOGRAPHY (ECT).
S. Huang, M. Phelps, E. Hoffman, D. Kuhl. UCLA School of Medicine, Los Angeles, CA.

In ECT, due to variability in photon statistics, sampling, and detector FWHM, ability to flexibly adjust reconstruction filter (RF) to reduce noise while maintaining image resolution is highly desirable. Use of cubic splines is investigated to provide design techniques for flexible ECT RF. Frequency response function (FRF) of ECT RF's should be 1) real and symmetric, 2) approximately equal to $|f|$ for $f \approx 0$, and 3) smooth,with response at high frequency adjustable to reduce noise. Thus, ECT RF's can be specified completely by defining the real part of its FRF at positive frequencies. Smoothness and low frequency requirements can be achieved by cubic splines, which are smooth curves (εC^3) that pass through arbitrarily selected points (knots). An interactive computer software system was developed to generate desired FRF with cubic splines. FRF values are specified at a few (<15) frequencies. The system generates and displays cubic spline that passes through these specified knots. One examines the curve and modifies locations of knots until satisfied with curve. Applying inverse FFT to FRF, system can generate an ECT RF with desired FRF. System is convenient and generated RF's tested on simulated and real ECT data gave faithful reconstructions. No artifacts were observed. With this system, ECT RF's of various cutoff characteristics can be generated conveniently to match ECT scanning parameters to optimize image signal to noise ratio. One such RF design was found to reduce image noise by 50% without significantly affecting image resolution. It is concluded that cubic spline is useful for convenient and flexible design of ECT RF to optimize image signal to noise ratio.

REMOVAL OF LONGITUDINAL EMISSION TOMOGRAPHIC BLUR BY LOCAL OPERATORS.
M.W. Vannier. Mallinckrodt Institute of Radiology, St. Louis, Mo. F.H. DeLand. University of Kentucky Medical Center, Lexington, Ky.

Longitudinal emission tomographic images are conventionally reconstructed by backprojection and contain defocused contributions of over and underlying structures. Removal of defocus blur may be performed by local image restoration operations that were developed for analogous purposes in the processing of light microscope images. The technique is based on the removal of a suitably convolved function of adjacent tomographic planes from the original backprojected image. The images may be contrast enhanced by removing the excess low frequency information from the adjacent plane images before restoration processing. The blurring contribution of adjacent tomoplanes was simulated by a circularly symmetric finite impulse response digital filter.

Emission tomographic images from a Searle Pho/Con scanner were acquired in raw scintigraphic form as a list mode data file on a PDP-11 computer using a specially designed interface. These data were reconstructed in multiple adjacent planes using conventional backprojection. Deblurred images were obtained as described above. The results were displayed on a 128x128 monitor in 16 color levels (GAMMA-11).

This method compares favorably with Fourier deconvolution and iterative deblurring techniques with reference to 1) generation of artifacts, 2) subjective quality of resulting images, and 3) computer processing time.

RESOLUTION RECOVERY IN PLANAR NUCLEAR IMAGES: APPLICATION TO HIGH PURITY GERMANIUM AND SCINTILLATION CAMERAS.
DA Ortendahl, DW Shosa, L Kaufman, W Rowan, JW O'Connell, RS Hattner, and R Herfkens, UCSF-RIL So. San Francisco, CA

Resolution recovery in images at depth with a high purity germanium (HPGe) camera has been achieved through the use of a weighted back projection (WBP) method (1,2). A modification of this algorithm is presented which is derivable either from simple geometrical arguments involving projection and reprojection of the image through the collimator or from a direct application of Bayes' theorem. With this approach the algorithm is reduced to a simple sequence of steps which are then applied iteratively to the image. Application of WBP has been shown to increase spatial resolution and improve contrast

without a concomitant reduction of signal to noise. The algorithm has been applied to the scintillation camera yielding significant resolution recovery despite the presence of scatter and textured noise not present in HPGe images. Improvement in image quality is obtained by reprojecting the final result back through the collimator and applying the algorithm again. Using both cameras a comparision between this new formulation and the previous method will be discussed. Although the new algorithm requires more iterations, artifact introduction is minimized. The techniques has been applied to a variety of images including phantoms, animals, and clinical subjects.

1. Williams SH, et al: Elimination of Loss of Resolution at Depth in Single-Photon Nuclear Images. IEEE Trans Nucl. Sci. NS-26: 590, 1979.
2. Ortendahl DA et al: High Resolution Emission Computed Tomography With a Small Germanium Camera. IEEE Trans. Nucl. Sci. NS-27 (In Press).

INVITED SPEAKER

Brent Baxter, University of Utah, Salt Lake City, UT
THREE-DIMENSIONAL DISPLAYS: IMPLICATIONS AND APPLICATIONS.

WEDNESDAY, JUNE 25, 1980

1:30-3:00 Room 2048

CLINICAL

KIDNEY

Session Chairman: Barry Grove
Session Co-Chairman: Peter Kirchner

SPLENIC BLOCKADE AND TRANSPLANT ACCUMULATION OF SULFUR COLLOID IN RENAL TRANSPLANT REJECTION. M.J. Chamberlain, P.A. Keown, C.R. Stiller, W.C. Vezina. University Hospital, London, Ont.

Uptake of Tc-99m Sulfur Colloid in liver, spleen and renal transplant was measured every second day for two weeks post-operatively and whenever rejection was suspected subsequently. 265 studies were performed in 30 patients encompassing 47 separate episodes of rejection. Transplant uptake, splenic uptake and liver/spleen ratio were correlated with the immune response as measured by lymphocyte-mediated cytotoxicity (LMC) assay complement dependent cytotoxicity (CDC) assay and with clinical evidence of rejection.
Acute rejection was associated with splenic blockade judged by falling spleen activity and rising liver/spleen ratio and by rising accumulation of activity in the transplant. The latter was strongly correlated with and often preceded rise in the LMC assay, whereas the splenic blockade generally followed other evidence of rejection. Differentiation of rejection from acute tubular necrosis is not a problem and routine sequential studies allow the patient to be used as his or her own control. Results of the sulfur colloid distribution study were commonly available 36 hours before the LMC assay.

QUANTITATIVE FUNCTIONAL EVALUATION OF KIDNEY TRANSPLANTS: DYNAMIC PATTERNS OF VARIOUS COMPLICATIONS BASED ON 1950 STUDIES IN 436 PATIENTS. E.V. Dubovsky, W.N. Tauxe, A.G. Diethelm, and J.D. Whelchel. The University of Alabama in Birmingham and VA Medical Center, Birmingham, AL.

Comprehensive renal studies using I-131-orthoiodohippurate (J Nucl Med 16:1115, 1975) accurately reflect graft function by scintigraphy, curve analysis, effective renal plasma flow (ERPF) and excretory index (EI). Using the values of ERPF and EI (Normal:N=1042; ERPF:375±73 ml/min, EI:0.98±0.08), the latter clearly separated the various groups of complications: acute rejection (AR), (N=301, ERPF:182±58 ml/min, EI:0.56), chronic rejection (CR), (N=260, ERPF:154±76 ml/min, EI:1.01±0.08) and acute tubular necrosis (ATN), (N=120, ERPF:160±80 ml/min, EI:0.14±0.10).

ERPF and EI data fell into patterns that were characteristic for each post-transplantation course. Their change in time had predictive value for the fate of the graft and for the effectiveness of the therapeutic regimen. The first day ERPF served as a baseline.

1. ATN: In anuric phase, initially the low ERPF gradually rose, followed by EI increase. The rate of ERPF increase was a good prognostic indicator. Early failure of ERPF to increase heralded irreversible ischemic changes, later (2nd week) along with stagnant EI suggested superimposed AR. 2. AR: Falling EI (pending rejection) was followed by decline in ERPF. Rising EI followed by ERPF increase typified the improvement phase. 3. CR: an irreversible process where ERPF slowly decreased while excretory function remained adequate (normal EI). When ERPF fell to approximately 100 ml/min, EI fell rapidly and the graft became non-functional. 4. Other tests, e.g., creatinine, were insensitive indicators especially in anuric ATN and stable CR.

INDIUM-111 OXINE LABELED LEUCOCYTES IN THE DIFFERENTIAL DIAGNOSIS OF REJECTION AND CYTOMEGALOVIRUS INFECTION IN RENAL TRANSPLANT PATIENTS. L.Forstrom, L.Gomez, B.Driscoll, B.Weiblen, J.McCullough, D.Hoogland, and M.Loken. University of Minnesota Hospitals, Minneapolis, MN 55455.

Indium-111 labeled leucocytes (In-111-WBC) have been shown to be useful in the localization of inflammatory processes, including renal transplant rejection. Using previously reported labeling methods, 63 studies with this agent have been performed in 53 renal transplant patients. Indications for study included suspected rejection or cytomegalovirus (CMV) infection. Studies were performed in 32 males and 20 females, with ages ranging from 6 to 68 years. Autologous cells were normally used for labeling, although leucocytes obtained from ABO-compatible donors were used in 3 subjects. Rectilinear scanner and/or scintillation camera images were obtained at 24 hours after intravenous administration of 0.1-0.5 mCi In-111-WBC. There was abnormal uptake of In-111-WBC in the transplanted kidney in 11 of 15 cases of rejection. In 3 additional cases of increased transplant uptake, CMV infection was present in 2. Abnormal lung uptake was present in 14 of 14 patients with CMV infection. In 4 additional cases, increased lung uptake was associated with other pulmonary inflammatory disease. Increased lung activity was not seen in patients with uncomplicated transplant rejection. These results suggest that In-111-WBC imaging may be useful in the differential diagnosis of rejection versus CMV infection in renal transplant patients.

ASSESSMENT OF DIURETIC RADIONUCLIDE UROGRAPHY (DRNU) IN CASES OF OBSTRUCTIVE UROPATHY (OU). M.K. Karimeddini, M.A. Testa, R.P. Spencer. University of Connecticut Health Center, Farmington, CT.

This study was undertaken to assess the diagnostic usefulness of DRNU as compared with the conventional radionuclide urogram (RNU) in patients with OU. Each patient had an intravenous pyelogram (IVP) performed, to determine the anatomic status of the urinary tract. Studies were carried out with a gamma camera and computer. The Tc-99m-DTPA was injected IV (12 mCi; weight adjusted for children). Data were collected from the posterior view with the patient supine. After 15 minutes, when furosemide (Lasix) was used, 20 mg were given IV (weight adjusted for children). Twelve patients had both the DRNU and RNU, while 29 had the DRNU alone and 8 had the RNU alone. The present examinations on these patients, plus their prior exams, presented 32 DRNU's for analysis and 55 RNU's.

		DRNU		RNU	
		normal	abnormal	normal	abnormal
IVP	normal	17	1	20	9
	abnormal	0	14	1	25

Statistical analysis of these results indicate that DRNU has a significantly lower false positive rate than RNU (6% versus 31%, $P < 0.05$). Routine or selective use of

diuretics, during a radionuclide investigation of the urinary tract in patients with known or suspected OU, may help to distinguish between true OU and conditions such as residual dilatation of the collecting system, extra-renal pelvis and other non obstructive urinary tract problems.

RENAL FUNCTION STUDY IN PATIENTS WITH SPINAL CORD INJURY, COMPARISON WITH EXCRETORY UROGRAPHY. E.V. Dubovsky, L.K. Lloyd, D.M. Witten, C. Metzker, K. Kuhlemeier, W.N. Tauxe, A.J. Bueschen, S.L. Stover. The University of Alabama in Birmingham, Birmingham, AL.

Renal disease is a leading cause of morbidity and mortality in spinal cord injury patients with neurogenic bladder. Lifelong follow-up is required to detect and treat urinary tract abnormalities.

341 patients (136 twice, 18 three times, 5 four times) were studied over a period of 3 years by excretory urography (EXU), cystography, plasma creatinine, BUN and I-131-orthoiodohippurate (OIH) renal function studies (RFS) (J Nucl Med Technol 5:81, 1977).

RFS with OIH requires no patient preparation or manipulation, has no adverse reaction and low radiation exposure. It accurately and reproducibly determines total and differential renal function by means of effective renal plasma flow, % OIH excreted in the urine, time-activity curve analysis and estimates volume of residual bladder urine.

The goal of this study was to determine if RFS could be utilized to follow such patients instead of the EXU. Both tests were compared in 500 studies. Both were normal in 125 patients and both abnormal in 205. The EXU was abnormal in 43 patients with normal RFS. Those abnormalities consisted of only minimal caliectasis and/or ureterectasis in all but 8 renal units. Abnormal RFS with normal EXU was seen in 127 cases. Follow-up studies confirmed significance of these findings.

Preliminary results suggest that after initial evaluation by the whole battery of tests, RFS could be used as simple, more accurate and quantitative way to follow spinal injury patients with neurogenic bladder. EXU is performed in selected cases.

RELATIVE RENAL FUNCTION WITH ORTHOIODOHIPPURATE (OIH): COMPARISON TO Tc99m DMSA. W.B. Nelp, T.G. Rudd, J. Ferens. University of Washington, Seattle, WA.

Relative renal function is often important when evaluating congenital urinary tract disease or chronic obstruction and/or infection. This study compared relative function determined by OIH to simultaneous differential localization of Tc99m DMSA. In this laboratory quantitative studies indicate relative tubular binding of DMSA is proportionate to relative renal blood flow and GFR (JNM 20:63, 1979).

36 children and adults were studied. They received .3 to 2.0 mCi of I-123 OIH (30 patients) or .15 to .3 mCi I-131 OIH, and serial 20 sec.digital images were obtained for 30 min. Static DMSA (1-5 mCi) images were made 2 hrs after IV injection.

In 15 patients the OIH background subtracted activity over each kidney was analyzed at 4 time intervals during the first 3 min. All intervals gave similar relative values; however the 60 to 180 sec. time provided the best combination of kidney (K) to background (B) ratio and statistical precision for counting.

In the 36 patients the correlation of relative OIH accumulation with that of DMSA localization was excellent, r= 0.98, y = 1.05 x + .022 (y = DMSA x = OIH). Patient creatinines ranged from 0.7 to 4.6, relative function (left kidney) ranged from 5 to 99% of the total. K/B ratios averaged 7/1 for DMSA and 4/1 with OIH. Mean counting precision for 123-OIH was 2% (coefficient of variation) and for Tc99m DMSA was 1%.

It is concluded that the net accumulated counts over each kidney from the 60 to 180 sec.period following IV OIH accurately reflects relative renal function, is identical to relative tubular accumulation of DMSA and is proportionate to differential renal blood flow and GFR.

THE EFFECT OF VARIOUS PATHOPHYSIOLOGIC CONDITIONS ON THE EXCRETION AND RENAL LOCALIZATION OF Tc-99m DIMERCAPTOSUCCINC ACID (DMSA). C.A.Yee, H.B.Lee, M.D.Blaufox. The Albert Einstein College of Medicine, New York, N.Y.

Because of the increasing use of DMSA for evaluation of individual renal function, it is important to know the effect of various pathophysiologic conditions on its excretion and renal localization.

Single injection clearance studies were done on 36 female Sprague-Dawley rats in six groups: I, control; II, dehydrated 24 hours; III, Mannitol infusion; IV, Probenecid; V Alkaline urine (sodium bicarbonate); and VI, Acid urine (Ammonium chloride). Plasma and urine concentrations of Tc-99m DMSA and I-125 Iothalamate were followed 80-90 min post injection and then the livers and kidneys were removed and samples counted.

There was a significant decrease in the plasma clearance of Tc-99m DMSA in group II (0.1±0.04 ml/min/100g) and group III (0.15±0.02 ml/min/100g) vs I (0.21±0.05 ml/min/100g). The GFR was increased in III ($p<0.0125$). There was a slight increase in renal localization in group II and a slight decrease in group III (p=n.s.). No statistically significant change was found in group IV and V. Group VI (acidosis), however, showed a marked decrease in renal accumulation with a concomitant increase in liver accumulation.

The data reveal: 1) little or no correlation of Tc-99m DMSA clearance with the GFR; 2) Tc-99m DMSA clearance and renal accumulation appear to have a weak urine flow dependence; 3) there is no statistically significant tubular secretion or reabsorption; and 4) Acidosis, which is frequently present in patients referred for renal scanning, markedly reduces renal concentration of Tc-99m DMSA in the rat. These results suggest that careful control of the state of hydration and acid-base balance may be necessary for accurate and reproducible DMSA studies in man.

THE CLINICAL CONTRIBUTION OF RENAL TRANSIT TIMES IN THE URONEPHROLOGICAL DISEASES OF THE CHILD AND THE ADULT : A PROSPECTIVE, INTERNATIONAL JOINT PROJECT. A. Piepsz, H.R. Ham, M. Hall, F. Erbsmann (Brussels), B.L. Diffey, M.J. Goggin, F.M. Hall, J.A. Miller (Canterbury), R. Di Paola, J. Lumbroso, J.P. Bazin, M. Di Paola (Paris).

The aim of the present international protocol is the study of the clinical usefulness of renal transit times. A common data sheet includes clinical, radiological, biological and radioisotopic data. Transit times are determined by the technique of mathematical deconvolution applied to Tc99m-DTPA renograms. Over 800 patients have now been entered into the study. The average and standard deviation of the mean transit time (MTT) in normal kidneys are 3'36" and 1'6" respectively. Urine flow rate has a moderate influence on MTT. If MTT>8'30", the diagnosis of obstruction or residual postoperative dilatation is incorrect in only 5 % of the cases studied. Both conditions cannot be differentiated from each other on the basis of transit times. Transit times in urinary tract infections are not different from normal. They are significantly longer in vesicoureteric reflux grade II and III compared with reflux grade I or with normals. This prolongation of transit time is not related to the grade of distension of the renal cavities, the kidney size, the cortical thickness or the separate glomerular filtration rate. Analysis of other renal pathologies is still in progress. This work was supported by the CNAMTS 75014 FRANCE and by the FWGO Grand n° 3003978 BELGIUM.

A SIMPLE METHOD FOR QUANTITATIVE EVALUATION OF SEPARATE KIDNEY FUNCTION WITH Tc-99m-DTPA. H.Seto, R.Futatsuya, M.Kakishita, T.Michigishi, N.Tonami, and K.Hisada. Toyama Medical and Pharmaceutical University, Toyama, and Kanazawa University School of Medicine, Ishikawa, Japan.

Quantitative measurement of separate kidney function, using a scintillation camera interfaced to a computer was evaluated in 466 patients. For quantitative analysis of the renogram [R(t)], the time-activity curve of the left ventricle [H(t)] was regarded as the plasma disappearance curve and several indices such as separate renal function ratios $[(C_2-C_1)/H_1, (C_2-C_1)/H_2]$ were calculated.

The count of each renogram from 80 to 140 sec after injection divided by the total count of both renograms gave the relative separate renal perfusion & function ratio(%). Separate renal Tc-99m-DTPA clearance was measured by the method of Piepsz (Eur.J.Nucl.Med.,2:173,1977). 1) $(C_2-C_1)/H_2$ ratios were correlated well with Tc-99m-DTPA clearance (n=13,r=0,977)and GFR(n=112,r=0.937) measured with sodium thiosulfate. The ratios of the diseased kidneys were significantly decreased ($p<0.01$) in comparison with normal kidneys. $(C_2-C_1)/H_1$ratios revealed a lesser correlation. 2) Relative separate renal perfusion & function ratios were correlated well with I-131 Hippuran. Normal values in 42 subjects were as follow; Left kidney:52.2±2.5%, Right kidney:47.8±2.5%.

$C_1=\int_{60}^{80}R(t)dt, C_2=\int_{120}^{140}R(t)dt, H_1=\int_{0}^{20}H(t)dt, H_2=\int_{1140}^{1200}H(t)dt,$

ROI of H(t):100 matrix points (time unit: sec.)

FUNCTIONAL IMAGING WITH I-123 HIPPURAN FOR RENOVASCULAR DISEASE. B.E. Oppenheim, C.R. Appledorn, H.Y. Yune, and C.E. Grim. Indiana University School of Medicine, Indianapolis, IN.

The functional image is a single image demonstrating time-related changes which are conventionally displayed as a sequence of images. It is formed by constructing the time-activity curve for each pixel in the image, measuring some parameter of curve shape for each curve, and displaying the parameter values as a digital image.

To achieve optimal functional renal imaging we used I-123 Hippuran (1 mCi) as the imaging agent and factor analysis for image processing. Iodine-123 Hippuran is superior to Tc-99m DTPA because it produces sharper, more characteristic renogram curves and has less extrarenal uptake, and is superior to I-131 Hippuran due to much higher photon yield for comparable radiation doses. Factor analysis is used to rapidly fit smooth curves to the noisy time-activity curves and greatly reduces the noisiness of the functional images.

A large number of curve shape parameters were examined, and 7 were identified as producers of clearly distinguishable and potentially useful functional images. Two represent time: TMAX (time to peak) and PI (persistence index). Five represent magnitude (after normalizing curves to unit area): RISE (peak minus first value), FALL (peak minus last value), RF (Rise X Fall), RISET (Rise corrected for curve trend), and RISMX (maximum rate of increase).

Thirteen studies were carried out, 4 in patients with proven and 5 in patients with suspected renovascular disease, and 4 in normal volunteers. The functional images appear to be far more sensitive than the standard images in demonstrating renal cortical function and in identifying subtle asymmetries and segmental abnormalities.

1:30-3:00 Room 2043

CLINICAL

IMAGE CORRELATION I

Session Chairman: Harry Agress Jr.
Session Co-Chairman: Frederick H. Gerber

EARLY DIAGNOSIS OF ACUTE COMMON BILE DUCT OBSTRUCTION BY Tc-99m-IDA (IMINODIACETIC ACID) CHOLESCINTIGRAPHY. H.S. Weissmann, R.R. Rosenblatt, L.A. Sugarman, J.D. Badia and L.M. Freeman. Montefiore Hospital and Medical Center, Bronx, NY.

Cases of obstruction without ductal dilatation, as well as dilatation without jaundice have been reported with ultrasonography(US). We have observed cholescintigraphy to be a sensitive and reliable method for detecting the functional abnormality of obstruction before the morphologic change of dilatation is seen on US, and even before the liver function tests(LFTs) are abnormal. Of 352 patients studied for suspected acute cholecystitis(AC), 27 exhibited a scintigraphic pattern which we have associated with significant common bile duct(CBD) obstruction: hepatocyte uptake with failure to visualize the gallbladder or common bile duct and absent or delayed intestinal visualization. No intestinal activity was noted in 25 of these patients; 2 had delayed intestinal visualization (2-4 hrs). CBD obstruction was confirmed in 26 cases, 23 by stones and 3 by tumor. The dilated ducts or obstructing neoplasm may be identified as photon-deficient areas on the cholescintigram. (In this group in addition to CBD obstruction, 19 had AC and 5 had chronic cholecystitis.) Of the 20 patients in this group who had both Tc-99m-IDA and US, a normal caliber CBD and intrahepatic radicles were identified in 14 (70%). Importantly, this scintigraphic pattern may be the first detectable evidence of CBD obstruction. In 1 individual, this pattern was observed before the bilirubin level (and other LFTs) were elevated and while US still revealed a normal caliber CBD. At surgery the CBD was completely obstructed by a stone at the ampulla.

COMPLIMENTARY ROLE OF Tc-99m-DIETHYL-IDA AND ULTRASOUND IN LARGE AND SMALL DUCT BILIARY TRACT OBSTRUCTION: W.C.-Klingensmith, M.L. Johnson, C.C. Kuni, M.G. Dunne, and A.R. Fritzberg. U. of Colorado Health Sciences Center, Denver, CO.

The relative role of Tc-99m-diethyl-IDA and ultrasound imaging in the evaluation of small or large bile duct obstruction was evaluated in 54 patients. Each patient was studied with both modalities; the average time between studies was 5.2 days. Eleven patients had partial or complete large bile duct obstruction, six patients had partial or complete intrahepatic diffuse small duct obstruction, e.g. biliary atresia, and 37 patients had no obstruction. In patients with large duct obstruction, Tc-99m-diethyl-IDA was abnormal in all eleven, but could not identify the level of obstruction in nine. Ultrasound was abnormal in nine (with correct identification of level), normal in one, and technically inadequate in one; ultrasound was also abnormal in six patients without obstruction. Combinations of the two modalities improved specificity without loss of sensitivity. A cost analysis indicated that in suspected large duct obstruction the most efficacious strategy was to perform ultrasound first and then Tc-99m-diethy-IDA in all positive or technically inadequate ultrasound studies. In small duct obstruction, Tc-99m-diethyl-IDA was abnormal in all six, but could not differentiate small from large duct obstruction in five. Ultrasound showed no large duct obstruction in all six and, thus, allowed identification of the level of obstruction in patients in whom the Tc-99m-diethyl-IDA study was equivocal. In suspected small duct obstruction the most efficacious strategy was to perform a Tc-99m-diethyl-IDA study first and then ultrasound in all Tc-99m-diethyl-IDA studies which were equivocal as to level of obstruction.

GALLIUM-67, ULTRASOUND AND COMPUTED TOMOGRAPHY IN PATIENTS WITH SEPSIS: ROC ANALYSES. B.J. McNeil, R. Sanders, H. Finberg, P.O. Alderson, S.J. Hessel, S.S. Siegelman, D.F. Adams, H.L. Abrams, Departments of Radiology Harvard Medical School and Johns Hopkins University, Boston, MA and Baltimore, MD.

The relative value of gallium-67 imaging (NM), ultrasound (US), and computed tomography (CT) was studied prospectively in over 140 patients suspected of having a focal source of sepsis. Patients were studied with fourth generation CT scanners and state of the art US. Patients in Boston had gallium studies performed on gamma cameras and those in Baltimore on rectilinear scanners. All images were interpreted prospectively using a 5 point rating scale and ROC curves then constructed.

At both institutions, the CT results fell on the same ROC curve which had a slope near 1.0. For a false positive (FP) ratio of 10% the true positive (TP) ratio was 61%, whereas for a FP ratio of 20%, the TP ratio rose to 71%. At both institutions, the US results also fell on the same ROC curve which had a slope slightly less than 1.0. For FP ratios of 10% and 20% the TP ratios were 48% and 61% respectively. The gallium data for both institutions did not fall on the same ROC curve. For FP ratios of 10% and 20% gallium scans performed on a gamma camera had TP ratios of 57% and 65% respectively, whereas those performed on rectilinear scanners had TP ratios of < 40% and 50% respectively.

When the Dorfman and Alf technique was used to identify

the best imaging technique, i.e., to identify the technique with the area closest to 1.0, the following results were obtained. CT had an area of 0.83, US 0.78, NM with a gamma camera 0.78, and NM with a rectilinear scanner 0.70. Thus, CT seems the best imaging modality and US and gamma camera gallium images are close seconds.

CORRELATION OF RADIOISOTOPE, X-RAY FLUORESCENT, AND ULTRASOUND SCANS IN PATIENTS WITH A SOLITARY THYROID NODULE
J.A. Harolds, J.A. Patton, and F.D. Rollo, Vanderbilt University Medical Center, Nashville, TN.

There are currently three imaging modalities which can be applied to the diagnosis of the solitary thryoid nodule. Radioisotope scans evaluate the trapping and organification capabilities, x-ray fluorescent scans measure the stable iodine content, and sonographic scans provide information on tissue structure. An x-ray fluorescence technique developed and previously reported, uses an iodine content ratio (ICR) of nodule vs. normal tissue as an indicator of benignancy (ICR > 0.6 → benign).

Ten patients with a solitary thyroid nodule were imaged by all three modalities prior to surgery. Nine of the ten nodules were "cold" on the radioisotope scan and one was "hot". The "hot" nodule was solid on ultrasound, had an ICR of 1.25, and was a colloid nodule with multiple cysts. Of the nine cold nodules, six were benign and four of the six had ICR's of 0.56 or higher. There was one case each of medullary, follicular, and papillary carcinoma with ICR's of 0.41, 0.49, and 0.53 respectively. In two of the benign nodules, no mass was identified by ultrasound. All of the other nodules were reported to be solid or complex by ultrasound. There were three adenomas with none reported as having a sonographic halo. In one carcinoma, the ultrasound appearance suggested an adenoma. One cystic lesion was missed by ultrasound.

In this limited series, it is concluded that the radioisotope scan is a good screening modality with a high ICR (> 0.6) as obtained by x-ray fluorescent scanning being a good indicator of benignancy. The fluorescent scanner provided more additional diagnostic information than ultrasound in this series.

EVALUATION OF A COMBINED DIAGNOSTIC APPROACH TO ABDOMINAL AORTIC ANEURYSM: RADIONUCLIDE ANGIOGRAPHY AND ULTRASOUND.
K. Yamamoto, Y. Ishii, D. Hamanaka, Y. Yonekura, and K. Torizuka. Kyoto University, Kyoto, Japan.

Thirty cases complaining of pulsating abdominal mass were imaged by both gray scale ultrasound (US) and radionuclide angiography (RN) to evaluate the abdominal aortic aneurysm. RN was performed on a bolus introduction of the Tc-99m in vivo labeled RBC, followed by US. All eighteen cases with an aneurysm, which were substantiated later, were successfully diagnosed by the combined use of these two. However, RN alone provided three false negative results and US alone provided one false positive result. Since US imaged the aneurysm as an enlarged echo-free space comprising laminated echo-genic mass due to thrombus, which is not imaged by RN, it is superior to RN for characterizing a mass as the aneurysm with thrombus. Four cases with pulsating abdominal mass not resulting from aneurysm could also be diagnosed by US alone. However, since RN revealed hemodynamic state of the aneurysm, it could help us evaluate the presence of such circulatory disturbance as of renal or iliac arteries and the presence of collateral circulation.

Thus RN should be considered in conjunction with US. In conclusion, the combined use of these two complementary modalities in patients suspected of the aneurysm established a rapid, accurate and safe diagnostic means. Thus, it provides an alternative to invasive contrast angiography.

NUCLEAR MEDICINE IN THE UNITED STATES.
Arthur B. McIntyre, Peter Paras, and Raymond C. Grant. Food and Drug Administration, Rockville, Maryland.

The Food and Drug Administration (FDA) recently completed a representative survey of nuclear medicine procedures performed in the United States in the year 1978. Data were collected for the Bureau of Radiological Health utilizing the FDA's Medically Oriented Data System (MODS).

More than 77,000 patient records were included in the analysis. The data include procedure type, radiopharmaceutical and administered dosage, patient age, and sex, and the physician's initial interpretation of the procedure result.

The relative frequency (in percent) of imaging procedures performed in 1978 were: brain, 24.1; liver, 20.3; bone, 18.1; lung, 16.5; thyroid, 10.9; renal, 3.2; tumor localization, 2.6; and cardiac, 2.5. Radionuclides use frequencies (in percent) were: Tc-99m, 88.2; I-131, 8.1; Xe-133, 3.7; Ga-67, 2.8; thalium 201, 1.1; and all other 0.7.

Results indicate that nuclear medicine procedures are increasing at a rate of 10 percent per year. This is a change in growth rates of up to 30 percent estimated prior to 1975. The analysis includes radiopharmaceutical dosage ranges and patient radiation absorbed dose estimates.

RENAL KINETICS: CORRELATION OF NUCLEAR MEDICINE AND COMPUTED TOMOGRAPHY.
C.L. Partain, E.V. Staab, F.D. Rollo, C.M. Coulam, and J.A. Patton. Vanderbilt University, Nashville, TN., and University of North Carolina, Chapel Hill, NC.

The purpose of this study was to compare two different glomerular agents and the associated different imaging modalities; namely, radionuclide flow study and serial contrast enhanced transmission CT in the evaluation of renal kinetics. The agents used were Tc-99m DTPA and Renografin-60. Studies were performed in three rhesus monkeys (Macaca mulatta). Time-activity and time-density curves were determined for each study.

The time to peak density in the renal cortex was approximately 4 minutes after injection, about the same time as the time-activity curve. However, the initial slope of the time-activity curve is much greater than the slope of the time-density curve implying a more rapid concentration of Tc-99m DTPA than Renografin-60. The cortical excretion appears essentially the same for both agents.

In the CT evaluation of the renal pelvis, the peak density was 6 minutes after injection. The initial slope of the time-density curve was less, and there was delayed excretion compared to the renal nuclear medicine study.

It appears that the cortical concentration of Renografin-60 is less rapid than for Tc-99m DTPA and the time to peak and excretion are essentially equivalent. In the renal pelvis Renografin-60 appears more slowly before the peak, peaks later, and persists longer than Tc-99m DTPA. These observations imply a different physiologic mechanism in the renal excretion of the two agents used. Also serial, contrast enhanced CT provides much greater temporal/density resolution than conventional intra-venous pyelography.

INVITED SPEAKER

Lawrence R. Muroff, MD,
University Community Hospital, Tampa FL
IMPACT OF COMPUTED TOMOGRAPHY ON THE PRACTICE OF NUCLEAR MEDICINE.
Sponsored by the Council of Correlated Imaging Modalities

1:30-3:00 **Room 3040**

CLINICAL

HEMATOLOGY

Session Chairman: Robert E. Henry
Session Co-Chairman: Rashid A. Fawwaz

LABELING HUMAN PLATELETS WITH IN-111 OXINE USING AN ALBUMIN DENSITY GRADIENT SEPARATION.
R.W. Bunting, R.J. Callahan, S. Finklestein, R.S. Lees and H.W. Strauss. Massachusetts General Hospital, Boston, MA.

Previously reported methods for labeling platelets in

which cells are spun against a hard surface during centrifugation have been limited by difficulty in resuspension of the cells. To minimize this problem, we have adapted the albumin density gradient separation of platelets to labeling with In-111 oxine. All samples were processed in capped conical centrifuge tubes (CT)under a laminar flow environment. Forty-three ml of blood was collected from each of 17 patients in 7.5ml of ACD-A solution and spun at 150 x g for 15 minutes. The platelet-rich plasma (PRP) was transferred to a second CT and 0.5 ml of 25% human serum albumin (HSA) was carefully layered under the PRP using a 2½" long needle. Centrifugation at 1500 x g for 15 minutes resulted in a platelet layer which was easily suspended in either 15% ACD-A in saline or 15% ACD-A in plasma. The cells were incubated with 0.5 - 1.0 mCi In-111 oxine for 30 minutes at 37°C. Labeling efficiency was 54.0 ± 11.4% (n=17) in ACD-saline and 47.3 ± 5.0% (n=3) in ACD plasma. In vitro aggregation after ADP stimulation was demonstrated in the final preparation of labeled cells and was equal in intensity to that demonstrated in PRP. Platelet survival studies in 5 patients ranged from 4.0 to 9.0 days and was consistent with their clinical condition. The addition of the albumin density gradient separation technique facilitates resuspension of the cells and preserves platelet viability during labeling.

CORRELATION BETWEEN INDIUM-111-OXINE PLATELET DEPOSITION AND THROMBUS FORMATION IN ARTERIAL THROMBOGENESIS. D.C. Price, M.J. Lipton, J.A. Hartmeyer and R.J. Prager. University of California, San Francisco, CA.

The technique of Thakur, McAfee et al for labeling platelets with Indium-111-oxine has opened many possibilities for in vivo evaluation of thrombus formation using routine scintigraphy. However, no systematic evaluation has yet documented true correlation between Indium-111-platelet deposition and quantitative clot formation. We have undertaken such a study in 24 mongrel dogs in which 200-400 µCi Indium-111-labeled autologous platelets were infused, a polyethylene angiographic catheter advanced to a carotid artery after percutaneous femoral insertion, routine scintigraphy performed, and the carotid with its thrombus-forming catheter excised at times ranging from 30-180 minutes. The Indium-111 activity was determined in vivo by region-of-interest computer processing of the scintigraphic images. Catheter clot was stripped after carotid excision, weighed, and the Indium-111 activity determined by well counting. Catheter activity was noted to peak at 30-80 minutes and fall thereafter. In vitro Indium-111 activity demonstrated a linear correlation with wet clot weight:

In-111 (% inj. dose) = 0.00209 x (mgm clot) + 0.00091 (r = 0.882)

In vivo correlation was also linear, but with a broader scatter of data points. At the peak, the in vitro label per cm of catheter was 0.060 ± 0.019%. Peak clot weight was 27.9 ± 5.6 mgm per cm of catheter. This study establishes that there is a valid correlation between Indium-111-platelet uptake and clot size in such an acute experimental situation.

THE EFFECT OF ANTICOAGULANTS AND ANTIPLATELET AGENTS ON INDIUM-111 PLATELET SCINTIGRAPHIC STUDIES IN MAN. M.D. Ezekowitz, E.O. Smith, S. Herren and F.B. Taylor, University of Oklahoma Health Sciences Center, Oklahoma City, OK.

Anticoagulants and antiplatelet agents are commonly used to inhibit active thrombosis. The purpose of this study was to determine retrospectively whether heparin (H) (systemic and subcutaneous) and aspirin (A) inhibited the incorporation of In-111 labelled platelets into thrombi (T) in man. Five patients all with positive scintiphotos were studied. Four had intracardiac T and a single patient had a pulmonary artery thrombus. (Two were surgically proven; in the patient with pulmonary artery thrombosis, the surface thrombus:blood In-111 activity was directly determined following surgical removal.) Two cardiac patients were treated with subcutaneous H, 5000 units daily. In both, treatment began 3 days prior to the study and continued for the duration of the study. Two other cardiac patients received A (600 mg B-I-D and 300 mg B-I-D) for a period of 6 weeks and 2 months respectively. In the second patient, A was discontinued two weeks prior to the study and for the duration of the study. The patient with the pulmonary artery thrombus had been on systemic H (25,000 units daily) for 6 weeks and throughout the study. The In-111 activity in the thrombus was 10 x blood per mg tissue. We conclude: 1) subcutaneous H and A, in the case of left ventricular T, and systemic H in the patient with PA thrombosis did not prevent incorporation of the platelets onto the surface of the clot. 2) These agents may not be effective in inhibiting thrombus propagation in these clinical situations. 3) In-111 platelet scintigraphy could be used to test the efficacy of anticoagulant and antiplatelet agents in different clinical situations.

MIGRATORY PATTERNS OF In-111 LABELED HUMAN LYMPHOCYTES IN CHRONIC INFLAMMATORY DISEASE. D.A. Goodwin, J.R. Hickman, L.F. Fajardo, A. Calin, S.L. Propst, and C.I. Diamanti. Veterans Administration Medical Center, Palo Alto, CA.

We have used the In-111 oxine method to label autologous lymphocytes and study their kinetics and migratory patterns in 12 patients with chronic inflammatory disease. Nearly pure lymphocyte preparations (10^8 cells) were obtained from the interface of a ficoll-hypaque gradient, resuspended in 5ml saline and incubated with 500 µCi In-111 oxine for 30 minutes. The labeling yield was 40-70%. Electron microscope radioautographs with 0.3 - 0.5 µ resolution showed nuclear as well as cytoplasmic labeling of leukocytes. Whole body images were made 18 - 24 hours after IV injections of 100-500 µC per 10^8 labeled autologous cells. Recovery at 15 min was 25% and blood disappearance $T_{½}$ for the slow phase was 53 hours. Normally activity is seen in spleen, liver and bone marrow (in descending order of concentration) as well as cervical and inguinal lymph nodes. Any concentration outside these areas, as well as asymmetrical uptake in lymph nodes was considered abnormal. Four patients also had In-111 WBC (mixed leukocyte) scans within 7-10 days for comparison. Five patients had abnormal scans and one had a large spleen and one expanded bone marrow. Two patients with chronic osteomyelitis (one histologically proven) had positive lymphocyte scans with normal or only faintly positive WBC scans, and a third with acute on chronic osteomyelitis and a positive WBC scan had abnormal regional nodes. All large joints were intensely positive in a patient with a plasma cell disorder and arthritis. The fifth, a paraplegic, had a positive bladder. Lymphocyte viability is shown by the ability of the labeled cells to concentrate in regional lymph nodes and chronically inflammed tissues, and diagnostic and functional information may be obtained by this technique.

SPLENIC SCAN FINDINGS IN SICKLE CELL-HEMOGLOBIN C DISEASE. C. H. Park, P. I. Wecsler, D. Lin and S. K. Ballas. Thomas Jefferson University Hospital, Philadelphia, Pa.

The purpose of the present study was to determine the relative frequency of scintigraphic splenomegaly and functional asplenia in sickle cell-hemoglobin C disease. (S-C disease) We have performed spleen scans on 18 patients proven to have S-C disease by electrophoresis. The patients' age ranged from 15 to 48 with the average age of 22.5 years. There were 7 males and 11 females. The spleen scans were performed within a few days after the crisis in 7 patients and the remaining 11 patients did not have a history of recent crisis at the time of the scan. All patients had spleen scans using 3mCi of Tc-99m sulfur colloid intravenously. A minimum of 3 views were obtained using gamma camera and some of them had a special view after shielding the non-splenic activity. Most of the patients had a mild anemia and only 5 cases had clinically palpable spleen - 4 cases agreed with the scan finding and 1 case had partial asplenia. Seven out of 18 showed a functional asplenia and 2 demonstrated a partial asplenia. (Table) Seven out of 18 revealed splenomegaly on scan. A literature survey shows splenomegaly in about two-thirds of the adult S-C disease patients and rare occurrence of asplenia. However, we found a high incidence of functional asplenia or partial asplenia (50%) and less frequent splenomegaly (38.9%) in our small group of S-C disease patients.

EFFECTS OF HEATING ON THE SIZE-DISTRIBUTION AND DIFFERENTIAL UPTAKE OF Tc-99m-RED BLOOD CELLS (RBC) BY SPLEEN AND LIVER. P. Som, A.N. Ansari, Z.H. Oster, H.L. Atkins, C.R. Sipe, F. Hosain, D.F. Sacker, G. Schidlovsky, R.G. Fairchild, G.E. Meinken and P. Richards. Brookhaven Nat'l Laboratory, Upton, NY, and Univ. of Conn., Farmington, CT.

For functional studies of spleen with RBC's, the degree of damage is critical. Routinely, heat damage is performed at 49-50°C for 15 min. The purpose of this study was to establish the minimal heating time for maximal splenic sequestration. Experiments were carried out in dogs using the BNL Tc-99m-RBC labeling kit with heating for 0,5,10,15, 30,45, and 60 min. at 49.5°C. Computer generated spleen/liver ratios at equilibrium were found to be 2.5, 2.7, 7.1, 5.4, .48, .23, and .15 for 0,5,10,15,30,45, and 60 min. heating respectively. Lengthening heating time enhances blood clearance by increasing rate of fast component clearance (10 min. heating: 58% clearance, $T_{\frac{1}{2}}$ 13 min; 60 min. heating: 90% clearance, $T_{\frac{1}{2}}$ 1.5 min) but for splenic imaging the 10 min. heating time was found to be the ideal.

The change in size-distribution of RBC with varying heating time was assessed with Coulter H4 system for both dog and human RBC's. Dog RBC's were found to increase in size with progressive heating (+2 to +13%) whereas human RBC's behaved differently; two distinct population of cells were observed. When heated for 10 min., 34% of the cells shrunk to 50% of their initial size. This population decreased with increasing heating time. The second population consisted mainly of normal size cells but they increased slightly in size with increased heating. This finding was also confirmed by scanning electron microscopy. It is concluded that optimal heating time is 10 min. and that changes in size-distribution can be used as a quality control parameter.

TIME COURSE OF IN VIVO LABELLING OF RED BLOOD CELLS. J.W. Froelich, R.J. Callahan, J. Leppo, K.A. McKusick and H.W. Strauss. Massachusetts General Hospital, Boston, MA.

In vivo labelling of red blood cells (RBC) results in gastric visualization (GV) in some patients. To determine if this visualization was due to incomplete binding of Tc-99m-O4 to RBC's, in vivo labeling kinetics were determined in 10 patients 20 minutes after injection of stannous pyrophosphate (SN-PYP) by collecting aliquots of whole blood from 1 to 10 minutes after IV injection of Tc-99mO4. The samples were added to tubes containing SN-DTPA which instantaneously stops the labelling of RBC's by chelating with unbound Tc-99mO4. In vivo labelling of RBC's follows an exponential curve plateauing at 10 min with a mean labelling efficiency of 93%.

To allow more time for RBC binding, 7 randomly selected patients undergoing cardiac gated blood pool imaging, had 10ml of blood withdrawn into a heparinized syringe containing 25mCi of Tc-99mO4, 20min after SN-PYP. The blood and Tc-99mO4 were allowed to incubate for 10 minutes prior to reinjection. To determine the kinetics of labelling within the syringe, aliquots were removed at 1 min intervals into tubes containing SN-DTPA. At 10 minutes, the labelling efficiency was 88% (n=4). To determine if this approach reduced GV, this group was compared with 6 randomly selected patients undergoing standard in vivo labelling. There was no GV in 6 of the 7 patients who were injected by the modified technique whereas there was GV in 5 of 6 patients injected with the standard technique.

These preliminary data suggest that this pre-labelling may alter the biodistribution of Tc-RBC's in man.

INTERFERENCE WITH Tc-99m LABELING OF RED BLOOD CELLS (RBCs) BY RBC ANTIBODIES. G.P. Leitl, H.M. Drew, M.E. Kelly, and P.O. Alderson. The Johns Hopkins Medical Institutions, Baltimore, MD.

RBC labeling efficiency was evaluated in 40 consecutive patients (pts) who underwent blood pool imaging with Tc-99m RBCs. Thirty min after a 10 ug/kg dose of Sn^{++}, 20 mCi of Tc-99m pertechnetate was injected. Thirty min later a blood sample was obtained and the % whole blood activity in RBCs was determined. Excellent RBC labeling (>90%) was found in 32 pts, but 8 showed poor (<50%) labeling. These 8 pts all had diseases or medications associated with RBC antibody formation; 2 had lupus, 1 had a recent transfusion reaction, and 5 were taking quinidine and/or aldomet. None were on heparin or were injected through a heparin lock. To further investigate the effect of RBC antibody formation on Tc-99m labeling an in vitro experiment was performed. Whole blood samples were obtained from 10 healthy volunteers with blood type O, Rh+. Packed RBCs were incubated with a 1:2 dilution of anti-RhD serum for 1 hr at 37°C, and a Coombs test was performed to verify that antibodies had been formed. These RBCs were then labeled with Tc-99m using the Brookhaven kit method, and the % activity in the RBC fraction was determined. The results were compared with control samples handled in the same manner, except that the RBCs were mixed with their own serum rather than anti-RhD serum. Eight of the 10 samples showed decreased labeling after anti-RhD incubation. The mean control labeling efficiency was 95% vs. 73% after incubation ($p<.01$). These clinical and experimental results suggest that RBC antibody formation may be responsible, in part, for inefficient labeling of RBCs in vivo with Tc-99m.

1:30-3:00 Room 3039

RADIOPHARMACEUTICAL CHEMISTRY

BIOINORGANIC CHEMISTRY SYMPOSIUM

Session Chairman: M.A. Davis
Session Co-Chairman: H. Donald Burns

PLATINUM COORDINATION COMPLEXES IN THE TREATMENT OF CANCER. B. Rosenberg. Michigan State University, E. Lansing, Mi.

Metal coordination complexes represent a new class of active, potent anticancer agents in animals and man. The first drug in general use, cis-dichlorodiammineplatinum (II) (cisplatin) is now considered curative, in appropriate combination chemotherapy, for testular cancers, ovarian cancers, and oat cell lung cancers. It is also of significant value in the treatment of bladder, head and neck, prostrate, cervical and uterine, and pediatric solid cancers.

The major side effects are nephrotoxicity and nausea and vomiting. Techniques for minimizing or ameliorating these are presently available or under study.

The drug passively penetrates cell membranes. It then undergoes an aquation exchange of the chloride leavings ligands within the intracellular cytoplasm. The aquated species are believed to produce the significant cellular lesion by reacting with DNA. While many reactions with DNA are possible and do occur, a specific reaction with guanine to form a closed ring chelate involving the O-6 site is most interesting. It has been postulated that this can lead to base mispairing and, therefore, base substitution mutations. This may explain not only the stereo-selectivity required for an active drug (the trans isomers are inactive but toxic), but, potentially, also the selective destruction of cancer cells with minimum destruction of normal cells.

Serious questions remain regarding the pharmacokinetics, the basic chemistry of aquation, the generality of the anticancer activity for other complexes and other metals, and the mechanisms of synergism with other drugs that is so prominent a characteristic of cisplatin.

SUPEROXIDE DISMUTASES: A DISPARATE CLASS OF METALLOPROTEINS. J. A. Fee, Biophysics Research Division and Department of Biological Chemistry, The University of Michigan, Ann Arbor, MI.

There are three classes of metalloproteins which catalyze the dismutation of superoxide, $2O_2^- + 2H^+ \rightarrow H_2O_2 + O_2$, which are distinguished by the metal ion co-factor required for activity. (1) The Zn/Cu protein is found in all eucaryotic cells, is composed of two identical subunits each binding one Zn and one Cu; only the latter is required for activity. A structure has been determined to

3 Å resolution. (2) The Mn protein is found in both eucaryotic (mitochondria) and procaryotic cells and is composed of either two or four identical subunits each binding 0.5-1 Mn. The resting valence state of the metal is Mn(III). (3) The Fe protein has been found only in procaryotes, including many strictly anaerobic bacteria, and has general properties similar to the Mn protein. The talk will deal primarily with the relation between the structural properties of the metal binding sites in these proteins and their ability to catalyze superoxide dismutation. However, some time will be devoted to the proposal that these proteins protect cells from oxygen toxicity.

1:30-3:00 Room 3035

RADIOASSAY

THYROID AND BERSON-YALOW AWARD

Session Chairman: Eileen Nicoloff
Session Co-Chairman: Linda A. Monroe

DETECTION OF TSH-RECEPTOR ANTIBODIES BY IMMUNOPRECIPITATION ASSAY. J. Konishi, Y. Iida, K. Kasagi, K. Endo, K. Ikekubo, and K. Torizuka. Kyoto University School of Medicine, Kyoto, Japan

This study was undertaken to develop a new radioassay for TSH-receptor antibodies by applying immunoprecipitation technique and to analyze the nature of the antibodies. The assay was tried by using Triton-solubilized TSH receptors from either Graves' thyroid or guinea pig epididymal fat. To the preformed I-125-TSH-receptor complex, 50 µg of IgG were added and precipitation was effected by addition of antihuman IgG. The antibody titer was expressed as the % radioactivity in the precipitate relative to the toral radioactivity bound to the receptor determined by polyethylene glycol precipitation. When the thyroid receptor was used, antibodies were positive in 9 of 14 patients with Graves' disease and also in 4 of 9 patients with Hashimoto's disease. But the antibody titers showed significant correlation with those of the anti-microsomal antibody. The assay using the fat receptor, on the other hand, revealed antibodies in 4 of 6 patients with Graves' disease and in only 1 of 5 patients with Hashimoto's disease, without any correlation with the anti-microsomal antibody. Neither was there any correlation between the antibody and TSH-binding inhibitor immunoglobulins detected by the radioreceptor assay. These data indicate that immunoprecipitation assay using the fat receptor is useful for detecting TSH receptor antibodies which are different from those detected by the radioreceptor assay.

ACUTE CHANGES IN THYROID HORMONES FOLLOWING ENDOTOXIN-INDUCED FEVER. R.B. Shafer, M.M. Oken, and M.K. Elson. V.A. Medical Center, Minneapolis, MN.

Reduction of serum levels of thyroid hormones in febrile euthyroid patients is well documented. Serial studies at daily or longer intervals have indicated reduction of thyroid hormones followed by rebound hypersecretion during recovery. To define acute changes in thyroid hormones, we produced fever by injection of 1 µg E. coli endotoxin in 3 kg rabbits, monitored temperatures continuously and measured thyroid hormone levels at 0, 2, 4, 6 and 24 hours. Results were compared to controls that received saline. Triiodothyronine (T-3), reverse T-3 (rT-3), thyroxine (T-4) and free T-4 (fT-4) were measured by radioimmunoassay. All rabbits receiving endotoxin developed fever with peaks at 1 hr (ΔT 1.1°C) and 3 hr (ΔT 1.4° C) and defervesced to base levels at 6 hours. Changes in hormone levels recorded as % of base level:

Hormone	Controls (n = 8)			Endotoxin (n = 16)		
	0	6 hr	24 hr	0	6 hr	24 hr
T-3	100	82	95	100	51	77
rT-3	100	143	117	100	870	360
T-4	100	98	127	100	81	173
fT-4	100	101	100	100	101	111

This study documents that the decrease in T-3 level is rapid following fever induction, but lags behind the temperature response. Increased T-4 levels at 24 hours suggest response to depleted thyroid hormones induced by fever. These observed thyroid hormone changes following endotoxin-induced fever suggest a role of thyroid hormones in modulating the febrile response.

HEPARIN EFFECTS ON FREE T4. L. Witherspoon, F. Husserl, S. Shuler, K. Middleton, L. Zollinger and M. Garcia. Ochsner Medical Institution, New Orleans, LA.

Heparin has been shown to increase apparent free thyroxine (fT4) concentration in some, but not all patients. This effect cannot be replicated by the addition of heparin to serum in vitro. It has therefore been suggested that heparin effects on thyroxine binding proteins are unlikely. While assessing thyroid functional status in 35 patients with chronic renal failure we observed heparin related changes in 17. Heparin effects were further studied in 7. Serum samples were obtained before and 10, 20 and 60 min. after i.v. heparin for hemodialysis in 4 patients and before and 15 minutes after heparin in 3. Total thyroxine (TT4), RT3U, fT4 by dialysis and methods of Corning, Clinical Assays and Damon, T3, rT3, TBG and TSH were measured in each sample. No change occurred in 3 patients. In the other 4 there was an immediate increase in the % dialyzed fraction, % Corning A tube binding, RT3U and apparent fT4 by dialysis, Clinical Assays and Damon. TT4 was depressed in all 4 patients. Reciprocal changes in TT4 and the two uptakes (RT3U and %A) resulted in no change in FTI or Corning fT4 estimate. All of these changes revert towards normal by 60 min. post heparin administration. Similar changes were observed in all 17 original dialysis patients studied early and late in dialysis. While changes in the % dialyzed fraction and RT3U are consistent with all three hypotheses, the increased % A and decreased TT4 cannot be explained by thyroidal secretion or T4 release from peripheral binding sites but are consistent with displacement of T4 from thyroxine binding proteins.

FREE T_4 ASSAY VS FREE THYROXINE INDEX. M.A. Swanson, T.R. Custer, C.M. Suey. University of California, Davis, CA.

The free thyroxine index (FTI) is designed for nonthyroidal alterations in total T_4 levels due to increase or decrease in serum thyroxine binding proteins. In the present study, comparison was made between the free thyroxin index and free T_4 levels of 37 euthyroid females, 17 of whom were on birth control pills. The purpose of this study was to determine the accuracy of each test and to assess the ability of the FTI to compensate for estrogen induced elevations in total T_4 concentrations. Biorad Quantacount and Quantimune Kits were used to measure T_3% Resin Uptake and total T_4 levels, respectively. Free T_4 was determined by the Corning relative rate reaction method.

The mean FTI in control women was 2.5 units (range: 2.3-2.9 units), with all values falling within the established normal range (1.4-3.4 units). The mean FTI in the birth control group was 3.0 units (range: 2.1-4.2 units), with 3 subjects having borderline high values (3.4 units) and 4 subjects having FTI's clearly above the normal range. The mean free T_4 in control and birth control women was 1.19 ng/dl (range: 0.7-1.7 ng/dl) and 1.16 ng/dl (range: 0.7-2.2 ng/dl), respectively. Only one birth control subject had a free T_4 above the normal range (0.7-2.1 ng/dl).

These findings indicate that the free thyroxine index only partially compensates for estrogen-induced elevations in thyroxine binding globulin levels and that the free T_4 by radioimmunoassay is the test of choice in women on oral contraceptives.

IN-HOUSE NEONATAL HYPOTHYROID SCREENING USING SERUM. H. Mermall, S. Pinsky, W. Paichel and L. Levitsky. Michael Reese Medical Center, Chicago, IL.

Neonatal hypothyroid screening done "in-house" has many advantages over external, centralized processing using filter paper spots. These include a turn-around time of less than 2 days as compared to 1 week or more, closer control of sample acquisition, and integrated quality control. Blood for the thyroid screen is drawn concurrently with samples for PKU assay and analyzed concurrently with all other T-4 samples, except that 10 µl duplicates are used instead of 20 µl. The remaining serum is preserved in case TSH and TBG are necessary.

A comparison of T-4 values from 1000 of the 10 µl samples to those from 2000 of the 20 µl samples shows similar means and variance of means (16.88 ± 4.285 vs. 16.99 ± 4.269 ng/dl). The smaller volumes decreased the number of samples rejected because of insufficient quantity from 0.7% to 0.4%. Of 3000 patients, 6 were recalled due to analytical failure; none were hypothyroid. Use of half volumes of serum is feasible because (1) the assay remains valid and (2) the normal for neonates is twice that of adults. When variance between duplicates was unacceptable, TSH analysis was performed. Using 10 µl reduced this number from 1.4% to 0.6%. Integrated, in-house, processing permits unified quality control, diminishes the likelihood of recall due to logistical or analytical failure, greatly reduces the time delay required for confirmation and recall of hypothyroid patients, which is critical, and reduces the loss of patients to follow-up.

Secretarial and scientific work flow pattern were considered in the project design.

BERSON-YALOW AWARD ABSTRACT

QUANTITATION OF PARASITE-SPECIFIC HUMAN IMMUNOGLOBULINS: COMPARISON OF RIA AND ELISA METHODS. *R.G. Hamilton, †R. Hussain, †E.A. Ottesen, *N.F. Adkinson, Jr., *Johns Hopkins Sch. of Med., Baltimore, MD; †NIAID, NIH, Bethesda, MD.

We have developed a non-competitive solid phase radioimmunoassay (SPRIA) to quantitate both human IgE and IgG antibodies (abs) against soluble adult antigens of Brugia malayi (B.m.), a filarial parasite causing extensive infection throughout the tropics. Previously, enzyme-linked immunoassays (ELISA) had been used to detect µg/ml levels of IgG anti-B.m., but IgE antibodies were difficult to detect in this system. Since the SPRIA successfully quantitates both IgG and IgE anti-B.m., we sought to examine the reasons for the SPRIA's apparent superiority in detecting IgE anti-B.m. by adding back specific IgG antibodies in increasing quantities to serum containing IgE anti-B.m. abs but depleted of IgG anti-B.m. IgE anti-B.m. was quantitated in these sera using both the SPRIA and ELISA methods. Results indicate that IgG anti-B.m. does not interfere with detection of specific IgE abs in the SPRIA but does interfere in the ELISA. While ELISA permits detection of IgE anti-B.m. in the absence of competing IgG anti-B.m., as levels of specific IgG increase, the IgE is no longer detectable. These differences between SPRIA and ELISA can be explained by SPRIA's antigen excess conditions which assure that there are sufficient antigens both to detect all anti-B.m. abs present in the serum and to adequately represent all antigen specificities in the crude B.m. extract. Our findings commend the use of SPRIA methods over ELISA in assessment of B.m. specific IgE abs in filariasis and indicate a potential role for SPRIA in both the standardization of parasite antigen extracts as well as in absolute quantitation of specific serum antibodies.

1:30-3:00 Room 2040

INSTRUMENTATION

COMPUTER CARDIOVASCULAR I

Session Chairman: Ronald Price
Session Co-Chairman: Peter Esser

VISUALIZATION OF THE PATTERN OF VENTRICULAR CONTRACTION IN PATIENTS WITH CONDUCTION ABNORMALITIES. J.M. Links, K.H. Douglass, and H.N. Wagner, Jr. The Johns Hopkins Medical Institutions, Baltimore, MD.

We have applied Fourier analysis to the processing of 64 x 64 matrix 16 frame gated blood pool studies to yield information about the pattern of ventricular contraction in normal persons and in pts with conduction abnormalities. The temporal Fourier transform at the fundamental frequency (the heart rate) was obtained on a pixel by pixel basis,and used to construct a cinematic display of the wave of contraction as it spread over the beating heart, by blacking out each pixel in the frame of the cycle when its fundamental frequency curve was maximally positive, and about to decrease, as determined from the phase of each pixel (Fourier space information), rather than from the first derivative of a Fourier filtered time-activity curve as proposed by Verba et al (J Nucl Med 20:625, 1979 (abst)). In normal persons, the wave of contraction traveled down the interventricular septum, and then spread over each ventricle from the free wall to the base. In pts with left bundle branch block, the wave traveled down the septum, spread over the right ventricle, and then over the left ventricle. In a pt with a right ventricular pacemaker, the wave started at the right ventricular apex, traveled up the right ventricular side of the septum, and then spread over the ventricles, with the left ventricle lagging behind the right. By permitting visualization of the pattern of ventricular contraction, temporal Fourier analysis should prove useful in the study of conduction abnormalities, and as an aid in the optimum placement of pacemakers.

TEMPORAL FOURIER ANALYSIS IN THE SELECTION OF RIGHT VENTRICULAR REGIONS OF INTEREST. K.H. Douglass, J.M. Links, P.O. Alderson, and H.N. Wagner, Jr. The Johns Hopkins Medical Institutions, Baltimore, MD.

Left-to-right stroke count ratios (SCRs) derived from equilibrium gated blood pool studies have been used as an index of valvular regurgitation. In individuals without regurgitation the SCR is near 1.0, and increases as the regurgitant fraction rises. Temporal Fourier analysis was studied in 20 control patients (pts) and 5 pts with documented aortic insufficiency (AI) in order to assess its effect on the SCR. The temporal Fourier transform (FT) at the fundamental frequency (i.e., heart rate) was calculated for each pixel of the 64 x 64 matrix size by 16 frame gated studies. The FT images were displayed in parametric form as both amplitude and phase images. Subjectively, these images facilitated outlining each ventricle by showing clear separation between the cardiac chambers. Two end-diastolic (ED) ROIs were drawn for the RV, the first using the ED image and the second using the FT images. A single LV ROI was drawn on the ED image and changes in SCR based on differences in the RV ROI were assessed. For 20 pts without regurgitation the SCR determined using the ED image was 1.66 ± 0.47 (SD). Using the FT image the average ratio decreased to 1.41 ± .35 ($p<.001$, paired t-test). When an end-systolic ROI was used to calculate systolic counts the mean SCR determined from standard images was 1.36 ± 0.72, and that from the FT images was 1.17 ± 0.51 ($p<.01$). In 5 pts with moderate to severe AI the SCRs were 6.52 ± 4.05 (ED images) and 5.02 ± 2.10 (FT images). These data suggest that temporal FT images are useful in the selection of RV ROIs.

LEAST-SQUARE FITTING OF SINUSOIDAL FUNCTIONS TO PIXEL TIME-ACTIVITY CURVES IN NUCLEAR MEDICINE CARDIAC BLOOD POOL STUDIES. P.L. Von Behren and M.W. Groch. Searle Radiographics Inc., Des Plaines, IL. D.A. Turner. Rush-Presbyterian St. Luke's Medical Center, Chicago, IL.

This study was done in order to understand the representation of cardiac motion by sinusoidal functions. The time-activity-curves of individual pixels in nuclear medicine cardiac blood pool studies were fit with cosine functions by a least-squares fitting technique. Several parameters were used in each fit: The average value (A_0), the amplitude (A_1), and the phase (P_1) of the cosine function. The frequency of the cosine function was derived from the systolic ejection periods of subregions of the ventricles.

Images of the fitted parameters, A_0, A_1, P_1, and of the goodness of fit parameters, χ^2, were formed. The A_1 images reduce to stroke volume images in the limit of two frames and are relatively insensitive to the chosen frequency. The P_1 images show the contraction sequence for normally- and-abnormally-contracting hearts and agree with cine' mode displays of the original data. The absolute phase of a pixel is quite sensitive to the chosen frequency value but the relative phases between any two pixels are not. The χ^2 images show that sinusoidal approximations to the pixel time-activity curves generally good but are better near the centers of ventricles than near the edges. Advantages of this method over Fourier techniques are the ability to vary the frequency and to use partial-cycle data. This is important because it allows the frequency of the fit to be based on the systolic ejection period and not on the RR interval. Also, a limited number of frames may be used over a fraction of the RR interval to obtain better time resolution.

ALGORITHM FOR QUANTIFICATION OF REGIONAL WALL MOTION ABNORMALITIES, USING THE PHASE IMAGE OF THE ECG-SYNCHRONIZED CARDIAC STUDY. E. Byrom, D.G. Pavel. University of Illinois Medical Center, Chicago, Illinois.

In a gated study, the time-variation of the count rate at each point of the image matrix may be approximated by the first term of its Fourier transform, and its amplitude and phase displayed as functional images. Algorithms have been made available recently to mask these functional images in order to isolate the cardiac chambers on the image, and to generate a histogram display of the number of matrix elements versus phase. These images have been shown to be useful in detecting regional wall motion (RWM) abnormality, which appear as regions of reduced amplitude and altered phase. We have evaluated the possibility of quantifying these phase images. This was done in two ways: 1) by measuring the maximum phase shift of the abnormal areas in relation to the remaining normal ventricle; 2) by measuring the surface of areas of similar phase shifts, and expressing them as % of the whole LV projection. The first procedure uses a vertical cursor on the histogram to mark on the image the following data: location of baseline setting (at the peak of the phase distribution of the normal area), location of the setting chosen at the abnormal phase and the amount of phase shift in degrees. Any number of measurements can be made and superimposed on the same histogram image. In the second procedure one or two areas are selected and displayed separately by indicating the range of phases to be included. The number of pixels in each of these areas is then displayed and compared to the area of the whole LV to give a measure of the extent of RWM abnormality. Single or multiple wall motion abnormalities can thus be quantified by two parameters.

A MEASURE OF EDGE DEFINITION IN NUCLEAR IMAGES AND ITS USE IN CHARACTERIZING SYSTEM PERFORMANCE. R.E. Wernikoff. Brattle Instrument Corporation, Cambridge, MA

The effects on edge definition of trade-offs among dose-time product, imaging system line spread function (LSF) and sensitivity, object size, contrast and motion are complicated and an analytical model that clarifies these effects, here proposed, is desirable. To quantify edge quality, including quantum effects, we imagine that edges are examined with two adjacent exploratory areas, each λ by λ in size; these areas are moved across the edge until the count difference (CD) between them is maximum, and then shrunk to the least λ for which CD is still statistically significant. The center-to-center distance, also λ, is what we define to be the edge width. It is shown that λ is the solution of

$$\int_0^{\lambda} f_0(x)dx = \lambda_0 \qquad (1)$$

$f_0(x)$, which summarizes LSF and motion effects, is the normalized anti-symmetric component of the count-density distribution (DD) obtained in the image when a step-function of activity in a plane distribution of photon sources is transformed by motion during imaging and by the LSF of the imaging system; λ_0 is an irreducible edge width that expresses quantum and contrast conditions at the edge. If ν_1, ν_2 are the hotter, colder limits of DD then

$$\lambda_0 = k/C\nu_a^{\frac{1}{2}},$$

where $C = (\nu_1 - \nu_2)/(\nu_1 + \nu_2)$ and $\nu_a = \frac{1}{2}(\nu_1 + \nu_2)$.

The preference order, λ_1 better than λ_2 if $\lambda_1 < \lambda_2$, seems to correspond to subjective preference, and the analytical formulation (1) facilitates study of trade-offs.

FUZZINESS AS A CONCEPT IN NUCLEAR MEDICINE. APPLICATION TO REGION OF INTEREST SELECTION. R. ITTI, L. PHILIPPE and S. ROSENBERG. Service de Médecine Nucleaire (Pr Th. PLANIOL) C.H.U. Bretonneau, 37000 - TOURS, France.

The non specific nature of radioisotopic labelling implies that there is no strict correspondance between a well defined anatomic structure and its nuclear imaging counterpart. As a consequence, we are naturally lead to interprete such pictures using the theory of fuzzy sets.

This is specially true when selecting regions of interest (R.O.I.),one of the most important steps in the processing of dynamic studies. As these R.O.I. will not have sharply defined boundaries, the degree of belonging to the R.O.I. for a given pixel of the digital frame matrix can only be computed in terms of probabilities, for a combination of some chosen temporal or spatial parameters.

Using this conception, an algorithm has been developed for the automatic selection of the left ventricular area in gated blood pool studies. After definition of the stroke volume image barycenter, several parameters are computed for every pixel : distance from the barycenter, end-diastolic activity, count rate changes amplitude and phase. From the combination of these parameters, the probability of belonging to the left ventricle is defined and its density histogram over the total matrix presents a well defined peak of high probability, which is assumed to correspond to the desired R.O.I..

This procedure allows, in most cases, a fully automatic and objective delineation of R.O.I.. Sometimes however, a manual intervention may be necessary after visual control of the results.

DETERMINATION OF VENTRICULAR BORDERS BY ADAPTIVE FILTERING. N.M. Alpert, H.W. Strauss, E.J. Tarolli, D.A. Chesler. Massachusetts General Hospital, Boston, MA.

To measure regional wall motion reproducibly, an operator independent means of defining the borders of the left ventricle is required. In an attempt to improve computer determined borders we have developed an algorithm which uses a non-stationary, adaptive filtering technique and heuristic rules. An estimate of ventricular border location is determined by approximating the second derivative of the image as the difference between an edge enhanced scene and the smoothed image. The Chesler filter is employed to compute the edge enhanced image. Use of this non-stationary filter allows for the matching of local statistical variations and precision of the edge detector.

Since other cardiac and non-cardiac structures can distort the second derivative edge even in the absence of statistical noise, heuristic criteria on continuity and border shape are imposed to determine the final border points.

Experience to date in studies performed in 20 patients with a variety of abnormalities indicates that the new algorithm is able to separate RV from LV when the chambers overlap in the anterior view and separate the superior margin of the LV from the left atrium in the LAO view. In particular this algorithm usually produces plausible borders in low count data such as exercise studies.

ANALYSIS OF STRESS OR NITROGLYCERINE GATED HEART STUDIES UTILIZING 3 DIMENSIONAL FILTERING AND MUGG, A NEW PROGRAM FOR AUTOMATIC ANALYSIS OF GATED HEART STUDIES. D.L.Yuille, St. Luke's Hospital, Milwaukee, WI.

The purpose of this paper is to describe a new program for rapidly analyzing gated heart studies. The program allows the computer to

automatically analyze one or a series of gated heart studies. The program provides RV and LV regions of interest, calculates RV and LV ejection fractions and other parameters for a maximum of 10 studies. Complete analysis of 10 studies is accomplished in under 20 minutes. The analysis program requires a two stage filtering process utilizing a previously described 3 dimensional smoothing filter SMVL (JNM 19:836, 1978) and a previously undescribed high emphasis filter. Filtering of 10 studies requires 40-45 minutes. Correlation of LV ejection fractions obtained utilizing the above filtering process and MUGE (a highly validated commercial program) with cardiac catheterization in 20 patients reveals a correlation coefficient of 0.90 and a regression line of Y = .992X -.07. For LV ejection fractions, the correlation of MUGG with MUGE (50 measurements in 24 patients) reveals a regression line Y = .972X -0.579 and a correlation coefficient of 0.97. Linear regression of RV ejection fractions for MUGG and Maddahi's method reveals a correlation coefficient of 0.91 and a regression line of Y=.747X + 9.23.

METHODS OF IMPROVING THE PRECISION OF LEFT VENTRICULAR VOLUME AND EJECTION FRACTION DETERMINATIONS.
W.I.Ganz,J.P.Wexler,A.M.Rabinowitz,A.I.Brenner, R.Steingart and M.D.Blaufox. Albert Einstein College of Medicine, Bronx, N.Y.

Accurate comparison of ventricular volume and left ventricular ejection fraction(LVEF)determined from gated studies requires a knowledge of the precision of end systolic(ESC)and end diastolic counts(EDC). LVEF, EDC, and ESC were determined in 21 pts by 5-13 serial 4-min gated studies during the hr after *in vivo* labeling of RBC with Tc-99m. The effect of correction for Tc-99m RBC biologic and physical decay was:

Parameter	Mean Counts($\bar{x}$) 100beats/20msec	$\bar{x}$(a) s.d.	$\bar{x}$(b)* s.d.	% Diff.	p($\bar{x}$(a)vs$\bar{x}$(b))
EDC	2,300	155	132	15	<0.001
ESC	1,000	92	81	12	<0.001

*Corrected for the effective half life of 4.5 hrs.

Single vs triplicate observation revealed:

Number of Observations	LVEF s.d. (EF Units)	Significant EF Unit Changes Confidence Level 60%	80%	90%	95%	99%
1	3.92	4.6	7.1	9.1	10.9	14.3
3	2.21	2.6	4.0	5.1	6.2	8.1

These data suggest that correction for effective $t_{\frac{1}{2}}$ and triplicate determination may be used to improve the precision of LVEF measurement.

REFERENCE-PLANE METHOD FOR HANDLING TISSUE CROSSTALK IN GATED EQUILIBRIUM CARDIAC STUDIES.
M.E. Read, D.D. Watson, and W.R. Janowitz.* University of VA, Charlottesville, VA.

A non-uniform "reference plane" method (RPM) was investigated as an alternative to the subtraction of a constant background from gated cardiac images. This background, more properly called tissue crosstalk (TC) is conventionally determined either by arbitrary choice, for wall motion visualization, or by using a horseshoe (HS) shaped region adjacent to the ventricle for left ventricular ejection fraction (EF) quantitation. Goris has recently pointed out that TC is not homogenously distributed across the region of interest. We have used a modification of Goris' interpolative background subtraction technique which will be referred to as the Reference-plane method (RPM), to restore the image's useful dynamic range for wall motion visualization. We also use the same RPM for handling TC in EF quantitation. Cardiac flow studies were performed on 71 sequential patients. All patients received a first pass study on a multicrystal camera. The EF was determined by standard first pass techniques. At equilibrium, gated studies were then performed. The EF was then determined using the conventional HS method and again using the RPM for TC estimation. The RPM compared quite well with the HS method having a correlation coefficient (R) of 0.951 and a standard error of the estimate (SE) of 0.053. In addition, the RPM correlated better with the first pass method than the HS method with R and SE of 0.894 and 0.076 vs 0.867 and 0.081 respectively. We feel the RPM gives a better dynamic range and thus facilitates visual assessment of wall motion as well as providing TC estimation which gives closer quantitative agreement with other methods for EF computation.
*University of Miami, Florida.

3:15-4:15 Room 2043

CLINICAL

HEART II

Session Chairman: Glen Hamilton, M.D.
Session Co-Chairman: Samuel Lewis

EFFECTS OF SUPINE BICYCLE EXERCISE ON BLOOD CONCENTRATIONS OF IN VIVO AND IN VITRO LABELED RED BLOOD CELLS FOR EQUILIBRIUM BLOOD POOL IMAGING.
E. Henze, G. Wisenberg, L. Morales, D. Kuhl, H.R. Schelbert. UCLA School of Medicine, Los Angeles, CA.

Changes (Δ) in cardiac chamber volumes measured by multiple gated acquisition blood pool imaging during supine exercise (E) could be affected by Δ in the indicator blood concentrations (IC). Using in vitro labeled RBC's (IVT) we found E caused an increase in IC. To examine this observation we randomly employed IVT or in vivo labeled RBC's (IVV) in 19 patients. Δ in IC were measured by well counting of serial blood samples and Δ in splenic activity (SA) by gamma camera imaging and expressed as %Δ from the control value obtained 10 min. after injection. At rest, IC's fell linearly but at different rates and were after 20 min. 4.4±1.3(SD)% with IVT and 11.9±4.5% ($p<0.01$) with IVV below control. With E, IC with IVV declined to -5.1±4.3% but increased with IVT to +3.0±4.0% ($p<0.01$) while SA fell with both to -37.7±17.5% and -33.4±33.9% ($p<0.01$ in both), respectively. Five minutes after E, IC with IVT decreased to -4.4±4.9% ($p<0.01$ compared to E) while SA rapidly rose to +1.7±24.9% ($p<0.01$ compared to E). IC with IVV continued to decline after E to -7.7±5% although SA increased to -16.0±6.5% ($p<0.01$). Δ in IC's varied considerably between individuals and between IVV and IVT. Thus, RBC's may be injured during in vitro labeling and preferentially extracted by the spleen. Splenic contraction reported in animals may also occur in man and account for the increase in IC's during E. We conclude that Δ in cardiac chamber activity during E should be normalized for changes in IC in order to accurately determine exercise induced Δ in ventricular volumes.

INTRACARDIAC THROMBI: IN-VIVO DETECTION BY IN-111 PLATELET IMAGING IN CARDIOMYOPATHY OR MYOCARDIAL INFARCTION.
J.R. Stratton, J.L. Ritchie, L.A. Harker, J.A. Werner, and G.W. Hamilton. Seattle V.A. Hospital and U. of Washington, Seattle, Wa.

Gamma camera imaging of In-111 labeled platelets may noninvasively identify pts with intracardiac thrombi (TH) at risk of embolization. To assess the efficacy of platelet (PLT) imaging, we studied 30 pts not on anticoagulants or PLT drugs and at risk for thrombi from cardiomyopathy (CM) (14 pts), defined as an ejection fraction (EF) < .40, or remote transmural myocardial infarction (TMI) (16 pts: 14 anterior). Mean EF was .27 (range .10-.61). Imaging was performed 24 hrs after autologous PLT labeling. Images were interpreted blindly and defined as positive for TH is there was a discrete area(s) of activity clearly greater than background blood pool.

Five pts had intracardiac TH and 1 pt had possible TH. Two pts had 2 TH. All 6 pts with TH had anterior TMI. Mean EF in pts with TH was .39 (range.22-.61); mean EF was .25 (range .10-.40)in other pts. 5/6 pts with TH had aneurysm

(AN) by either echo (5) and/or contrast angiography (angio) (2). 4/24 without TH had AN. Confirmation of TH was available in 5/6 pts by operation (2), echo (5) and/or angio (2). One pt with TH by scan and at operation had probable embolic events. All pts with TH by echo or angio had definite or possible TH by PLT imaging.

We conclude that In-111 PLT imaging detects mural thrombi in some high risk pts with prior transmural infarction. PLT imaging may help define pts at risk for embolization and be useful for detection of TH in other settings, such as acute MI, and for in vivo assessment of antithrombotic drugs.

MYOCARDIAL UPTAKE OF TECHNETIUM-99M PYROPHOSPHATE IN PATIENTS WITH AMYLOIDOSIS. J. Muz, T. Wizenberg, W. Samlowski and Y. Sohn. Harper Division, Harper-Grace Hospitals, Detroit, MI.

Imaging of the heart with Technetium-99m Pyrophosphate (Tc-99m-PYP) for detection of myocardial infarction (MI) has become a well-established diagnostic modality. Increased uptake of Tc-99m-PYP in myocardium, particularly when it is diffuse and extensive, does not necessarily imply myocardial damage due to MI. It can be associated with cardiomyopathy secondary to amyloidosis, and possibly other conditions.

Of 681 Tc-99m-PYP cardiac studies performed in our department between 1/1/77 and 12/31/79, we have found 17 cases with diffuse extensive myocardial uptake of Tc-99m-PYP, without clinical and/or laboratory evidence of MI. Five patients of this group (two male and three female, ranging in age from 67 to 84 years) had histologically proven amyloidosis and clinical signs of cardiomyopathy.

The exact mechanism of Tc-99m-PYP uptake in amyloid cardiomyopathy is not known. It is probably related to the composition of protein in amyloid deposits in the myocardium. In our opinion, Tc-99m-PYP cardiac scintigraphy is an important noninvasive test in the diagnosis of amyloid cardiomyopathy.

DOES CORONARY BYPASS SURGERY IMPROVE GLOBAL AND REGIONAL LEFT AND RIGHT VENTRICULAR RESPONSE TO EXERCISE? M. Freeman, R. Gray, D. Berman, M. Raymond, J. Maddahi, J. Matloff, J. Forrester, H.J.C. Swan, and A. Waxman, Cedars-Sinai Medical Center, Los Angeles, CA.

To clarify the controversial effects of coronary artery bypass surgery (CABG) on ventricular function, 19 males had multiple gated equilibrium scintigraphy (MGES) with Tc-99m-RBC's in the 45° LAO view at rest (R) and maximal upright bicycle exercise (Ex) before (pre-op) and 5 months after (post-op) CABG. The left ventricle (LV) was divided into 5 segments and scored with a 5 point system (3=normal (nl), -1=dyskinesis). A total wall motion score (WMS) was obtained by summing the scores of the 5 segments. A $\leq$10% rise in ejection fraction (EF) or a WMS decrease of $\geq$1 during Ex from R was considered abnormal (abn). Of the 18 pts symptomatic pre-op, 12 were asymptomatic, 2 were improved and 4 were unchanged post-op. A positive stress ECG was present in 13 pts pre-op, but in only 3 post-op. Ex heart rate improved ($p \leq .05$) from 129±23 pre-op to 150±19 post-op. Although mean post-op R and Ex LVEF, right ventricular (RV) EF, and WMS were not significantly different from pre-op, Ex LV and RVEF tended to improve post-op. Importantly, LVEF rose post-op (.55 to .60) from R to Ex ($p \leq .05$), but did not pre-op (.55 to .55). Of the pts with abn pre-op response to Ex, nl post-op response of LVEF, RVEF, and WMS was noted in 11/14, 6/10 and 8/16, respectively. Of the pts with nl pre-op Ex response, abn post-op response of LVEF, RVEF, and WMS was noted in 3/5, 2/9 and 1/3, respectively. Symptomatic improvement was associated with nl post-op LVEF Ex response. Thus, clinical improvement was associated with improved LV functional reserve post-op. Furthermore, the data suggest that pts with nl function pre-op frequently demonstrate abn LV reserve post-op.

EXERCISE THALLIUM-201 IMAGING IN ASSESSMENT OF AORTO-CORONARY BYPASS SURGERY. W. Haaz, A. S. Iskandrian, S. Kane and B. L. Segal. Cardiovascular Institute, Hahnemann Medical College and Hospital, Philadelphia, Pennsylvania.

Thirty patients (pts) with recurrent symptoms, following aortocoronary bypass graft surgery, underwent angiography as well as exercise thallium-201 imaging (EX-Tl). There were 27 men and three women (age 34-70). They were divided as follows: Group I (10 pts, 2.4 grafts per pt) had normal EX-Tl. These pts had complete revascularization (CR), i.e. all grafts were patent, all diseased vessels were grafted and there was no progression of disease in the nongrafted vessels. Group II (7 pts, 2.3 grafts per pt) had normal EX-Tl in the presence of incomplete revascularization (IR), i.e., either graft occlusion or presence of nongrafted diseased vessels, however, each pt had at least one patent graft. Three pts had occlusion of grafts to diagonal branches {with either patent grafts to the left anterior descending (LAD) or a normal LAD} or occlusion of the graft to the right coronary artery (RCA) or disease of RCA. Group III (13 pts, 1.7 grafts per pt) had exercise-induced perfusion defects. Each pt had IR. The perfusion defect corresponded to the diseased vessel or occluded graft in each pt. The exercise electrocardiograms were not useful in predicting the status of revascularization.

We conclude, exercise imaging is highly specific (100%) in the evaluation of pts following bypass surgery. Pts with CR have normal images. Similarly, exercise-induced defects are only seen in the presence of IR. Normal images may be seen in some pts with IR; however, these pts generally have at least one patent graft and none had disease of LAD or its graft. Moreover, the disease in these pts is limited to RCA or diagonal branches or their grafts.

EXERCISE LV/RV STROKE INDEX RATIOS MEASURED BY GATED BLOOD POOL SCANS IN AORTIC REGURGITATION PRE AND POST VALVE REPLACEMENT. M. Besozzi, J. Clare, J. Santinga, J. Thrall and B. Pitt, University of Michigan Medical Center, Ann Arbor, MI.

Left ventricular (LV)/right ventricular (RV) stroke index ratios (SIR) were calculated in 10 patients with angiographically determined severe aortic regurgitation (AR), 3 with moderate AR, 3 minimal AR and 2 with aortic stenosis. The SIR was calculated at rest and at peak exercise before and after valve replacement. Controls were calculated on 20 patients without valve disease. Equilibrium gated radionuclide ventriculograms were acquired in the LAO 45° projection at rest and during maximal supine bicycle exercise. Fixed end diastolic regions of interest were drawn over the LV and RV and time activity were generated. The minimum (end systolic) counts determined from these curves were subtracted from the maximum (end diastolic) counts for each ventricle to give a stroke index (SI). SIR was calculated for each patient by dividing the LVSI by the RVSI (SIR = LVSI/RVSI). The normal SIR was 1.01 ± 0.08 (95% confidence interval). There was no significant change with exercise 1.06 ± 0.06 (.4>p>.3). The values for AR were: Severe = 3.59± .85, moderate = 1.99, minimal =1.77 and aortic stenosis = 1.02. In all patients with AR the SIR decreased with exercise (severe AR ex.=2.53 ± 0.78). Post operative values (0.97±0.09) were not significantly different than controls (.5>p>.4) except in one patient with perivalvular AR (2.91). This technique provides a non invasive means to quantitate AR, evaluate physical and pharmachologic effects on AR and evaluate prosthetic valve dysfunction.

EFFECTS OF EXERCISE ON REGURGITANT FRACTION AND RIGHT AND LEFT VENTRICULAR FUNCTION IN AORTIC AND MITRAL INSUFFICIENCY. E. Henze, G. Wisenberg, H.R. Schelbert. UCLA School of Medicine, Los Angeles, CA.

The hemodynamic response to supine exercise was studied with equilibrium blood pool imaging in 9 patients with isolated mitral (MI) or aortic (AI) insufficiency and compared to that in 9 normals. In order to calculate right ventricular (RV) ejection fractions (EF) and regurgitant fractions (RF) a technique was developed that corrects for the contribution of right atrial activity to right ventricular activity. At rest, mean LVEF in AI was 57.0±7.6 (SD) and not significantly different from N (59.6±4.2) but was lower in MI (51.5±7.6; $p<0.01$). Resting RVEF were slightly but significantly depressed in MI when compared to N (44.0±10.7 vs. 52.5±6.4; $p<0.05$) but not in AI (51.8±6.6). With this new approach RF in N at rest was negligible (1.9 ±8.6%), but was 53.2±4.8% in AI and 51.8±10.8% in MI (AI vs. MI not significant). With exercise, LVEF and RVEF in-

creased in N significantly to 70.5±3.8 ($p<0.01$) and 68.0±7.3 ($p<0.01$), respectively, without a significant change in calculated RF (2.3±14.1%). However, in both AI and MI, LVEF fell to 46.8±11.8 ($p<0.05$) and 41.8±6.1 ($p<0.05$) with no significant difference between AI and MI. The RVEF response, however, was distinctly different: it decreased in MI to 33.3±6.8 ($p<0.05$) but increased in AI to 65.8±8.3 ($p<0.01$). In both AI and MI the RF declined with exercise to 31.4±12.9 and 34.0±12.7, respectively ($p<0.01$ in both). Thus, in response to exercise RF declined in both AI and MI; and RVEF increased in AI but declined in MI. We conclude that exercise multiple gated acquisition blood pool imaging permits evaluation of the hemodynamic response and changes in RF in patients with valvular insufficiency.

QUANTITATION OF RIGHT VENTRICULAR VOLUME OVERLOAD BY GATED EQUILIBRIUM RADIONUCLIDE ANGIOGRAPHY. S. Sorensen, R. O'Rourke, T.K. Chaudhuri, University of Texas Health Science Center, San Antonio, TX

R-wave synchronous equilibrium radionuclide angiography (RNA) provides time-activity curve count information proportional to ventricular volumes which may be used for relative volume comparisons within either ventricle to derive ejection fraction (EF). Accordingly, comparisons of count output (CO) between right (RV) and left (LV) ventricles may permit quantitation of intracardiac shunt.

Employing an R-wave synchronized camera-computer system, we performed resting equilibrium RNA in 8 consecutive patients undergoing cardiac catheterization (CATH) for atrial septal defect. RNA pulmonary-to-systemic flow ratios (Qp/Qs) were calculated as Qp/Qs=RVCO/LVCO, where CO was derived from processed composite time-activity curves for each ventricle by subtracting end-systolic from end-diastolic counts (EDC). Mean (±SEM) systolic blood pressure (BP), heart rate (HR), LVEF, RVEF, Qp/Qs, and RV/LV EDC ratio were:

N=8	SBP	HR	LVEF	RVEF	QP/QS	R/L EDC
CATH	133±10	80±6	--	--	(2.6±.3)/1	--
RNA	123±6	71±3	.53±.03	.41±.01	(2.4±.3)/1	1.92±.13
P	NS	NS	--	--	NS	--

RNA Qp/Qs correlated well with CATH Qp/Qs (r=.95). RNA Qp/Qs was obtained in 4 pts before and after successful surgical atrial septal defect repair. (RNA Qp/Qs preoperative 2.9±.51; postoperative = 1.06±.82, $p<.05$). Mean (±SEM) RNA Qp/Qs calculated in 20 control pts (10 normal, 10 cardiac disease) without regurgitation or shunt was .99±.03 (range .80-1.23). We conclude that left-to-right shunting at the atrial level may be accurately detected, quantitated, and followed serially after therapeutic intervention using gated equilibrium RNA.

LEFT VENTRICULAR VOLUME AND CARDIAC OUTPUT DETERMINED FROM GATED BLOOD POOL IMAGING WITH AN ATTENUATION CORRECTED COUNT RATE METHOD. J.M. Links, L.C. Becker, J.G. Shindledecker, A.H. Maurer, and H.N. Wagner,Jr. The Johns Hopkins Medical Institutions, Baltimore, MD.

A new method for determination of left ventricular volume (LVV) was validated in 22 pts who had gated blood pool (GBP) imaging and single plane contrast ventriculography (CV), and in 9 other pts who had GBP imaging and thermal dilution (TD) analysis of cardiac output (CO) via Swan-Gantz catheterization. Gated LAO 40° and static anterior views were acquired. A radioactive marker was placed on the skin over the LV in the LAO view, and imaged during the anterior view. A blood sample was withdrawn during the LAO view, and counted on the collimator face after completion of both views. LVV at end-diastole (ED) was given by the ratio of the attenuation corrected LVED count rate in the LAO view to the count rate/ml from the blood sample. Attenuation correction was made by dividing the LVED count rate by e^{-ud} (u=u of water, d=distance from skin marker to center of LV in anterior view/sin 40° to yield depth of LV in LAO view). This LVEDV was used to calibrate the LV time-activity curve, yielding LV stroke volume. CO was obtained by multiplying the stroke volume by the average heart rate. The correlation between GBP and CV EDV was 0.96 (GBP = 1.06CV - 12 ml); between GBP and CV ESV was 0.96 (GBP = 1.19CV - 13 ml); between GBP and TD CO was 0.88 (GBP = 1.03TD + 0.21 l/min). This method permits non-invasive determination of LVV and CO without geometric assumptions, the use of a regression equation, or the need for determination of total blood volume.

LEFT VENTRICULAR VOLUME USING ATTENUATION-CORRECTED MULTIGATED DATA. R.J. Jaszczak, K.G. Morris, F.R. Cobb R.E. Coleman. Duke University Medical Center, Durham, NC.

We have investigated the feasibility of quantitating left ventricular blood volume from multigated cardiac studies. Initial phantom studies were performed using water-filled polyethylene bottles (representing "ventricles") placed in a water-filled Alderson body phantom. To simulate patient studies Tc-99m was distributed in the "ventricle" and "body" in a 10:1 concentration ratio R, respectively. The LAO view was used to obtain the background corrected ventricular count rate CV and signal-to-background ratio S/B. Data from two LPO views, one using an energy window centered on the primary photopeak (126-154 keV) and the other using an energy window positioned to accept scattered gamma rays (90-120 keV), were used to compute a ventricular length L and depth ƶ. A 1 ml sample was removed from the "ventricle" and counted with the camera (CS).

An initial volume $U=\{(CV)/(CS)\}\exp(\mu ƶ)$, where μ is the photopeak attenuation coefficient, is first computed. The measured parameters L, ƶ, S/B and D (LPO-RPO diameter) are then used to calculate the "unknown" concentration ratio R yielding a corrected volume V=U+U/R. The computed volumes for the phantoms were 34, 63, 141, 211, 323 and 633 ml for actual bottle volumes of 35, 65, 141, 206, 311 and 582 ml. End diastolic left ventricular volumes were calculated from five patient studies using the above algorithm and compared with biplane catheterization volumes. The radionuclide (cath) volumes are as follows: males-107 (119), 152 (138); females-101 (116) ml, 124 (188), 114 (228).

Thus ventricular volumes can be quantitated from multigated studies by correcting for attenuation, scatter and extra-ventricular activity. The depth ƶ and volume may be underestimated in patients with large breasts.

3:15-4:15 Room 3037

CLINICAL

HEART III

Session Chairman: Charles Boucher
Session Co-Chairman: Paul M. Weber

THALLIUM SCANNING: A COMMUNITY HOSPITAL'S EXPERIENCE. D.R.Spiegelhoff, D.L.Yuille, and A.E. Beranek, St. Luke's Hospital, Milwaukee, Wi.

Approximately 700 Thallium Stress-redistribution studies were performed between December 1976 and July 1978 at our institution. We have retrospectively located 154 cases from this time period with suitable cardiac catheterization data for comparison with the results of Thallium stress-redistribution imaging. These 154 cases are the basis for this paper. The patients in this series were taken to maximum stress by an experienced cardiologist, injected with Thallium and exercised for an additional 30-60 seconds. Multiple view stress imaging was begun 5-10 minutes post-exercise. Redistribution imaging was obtained 4-6 hours post-stress. Cameras and imaging techniques varied during this time interval. No cases were rejected because of poor technique and no computer processing was used. The overall series sensitivity for detecting coronary artery disease (CAD) with stenoses > 50% is 84.6% with a specificity of 92%. The sensitivity of the ECG stress test is 58.1% with a specificity of 83.8%. The sensitivity of Thallium scanning for one vessel disease is 76.2% for two vessel disease is 90.2% and for three vessel disease is 87.8%. We conclude that Thallium scanning is an effective screening procedure for CAD and that this series will provide a useful baseline for future comparison with computer processed Thallium scans.

IS THE ACCURACY OF DETECTION OF CORONARY ARTERY DISEASE CHANGED BY ECG GATING OF THALLIUM-201 MYOCARDIAL IMAGES?

J.H. McKillop, M.L. Goris, H.D. Fawcett, and J.E. Baumert, Stanford University School of Medicine, Stanford, CA.

Thirty-four patients undergoing selective coronary arteriorgraphy had stress Thallium-201 (Tl-201) myocardial imaging in anterior, 45° and 65° LAO projections acquired using ECG gating (16 images per cycle). Nongated images were created by adding the 16 images together to produce a composite for each projection. The Tl-201 images were processed by interpolative background subtraction and interpreted both in ECG gated diastolic and nongated forms by 3 independent observers who were unaware of the patient identity, the arteriogram results and whether the study was gated. Each observer classified every study as normal, probably normal, probably abnormal, or abnormal. In cases of disagreement, a majority verdict was obtained.

In 28 patients with abnormal arteriograms (>50% stenosis of luminal diameter of any major vessel), gated images were abnormal in 24 (sensitivity 86%) and the ungated images in 22 (sensitivity 79%). Three patients had false negative results both on gated and nongated images. Four of six patients with normal arteriograms had normal gated images (specificity 67%) and 5 normal ungated images (specificity 83%). There was greater uncertainty in interpreting the gated images, individual observers reading studies as probably normal or probably abnormal with a greater frequency on gated (24/102) compared to ungated (18/102) images.

These initial results suggest that any improvement in the accuracy of detection of coronary artery disease obtained by ECG gating of Tl-201 images is likely to be marginal.

THE EFFECT OF DIFFERENT LEVELS OF Tl-202 AND Tl-200 RADIOCONTAMINATION ON Tl-201 IMAGING, H.H. Hines, M.C. Lagunas-Solar, University of California Davis, Sacramento, CA

Tl-201 can be produced by (p,xn) reactions on Tl-203 and Tl-205 targets. The proton energy and target thickness particularly determine the yield of Tl-201, Tl-202, and Tl-200. Tl-202 and Tl-200 emit high energy photons that contribute significant Compton scatter into the low energy window and septal penetration to degrade Tl-201 images. We studied the effect of different levels of Tl-202 and Tl-200 radiocontaminants on Anger camera images.

The effects on image quality were evaluated from FWHM and FWM-10% determined from line spread function measurements made on a 37PM camera (0.25" crystal, GP collimator). The line sources, 1mm ID tubes filled with Tl-201, were placed at mid depth in a water bath 10cm deep. The sources were images at several different times post irradiation to get different levels of Tl-202 and Tl-200 by radiodecay.

When the Tl-202 levels were <5% (<.03% Tl-200) the FWHM was constant at 9.3mm (±.6mm) and the FWM-10% at 23mm (±.9mm). When Tl-202 levels ranged from 5 to 20% (<.03% Tl-200) the FWHM went from 9.2 to 9.9mm (±.6mm) and the FWM-10% from 23 to 45mm (±.9mm). When the Tl-200 levels ranged from 0.2 to 2.9% (<.01% Tl-202) the FWHM were 9.3± .6mm and the FWM-10% ranged from 20.7 to 22.7mm (±.9mm).

To preserve image quality, production parameters should be chosen to keep Tl-202 levels <5%. Also, Tl-200 levels should be kept <2%. If both Tl-202 and Tl-200 are present in the same sample, lower levels of both radiocontaminants should be maintained.

THALLIUM REDISTRIBUTION IN STUDIES THAT USE VASODILATORS.

Jeffrey Leppo, Tada Yipintsoi, and H. William Strauss. Massachusetts General Hospital, Boston, MA., and Montefiore Hospital, Bronx, N.Y.

The significance of Thallium-201 (Tl) redistribution after vasodilator administration is unknown. Accordingly, a left circumflex (LCX) stenosis that did not alter basal flow, but attenuated reactive hyperemia was produced in 10 dogs. Tl and radioactive microspheres (Ø1) were injected near the end of an 8 min I.V. infusion of adenosine (Ad) and sequential Tl scans were collected. Additional labeled Ø (Ø2-4) were injected before the end of a study (80-220 min). Left anterior descending (LAD) and LCX regional flow (ml/g/min) and Tl content (cpm/g) were determined by gamma well counting of all heart samples. Regional Ø1 flow (Q) defined 2 groups of hearts which had elevated Q as compared to Ø2-4 determinations; I-elevated Q in both LAD and LCX and II-elevated LAD Q only.

(Mean ± sd *=p<.05)

GROUP	Ad LAD Q	Ad LCX Q	Ad LAD/LCX Q	FINAL TL LAD/LCX
I(n=6)	4.26±1.07 *	1.85±.27 *	2.30±.47	1.10±.04 *
II(n=4)	1.95±0.86	0.91±.19	2.11±.60	1.25±.15

The Ø2-4 injections demonstrated homogeneous (LAD Q=LCX Q) perfusion during Tl redistribution. Initial Tl scan defects disappeared faster in group I than II as confirmed by the final Tl LAD/LCX ratios and despite similar initial flow ratios. We have demonstrated that substantial Tl redistribution occurs within 80-220 min after an initial flow disparity averaging 2 to 1 during the Tl injection and that higher loss of Tl from the normal scan area (LAD) rather than an increase of Tl in the defect (LCX) area is the mechanism for Tl redistribution in this type of study. These data also suggest that serial, imaging after vasodilators could differentiate between an initial defect produced by underperfusion secondary to a coronary stenosis and one caused by a scar.

RAPID RELATIVE REGIONAL WASHOUT (R^3WO) AS AN ATTRIBUTE OF Tl-201 IMAGING.

K.A. McKusick, P.C. Voukydis, M. Johnson and H.W. Strauss. Massachusetts General Hospital, Boston, MA and Mount Auburn Hospital, Cambridge, MA.

A normal area on an initial Tl-201 (Tl) image which demonstrates marked decrease or absent Tl concentration on the delayed image, in comparison to adjacent myocardium, is R^3WO. Correlation of R^3WO to the other attributes of Tl imaging (i.e., scar (S), ischemia (I), initial increased lung Tl and left ventricular size (F)) was sought in 95 patients (P) undergoing Tl - ECG stress exercise testing, of whom 20 (C) had catheterization because of intractable symptoms. 400k count Tl initial and 3-hour images were made with a large field of view camera by standard technique in 3 views. Interpretation was by consensus of two experienced observers who reviewed the images made on two intensity transparency and triple lens Polaroid films twice, without knowledge of the clinical data.

Tl RESULTS

PT	No.	NORMAL	I	S	F	R^3WO	
P	95	17%	32%	54%	27%	47%	(>1 Abnormality
C	20	5%	40%	75%	25%	60%	in some Patients)

In 2/20C, no CAD was found although S and R^3WO were present in both. In 12/14 segments with R^3WO, corresponding significant coronary artery disease (CAD) (>50% stenosis) was present. R^3WO was found most commonly with S (9/20C), and was the only attribute of CAD in 2/20C. Thus, R^3WO is a pattern of Tl clearance which occurs not uncommonly, and may be the only Tl indicator of CAD, but may not be specific.

QUANTITATIVE ANALYSIS OF STRESS AND REDISTRIBUTION TL-201 MYOCARDIAL SCINTIGRAMS IMPROVES DETECTION AND EVALUATION OF EXTENT OF CORONARY ARTERY DISEASE.

J. Maddahi, E. Garcia, D. Berman, J. Forrester, H.J.C. Swan, and A. Waxman. Cedars-Sinai Medical Center, Los Angeles, CA.

Visual interpretation (VIS) of Tl-201 scintigrams is suboptimal for detection and evaluation of coronary artery (CA) disease (D). Thus, we have recently developed a computerized technique that expresses the relative space-time distribution of Tl. Ten min images were obtained in the anterior, 45° and 70° LAO views 6 min, 40 min, 4 hrs, and 24 hrs after maximum (max) exercise in 67 pts: 32 normals (nls) and 35 with CAD (>50% stenosis). Multiple view max counts circumferential profiles (CPs) and washout (W) CPs were plotted to represent the Tl distribution and % W of 60 6° arcs of the myocardium. Pt CPs and WCPs were compared to the corresponding mean ±2 SD calculated from the pooled nl CPs and WCPs. Abnormalities were defined for both distribution and W patterns. CP was compared to VIS by 3 experienced observers to demonstrate the sensitivity (SENS) and specificity (SPEC) of each technique for detection of CAD pts and D in specific CA's.

	CAD	LAD	LCX	RCA	Total
SENS and CP	94%	83%	78%	96%	86%
(SPEC) of	(94%)	(78%)	(92%)	(75%)	(82%)
SENS and VIS	86%	57%	44%	78%	60%
(SPEC) of	(94%)	(78%)	(92%)	(92%)	(88%)

Regarding extent of CAD, both CP and VIS correctly iden-

tified single vessel D in only 40% of pts. However, CP correctly identified multi-vessel D in 87% of pts in contrast to 57% by VIS. Therefore, this new, quantitative method appears to be more SENS than VIS for both detection and evaluation of the extent of CAD with minimal loss of SPEC and offers the important advantage of objectivity.

AN OBJECTIVE AND QUANTITATIVE METHOD FOR ASSESSMENT OF REGIONAL LEFT VENTRICULAR WALL MOTION USING MULTIPLE GATED EQUILIBRIUM SCINTIGRAPHY. M. Freeman, E. Garcia, D. Berman, J. Maddahi, J. Forrester, H.J.C. Swan and A. Waxman, Cedars-Sinai Medical Center, Los Angeles, CA

The visual interpretation of left ventricular (LV) regional wall motion (RWM) from multiple gated equilibrium scintigraphy (MGES) is subject to inter- and intraobserver error. In this study we describe a new method for quantifying LV RWM using MGES in the 45° LAO view, and apply the technique in 15 normal volunteers and 15 pts with RWM abnormalities (ABN) demonstrated by contrast ventriculography. LV end-diastolic (ED) and end-systolic (ES) regions are obtained semiautomatically and are divided into 12 equal sectors originating at the center of mass of ES, and numbered as a clock's face. A contraction fraction (CF) is measured for each sector as the % change in sector area from ED to ES. The program runs on a small computer (32K) in less than 10 seconds. From the 15 volunteers, the normal range of RWM was established as the mean CF -2SD for each sector. In the abnormal pts the results of this new objective method were compared with visual assessment of RWM from MGES, performed by 2 experienced independent observers. RWM was evaluated as normal or abnormal in the proximal posterolateral segments (PLS) (sectors 2 and 3), distal PLS (sectors 4 and 5), apex (sectors 6 and 7) and septum (sectors 8 and 9). Of 30 segments with normal visual RWM, 19 (63%) were identified by the objective method as normal, with 9 of the 11 disagreements being associated with severe RWM in contiguous segments. Of the 34 segments with visual RWM ABN, 33 (97%) were correctly identified by the computer method. Therefore, this new quantitative method is effective in identifying normal and abnormal LV RWM in the 45° LAO view and offers promise for objective MGES assessment of RWM.

INSENSITIVITY OF THE INTERVAL EJECTION FRACTION TO DIFFERENTIATE NORMALS FROM PATIENTS WITH CORONARY DISEASE (CAD). A.J. Kemper, J.A. Bianco, P.H. Swerdlow, E.D. Folland, R. Shulman, A.F. Parisi and D.E. Tow. Nuclear Medicine and Cardiology Services, West Roxbury VA Medical Center and Harvard Medical School, Boston, MA.

The contribution to global left ventricular ejection fraction (LVEF) from various portions of LV systole defines interval global LVEF's. The usefulness of this parameter in differentiating patients with coronary artery disease (CAD) from normal volunteers was studied using first-pass RVG's with a multicrystal camera at 25 msec temporal resolution. The interval global LVEF during the initial, middle and last thirds of systole (end diastole to end systole) was computed for 10 normal volunteers and 13 patients with prior transmural myocardial infarction (by ECG and at least one asynergic area on contrast ventriculography). Results are as follows:

	Normals	CAD	P
First 1/3 EF (± SD)	0.16 ± 0.04	0.15 ± 0.04	NS
Second 1/3 EF	0.30 ± 0.04	0.27 ± 0.06	NS
Last 1/3 EF	0.14 ± 0.02	0.11 ± 0.04	<.05
Global EF	0.60 ± 0.03	0.52 ± 0.06	<.05

Additionally, the systolic time interval was divided into ten equal segments. The change in LV counts during each time segment was computed as a fraction of the total change in counts (end diastole to end systole). There were no significant differences between the normal subjects and the CAD patients. It is concluded that interval global LVEF's provide no information beyond that available in global LVEF in predicting the presence of CAD.

INCREASED LUNG UPTAKE OF THALLIUM-201: A NONINVASIVE MARKER OF EXERCISE-INDUCED HEART FAILURE
C.A. Boucher, L.M. Zir, G.A. Beller, H.W. Strauss, R.D. Okada, J.B. Bingham, G.M. Pohost, Massachusetts General Hospital, Boston, MA

We have noted increased lung uptake of Tl-201 (LUT) during exercise (ex) myocardial imaging in patients with severe coronary artery disease (CAD). To define the hemodynamic changes associated with LUT, 12 patients underwent supine ex Tl-201 testing during cardiac catheterization to monitor pulmonary capillary wedge pressure (PCWP) during ex. LUT on anterior images was assessed qualitatively as normal (N) or increased (I) and quantitatively by computing a lung-to-heart (L/H) activity ratio. Mean ± 1SD values in 7 patients with N-LUT were compared to those in 5 patients with I-LUT:

		N-LUT (n=7)	I-LUT (n=5)	P
L/H ratio		0.30±.03	0.51±.09	
CAD present		3/7 (43%)	5/5 (100%)	
Ex time (min)		9±2	5±3	<.05
PCWP	-rest	10±3	12±1	NS
(mmHg)	-ex	12±2	24±4*	<05

*ex value is greater than rest value ($p < 05$)

A qualitative increase in LUT was confirmed by quantitation and was associated with a shorter duration of ex and a large rise in PCWP during ex. Therefore, I-LUT appears to be a noninvasive marker of the development of heart failure during ex and should be added to the routine interpretation of thallium images.

CONTRIBUTION OF SEGMENTAL WALL MOTION TO EJECTION FRACTION IN PATIENTS WITH ACUTE MYOCARDIAL INFARCTION. F. Ohsuzu, C.A. Boucher, M.D. Osbakken, J.B. Bingham, J.B. Newell, H.K. Gold, R.C. Leinbach, G.M. Pohost, and H.W. Strauss. Massachusetts General Hospital, Boston, MA.

To determine the impact of the location of infarction on ventricular function, a series of 127 patients with acute myocardial infarction had gated blood pool imaging within 18 hours of the onset of symptoms in both the anterior and LAO positions. The left ventricular circumference was divided into 5 segments on the anterior view, and 5 segments in the LAO view. The regional wall motion was graded subjectively from 4 if normal to 0 if dyskinetic. The ejection fraction (EF) was determined using a varying region of interest-counts method. The contribution of each segment to the global EF was then determined by multiple linear regression analysis. The apical-septal, anterobasal, posterolateral walls were found to have the dominant influence on the EF; EF=-15.35+7.379x(anterobasal) + 3.361x(apical-septal) + 3.321x(posterolateral) + 2.950x (anterolateral) + 3.946x(superior-lateral).

These data suggest that during the acute phase of myocardial infarction, lesions involving the apical-septal, anterobasal, posterolateral, anterolateral, and superior-lateral segments are more consistently serious than those involving the apical, diaphragmatic, posterobasal, basal-septal, and inferior-lateral segments.

TWO INJECTION METHOD AND REVERSE TWO INJECTION METHOD FOR ESTIMATING THE REDISTRIBUTION OF PULMONARY BLOOD FLOW UNDER EXERCISE. T.Tanaka,K.Hirosawa,K.Kusakabe,and T.Yamazaki. Heart Institue Japan,Department of Radiology, Tokyo Women's Medical College,Tokyo,Japan.

To detect noninvasively the redistribution of pulmonary blood flow,changes of digital perfusion images(DPI),caused by various stimuli two injection method was introduced.

For the control DPI 1 mCi dose of Tc-99m MAA was injected in the errect posture,then data were collected during 200 seconds period of quiet breathing by using GCA-401(Toshiba).After desired stress test 10 mCi dose of Tc-99m MAA was injected in the same way.Data were collected during 20 seconds period.The DPI were obtained by using Varicam system.By comparing both DPI the changes of pulmonary blood flow caused various stress test were estimated.Reverse method consists of reverse procedure,i.e. first desired stress test then injection of 1 mCi,after data collection control DPI were obtained by using 10 mCi.

By using this method new findings were easily obtained. In normal subjects the basal hyperperfused area unchanged, though apical hypoperfused area diminished after exercise. A remarkable changes were noted in the DPI of the patients with mitral stenosis after exercise.Postual change also caused considerable changes in DPI.A tab. of NTG caused some changes in DPI of the patients with ischemic heart disease.The reverse method was useful for serious case.

The possibility of estimating the changes of DPI, distribution of pulmonary blood flow,were showed.It might

be possible to estimate noninvasively pulmonary hemodynamic changes under various stress test.

3:15-4:15 Room 3039

RADIOPHARMACEUTICAL CHEMISTRY

BIOINORGANIC CHEMISTRY SYMPOSIUM (cont'd)

Session Chairman: Michael A. Davis
Session Co-Chairman: H. Donald Burns

SPECIFIC ATTACHMENT OF SUBSTITUTION INERT METAL CENTERS - PRACTICE AND PROSPECTS. H. Taube. Stanford University, Palo Alto, CA

The features of structure, electronic and molecular, that lead to the formation of robust complexes will be reviewed and the advantages and some of the limitations of the use of substitution inert metal centers will be discussed. Special emphasis will be given to the chemistry of a particularly versatile system, comprised by ruthenium in the 2+ and 3+ oxidation states. Added to the usual features of substitution inert centers, is the facile electron transfer which is an important factor in the loading of a substrate as well as in the way the properties of the substrate are altered. Futhermore, loading under equilibrium as well as kinetic control is possible. Prospects with osmium complexes and with organometallic combinations will be discussed.

3:15-4:15 Room 2040

INSTRUMENTATION

COMPUTERS: INSTRUMENT EVALUATION

Session Chairman: William Hunter
Session Co-Chairman: Gene Johnston

A PROGRAM FOR QUANTIFICATION OF GAMMA CAMERA SPATIAL LINEARITY. NH Clinthorne, WL Rogers, and KF Koral. Department of Internal Medicine, University of Michigan Medical Center, Ann Arbor, MI.

Frequent assessment of gamma camera linearity is essential to avoid acquisition of data which may generate artifacts in reconstructed tomograms. An automatic peak-finding and linear fitting computer program has been written to provide a simple measure of camera linearity using data from an orthogonal hole calibration plate illuminated by a flood source.

The calibration plate is oriented on the camera face such that the rows and columns of holes lie along the X and Y axes of the camera. The algorithm determines centroids of the point images and performs a least squares linear fit to the rows and columns of the hole pattern. Linearity parameters calculated include worst case and overall goodness of fit of centroids to the least squares lines, the skewness of the fitted lines, and non-uniformity in X and Y camera gains. These parameters can be calculated within circular regions of desired radius concentric with the center of the camera field. The algorithm is implemented in FORTRAN IV, requires 16k words of memory and analyzes 128 x 128 data in 100 seconds on a Data General NOVA 1200 computer.

Evaluation of the program was accomplished with a wide-field camera having mild barrel distortion. The correction of this distortion with a commercial linearity corrector showed up as a reduction of 33% in the mean absolute deviation from the fitted lines. The program is a straight forword and sensitive method of quantifying camera linearity.

A General Measure of Anger Camera Linearity And Results With And Without An On-Line Corrector
K. F. Koral, M. E. Schrader, and G. F. Knoll, Medical Data Systems, Ann Arbor, Michigan

A new technique is presented for characterizing the linearity of an Anger camera over a circular field of view of a given diameter. Required for the measurement is a lead plate with thin grooves machined parallel to one another and at equal known spacing. High resolution images are acquired by a computer with the plate illuminated by a point source and oriented first in the x and then the y direction. These x and y images are processed separately. The procedure, which follows, is equivalent to requiring a simultaneous best fit to a set of parallel and equally-spaced lines in each direction. First, the apparent location of each line is found at equally-spaced values of the orthogoual coordinate by a centroid-locating program. Then these locations are fit by the method of least squares to the true values over the entire camera surface using the equation of a plane. (One of the coefficients from each fit gives the value of camera gain in the respective direction.) Finally, discrepancies between the data points and the fit values are calculated and a mean of the absolute values found. These means, one for x and one for y, are the measures of linearity in the respective directions.

The technique was applied to the computer images of selected Anger cameras with and without the preprocessing of output signals by an on-line linearity corrector. Comparative results are presented as a function of the diameter of the field of view.

A MINICOMPUTER BASED ANGER CAMERA QUALITY CONTROL PROTOCOL. B.H. Hasegawa, M.T. LeFree, D.L. Kirch, R.A. Vogel, W.R. Hendee, P.P. Steele, University of Colorado Health Sciences Center and Denver VA Medical Center, Denver, CO.

Anger camera quality control procedures traditionally are based on subjective visual interpretation of test images and lack the reliability, sensitivity, and reproducibility of quantitative performance evaluations. A quantitative quality control protocol with accompanying software has been developed for a Picker Dyna 4/15 Anger camera-ADAC CDS minicomputer system at the Denver VA Medical Center. The quality control analysis is derived from an orthogonal hole phantom digital image from which quantitative and regional measurements of point source sensitivity, spatial resolution, and spatial linearity are calculated for each of approximately 700 orthogonal hole locations across the crystal face. Information is presented as a series of functional images and histograms showing the distribution of values for each measurement. Two versions of the software have been developed. One version is designed specifically for technologist performed routine quality control evaluations. Minimal operator intervention is required and the entire protocol can be completed in less than 30 minutes. Functional images and histograms, as well as relevant demographic data, are automatically compiled and furnished to the system multiformat camera for recording on film as a hard copy quality control record. The second software version is designed as a diagnostic and research tool. It allows a physicist or engineer to interactively and selectively display specific features of camera performance. This quantitative methodology provides more complete, sensitive, and reliable results than conventional methods for absolute and comparative Anger camera performance evaluations.

EVALUATION OF COMPUTER IMAGE DISPLAY SYSTEMS USING DIGITAL TEST PATTERNS. T. R. Miller, K. S. Sampathkumaran, D. R. Biello, and M. W. Vannier. Mallinckrodt Institute of Radiology, St. Louis, MO.

With the increasing use of digital images in nuclear medicine, a method is needed to qualitatively and quantitatively evaluate and adjust computer-video monitor-film systems. Three computer generated digital test patterns were used to evaluate several computer display systems. One pattern, consisting of linear and logarithmic gray scale wedges and horizontal and vertical bars of varying pixel widths, was used for gray scale, resolution, and edge sharpness evaluation. The other two patterns, a cross-

hatch and a "pin cushion" dot pattern, permitted assessment of spatial linearity and resolution. In addition to qualitative determinations, quantitative optical densitometry measurements were performed to evaluate gray scale linearity and saturation. Several black-and-white and color computer display systems with differing gray scales and resolutions were tested using this method. The images were recorded on polaroid and x-ray film and videotape. Significant differences, many of which had not been appreciated in routine clinical use, were found among the various systems using these patterns. In some cases, unexpected important misalignments were discovered. Adjustment of the systems was much more precise and reproducible than when conventional gray scale wedges or clinical images were employed. In conclusion, using these computer generated digital test patterns one can: 1)assess the performance of computer display systems qualitatively and quantitatively; 2)optimize the adjustment of these systems; and 3)perform routine quality control measurements.

AN AUTOMATED PROGRAM TO CONVERT DATA FROM A SCANNING CAMERA INTO A WHOLE BODY COMPUTER IMAGE. M.A. King and P.W. Doherty. The University of Massachusetts Medical School, Worcester, MA.

An automated program was written to convert the output of a scanning camera into a whole body computer image which can then be used to study regional and whole body radiopharmaceutical localization and retention. The electronically masked output of the camera is collected as a dynamic study on the computer with the time per frame set according to scan speed. The program overlays these frames onto a matrix in memory to form the image. The overlayed frame is incremented 1 pixel in the direction of camera motion during camera scanning or positioned on top of the last frame during electronic scanning. The timing of camera motion is automatically determined by the program. Both single and double pass studies can be reconstructed. Upon completion the program stores the matrix as a patient study. The standard software of the computer system can then be used to analyze the study. By using the geometric mean of the anterior and posterior scans and appropriate phantom data, uptake in % of dose can be estimated. We are investigating the usefulness of the program in quantitating: 1) regional uptake in metabolic bone diseases, 2) % of dose of 111-In labeled white blood cells at sites of infection and abscesses, and 3) R to L shunts with 99m-Tc MAA.

THURSDAY, JUNE 26, 1980

2:00-3:30 Room 2043

CLINICAL

RADIOLABELED ANTIBODIES

Session Chairman: Frank DeLand
Session Co-Chairman: Kenneth McKusick

INVITED SPEAKER
Edgar Haber, MD, Massachusetts General Hospital, Boston, MA
CONCEPT OF RADIOLABELED ANTIBODIES FOR DIAGNOSIS.

RADIOIMMUNODETECTION OF LUNG CANCERS USING RADIOLABELED ANTIBODIES TO CARCINOEMBRYONIC ANTIGEN (CEA), ALPHA-FETOPROTEIN (AFP) AND HUMAN CHORIONIC GONADOTROPIN (HCG). E.E. Kim, F.H. DeLand, P.A. Domstad, S.J. Bennett, G.H. Simmons, and D.M. Goldenberg. University of Kentucky and Veterans Administration Medical Centers, and McDowell Cancer Network Lexington, KY.

The detection of primary pulmonary tumors (20 carcinomas, 1 carcinoid, 1 giant cell tumor) by radioimmunoscans with I-131 labeled antibodies to CEA, AFP or HCG was evaluated in 22 patients. At 24 and 48 hours after injection of the radioactive antibodies, images of the chest and abdomen were made with a scintillation camera and computer-assisted processing was performed to minimize background activity. In 16 patients with 22 lesions by chest radiographs studies with anti-CEA scans detected 16 lesions. Of the six false negative results, three lesions were less than 2 cm in diameter and the other three (3-5 cm) were obscured by excessive radioactivity in adjacent axillary lymph nodes or technical limitations of processing. Six patients with solitary lung tumors were examined with anti-AFP (3) and anti-HCG (3). Tumor localization was observed in 2 of 3 cases with each of these radioantibodies. Metastatic lesions in the liver corroborated by liver-spleen scans in 3 patients were also demonstrated by radioimmunoscans (CEA 2, HCG 1) and no false positive radioantibody localization was seen in 23 secondary sites presumably free of tumor byoother diagnostic studies. The average tumor to non-tumor count density ratio was 1.51: the tumor to non-tumor image contrast was enhanced more than two-fold by the subtraction process. Circulating blood levels of these antigens showed no correlation or interference with radioantibody tumor localization. Radioimmunodetection offers tumor localization and information on tumor endocrine secretion.

TUMOR IMAGING IN MICE WITH I-131 LABELED MONOCLONAL ANTIBODY. G. Levine, B. Ballou, J. Reiland, D. Solter, L.W. Gumerman, and T. Hakala. University of Pittsburgh Schools of Medicine and Pharmacy, Pittsburgh, PA.

The use of specific antibodies for tumor localization and treatment has been suggested and attempted for some time. The recent development of tumor specific monoclonal antibodies derived from hybridomas offers a potent tool for tumor detection. We report three related studies in which a tumor specific monoclonal antibody was labeled with I-131 and injected into MH-15 teratocarcinoma bearing BALB/C mice. For Kinetic studies 15 μCi were administered in 0.2 ml, I.V.; for imaging studies 150 μCi were used. In the first study using only antibody specific to human and mouse teratocarcinomas we found tumor to muscle ratios of 150:1, and tumor to blood ratios of 15:1 at five days post administration with an accumulation of 15% of the administered dose per gram in the tumor. Following administration, the labeled specific anti-tumor antibody was eliminated from the various non-tumor tissues, presumably as a function of the perfusion kinetics. In the second study mice were implanted with a non-specific (control) tumor and the teratocarcinoma. Antigenic (test) to non-antigenic (control) tumor tissue ratios approach 30:1. In the third study sets of three mice bearing only the teratocarcinoma were used; one mouse received I-131 specific antibody, one received I-123 non-specific antibody and the third received both. The image with the I-123 non-specific antibody was subtracted by computer from the image with both specific and non-specific antibodies, leaving the specific tumor image only at 48 hours post administration.

A KIT FOR DIRECT LABELING OF ANTIBODIES AND ANTIBODY FRAGMENTS WITH TC-99m. B.A. Rhodes, D.A. Torvestad, S.W. Burchiel and R.K. Austin. University of New Mexico Radiopharmacy, Albuquerque, NM

The purpose of this study was to develop a method of preparing IgG and fragments (FAB) in a freeze-dried form that could be readily labeled to high specific activities with Tc-99m. The radiolabeled antibodies are intended for tumor imaging. Three Hundred (300) mg of protein in a phthalate/tartrate buffer are incubated with 0.12 mg of stannous ions for 21 hours at 25° C and under N-2. One Hundred Fifty (150) μgm aliquots of the protein are freeze-dried. Labeling is achieved by the addition of up to 50 mCi of Tc-99m in 1 cc of saline. Tc-99m, other than that firmly bound to the protein, is removed by a passage through a 0.9 cm x 20 cm pretreated Sephadex G-25 column. Studies were completed to show optimum pH, concentration of stannous ions, and incubation times. Also, the absence of colloidal Tc was shown; however 5-10% of the protein-bound Tc can exchange onto albumin. Labeling yields of up to 90% have been achieved. The Tc-labeled product showed antigen titration curves similar to that of the original antisera. When anti-IgG

was the labeled antibody, it was demonstrated that it could be used to obtain specific labeling with Tc of 12 different human tumor cells grown in tissue culture. It is concluded that it is feasible to prepare Tc-labeling kits which produce strongly bound Tc-99m in high specific activity and preserve the immunoreactivity of the antibodies or antibody fragments.

2:00-3:30 Room 3037

CLINICAL

BONE II

Session Chairman: Brian Lentle
Session Co-Chairman: Gopal Subramanian

INVITED SPEAKER
Ignac Fogelman, University Dept. of Medicine & Nuclear Medicine, Royal Infirmary, Newton-Mearns, Glasgow, Scotland
METABOLIC BONE DISEASE

SYMPATHETIC NERVOUS SYSTEM DISORDERS OF BONE: SCINTIGRAPHIC DETECTION. N.D. Charkes and E.W. Fordham. Temple University Hospital, Philadelphia, PA and Presbyterian-St. Luke's Hospital, Chicago, IL

We have recently shown that the kinetics of 18F-fluoride, a bone-seeking tracer, can be simulated by a multicompartmental model, the underlying assumptions of which have been verified in animal experiments (JNM 20:1150,1979). We have extended these studies to the modelling of 99mTc-MDP, and have proposed a parallel-flow model of the microcirculation in bone to account for certain experimental observations (JNM 20:1257,1979). This blood flow model postulates that about 1/3 of the bone microcirculation is normally closed, by sympathetic tone, since severing the sympathetic supply to bone at supranormal flow rates increases MDP uptake in bone by about 50%. In this study we have sought for scintigraphic abnormalities in sympathetic nervous system disorders, as predicted by the model, by reviewing bone scans done and interpreted by one of us. The typical scintigraphic appearance which we found was that of a diffuse increase in counting rate over one or more long bones of an extremity ("recruitment" or "hyperemic effect"). Disorders demonstrating the abnormality include stroke, sympathetctomy, lumbar discogenic disease with sciatica, peripheral neuropathy (diabetes), reflex sympathetic dystrophy syndrome (viz., shoulder-hand syndrome after myocardial infarction) and intraosseous disorders such as fracture, osteomyelitis, and certain tumors. Conclusions: Kinetic modelling predicts a characteristic bone scan abnormality in patients with extraosseous and intraosseous disorders of the sympathetic nervous system. The abnormality has been sought for and found in clinical studies. Identification of this pattern is an important advance in bone scan interpretation.

SCINTIGRAPHIC AND BIOPTIC FINDINGS EARLY AFTER INTRACAPSULAR FRACTURE OF THE FEMORAL NECK. P.F. Høilund-Carlsen, A. Widding, A. Uhrenholdt, P. Christoffersen and J. Greiff. Hvidovre Hospital, University of Copenhagen, Denmark.

The purpose of this investigation was to evaluate the value of hip scintigraphy for the detection of avascularity of the femoral head shortly after intracapsular fracture of the femoral neck.

So far 15 patients were investigated in a controlled clinical trial. During operative treatment biopsy samples were taken from the femoral head and the trochanteric region 2 hours after the intravenous injection of lo mCi Tc-99m-Sn-pyrophosphate. Before histological examination the activity in each biopsy was counted and expressed as the ratio: specific activity in femoral head/specific activity in trochanteric region. Hip scintigraphy was performed at the time of operation, a week later, and 6 weeks after the fracture. Anterior views were taken using a 6 mm pin-hole collimator and the same collection time on both sides.

There were no histological differences between femoral head and trochanteric biopsies. Eight patients had normal activity in the femoral head at all scintigraphic examinations and also high biopsy activity ratios (1/1 - 1/9). In four patients with changing scintigraphic findings ratios were high (1/4 - 1/6) in three and low (1/28) in one. Three patients with repeatedly low uptake in the femoral head at scintigraphic examination had all low ratios (1/22 - 1/1o2).

Hip scintigraphy with bone seeking radionuclides is likely to image the vascularity of the femoral head. But the earliest scintigrams are difficult to interpret and the vascularity seems to be too changeable in the first few weeks after the fracture to allow reliable prediction of the viability of the femoral head at this early stage.

SKELETAL RESPONSE TO RADIATION INJURY. P.O. Alderson, B.A. Siegel, R.L. Donovan, and E.R. Barron. Armed Forces Radiobiology Research Institute, Bethesda, MD.

To evaluate the response of the skeleton to radiation injury, male rats underwent a 1000,1500 or 2500 rad single exposure of the right tibia with 250 KVP x-rays. Tibial accumulation of Tc-99m EHDP was evaluated at 1,3,5 and 7d, and at 2-4,6,8,12,16 and 24 wks post-exposure. Each group contained at least 5 animals. Each anesthesized animal received a 15 uCi i.v. dose of EHDP. Three hrs later animals were sacrificed and cts/gm in the whole rt tibia were compared to those in the unirradiated lt. tibia. Thirty-two animals in various dose groups also received an intracardiac injection of 600-900,000 Sr-85 microspheres (15 ± 5u) one minute prior to sacrifice and the R/L cts/gm ratio was used to determine relative blood flow. Each group initially showed about a 20% increase ($p<.001$) in EHDP accumulation in the irradiated tibia, but returned to baseline by 1-2 wks post-exposure. Subsequently significant decreases in EHDP accumulation occurred. In the 1000 and 1500 rad groups the maximum decrease occurred approximately 10 wks post-exposure, when rt tibia activity averaged 90% of control levels. Both these groups showed a return to normal EHDP accumulation by 24 wks. Tibial activity in the 2500 rad group fell to 60% of control levels at 10 wks and did not change thereafter. There was a significant linear relationship between relative EHDP accumulation and microsphere activity in the 32 animals that received both tracers ($r = 0.82$, $p<.001$). The results demonstrate that the skeletal response to radiation injury depends on the dose received and the time after exposure, and that bone tracer accumulation is closely related to changes in blood flow in the irradiated area.

ACCURACY OF BONE AND GALLIUM IMAGING IN PATIENTS WITH PAINFUL PROSTHESES. N.P. Alazraki, M.M. Convery, and F.R. Convery. University of California and Veterans Administration Medical Center, San Diego, CA.

Painful prostheses can be caused by infection, loosening, or both. This study evaluated the ability of the 67-Ga and 99m-Tc MDP bone scan to correctly diagnose the cause of pain.

Twenty-six patients with hip or knee prostheses had bone and gallium scans within 48 hours of surgery. Arthrogram, sedimentation rate, hematocrit, and joint aspiration were also performed preoperatively.

Scan criteria for infection were: 3+ or 4+ focal increased uptake on both bone and gallium images, where zero is normal and 4+ is severe increased uptake. Scan criteria for loosening included: abnormal bone scan (1+ - 4+) and gallium scan normal or mildly abnormal (0 - 2+).

Scans correctly diagnosed infection in 3 of 4 patients; in one patient the scans were falsely negative. There were 6 false-positive scan interpretations of infection. Sensitivity for diagnosis of infection by scans was 75%; specificity was 73%.

Scan diagnosis of loosening was in agreement with surgical impression in 18 patients. There were 3 false-positive scans for loosening and no false-negatives. Scan sensitivity for loosening was 100%; specificity was 40%. Overall scan accuracy for correctly diagnosing loosening and/or infection was 80%. Arthrogram correlated with 72% accuracy.

Joint aspiration correlated best with infection, yielding a 96% accuracy.

Since a normal 99m-Tc bone scan appears to exclude a surgically correctable abnormality, we conclude that bone scans alone may be worthwhile in selected patients.

THE ROLE OF Tc-99m PHOSPHATE COMPOUNDS AND GALLIUM-67 IN THE MANAGEMENT OF MAXILLARY-FACIAL DISEASE. R.B. Shafer, J.M. Marlette, G.A. Browne, and M.K. Elson. V.A. Medical Center, Nuclear Medicine Service, Minneapolis, MN.

Osteomyelitis of maxillary-facial bones is difficult to differentiate from trauma or malignancy, yet successful management is dependent upon early diagnosis, appropriate therapy and documentation of effective treatment. To differentiate osteomyelitis from trauma, 46 Tc-99m phosphate compound (Tc-99m PP) and gallium-67 studies were done in 35 patients with maxillary-facial disease. In all patients the definitive diagnosis was determined by surgery and/or clinical follow-up. Specific diagnoses included active osteomyelitis, chronic osteomyelitis, non-union or healed fractures and recurrent malignancy. In 31 of 34 patients the bone scan was positive. In the 4 negative studies, no bony abnormalities were subsequently demonstrated. Ten of 34 gallium-67 studies were interpreted as positive for osteomyelitis. Subsequent surgery and/or clinical follow-up demonstrated active osteomyelitis in all 10 patients. Of the 24 negative gallium-67 scans, one patient was demonstrated at surgery to have actinomycosis and a second patient had chronic, low-grade osteomyelitis. Four patients with active osteomyelitis and positive gallium-67 scans were restudied following therapy and found to have negative scans. Conclusions: 1) The addition of gallium-67 to the bone scan study of maxillary-facial disease contributes significantly to differentiating trauma from osteomyelitis. 2) Radiographic changes do not accurately reflect bone activity, nor differentiate trauma from osteomyelitis. 3) Although follow-up scans were obtained in only 4 patients, the data suggest that gallium-67 and Tc-99m PP are useful in evaluating effectiveness of therapy in patients with maxillary-facial disease.

FLUORINE-18 POSITRON EMISSION TOMOGRAPHY OF BONE LESIONS. S.D.J. Yeh, R.S. Benua, R. Grando, M.C. Graham. Memorial Sloan-Kettering Cancer Ctr.,Cornell.Med.Coll., N.Y.,N.Y.

Conventional bone scans display 3D distribution of increased mineral turnover as 2D images, thus making interpretation difficult in some patients. The purpose of this study is to evaluate whether or not positron emission tomography of F-18 bone scans will increase diagnostic accuracy over that of conventional Tc-99m diphosphonate bone scans.

Fourteen patients with pelvic, 19 with thoracic, 4 with calvarial and 11 with limb lesions were studied. The majority of patients had osteogenic sarcoma, breast or prostate carcinoma. Images were made on the Positron Camera PC 4200. This camera has 280 NaI(Tl) crystals, 2 cm in diameter and 3.8 cm in thickness. A total 2848 coincidence lines were collected from an area 30 x 30 cm over a period of 30 minutes and stored in the buffer memory. A longitudinal plane image and reconstructed transaxial images were produced on the video display.

Positron emission tomography has been most useful in differentiating parenchymal lung metastases of osteogenic sarcoma from rib or spine lesions. In the pelvic area, ileal conduit or bladder activity can be separated from adjacent bony structures. The location of calvarial lesions was precisely determined. Compared with Tc-99m scans, the tomograms improved localization for selected lesions of the thorax, skull or extremities. Only 3 of 14 pelvic studies were helpful.

Data from this study suggests that 3D images of bony structures can be successfully reconstructed with the PET. Additional information permits the determination of precise location, extent of lesion and its relationship to neighboring structures.

THE USE OF A STERILIZABLE RADIATION PROBE DURING BONE SURGERY. C.L. Colton and J.G. Hardy. Queen's Medical Centre, Nottingham, U.K.

A technique has been developed which enables bone lesions to be located easily and accurately at surgical exploration.

The method is applicable to lesions showing enhanced uptake of radiopharmaceutical by gamma camera scintigraphy. The patient is injected with 10 - 15 mCi Tc-99m methylene diphosphonate four hours prior to surgery. Following surgical exposure the sterile probe is scanned over the surface of the bone thereby pinpointing the site of the lesion. The probe has a maximum diameter of 9 mm, and comprises a well-collimated sodium iodide detector coupled with a photomultiplier tube via a 1.5 m light guide. The assembly is sterilizable by ethylene oxide.

The technique has been applied to the localization of osteoid osteomata in four patients. In each case the count rate monitored over the tumor was about four times that detected over the surrounding bone. Thus for each patient it was possible to accurately localize the tumor and to curette the nidus whilst minimizing the amount of overlying cortex resected. Autoradiography has been undertaken on the tissue specimens. Follow-up has shown that the patients have been relieved of all pre-operative pain.

The technique described is applicable in other situations, for example the selection of biopsy sites.

2:00-3:30 Room 3039

RADIOPHARMACEUTICAL CHEMISTRY

MYOCARDIAL

Session Chairman: Thomas F. Budinger
Session Co-Chairman: Donald M. Wieland

DEVELOPMENT OF A Tc-99m MYOCARDIAL IMAGING AGENT TO REPLACE Tl-201. E. Deutsch, K. A. Glavan and D. L. Ferguson, Department of Chemistry, University of Cincinnati, and S. J. Lukes, H. Nishiyama and V. J. Sodd, Nuclear Medicine Laboratory, BRH, FDA, Cincinnati, OH.

For some time there has been keen interest in developing a Tc-99m based replacement for Tl-201. While Tl-201 is currently the agent of choice for imaging normal myocardium, it is subject to several limitations (high cost, low photo-peak energy, low count rate per dose) which would be largely eliminated by use of a Tc-99m agent. We have evaluated several cationic technetium complexes as potential myocardial perfusion agents, and find that at least one of these exhibits myocardial uptake comparable to that obtained with Tl-201. This well-defined inorganic complex is prepared with "no carrier added" Tc-99m under clinical conditions. Images of normal dogs obtained with a high sensitivity collimator clearly visualize the myocardium with maximum myocardial uptake occurring about 20 min post injection. The bulk of the activity is taken up by the hepatobiliary system. Tissue distribution studies in three purebred beagle dogs sacrificed 20 min post injection yield the following average %dose/g values: bile, 0.073; liver, 0.044; gallbladder, 0.030; myocardium, 0.022; pancreas, 0.015; lung, 0.009; skeletal muscle, 0.008; blood, 0.004; rib, 0.003; pericardium, 0.002. Time dependent tissue distribution studies in normal rats also show significant myocardial uptake (2.3 %dose/g in myocardium at 10 min post injection). These nascent investigations firmly establish that Tc-99m complexes can accumulate in, and image, the normal myocardium; they also lay the groundwork for future development of more efficacious Tc-99m myocardial imaging agents.

3-(C^{11})-METHYL GLUCOSE, A PROMISING AGENT FOR IN VIVO ASSESSMENT OF FUNCTION OF MYOCARDIAL CELL MEMBRANE. K. Vyska, A. Höck, C. Freundlieb, L.E. Feinendegen, G. Kloster, G. Stöcklin, Institute of Medicine and Institute of Nuclear Chemistry, Nuclear Research Center Jülich, FR Germany.

In vitro studies demonstrated that O-methyl-D-glucose - a non-metabolisable analogue of glucose - is an excellent indicator for investigating the sugar transport across the

cardiac cell membranes. Since the transmembrane transport is known to be a limiting factor for cardiac utilisation of glucose, we concluded that 3-(C^{11})-methyl glucose (MG) might provide valuable clinical information.

The MG was synthesized by methylation via $^{11}CH_3I$ of the potassium salt of diacetone-D-glucose [1]. 1-1.5 mCi of MG were i.v. injected in 9 rabbits. Whole body distribution was detected with a large-field-of-view gamma camera, equipped with a special high energy (511 KeV) collimator. The serial scintigrams were registered in AP projection with a frame frequency of 1 per minute.

MG is preferably accumulated in heart, liver, and kidney. The myocardium is clearly delineated from all surrounding tissues. The heart/lung and heart/liver ratios were 3.3 and 1 respectively. The turnover of MG in the myocardium was rapid, with accumulation and elimination half lifes of 2 and 5 minutes respectively.

MG seems to provide an excellent indicator for myocardial imaging; MG-turnover in vivo is easily detected. The method promises quantification of membrane processes in vivo.

[1] G. Kloster et al. Proc. of 17th Ann. meeting of ESNM Innsbruck 1979 (in press).

THE EFFECT OF DIPHENYLHYDANTOIN (DILANTIN) ON THALLIUM-201 CHLORIDE UPTAKE. E.R. Schachner, Z.H. Oster, N. Cicale, D.F. Sacker, P. Som, H.L. Atkins and A.B. Brill. Brookhaven National Laboratory, Upton, New York.

Thallium-201-chloride (Tl-201) is widely used for myocardial imaging. It is a potassium analogue and both cations behave similarly. Dilantin is a widely used drug for most types of epilepsy. It is also used in the treatment of ventricular tachycardia and digitalis-induced arrhythmias. Dilantin acts primarily by increasing membrane-potassium conductance by acting on the sodium-pump. In view of these facts we have looked for possible effects of Dilantin on Tl-201 uptake by the heart. A dose of 1.25 mg of Dilantin was injected intravenously to six Sprague-Dowley rats, while another group of six was used as control. After 30 min., 15 µCi of Tl-201 was injected intravenously to both groups of rats (12) and after another 30 min. all animals were sacrificed. The results showed a significant decrease of Tl-201 uptake in the rats previously treated with Dilantin. The biological distribution reveals a concentration of 0.90 ± 0.17%/organ and 1.31 ± 0.29%/gram in Dilantin treated rats and 1.47 ± 0.38%/organ and 2.04 ± 0.55%/gram in the control group. The decrease of 38.80% uptake of Tl-201 in the Dilantin treated rat-heart is statistically significant ($p<0.01$). In conclusion, Dilantin decreases the uptake of Tl-201 in the rat and similar mechanism may be present in humans treated with Dilantin. Studies are in progress with drugs which behave like Dilantin (procainamide, lydocaine) to assess the possible effect of these drugs on the washout of the thallium from the heart.

IN VIVO RECEPTOR BINDING OR IODINATED BETA ADRENOCEPTOR BLOCKERS. W.C. Eckelman, R.E. Gibson, F. Vieras, W.J. Rzeszotarski, B. Francis and R.C. Reba. George Washington University Medical Center, Washington, D.C., and the Armed Forces Radiobiology Research Institute, Bethesda, MD.

Four radioiodinated derivatives and two tritium labeled beta adrenoceptor blocking agents with a range of affinity constants were evaluated as radioindicators for adrenoceptors in guinea pig heart and lung. These receptor binding radiopharmaceuticals may be useful as myocardial imaging agents. In vitro receptor assays using rat ventricular muscle and rat lung microsomal fraction showed that the radiolabeled beta adrenoceptor blocking agents had receptor affinities ranging from 10^4 M^{-1} to 1.6×10^9 M^{-1}. All concentrated in the heart and lung at levels in excess of 0.1% Dose/g tissue. However, based on in vivo displacement studies using excess propranolol only two of the six compounds - [I-125] iodohydroxybenzyl pindolol and [H-3] carazolol - showed beta adrenoceptor binding in the lung and only one - [H-3] carazolol - showed receptor binding in the heart. This latter study is the first example in vivo of detectable beta adrenoceptor binding in the heart. These results agree qualitatively with a bimolecular reversible equilibrium model which predicted a H/B ratio greater than one for carazolol and a L/B ratio greater than one for [I-125] iodohydroxybenzyl pindolol and carazolol. Since carazolol has the highest receptor affinity of presently available beta receptor blockers, we propose that the beta adrenoceptor blockers as a group will not be useful as in vivo probes of receptor concentration in the heart because of their generally low affinity constants and high levels of nonreceptor binding. Beta adrenoceptor blocking agents with affinity constants in excess of 10^9 will be needed to give heart-to-blood ratios of 10.

THE POTENTIAL ROLE OF 123 IODINE-HEXADECENOIC ACID IN ASSESSING NORMAL AND ABNORMAL MYOCARDIAL METABOLISM. V.F. Huckell, D.M. Lyster, and R.T. Morrison, Divisions of Cardiology and Nuclear Medicine, University of British Columbia and Vancouver General Hospital, B.C., Canada

We measured the rate of metabolism of 123 iodine labelled hexadecenoic acid (I-HDA) in patients with normal, ischemic, and infarcted myocardium (MI). Twenty patients (mean age 59 years) were studied using I-HDA prepared by standard techniques: 3 normal, 9 old MI, 8 acute MI (less than 21 days). Immediately after injection, data was collected dynamically for ten minutes. Regions of interest (ROI) were generated over normal and abnormal myocardium (MYO) and time activity curves were plotted. Static imaging was also performed in standard views. After background subtraction, compartmental analysis was carried out using standard techniques.

After an initial rapid increase of radioactivity, a bi-exponential elimination is noted. A long lived component represents free iodine; a rapid component represents myocardial metabolism. For the rapid component three characteristic elimination slopes are seen. Normal MYO and old MI's have a rapid downslope. Lack of differentiation of old MI's from normal MYO may be due to an inability to select small ROI's. Subacute MI and ischemic MYO have a delayed downslope suggesting normal perfusion and abnormal metabolism. Acute MI's have no downslope suggesting perfusion with no metabolism.

Conclusions: the elimination of I-HDA is significantly different between normal, acutely infarcted, and ischemic MYO. The change in slope of the elimination phase varies with the age of the MI and may be useful in following the course of ischemia.

Supported by B.C. Heart Foundation

RADIOHALOGENATED PHENYLFATTY ACIDS FOR METABOLIC STUDIES OF THE MYOCARD

H.-J.Machulla, M.Marsmann, K.Dutschka and D. van Beuningen Institute for Radiation Physics and Radiation Biology of the University Hospital Essen,F.R.G.

I-123-Heptadecanoic acid (IHA) was shown to be suitable for tracing the myocardial metabolism of fatty acids.(1) As an alternative approach ω-phenylpentadecanoic acid (PPA) carrying the label at the benzene ring has been proposed with the advantage of well-studied biochemical pathways.(2) PPA is catabolized via ß-oxidation ending up in the release of benzoic acid known to be excreted mainly as hippuric acid.

In mice both para *IPPA and *BrPPA show a fast extraction out of the blood within the first minute and a rapid myocardial uptake of about 35% inj.dose(id)/g whereas the corresponding ortho isomers are less accumulated (27% id/g) A maximal heart to blood ratio of twenty is observed for both para isomers as it was found only for C-11-palmitic acid, so far.

Sixty minutes after administration of *IPPA the radioactivity in the stomach is still below 2% id/organ,thus indicating the absence of metabolically released radioiodide as observed in case of IHA (16% id/stomach). (1)

In case of *IPPA the myocardial activity is eliminated with a fast and a slow component, half lives of 3.5min and 35min are found similar to IHA.

Due to the advantageous properties of I-123 it is therefore concluded that para *IPPA is a highly promising radiopharmaceutical for both imaging and metabolic studies of the myocard.

(1) H.-J.Machulla et al.J.Nucl.Med. 19,298(1978)
(2) H.-J.Machulla,M.Marsmann,K.Dutschka Europ.J.Nucl.Med. in press (1980)

15-(p-BROMOPHENYL-)PENTADECANOIC ACID: A NEW POTENTIAL AGENT FOR MYOCARDIAL IMAGING. G. Stöcklin, H.H. Coenen, M.F. Harmand, G. Kloster, R. Weinreich, L.E. Feinendegen, K. Vyska, A. Höck, C. Freundlieb. Institut für Chemie 1: Nuklearchemie und Institut für Medizin, Kernforschungsanlage Jülich, Federal Republic of Germany.

Among the positron emitting bromine isotopes, Br-75(T=98min) is the most promising and can efficiently be produced via the As-75(He-3,3n)Br-75-reaction. In continuation of our studies on radiohalogenated fatty acids as indicators for regional myocardial metabolism we have now chosen 15-(p-bromophenyl-)pentadecanoic acid (BPPA) as a potential indicator. BPPA was prepared practically carrier-free by electrophilic substitution on 15-phenylpentadecanoic acid using CF_3SO_3Cl as oxidizing agent. Pharmacokinetic studies in mice show that BPPA is rapidly accumulated in the myocardium; a maximum uptake of 4.5% dose/heart is obtained already 0.5 min after injection, an enrichment comparable to that of 17-I-123-heptadecanoic acid (IHA). The elimination of BPPA is considerably slower than that of IHA. Analysis of the labelled catabolites in the heart muscle indicates that this is due to the fact i) that binding to the enzyme complex effecting ß-oxidation is less efficient due to the phenyl ring and ii) that the final catabolites are lipophilic organic acids like p-bromobenzoic acid which are retained in the cell. In contrast to ω-halofatty acids a much larger activity fraction is still present as free fatty acid in the heart muscle at the time of maximum accumulation. No free bromide is formed during the turnover phase, all catabolites appear as halogenated organic acids. The fast uptake in conjunction with the relatively slow elimination makes BPPA a promising agent for myocardial positron emission tomography and possibly for measuring regional metabolism. Such in-vivo studies are presently in progress.

123m-Te-9-TELLURAHEPTADECANOIC ACID AS MYOCARDIAL IMAGING AGENT. D.R. Elmaleh, F.F. Knapp*, T. Yasuda, S. Kopiwoda, K.A. McKusick, and H.W. Strauss, Mass. General Hospital, Boston, MA and Oak Ridge National Laboratory* Oakridge, TN.

123m-Te-9-telluraheptadecanoic acid (THDA), an oleic acid iosoter, was prepared by basic hydrolysis of the product formed by the coupling of 123m-Te-sodium octyl tellurol with methyl-9-bromo-octadecanoate. Tissue distribution studies were performed in normal fasted rats (I), and rats fed a high fat diet of food pellets soaked in olive oil (II) for 24 hours prior to study. Groups of six rats were anesthetized, injected with 5µCi THDA and sacrificed 30 min later. The heart, lung, liver and blood tissues were weighed and counted in a well counter to determine the % dose THDA uptake (see table). The lung uptake increased 79% from 3.66 in (I) to 6.07 in (II). Myocardial uptake was slightly lower and liver uptake higher in group I than group II.

Tissue	(I) M ± SE		(II) M ± SE	
Blood	.43	.03	.44	.04
Heart	5.36	.53	6.22	.51
Lung	3.66	.56	6.07	.59
Liver	4.03	.15	2.93	.23

*mean-6 animals

Imaging studies using the pinhole collimator were performed in 2 rats. The heart uptake was quantified as 4.2±.3% using an Aliquot of Dose for calibration. Serial images from 5 minutes to one hour revealed no change in the myocardial activity. Dosimetry for this agent was shown to be 1.7 rad/mCi for liver as critical organ.

The metabolic properties of 123m-Te-THDA make this fatty acid analog a potential agent for myocardial imaging.

BIODISTRIBUTION OF 123m-9-TELLURAHEPTADECANOIC ACID: LARGE DIFFERENCE OF UPTAKE IN NORMAL AND INFARCTED MYOCARDIUM. T. Yasuda, F.F. Knapp, D. Elmaleh, S. Kopiwoda, K.A. McKusick and H.W. Strauss. Massachusetts General Hospital, Boston, MA and Oak Ridge National Laboratory, Oak Ridge, TN.

Biodistribution of 123mTe fatty acid (123mTe-9-telluraheptadecanoic acid) was investigated on eleven infarcted male Sprague-Dawley rats (weight 200-210gm/rat). The infarction was produced surgically by ligation of the left anterior descending coronary artery. One hour after the ligation, five microcuries of Te-123m-9-telluraheptadecanoic acid in 6% albumin in normal saline was then injected intravenously. Thirty minutes later, the animals were sacrificed by intravenous injection of triphenol tetrazolium chloride (TTC). Infarcted and normal myocardium was separated by the difference of TTC staining and multiple organs were removed, weighed and counted in a gamma scintillation counter.

ORGAN	SAMPLE #	MEAN % Dose/gm	SE
Blood	11	.180	± .020
Lung	11	1.227	± .104
Infarcted Myocardium	9	1.115	± .177
Normal Myocardium	11	3.702	± .281
Liver	6	1.609	± .156
Pancreas	6	.511	± .710
Kidney	6	1.009	± .069
Bone	6	.134	± .017
Muscle	6	.178	± .026
Whole Intestine	6	.216	± .050

In conclusion, 123mTe-9-telluraheptadecanoic acid concentrates in normal myocardium to a 3 fold greater extent than in zone of infarction and lung. This radiopharmaceutical agent may be useful for myocardial imaging.

CARDIOSELECTIVE RADIOLABELED BETA ADRENERGIC ANTAGONISTS AS POTENTIAL MYOCARDIAL IMAGING AGENTS. Robert N. Hanson, Michael A. Davis, and Zvi Cohen. Joint Program in Nuclear Medicine, Harvard Medical School, Boston, MA.

In our program to develop new radiopharmaceuticals we have examined radiolabeled beta adrenergic antagonists as potential myocardial imaging agents. The present study was designed to evaluate new compounds having increased myocardial uptake and selectivity (heart-to-nontarget ratios). A series of six radioiodinated beta antagonists (1-6) was prepared by conventional methods and labeled by isotope exchange. Biodistributional results in rats at 15 and 60 min using subpharmacologic doses (10 nmol/rat) indicated that the $CH_2CH_2C_6H_3(OCH_3)_2$ group enhanced both myocardial uptake and selectivity compared to the isopropyl (i-Pr) analogs. Hydrogen bonding groups at R_3 also improved uptake and selectivity with $CH_3CONH > IC_6H_4CONH > H$. Compound 6 was the best of the series with a myocardial uptake of 1.47% ID/g and heart-to-blood and -lung ratios of 5.4 and 1.1, respectively.

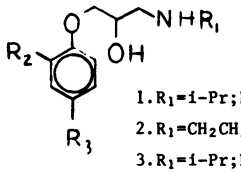

1. R_1=i-Pr; R_2=^{125}I; R_3=H
2. R_1=$CH_2CH_2C_6H_3(OCH_3)_2$; R_2=^{125}I; R_3=H
3. R_1=i-Pr; R_2=H; R_3=$NHCOC_6H_4{}^{125}I$
4. R_1=$CH_2CH_2C_6H_3(OCH_3)_2$; R_2=H; R_3=$NHCOC_6H_4{}^{125}I$
5. R_1=i-Pr; R_2=^{125}I; R_3=$NHCOCH_3$
6. R_1=$CH_2CH_2C_6H_3(OCH_3)_2$; R_2=^{125}I; R_3=$NHCOCH_3$

LOCALIZATION OF Tc-99m-COLLOIDS IN ACUTE MYOCARDIAL INFARCTIONS. D.P. Swanson, T.J. Brady, L.E. Brown, and J.W. Keyes. Univ. of Mich. Medical Center, Ann Arbor, MI.

Based on the observation that colloidal carbon black localizes in areas of acute vascular damage including acute myocardial infarction (MI), we investigated the localization of Tc-99m-colloids in 1-2 hr old MI's.

Dogs were infarcted using a reflow method. Tetracycline (500mg) was injected I.V. 10 min after release of occlusion. Ten mCi of Tc-99m-sulfur colloid (TcSC) or Tc-99m-antimony sulfide colloid (TcAS), prepared from commercial kits, were injected 1 hr after occlusion release. In the histamine (H) experiments, 0.1µg/ml estimated blood volume H-base was slowly injected I.V. 2 min preceding colloid administration. Dogs were sacrificed 1 hr after injecting colloid. Samples of blood, normal myocardium (right and left ventricle) and center of infarct (INF) (determined by tetracycline staining) were assayed for radioactivity content. The mean results (% kg-dose/gm x 10^{-2}) are listed

below. Normal myocardium (NOR)=average of right and left ventricular uptake.

Agent	NOR	INF	INF/NOR	INF/BLOOD
TcSc (n=4)	1.21	2.77	2.90	0.51
TcSc + H (n=3)	0.86	4.73	5.50	1.06
TcAs (n=2)	2.90	5.03	1.73	0.17
TcAS + H (n=3)	2.70	9.72	3.60	0.66

TcSC and TcAS, alone, possess some specificity for MI. This may be based upon passage of colloidal particles through open intracellular junctions formed between the damaged endothelial cells of minute blood vessels, followed by filtering and retention by the intact basement membrane. Histamine, known to increase vascular permeability, enhances the opening of these junctions. Optimization of this technique may result in the ability to image acute MI.

2:00-3:30 Room 3035

RADIOASSAY

NEW TECHNIQUES IN TECHNOLOGY

Session Chairman: Lynn R. Witherspoon
Session Co-Chairman: Nicholas Kutka

A TERMINAL LABELING, IMMUNORADIOMETRIC ASSAY USING GENERATOR PRODUCED SHORT LIVED RADIONUCLIDES. W. Wolf, R. Nakamura, A. Gökce, M. Tubis, T. O'Brien, J. Harwig and G. Oflaz. Radiopharmacy Program and Dept. of Obstetrics and Gynecology, Univ. Sou. Calif., Los Angeles, CA.

We wish to present here a novel method of performing immunoradiometric (and competitive binding) assays, using an antibody or an antigen coupled to a non-radioactive chelating agent, which can then be terminally labeled with a short lived radionuclide. This method requires no iodination, and hence leads neither to products of limited shelf life nor to degradation products because of oxidation during the iodination step. Furthermore, the use of short lived radionuclides such as In-113m or Ga-68 generates no radioactive waste.

The methodology is illustrated by an immunoradiometric assay of hGH. Theantigen is reacted with a specific anti-hGH antibody that had been coupled to a solid support. This first antigen-antibody complex is now reacted with a second antibody, also specific for hGH, but produced in a different species. Separately, an antibody to the second (which, because it recognizes the Fc region, is a "universal" antibody), has been coupled to a chelating molecule such as transferrin. Complexation of the antigen complexed with the first two antibodies is now effected with the universal antibody carrying the chelating moiety. This final complex is now labeled with a solution of In-113m that has been stabilized at pH 7. The free/bound ratio of the radioactivity is plotted as a function of the hGH with a sensitivity and a precision equivalent to the most precise tests currently available. Full details on the scope of this novel methodology will be presented.

RADIOIMMUNOASSAY FOR ATROPINE IN HUMAN PLASMA. P.W. Hayden, S.M. Larson, S.L. Lakshminarayanan. University of Washington and Veterans Administration Hospital, Seattle, WA.

The sensitivity of a new radioimmunoassay (RIA) for atropine has been tested in clinical samples. Six adult males with chronic bronchitis and bronchospasm refractory to usual adrenergic bronchodilators received .05 mg/K doses of atropine sulfate by inhalation. Two diabetic patients received 1 mg bolus injections of atropine followed by continuous I.V. infusion at .01 mg/minute. The RIA is done by incubating duplicate 100 ul plasma samples overnight at 4° C with 100 ul rabbit anti-atropine antibody and 100 ul tritiated atropine in phosphate buffered saline. After precipitation with ammonium sulfate the bound atropine is measured by liquid scintillation counting. Utilizing a standard curve from known dilutions of atropine concentrations as low as 0.6 ng/ml. can be measured. Atropine plasma values from patient samples were compared to plasma clearance curves from 4 volunteers given single 0.3 mg doses. Following 0.3 mg atropine I.V. there is rapid (<5 minute) distribution into an apparent volume of over 150 liters. Clearance half time is 2 to 3 hours. Following inhalation of .05 mg/K atropine there is a highly variable rate of absorption with peak levels not attained for 1 to 2 hours and then slow clearance over 6 to 24 hours. Serial samples during slow infusion showed atropine levels as high as 10 ng/ml. accompanied by significant increase in heart rate. These preliminary studies indicate this RIA is sufficiently sensitive to measure the low plasma levels attained after pharmacologic doses of atropine. Further studies relate the delayed plasma clearance after inhalation of atropine to toxicity which gradually occurs with chronic use of atropine by inhalation.

RELATIONSHIP BETWEEN AMINO ACID METABOLISM AND DRUG RESISTANCE OF M. TUBERCULOSIS. E.E. Camargo, T.A. Milkowski, H.N. Wagner Jr. The Johns Hopkins Medical Institutions, Baltimore, MD.

We have previously reported that drug resistance of M. tuberculosis was associated with an increased oxidation rate of long chain fatty acids and reduced niacin production. We have now found that drug resistance is also related to amino acid metabolism. Using our new radiometric assay for niacin, we observed that administration of the amino acid aspartate to M. tuberculosis cultures resulted in stimulation of niacin production, previously found by us to be related to increased susceptibility of the organism to drugs. This led us to a systematic investigation of amino acid metabolism by M. tuberculosis. Two similar strains of M. tuberculosis, H37Rv(susceptible to all drugs, S), H37Rv (resistant to isoniazid, R) and M. avium serotype 1 (resistant to all drugs) were compared. The bacteria were suspended in 1 ml of 7H9 medium with 1μCi of one of the following (U-C-14) L-amino acids: glycine, alanine, serine, aspartate, glutamate, threonine, leucine, isoleucine, methionine, arginine, proline, phenylalanine, tyrosine, histidine and DL-valine. The C-14 carbon dioxide production was measured radiometrically. Alanine, aspartate, glutamate, serine and glycine were found to be the best substrates with both S and R strains, but having lower oxidation rates with R. The remaining amino acids were poorly oxidized. With M. avium all the amino acids showed even lower oxidation rates than R. Thus, the more drug resistant strains are less able to metabolize amino acids even in the absence of the drug. Combined evaluation of fatty acid and amino acid metabolism by strains of M. tuberculosis may make possible a biochemical assay of drug susceptibility that would be simpler and faster than current microbiological methods.

EVALUATION OF ALTERNATE PROCEDURES FOR MEASURING NSB. M. Daniels, H. Mermall and S. Pinsky. Michael Reese Medical Center, Chicago, IL

Nonspecific binding (NSB) is one quality control parameter of radioimmunoassay systems. Some methodologies permit direct measurement of NSB, others do not. This work; 1) obtained parallel measurements of NSB in both types with systems using methods such as saturating the system with antigen, heating the antibody, or omitting it; 2) compared the NSB values obtained; and 3) examined the value of NSB as the absolute analytical limit of the procedure.

The CEA-Roche assay, a single antibody system, when saturated with antigen produced a NSB of about 11% of the total counts compared to 10% without anti-CEA. This represents an upper limit for the indirect assay equivalent to 40 ng/dl. An immobilized single antibody system for digoxin shows a NSB equal to 6-7% of the total with heat inactivated antibody compared to 7% by antigen saturation. This represents an upper limit of about 15-16 ng/dl; 5.5.% of total, was due to adsorption of radiolabel onto the tube wall. A double antibody T-3 system bound about 2.8% of the total when antiserum was omitted. The system saturated at 3.3% when antigen concentration was ≈ 12,800 ng/dl. Mechanical binding accounted for 2.9% of the total. A solid phase, double antibody, assay for T-4 bound 7-8% of the total counts when T-4 antiserum was omitted; the same as the % bound at antigen saturation (128 μg/dl). Mechanical binding was 0.9-1.5%; the least of any studied.

Determination of NSB should be part of RIA evaluation and quality control procedures. One or more of the procedures used in this study will work with any radioimmunoassay.

EVALUATION AND COMPARISON OF TWO FULLY AUTOMATED RADIOIMMUNOASSAY SYSTEMS WITH DISTINCTLY DIFFERENT ANALYSIS MODES. I.W. Chen, H.R. Maxon, L.A. Heminger, K.S. Ellis, and C.P. Volle. Eugene L. Saenger Radioisotope Laboratory, Univ. of Cincinnati, Cincinnati, OH.

Two fully automated radioimmunoassay systems with batch and sequential modes of analysis were used to assay serum thyroxine (T_4), triiodothyronine (T_3), and digoxin (D) and results were compared with those obtained by manual methods. The batch system (Concept 4, Micromedic Systems) uses antibody coated tubes while the sequential system (Aria II, Becton Dickinson) uses immobilized antibody columns. Mean intraassay (Intra) and interassay (Inter) coefficients of variation and correlation coefficients (r) with respect to the manual methods are shown in the following table:

	Batch			Sequential			Manual		
	T_4	T_3	D	T_4	T_3	D	T_4	T_3	D
Intra	7.2	11.1	11.7	6.2	6.2	4.3	5.9	7.1	7.9
Inter	8.6	9.6	12.0	3.8	6.5	5.0	6.5	8.9	7.6
r	0.97	0.96	0.93	0.95	0.92	0.92	-	-	-

Carryover was evaluated by analyzing alternating groups of 3 serum samples with high and low T_4 values (about 18 and 3 µg/dl). There was statistically significant carryover in sequential system (unpaired t test, $p<0.001$, 15 pairs) of about 10% deviation from true values, but the carryover was not significant in batch system. Although the sequential system appears to give better precision, carryover may cause significant errors when values of adjacent samples are far apart. Sequential system also showed slight but statistically significant drift in T_4 values (e.g. 5.8→6.1 µg/dl over a span of 97 cycles, $r=0.358$; $p<0.001$). The analytical throughput in terms of number of hours required to assay 30 samples in duplicate is about 1.5-3 hours for the batch system and 3-5 hours for the sequential system.

EVALUATION OF T3 RIA BY THE ARIA II AUTOMATED RIA SYSTEM. A. Heal and L. Blazak, Nuclear Medicine, University of Mia. Jackson Memorial Hosp., Miami, Fla., and LaVell Johnson, T.R. Witty, K. Lamont Hadfield and Liza Larriva, B-D Immunodiagnostics Salt Lake City, Utah.

The ARIA II is a fully automated flow-through RIA system using a reusable antibody coated chamber. The purpose of this study was to evaluate the automated T_3 RIA and compare it to established reference methods.

A total of 17 full carousels were performed, consisting of 60 samples per carousel in duplicate.

Confidence factors ranged from 0.90 to 0.99 and total count C.V.'s from 1.5% to 7.09%. Intra assay C.V.'s were all below 9%. The C.V.'s for patient samples indicated all ran 10% or less. A randomized study with patient samples indicated no evidence of carry over. Storage effect studies indicated that there was less effect when samples were stored at room temperature.

Patient results were correlated to T3 RIA kits from Corning, Abbott Diagnostic Products, and Concept IV. Good correlation (>0.95) was shown with all kits except Corning

EVALUATION OF AN AUTOMATED MICRO-DIGOXIN OF THE ARIA II. A. Heal and L. Blazak, Nuclear Medicine, University of Mia. Jackson Memorial Hosp., Miami, Fla. and LaVell Johnson, T.R. Witty, K. Lamont Hadfield and Liza Larriva, B-D Immunodiagnostics Salt Lake City, Utah.

The ARIA II is a fully automated RIA system utilizing a flow-through system and reusable antibody coated chambers. The purpose of this research was to evaluate the automated micro-digoxin assay and compare it to several references methods presently used.

The method consisted of a pre-incubation in the instrument carousel and the second incubation and separation performed in the ARIA II. A total of 18 full carousels were run which consisted of 60 samples per carousel.

Confidence factors for all runs were 0.93 or better. The curve sensitivity averaged 55.3 ± 8.9% and the % recoveries ranged from 90-118%. Intra-assay C.V.'s ranged from 1.34% to 6.58% and inter-assay C.V.'s were 4.71% or less. The C.V.'s on the clinical samples were 4.31% or less, thus demonstrating a lack of carry-over from one sample to the next. Comparison of results under various storage condition indicate that frozen storage maintained the specimens best. Correlation of results with S/M (charcoal), Kallestad and Clinical Assays methods gave correlation coefficients of 0.95% or better.

2:00-3:30 Room 2040

INSTRUMENTATION

COMPUTERS: CARDIOVASCULAR II

Session Chairman: Sherman Heller
Session Co-Chairman: James Patton

EDGE TRACING FOR THE DETERMINATION OF THE LEFT VENTRICULAR PROJECTION AREA. M.L. Goris, J.H. McKillop, H.D. Fawcett, and P.A. Briandet. Stanford University School of Medicine, Stanford, CA, and Informatek States, S.A., Atlanta, GA.

The precise delineation of the left ventricular (LV) projection area (ROI) is an essential part in the quantitative analysis of nuclear angiocardiographies (NA).

We have devised an algorithm which permits automation of this step, based on a one dimensional Laplace operator whose kernel is 2,2,-2,-4,-2,2,2. The operator characteristically enhances "valleys" more than edges and therefore favors septal and the valve plane detection. The operator is applied vertically, horizontally and along both diagonals. Each pass is immediately followed by a local maximum search during which the image resulting from the Laplacian operator is reduced to a binary one, with zeros everywhere except where a local maximum was found along the path of the operator.

This resultant image yields a closed "edge" around LV, even though many structures outside of LV are also delineated. However, the centroid of LV is defined from functional criteria and LV ROI is defined from centroid to first edge.

The method has been applied to first pass (FPNA) and gated studies (EGNA) in anterior and 45° LAO views. The table indicates the success rate.

	Anterior	LAO	Total
FPNA	.72 (8/11)	.86 (19/22)	.82 (27/33)
EGNA	.76 (13/17)	.92 (58/63)	.89 (71/80)

In 100 successive cases the ejection fraction obtained automatically (AEF) was compared to the manual result (MEF). The regression equation yielded an identity relation: $AEF(\%) = 1.7 + 1.0\ MEF(\%) \pm 2\%$. ($r = .995$)

In conclusion, a fully automated region of interest selection has been implemented.

VISUAL DETECTION OF 1mm MOTION UNDER CONDITIONS SIMULATING CLINICAL GATED EQUILIBRIUM BLOOD POOL SCINTIGRAPHY. D. Chapman, E. Garcia, D. Berman, M. Freeman, J. Maddahi, K. Van Train, and A. Waxman, Cedars-Sinai Med. Center, L.A., CA.

To answer a frequent clinical question regarding minimum detectable motion, this study evaluates wall motion under conditions simulating rest (simR) and exercise (simEx) multiple gated equilibrium cardiac blood pool scintigraphy (MUGES). The two ventricles were simulated with cylinders containing Tc-99m. A Tc-99m flood source was used to create a target to background ratio of 2:1. One or both cylinders were moved in 5-8 equal increments to produce 0, 1,2 or 5mm inward motion. Data were acquired in 64x64 byte mode with a mobile camera (Picker) and a minicomputer (MDS A^2). SimR images were acquired with high resolution collimation, obtaining 200K cts/frame. SimEx images were acquired with all-purpose collimation for 100K cts/frame. Images were cine displayed on the computer video. Six blinded observers read a randomly selected series of 5 simR and 5 simEx studies for presence and location of motion. Results were as follows: (Correct observations/total observations)

	One Cylinder		Both Cylinders		Total
Movement	5mm	1mm	1mm	no motion	
simR		12/12	4/6	6/6	22/24
simEx	6/6	5/6	1/6	6/6	18/24

Of 18 observations of 1mm motion on the simR studies, there were 16 correct responses. Of 12 observations of 1mm motion on the simEx studies, there were 6 correct answers. However, motion or its absence was correctly identified in all 48 tests. The results show that 1mm motion was accurately observed and localized under simR conditions. In simEx studies 1mm motion was recognized, but not accurately localized. Thus, motion far less than system resolution is readily detected in simulated MGES.

ELIMINATION OF PATIENT-DETECTOR MOTION DURING UPRIGHT BICYCLE EXERCISE. C. Eubig, W. Covitz, and R.F. Greene, Medical College of Georgia, Augusta, Ga.

An adjustable wedge mold (M) and harness (H) were designed to eliminate blurring of gated blood pool images during upright bicycle exercise. This study quantitated patient motion relative to the gamma camera using 3 methods of immobilization: a foam wedge with tape (F/T), F/H, and M/H. Horizontal and vertical motion were determined by measuring the change due to exercise (ΔEX) in the full width at half maximum (FWHM) of the intensity profile of a point source attached to the chests of 4 subjects. These changes were related to motion in mm by determining the FWHM for a mechanically oscillating point source at varying amplitudes and distances from the collimator.

	F/T		F/H		M/H	
	mean	maximum	mean	maximum	mean	maximum
ΔEX (%)	12	46	7	35	1.5	7
Motion (mm)	4.6	8.2	4.2	7.2	0.6	2.6
n	8		7		8	

Motion with M/H was nearly imperceptible while the other methods allowed significant movement. Complementary studies revealed a 50% increase in FWHM with F/H when the exercise was prolonged; and with excessive workload, a 200% increase in FWHM was seen with F/T and F/H while M/H held it to 29%. FWHM increases in the range of 200% were due to gross subject slippage and occurred only with F/T and F/H. M/H eliminated patient motion which was significant with the other methods and most pronounced with prolonged or excessive exercise. Failure to eliminate motion is likely to cause the greatest error in patients who fatigue easily and at maximum effort, and result in misdiagnosis.

RECIRCULATION SUBTRACTION FOR LEFT TO RIGHT CARDIAC SHUNT ANALYSIS. T.S. Houser, W.J.MacIntyre, M. Siegel, D.S. Moodie, J.H. Gallagher, and S.A. Cook.
Cleveland Clinic Foundation, Cleveland, Ohio

The analysis of indication dilution time-activity curves has been used for cardiac shunt analysis for almost twenty years. Most of the current techniques involve recording the dilution curve from the lung field following a fast bolus injection and measuring the departure of the recorded curve from an expected exponential clearance or gamma variate fit that would be indicative of normal blood flow through the lung. When a left to right cardiac shunt occurs, the trailing edge of the primary dilution curve is distorted with the area of the distortion dependent on the magnitude of the shunt.

Although distortion may be readily observed in large shunts, in many cases it is obscured by activity returning by recirculation. The object of this study is to improve the quantification of the shunt curve by separating the effects of recirculation from direct shunt return.

In the present study when recirculation could not be identified by a secondary peak occurring beyond the time of shunt activity, the time was estimated by determination of the similar appearance time from the cardiac chambers. Following this time selection, a gamma variate fit based on the distribution of points at that segment was effected and subtracted from the original lung dilution curve. Similar gamma variate fitting was performed for both primary and shunt curves.

Greater accuracy of the gamma variate fit of the shunt was obtained since a trailing edge of the curve is apparent following recirculation subtraction. Secondly, the algorithm is completely automatic with no operation intervention or selection of curve fitting regions required.

RADIONUCLIDE QUANTIFICATION OF LEFT TO RIGHT CARDIAC SHUNTS WITH THE PULMONARY TRANSFER FUNCTION. M.H. Bourguignon, J.M. Links, K.H. Douglass, P.O. Alderson, and H.N. Wagner, Jr. The Johns Hopkins Medical Institutions, Baltimore, MD.

A new method for quantification of left to right (L-R) cardiac shunts was studied in 14 children and 3 adults with suspected L-R shunts who had radionuclide angiocardiography and independent determination of shunt size by oximetry. The original pulmonary transit curve was deconvoluted in 2 different ways: (1) by the superior vena cava bolus curve, to yield the deconvoluted pulmonary transit curve (DPTC), which represented the theoretical pulmonary transit curve with a perfect bolus injection, and (2) by the right ventricular transit curve, to yield the pulmonary transfer function (PTF), which represented the theoretical pulmonary transit curve with a perfect bolus injection and with no intracardiac shunts. The PTF was scaled to fit the first peak of the DPTC, and the area A under the scaled PTF obtained. The scaled PTF was then subtracted from the DPTC. The PTF was rescaled to fit the resulting shunt recirculation peak in the difference curve, and the area B under this rescaled PTF obtained. Shunt size was quantified with the formula $QP/QS = A/(A - B)$. The method correlated closely with oximetry ($r = 0.93$, $p<.001$). Use of the PTF provides accurate shunt quantification and reduces subjective operator decisions.

A METHOD FOR AUTOMATIC OVERLAPPING OF SEQUENTIAL SCINTIPHOTO IMAGES.
M.E. Read, D.D. Watson, E.K. Read, E. Leidholtz.
University of VA, Charlottesville, VA.

An operator independent algorithm to achieve superimposition of sequential scintiphoto images has been developed and is used clinically on a dedicated nuclear medicine computer system. In attempting to compare the relative myocardial uptake of thallium-201 in initial and delayed images, some method was necessary to assure that the same myocardial regions were being sampled in both images. It is a relatively simple task to maintain an angle of 90 degrees between the long axis of the patient and arm of the camera, the proper angle of obliquity, and the distance from the chest wall to the camera. However, repositioning to place the myocardial image in exactly the same x and y location in the computer image matrix becomes a far more delicate and difficult task. Our algorithm initially determines the centroid for the initial and delayed images. The initial image is first shifted so it's centroid is in the center of the matrix. The delayed image is then shifted in the x and y directions to align the centroids. After this initial repositioning the delayed image is further shifted in the x and y directions until the cross correlation between the two images is maximized. This is mathematically equivalent to minimizing the sum of the squares of the differences between the images and thus defines image overlap according to an objective least squares criteria. The program was tested on clinical data as well as various test patterns. By maximizing the cross correlation between the images in a hands off manner, good alignment with complete reproducibility is accomplished even in the face of significant radionuclide redistribution between the initial and delayed images.

DEFECT PERCEPTION IN MYOCARDIAL PERFUSION IMAGES.
D.D. Watson, E. Leidholtz, G.A. Beller, C.D. Teates.
University of VA, Charlottesville, VA.

It has been known since the early 19th century that the human eye perceives equal increments of intensity or density if the increments are arranged in geometric proportion. However, nuclear medicine imaging devices conventionally employ gray scales which are arranged in linear proportion. This causes a loss of ability to perceive small changes in intensity in the high count portion of the images. This is a problem in "cold spot" thallium-201 myocardial imaging. We have accordingly altered the computer gray scale so that each intensity step increases by a constant fraction of the previous intensity level. The same principle was also used with the color video monitor but further augmentation of brightness increments was achieved by adding white to a base color of saturated green. This

technique avoids the confusing affect of multiple color displays by maintaining a constant hue but still uses color to enhance visual perception by adding increments of "whiteness" to enhance the perception of brightness. Visual perception of defects in thallium myocardial images was compared to results by computer quantitation. Myocardial target regions were defined as having defects of minimum statistical significance if they varied by one standard deviation determined from sampling a normal patient population, and to be clinically significant defects at the 90 percentile limits of the normal population distribution. Using these display scales thallium defects of minimal statistical significance be readily perceived without the use of variable background or contrast adjustment. This permits standardized image formation without risking the loss of significant information, and the standardization promotes a more rapid and accurate learning curve.

IN VIVO QUANTITATION OF MYOCARDIAL UPTAKE OF TL-201 IN MAN. J.J. Frost, J.M. Links, K.H. Douglass, and H.N. Wagner,Jr. Johns Hopkins Medical Institutions, Baltimore, MD.

A method for quantitation of myocardial uptake of Tl-201 was studied in normal persons, those with known severe CHD and those with known noncoronary cardiomyopathies. In order that the injected dose and myocardial activity be measured under near identical geometry and attenuation conditions, the injected dose was measured during its first transit through the left ventricle (LV) in the LAO 40° projection. The area under the LV transit curve is proportional to both the total activity passing through the LV and the chamber mean transit time (MTT). A gamma variate function was fitted to the first pass curve, and the area under it determined. A second gamma variate fit to the LV transit curve after its deconvolution from the pulmonary transit curve was used to determine the MTT. The area under the first gamma variate function was divided by this LV MTT, yielding the count rate of the injected dose available for myocardial uptake. Therefore any activity remaining in the lung is not included. The LV myocardial count rate in a 10 min post injection LAO 40° static image was obtained by dividing the total myocardial counts by the acquisition time, after background correction using an annular region of interest around the myocardium. Myocardial uptake was then given as the ratio of the myocardial count rate in the static image to the first pass count rate. Preliminary studies in normal persons demonstrated uptakes of $3.9\pm0.3\%$ whereas those with severe multivessel CAD had uptakes of $1.3\pm0.3\%$. Persons with known noncoronary cardiomyopathies had uptakes of $8.2\pm0.6\%$. Thus this quantitative method may well aid the differentiation of normal and specific disease states using Tl-201 myocardial scanning.

SPACE-TIME QUANTITATION OF SEQUENTIAL THALLIUM-201 MYOCARDIAL SCINTIGRAMS: DESCRIPTION AND APPLICATION OF A NEW METHOD. E. Garcia, J. Maddahi, D. Berman, and A. Waxman, Cedars-Sinai Medical Center, Los Angeles, CA.

Visual interpretation of Tl-201 scintigrams is imprecise and subject to observer variability. Thus we have developed a new computer method to objectively express the relative space-time myocardial (myo) distribution of Tl. Ten minute (min) planar images were obtained in the anterior, 45° and 70° LAO views 6 min, 40 min, 4 hrs, and 24 hrs after exercise Tl injection in 32 normal pts (NLS) and 35 with coronary artery disease (CAD) (>50% stenosis). Multiple view circumferential profiles (CP) of maximum cts were obtained for each time interval following interpolative background subtraction and 9 point smoothing and were plotted to represent the distribution characteristics of 60 6° arcs of the myo. Washout (W) CPs were calculated as %W from stress. The mean ±2 SD were calculated from the pooled NLS for each 6° arc of each CP and WCP. The computer compared each pt's CPs and WCPs to the corresponding mean ±2SD. Four types of abnormality were defined: 1)a "defect" occured when a 6 min post-stress CP arc fell >2 SD below the mean; 2)"late peaking" was when any arc of the 40 min CP was >2 SD above the mean; 3)"slow W" was defined when any arc of the 4 hr CP was >2 SD above the mean or the corresponding WCP was >2 SD below; 4)"very slow W" occured when any arc of the 24 hr CP was >2 SD above, or the corresponding WCP was >2 SD below the mean. The biological $T_{\frac{1}{2}}$ of myo Tl in NLS was 4.4 hrs, and was the same for all regions. CPs and WCPs correctly identified 33/35 CAD pts and 30/32 NLS. Although all 33 CAD pts detected had regional CP abnormality, addition of WCP frequently identified other segments with CAD. This new objective method of quantifying distribution and washout of myo Tl provides accurate assessment of CAD.

4:00-5:30 **Room 3037**

CLINICAL

HEART IV

Session Chairman: Richard N. Pierson
Session Co-Chairman: Robert A. Vogel

QUANTIFICATION OF REGIONAL WALL MOTION ABNORMALITIES (RWMA) DETECTED BY PHASE ANALYSIS OF GATED CARDIAC STUDIES. D. Pavel, R. Pietras, W. Lam, E. Byrom, C. Meyer Pavel, S. Swiryn, D. Witham, K. Rosen. University of Illinois Medical Center, Chicago, IL.

The functional phase images (PHI) obtained by Fourier analysis of the equilibrium gated studies (GS) has proven useful in the detection or RWMA. We have evaluated the possibility to use this method to obtain, in addition, a quantification of RWMA, in two ways: 1) by measuring the maximum phase shift of the abnormal areas in relation to the remaining normal ventricle; 2) by measuring the surface areas of similar phase shifts and expressing them as % of the whole LV projection. The present data are based on 28 patients in whom contrast angiography (CAG) was also performed. Only LAO views were correlated because not all patients had GS in two views, and only the free borders were considered (inferior and postero-lat. wall), total of 56 segments. Results: Method #1 showed, by the Fisher's exact test, a strong association when normal versus abnormal segments are considered ($p<.0001$). The correlation coefficient calculated by assigning a code (from 1 to 4) to the 4 possible categories of RWMA is 0.93 ($p<.001$). In general the higher the phase lag the more accentuated the abnormality. Method #2. when correlated with the qualitative impressions obtained during CAG showed a good correlation: The larger the surface of high phase shifts, the more probable the suggestion of extensive RWMA on CAG. Conclusion: The two methods described enable each of them to quantitate a certain aspect of RWMA. Interpreted together they allow a precise assessment of the degree and of the extent of abnormalities.

IDENTIFICATION OF SITE OF ONSET OF VENTRICULAR CONTRACTION BY LEAST SQUARES PHASE ANALYSIS (LSPA) OF RADIONUCLIDE CINEANGIOGRAMS (RCA). D.A. Turner, P.L. Von Behren, N.T. Ruggie, R.G. Hauser, P. Denes, J.V. Messer, E.W. Fordham and M.W. Groch. Rush Medical College Chicago, IL. and Searle Radiographics Inc., Des Plaines, IL.

Von Behren et al. have described a method intended to display the sequence of onset inward ventricular movement, namely LSPA of RCA. To determine whether or not this technique can identify the site of onset of ventricular contraction, seven patients with transvenous pacemakers underwent equilibrium, ECG-gated RCA in 30° RAO and 45° MLAO projections during pacing; 1 of 7 was studied twice with the pacing electrode in 2 different locations. Six of 7 were also studied in normal sinus rhythm (NSR). Three independent observers inspected Polaroid film displays of LSPAs of the 14 RCAs. In all cases, studies in NSR were easily identified, as were the sites of the pacing electrode tip during pacing. Estimates were made (from the LSPAs) of the time-interval of spread of onset of ventricular movement: these estimates correlated well (r=0.88) with the duration of the corresponding QRS complexes in a range from 60 to 200 msec. Finally, an 8th patient was studied in hemodynamically stable ventricular tachycardia. The LSPA correctly identified the site of origin of the arrhythmia as determined by electrophysiological endocardial mapping. Furthermore, the sequence of onset of ventricular movement paralleled the sequence of endocardial depolarization. These preliminary

studies suggest that a) LSPA of RCA can correctly identify abnormal sites of ventricular activation and b) the sequence of onset of ventricular contraction as depicted by LSPA may be a valid representation of the actual sequence of contraction.

Quantitative Analysis of Regional Left Ventricular Function
M.V. Yester, S.E. Papapietro, J.R. Logic, W.N. Tauxe, C.E. Rackley, R.O. Russell, W.J. Rogers, J.A. Mantle. University of Alabama School of Medicine, Birmingham, AL

Quantitative regional left ventricular function was studied in a group of 22 patients with first pass (FP) and equilibrium gated (EG) radionuclide angiocardiography. The results were compared to biplane contrast cineangiograms (CA) performed on the same patients within 3 hours of the radionuclide studies. The FP studies were performed in a RAO projection and the EG studies in a LAO projection with caudal angulation corresponding to the views used for CA. A computer program was written to divide the left ventricle into five segments from the center of the end-diastolic outline for each view. The ejection fraction of each segment was calculated for quantitative regional function. The same algorithm was used for the CA end-diastolic and end-systolic silhouettes. Good correlations were obtained for the anterobasal (R=0.74), anterolateral (R=0.78), apical (R=0.85), apical septal (R=0.78), and posterolateral (R=0.77) segments, where the criterion of the AHA was followed in assigning the labels. Poorer correlations were obtained for the diaphragmatic (R=0.63) and inferior lateral (R=0.53) segments. No correlation was observed for the basal septal, posterobasal, and superior lateral segments. The global ejection fraction correlation was R=0.87 for RAO FP vs biplane CA and R=0.83 for the LAO EG vs biplane CA. Regional ejection fraction by both radionuclide techniques correctly identifies and quantitates dyskinesis and degrees of hypokinesis and adds clinically to the evaluation of regional left ventricular function especially in coronary artery disease.

SCREENING FOR CARDIAC DYSFUNCTION WITH THE NUCLEAR STETHOSCOPE. *A. Strashun, S.F. Horowitz, S.J. Goldsmith, A. Dicker. Mt. Sinai Med. Ctr., NY, NY.*

The utility of left ventricular(LV) function parameters from an ECG-gated scintillation probe, the Nuclear Stethoscope(NS), to predict LV dysfunction was analyzed in 68 patients. Pulmonary transit time, ejection fraction(EF), ejection rate(EJR), fast-filling rate(FFR), rate-related subdivisions of the cardiac cycle including the fast-filling time(FFT), relative end diastolic and stroke volumes, and relative cardiac output(RCO) were displayed by the NS within 10 minutes following injection of 15mCi Tc-99m blood pool agent. Independently obtained scintangiographic studies(ANG) identified LV dysfunction(ABNL) in 50 of 68 patients. Mean (x̄) and standard deviation(SD) of NS parameters were determined from the normal population(NL).

ANG	*EF***	*RCO**	*EJR**	*FFR**	*EF/FFT**	*RCO, EJR, FFR, EF/FFT*
NL(18)	*18(>)*	*18(>)*	*16(>)*	*16(>)*	*16(>)*	*18(2of3>)*
ABNL(50)	*44(<)*	*49(<)*	*48(<)*	*47(<)*	*46(<)*	*50(2of3<)*
Sensitivity	*88*	*98*	*96*	*94*	*92*	*100*
Specificity	*100*	*100*	*89*	*89*	*88*	*100*
	p<.005	*<.005*	*<.005*	*<.005*	*<.005*	*<.005*

**x̄ - SD, **x̄ - 2SD*

Thus, the RCO,EJR,FFR,and EF/FFT individually and especially together expand the ability of the NS to predict ABNL beyond simple EF analysis. These parameters may represent abnormal ventricular compliance(FFR,EF/FFT), diminished contractility (EJR), or regional asynergy(RCO) despite a compensated EF. The data suggests the NS can serve as a portable,cost-effective noninvasive screening device for LV dysfunction.

VARIABILITY OF RESTING GATED EJECTION FRACTION.
W.I. Ganz, J.P. Wexler, A.I. Brenner, R.Bontemps, R. Steingart, and M.D. Blaufox. Albert Einstein College of Medicine, Bronx, N.Y.

Stress induced changes in radionuclide left ventricular ejection fraction (LVEF) may detect abnormalities in cardiac function not apparent at rest. A knowledge of the reproducibility of LVEF is required to determine if a change in LVEF is statistically significant. The variability of LVEF was evaluated by obtaining 5-13 sequential 4-minute gated acquisitions in 21 clinically stable resting patients during the hour immediately following in vivo labeling of red blood cells with Tc-99m. Processing was by an automated method which was correlated with biplane cineangiography (LVEF(cath)=0.88 LVEF(gated)+8.35,n=57, r=0.90,p<0.001). Repetitive processing of the same study by a single observer yielded s.d.<1.0 EF units for LVEF from 10-75. The mean s.d. of the steady state LVEF was 3.6 ± 1.3 EF units for LVEF in the range of 10-75. The s.d. was relatively independent of the value of LVEF being measured in this range. Changes in LVEF determined with this method by a single observation must exceed 4.2, 6.5, 8.4, 10.0 and 13.2 EF units to be significant at the 60%, 80%, 90%, 95%, and 99% confidence level respectively. These values should be calculated for each laboratory to evaluate the significance of changes in LVEF.

CRITERIA TO OPTIMIZE DIAGNOSIS OF CORONARY ARTERY DISEASE FROM REST-EXERCISE RADIONUCLIDE ANGIOGRAPHY.
R.E. Coleman, F.R. Cobb, and R.H. Jones. Duke University Medical Center, Durham, NC.

Coronary artery disease (CAD) may result in myocardial fibrosis reflected by a wall motion abnormality (WMA) or low ejection fraction (EF) at rest or myocardial ischemia reflected by a decrease in EF, increase in end diastolic or systolic volumes (EDV, ESV) and/or a WMA during exercise. The purpose of this investigation is to determine the parameters which detect at least 90% of patients with CAD. Rest and exercise first-pass radionuclide angiograms (RNA) were obtained in 342 patients who had cardiac catheterization for suspected CAD. At least 75% stenosis (CAD) was present in one or more coronary arteries in 74% of these patients.

The resting EF which best separated patients with CAD was .46, and 95% of 57 patients with resting EF below this had CAD. Additionally, 96% of these patients had WMA at rest. In the 285 patients with resting EF >.46, CAD was present in 90% of patients who decreased their EF by .12 or more during exercise. A change in EDV was not a sensitive discriminator of CAD. CAD was present in 87 of 97 (97%) of patients with an increase in ESV >20 ml. CAD was present in 107 of 119 (90%) of patients who developed a new or increased WMA.

CAD was detected with a probability of >.90 in 125 (44%) of the 285 patients who had at least one of the parameters abnormal. If all three parameters were abnormal, 54 of 57 (95%) patients had CAD. Therefore, abnormal criteria define a group of patients with a high likelihood of CAD.

VALUE AND LIMITATIONS OF LEFT VENTRICULAR FUNCTION INDICES DERIVED BY EXERCISE EQUILIBRIUM BLOOD POOL IMAGING IN THE DIAGNOSIS OF CORONARY ARTERY DISEASE.
G. Wisenberg, H. Schön, R. Marshall, E. Henze, H. Schelbert. UCLA School of Medicine, Los Angeles, CA.

An abnormal response in ejection fraction (EF) to exercise is considered as both highly sensitive and specific for coronary artery disease (CAD). In this study, we compared the sensitivity (SE) and specificity (SP) of exercise induced changes (Δ) in EF, enddiastolic counts (EDC), heart rate corrected - ejection and filling rates (ER and FR), and regional EF (REF) during supine exercise for detection of (CAD) and cardiac disease (CD) in 10 normals (N), 36 CAD patients, and 9 patients with valvular regurgitation (VR). The mean changes in each patient group were:

	ΔEF	ΔEDC	ΔER	ΔFR
N	+6.5±8.4%	-7±5%	+0.64±.71	+1.10±1.23
CAD	-3.7±9.0*	+22±12**	+0.21±.58*	+0.63±1.12
VR	-6.1±7.2*	-1±17	+0.16±.46*	+0.25±0.85*

*p<.05 **p<.001 to N

Defining ΔEF<5%; asymmetric REF response with <5% increase in at least one region; ΔEDC>5%, ΔER<.65; and ΔFR 1.10 as abnormal responses, the SE and SP for CAD and CD in this patient population for each parameter were:

	ΔEF	ΔEDC	ΔER	ΔFR	REF
SE-CAD	86%	100%	75%	75%	94%
SE-CD	87%	71%	76%	87%	75%
SP-CAD	42%	84%	53%	37%	100%
SP-CD	70%	100%	70%	50%	100%

We conclude that 1) ΔEF is sensitive but non-specific for CAD; 2) the variability of ΔER and ΔFR limit their diagnostic value; and 3) in this population, ΔEDC is most sensitive and REF most specific for diagnosing CAD by exercise equilibrium blood pool imaging.

QUANTITATIVE STANDARDS FOR TL-201 MYOCARDIAL DISTRIBUTION AND WASHOUT.

D.D. Watson, G.A. Beller, M.E. Read, and C.D. Teates. University of VA, Charlottesville, VA.

A computer method has been developed to determine the relative initial uptake and washout rates of thallium-201 sequential myocardial images following exercise stress. Images are obtained at 10 min, 1 hr, and 2 hrs following injection. A modified bilinear interpolative method as suggested by Goris was used to construct a reference plane and net myocardial counts above this reference plane were determined by multiple profiles. Washout rates were determined by linear regression of time activity curves constructed from the sequential images. Normal standards were obtained from studies on 25 subjects who had normal coronary angiograms and ventriculograms. Data from the normal population was used to establish numerical criteria of 25% for a focal defect and 0.05 hr^{-1} for abnormal segmental washout slope. These values were beyond the 90 percentile limits of the distribution of values obtained from the normal population. Angiographic correlations were obtained for 140 patients which yielded a sensitivity of 91 percent and specificity of 90% for detection of coronary disease, and specificity of 68% for differentiation of single from multivessel disease. Blind visual assessment was performed independently by three people on 91 of these studies with consensus readings (agreement by at least two readers) providing respectively 87%, 80%, and 40% for sensitivity, specificity, and detection of multivessel involvement. This method is simple, reproducible, and gives somewhat better results than we could achieve by objective evaluation using highly experienced readers.

EXCESS REGIONAL THALLIUM UPTAKE: POSSIBLE DEMONSTRATION OF REACTIVE HYPEREMIA IN MAN. R.A. Steckley, R.M. Robertson, M.W. Kronenberg, M.L. Born, D.H. Robertson, G.C. Friesinger, F.D. Rollo. Vanderbilt University Medical Center, Nashville, TN.

Initial myocardial thallium (TL) distribution is dependent upon regional myocardial blood flow. Release of coronary occlusion in canine models results in reactive hyperemia with excess flow debt repayment when proximal stenoses are not severe. To determine whether reactive hyperemia can be demonstrated in man, 36 serial TL images were obtained in 3 patients with variant angina, a syndrome in which coronary atherosclerosis of any degree may coexist with coronary spasm, producing angina at rest. In 2 patients with angiographically-documented coronary spasm and minimal atherosclerosis in the vessel involved, TL was injected at the onset of an ischemic episode of short duration (1-2 min). Initial images revealed pronounced excess activity in the area corresponding to the artery involved. Subsequent images obtained over 5 hours showed progressive normalization. In contrast, TL injected during a prolonged episode of ischemia in the third patient, who had severe atherosclerosis in the vessel involved, demonstrated a classic initial perfusion defect with delayed resolution over 4 hours. This excess TL uptake distal to vasospastic lesions has not previously been demonstrated in man; it does confirm prior canine studies. The occurrence of reactive hyperemia is likely to depend on the precise relationship between the degree of coronary atherosclerosis and the spasm superimposed. Thus, "thallium hyperemia" may provide a means to assess coronary reactivity and the significance of coexisting atherosclerosis in man.

CALCULATION OF LEFT VENTRICULAR EJECTION FRACTION WITHOUT DIRECT BACKGROUND CORRECTION. E.J.Gandsman, R.S.Shulman, I.B. Tyson and E.W. Bough. The Miriam Hospital, Providence R.I.

The mathematical characteristics of the cardiac background (B) were studied in 34 patients who underwent both gated radionuclide angiography (GRA) and single plane cardiac catheterization. The background-corrected ejection fraction (BCEF) was calculated in the standard manner using an operator-defined periventricular background region. The "uncorrected" ejection fraction (UEF) was also calculated from the uncorrected left ventricular time-activity curve and compared to both the BCEF and the angiographic ejection fraction (AEF). UEF exhibited a remarkable linear correlation with both BCEF and AEF. The calculated linear regression equation (AEF = 2.89 UEF) allowed the calculation of a true ejection fraction without direct background correction. The measurement of left ventricular ejection fraction using this linear regression methodology was tested prospectively in an additional group of 20 catheterized patients. The regression ejection fractions (REF) showed excellent linear correlation with AEF (r = .89) and minimal interobserver variability.

NONINVASIVE DETERMINATION OF LEFT VENTRICULAR ENDSYSTOLIC PRESSURE VOLUME RELATION BY RADIONUCLIDE ANGIOGRAPHY

G.Schuler, K.v.Olshausen, H.Hehmel, H.J.Herrmann, F.Schwarz, J.Kübler; Univ. of Heidelberg, Germany

Recent reports indicate that left ventricular (LV) endsystolic pressure volume relation (ESPV) is a parameter of myocardial contractility independent of pre- and afterload. The aim of this study was to define ESPV noninvasively in patients (p) with aortic regurgitation (n=8), cardiomyopathy (n=2), coronary artery disease (n=4) and normals (n=4). Changes in endsystolic volume were determined by equilibrium radionuclide angiography and expressed in dimensionless units. Peak systolic pressure was measured by automated cuff and substituted for endsystolic pressure. Variations in blood pressure were achieved by nitrates and methoxamine, while heart rate was kept within a narrow range (± 4) by atropin. An average of 11 measurements was obtained in each p while endsystolic pressure varied by 55±11 mmHg. The slope of ESPV was determined from the regression equation, which showed a close linear correlation (r=0.9). The slope k had a normal range of 8.8 to 4 and correlated to LV ejection fraction in an exponential fashion (r=0.85). All p with depressed LV function were correctly identified, and p, whose LV ejection fraction was only borderline abnormal, had a markedly depressed slope (k<1.5). We conclude that the slope of ESPV is a sensitive parameter of LV contractility. It is particularly useful to identify p with discrete and not yet significantly depressed LV function.

RV FUNCTION EVALUATION USING VOLUME-PRESSURE LOOP BY ECG-GATED EQUILIBRIUM RADIONUCLIDE ANGIOGRAPHY AND SIMULTANEOUSLY ACQUIRED RV PRESSURE DATA.

S. Watanbe, T. Yasue, H. Mori, M. Hosoba, J. Soramoto and S. Wakabayashi. Gifu Prefectual Hospital and Shimadzu Corporation, Gifu and Kyoto, Japan.

This study was undertaken to evaluate the right ventricular (RV) function in various cardiac disease using volume-pressure relationship which was produced from ECG-gated equilibrium (EQ) radionuclide angiography and RV pressure data measured with Swan-Gantz catheter. Computerized methods for LIST mode data acquisition were developed to collect the data from gamma camera, ECG wave and RV pressure simultaneously. ECG-gated pool images summing about 200 beats and average pressure curve spanning a complete cardiac cycle were generated from LIST mode data which were acquired in the LAO 30° view with 3-min collection period using 15 mci Tc-99m HSA. A time-activity curve (TAC) of the RV activity over the cardiac cycle and RV ejection fraction (EF) were calculated chosing RV ROI for end diastole (ED) image after background

correction. In order to determine ROI without inter-observer variation, RV ROI could be selected on both ED and absolute value image of (ED–ES) that emphasised the changing part in RV and right atrium. RV volume curve was obtained calibrating TAC with ED volume calculated from the relation of EF and cardiac output measured by thermodilution method. From pressure curve and volume curve, volume-pressure loop was created. RV regional wall motion analysis was also performed by producing regional EF functional image.
With this EQ method using simultaneously acquired RV pressure data we obtained accurate RVEF, volume curve and volume-pressure relationship repeatedly that would be rarely available by traditional contrast angiography.

MYOCARDIAL FUNCTION ASSESSED BY RADIONUCLIDE ANGIOGRAPHY FOLLOWING CHEST TRAUMA. G.A. Sutherland, A.A. Driedger, W.J. Sibbald, J.E. Calvin, and R.L. Holliday. Victoria Hospital, London, Ontario, Canada.

Left and right ventricular ejection fractions and wall motion were assessed by Tc-99m-RBC equilibrium ECG gated angiography in 25 consecutive patients who had sustained severe blunt chest trauma.

Abnormalities of wall motion were defined in 17 patients altogether with 12 right ventricular, 2 left ventricular, and 3 biventricular findings. Two patients had traumatic tricuspid insufficiency demonstrated by first pass radionuclide angiography and verified by contrast angiography. Alterations of ECG were diagnostic of myocardial injury in only 7 of the 17 patients. Scans with Tc-99m pyrophosphate were generally unhelpful being positive in only 2 of 8 instances. Enzyme elevations were of no diagnostic benefit.

Two of 5 deaths were attributed to refractory arrhythmias. Surgical or post mortem evidence of myocardial contusion was obtained in 5 instances. Of the 13 patients available for follow up examinations, 11 showed complete or partial resolution of the abnormality and 2 were unchanged.

In the traumatized chest, altered myocardial function may be due to direct myocardial injury or possibly secondarily to altered vasomotor tone, thoracic mechanics, etc. We believe that a positive radionuclide angiogram constitutes prima facie evidence of myocardial injury.

BIPLANE RADIONUCLIDE QUANTITATION OF EXERCISE GLOBAL AND SEGMENTAL LEFT VENTRICULAR RESPONSE IN CORONARY DISEASE. V. Kalff, Y.Lim, M.Kelly, P.Mason, R. Harper, S.Anderson, J.Federman, A.Pitt. Alfred Hospital, Melbourne, Australia.

Sequential gated RAO first pass and LAO equilibrium radionuclide (RN) angiograms were obtained at rest (R) and peak supine bicycle exercise (Ex) to assess global (GEF) and segmental (SEF) left ventricular (LV) ejection fraction. To define normal GEF and SEF, 14 healthy volunteers were studied. Thirty-two patients (PT) with chest pain were studied, 28 with coronary artery disease (CAD) defined at coronary angiography as having >50% luminal stenosis.

Counts based GEF and SEF (interobserver r≥.97) were obtained with computer defined standardised isocount, variable LV regions of interest. RN segments were assigned to left anterior descending (LAD), left circumflex (LCX) and posterior descending (PD) coronary artery territories. Abnormal (ABN) responses were defined as (a) GEF or SEF > 2 SD outside normal R or Ex mean range or (b) GEF rising <5% or (c) SEF falling > 2 SD of interobserver mean variance for each segment.

	PD	LCX	LAO LAD	RAO LAD	BIPLANE LAD
ABN SEF/CAD > 50%	19/22	17/22	21/25	21/25	25/25
ABN SEF/CAD 30-50%	2/2	2/2	1/1	1/1	1/1
ABN SEF/CAD 0-30%	2/8	2/10	1/6	0/6	1/6

GEF responses were ABN in one or both views in 27/28 PT with CAD (26 RAO and 27 LAO). When SEF was combined with GEF in either view all PT with CAD demonstrated ABN stress LV function. GEF and SEF responses were normal in the 4 PT with no CAD.

The addition of quantitative SEF to stress GEF improves the overall sensitivity of RN detection of CAD and biplane SEF reliably localises CAD.

LEFT VENTRICULAR EJECTION FRACTION FUNCTIONAL IMAGES AT REST AND BICYCLE EXERCISE: DEFINITION OF NORMAL AND ABNORMAL REGIONAL RESPONSES IN CORONARY ARTERY DISEASE. B. Williams, H. Berger, F. Wackers, A. Brendel, S. Lewis, A. Gottschalk, and B. Zaret. Yale University, New Haven, Ct.

Computerized ejection fraction functional images (EFFI) display the relative contribution of individual left ventricular (LV) regions to global LVEF. EFFI's were obtained by anterior first-pass technique using a multicrystal camera at rest (R) and peak bicycle exercise (EX) in 143 patients (pts) {76 with coronary artery disease (CAD), 35 with aortic regurgitation (AR) and 32 normals (nl)}. At R, nls showed 2 EFFI patterns: symmetric regional contribution to LVEF (23 pts); and asymmetric, with relatively decreased inferobasilar contribution (9 pts). At EX, 31/32 nls augmented EFFI ≥1 region (12 pts anterior and inferior symmetrically, 19 pts 1 region). No region became worse at EX in nls. In CAD, 29/76 pts were abnl at R, and 51/76 had abnl EX response (worsening or failure to augment in any region). 60/76 had abnl global EX LVEF response. 95% of 3 vessel CAD pts had abnl EX EFFI response, whereas 59% of 1 and 2 vessel pts had abnl EX EFFI response. In a subgroup of 16 pts with LVEF at R <40%, EX EFFI revealed new regional changes in 9 pts not appreciable by visual wall motion analysis or EX LVEF response. Of 15 pts with AR and abnl EX LVEF response, only 2 pts had abnl EX EFFI (both had normal CA), while only 1/20 AR pts with nl EX LVEF responses had abnl EX EFFI.

Thus, EFFI permits evaluation of regional function at R and EX. Abnl EX EFFI usually indicates CAD. For CAD detection, EX EFFI is similar to EX LVEF response, but EFFI analysis may have potential value in appreciating induced regional changes, particularly in pts with compromised resting LV function.

ACEBUTOLOL, A NEW BETA-BLOCKER: EFFECTS ON RESTING AND EXERCISE VENTRICULAR FUNCTION IN CORONARY ARTERY DISEASE AS DETERMINED BY RADIONUCLIDE ANGIOGRAPHY. R.J. Katz, R. DiBianco, S. Singh, B. Sauerbrunn, H.R. Bates, R.D. Fletcher. Veterans Administration and Georgetown University Medical Centers, Washington, D.C.

Though beneficial in the treatment of coronary artery disease (CAD), beta-adrenergic blockade may produce adverse effects on ventricular function. Acebutolol (Acb), a new cardioselective beta-blocker, was studied to assess its effects on global and regional ventricular function in 26 patients with chronic angina. All patients underwent rest and maximal supine bicycle exercise radionuclide angiography during placebo (P) and on oral Acb (400 mg TID). Resting heart rate and anginal frequency decreased after Acb (↓10%, p<.005; and ↓22%, p<.02, respectively). Resting ejection fraction (EF) on P was .51±.03 (range .28-.72) and increased on A to .54±.03 (p<.05). No resting EF decreased >.07. One patient with resting EF .28 on P had resting EF .21 on Acb and developed signs of fluid retention. No other patients had signs or symptoms of heart failure. Exercise nuclear studies on P revealed 24/26 with response consistent with CAD (19/26<.05 increase EF with exercise; 24/26 regional wall motion abnormalities on exercise). Exercise protocols were similar on and off Acb, and chest pain limited most studies (22/26 placebo, 19/26 Acb). Acb produced lower peak exercise heart rates (98 vs 110±3, p<.005) and rate-pressure products (17,344 vs 20,898±1700; p<.005). Peak exercise EF, was similar on P and Acb (.51±.03 to .54±.03, respectively, pNS). Four patients normalized exercise EF response (≥.05↑) and 5 patients normalized all RWMA on Acb. Cardioselective beta blockade with Acb in effective antianginal doses is safe and may improve resting and exercise ventricular function.

LEFT VENTRICULAR PERFORMANCE AT REST, EXERCISE AND DURING ACUTE BETA RECEPTOR BLOCKADE IN NORMAL MAN. R.Bauer, E.Sauer, H.Langhammer, H.W.Pabst, A.Hirzfeld, H.Sebening. Technische Universität, München, Germany

10 healthy subjects with invasively proven normal heart function were tested by radionuclide ventriculography to evaluate ejection fraction EF and relative emptin and filling velocities VE and VF, respectively (VE = dV/dt / EDV).

Scintigrams were taken at rest, under maximal exercise with a bicycle ergometer, under stimulation with Dobutamin and after acute beta blockade

with Metoprolol. Under exercise EF increased from 55% at rest to 78%, VE and VF from -2.5 and +2.5 to -6.2 and +8.2, respectively. Heart rate increased from 68 to 170 /min. One hour after exercise Dobutamin was infunded at 7.5 and 15 ug/kg/min over periods of 15 min each. EF, VE and VF increased from 53%, -2.9 and +2.9 to 80%, -6.0 and +4.5 at 15 ug Dobutamin. Following acute beta blockade with 0.2 mg/kg Metoprolol i.v. we found no change in cardiac function (53%, -2.6 and +2.6) Patients were submitted to exercise a second time, now EF and velocities increased to only 63%, -4.3 and +6.0 at a heart rate of 130 /min.

The data show that both ergometric exercise and pharmacological beta stimulation result in the same maximal cardiac performance revealed by EF and VE, whereas under acute beta blockade cardiac performance is limited.

(Supported by Fritz-Thyssen-Stiftung and DFG)

4:00-5:30 Room 2048

CLINICAL

GI II

Session Chairman: Robert Stadalnick
Session Co-Chairman: Leon S. Malmud

ESOPHAGEAL TRANSIT OF GELATIN CAPSULES-THERAPEUTIC IMPLICATIONS. L.S. Malmud, E. Rock, G. Applegate, J. Reilley, R.S. Fisher. Temple University Hopital, Philadelphia, PA.

The purpose of this study was to measure the effect of patient position and the use of water on the movement through the esophagus of a standard commonly employed gelatin capsule. Orally administered medications have been implicated in the etiology of esophageal erosions. Many patients have learned to swallow capsules without water or with one swallow of water. This study was designed to determine if such practices might result in delayed transit of the capsule through the esophagus, with resultant esophageal symptoms or frank erosions. Twenty-five normal, asymptomatic subjects were studied in both the upright and supine positions, and with or without swallowing water. The patients were positioned against a gamma camera detector on line to a digital computer. Images and counts were obtained at 1 second intervals for 30 seconds and then at 15 second intervals for 10 minutes. Each capsule contained less than 100 microcuries of Tc-99m sulfur colloid absorbed onto a fragment of filter paper. The total clearance of the capsule was expressed in minutes following ingestion. In one half of the normal subjects studied upright, the capsule remained in the esophagus for a period of 10 minutes or longer, if it was not administered with water. Similarly, the transit of the capsule was delayed over 10 minutes in 50% of the normal subjects studied supine, with or without water. When the capsule was swallowed with water in the upright position, it cleared in less than 10 seconds in all subjects.

In conclusion, these data suggest that orally administered capsules should be swallowed in the upright position with water in order to protect the esophagus.

RADIONUCLIDE QUANTITATION OF ESOPHAGEAL EMPTYING OF SOLID FOOD IN ACHALASIA. G.A.Krosin, T.Saladino, R.W. McCallum. Yale University, New Haven, CT.

The purposes of the present study were: 1) develop a technique to quantitate esophageal emptying of an isotope-labeled solid meal in normal subjects; 2) compare esophageal emptying in normals with achalasia patients, both untreated and after myotomy. 7 normal adult subjects and 10 patients with documented achalasia (7 untreated and 3 failed pneumatic dilatations) ingested an egg salad sandwich labeled with ^{99m}Tc-DTPA. All patients were studied in the sitting position with posterior positioning of the gamma camera. Counts were obtained every minute for 15 minutes beginning on completion of the meal. The total count of the ingested meal was the sum of initial gastric and esophageal counts. Esophageal retention was calculated as the percent of total ingested isotope remaining in the esophagus over time. 4 achalasia patients underwent Heller myotomy and were restudied.

		% Isotope Remaining in Esophagus			
Group	N	1 MIN	5 MIN	10 MIN	15 MIN
Normals	7	6.9±2.7	3.4±1.1	3.3±1.1	2.8±1.0
Achalasia	10	27.7±4.7	24.6±4.9	22.7±4.6	21.1±4.8
Pre-myotomy	4	20.9±7.0	17.5±6.7	14.3±4.8	12.0±3.9
Post-myotomy	4	4.9±3.4	3.4±2.4	2.8±2.2	1.9±1.4

Compared to normals, untreated achalasia patients had marked and significantly increased esophageal isotope retention from 1 to 15 minutes after the meal ($p<0.01$). Esophageal emptying significantly improved after surgery, returning to the normal range and correlated with marked symptomatic improvement. We conclude that quantitation of esophageal emptying of radiolabeled solid food is a physiologic test for evaluating the efficacy of achalasia therapy and to study esophageal dysfunction.

COMBINED GALLBLADDER-GASTRIC EMPTYING IN MAN: EFFECTS OF VARYING MEAL COMPOSITION. E.Rock, L.S.Malmud, P.Bandini, G. Applegate, J. Reilley, R.S. Fisher. Temple University Hospital, Philadelphia, PA.

The purpose of this study was to simultaneously measure the rates of gallbladder and gastric emptying after ingestion of meals of varying protein, cardohydrate, and fat content without altering total caloric or volume intake. Fifty paired experiments in 25 normal subjects were performed using the technique of dual radionuclide cholescystogastric scintigraphy. One minute images and counts were obtained at 15 minute intervals for a period of 2 hours using the gamma camera on line to a digital computer.

Following a saline liquid meal, no significant gallbladder evacuation was observed. A monocomponent fat meal and a multicomponent meal that induced gallbladder emptying which was more rapid and more complete than that which followed either a protein or carbohydrate meal. Fat emptied from the stomach more quickly than protein, or carbohydrate, or a mixed meal, but more slowly than a saline load. The temporal relationship between the gallbladder emptying and gastric emptying, expressed as a ratio, was similar for each monocomponent meal. The ratios were significantly higher after a multicomponent meal.

In conclusion, both gallbladder and gastric emptying were affected significantly by varying meal composition. Gallbladder evacuation was stimulated not only by fat, protein, or mixed meals, but also by a pure carbohydrate meal. This technique appears to be a useful one in studying the relationship between gallbladder and gastric emptying in man under a variety of circumstances.

DUAL RADIONUCLIDE STUDIES OF GASTRIC EMPTYING USING A PHYSIOLOGIC MEAL. P. Bandini, L. Malmud, G. Applegate, J. Reilley, E. Rock, R.S. Fisher. Temple University Hospital, Philadelphia, PA.

The technique of dual radionuclide scintigraphy was employed to quantitate simultaneously gastric emptying of solids and liquids, to establish normal values for gastric emptying of a physiologic meal, to determine the effect on gastric emptying of anti-cholinergic medication, and to evaluate patients with gastric outlet obstruction. The study was performed in 25 normal subjects employing Tc-99m labeled chicken liver as the solid meal, and Indium-111-DTPA in water as the liquid component.

Water, when ingested alone, emptied from the stomach faster than did the liver. When ingested simultaneously there was delayed emptying of the water. Cholinergic blockade slowed emptying of both water and liver. Delayed emptying of both water and liver was observed in 8 of 10 patients studied with the gastric outlet obstruction syndrome. In the other two patients, only emptying of the solid was decreased, as confirmed by a normal saline load test.

In conclusion, this technique demonstrates different rates of emptying of liquids and solids. When ingested simultaneously the solid slowed the rate of gastric emptying of the liquid, there was inhibition of emptying of both liquids and solids by atropine. In some patients with a

gastric outlet obstruction, only solids demonstrated delayed gastric emptying, but not liquids. These studies suggest that this technique can provide quantitative information about gastric emptying which correlates better with patient symptoms than does the standard saline load test. It is also suitable for measuring the effects of various pharmaceuticals on gastric emptying.

THE GASTRIC UPTAKE AND SECRETION OF Tc-99m PERTECHNETATE AFTER H_2 RECEPTOR BLOCKAGE IN DOGS. V. V. Sagar and J. M. Piccone. V. A. Center, Wilmington, DE.

This research investigation describes the effect of cimetidine, a H_2 receptor blocking agent, on the gastric secretion of Tc-99m pertechnetate.

Eleven beagle dogs were anesthetized, opened and the gastric contents aspirated. The six experimental animals were administered 300mg of cimetidine. All animals were administered 2mCi of Tc-99m pertechnetate and, 4 hours after administration, the gastric contents aspirated. The stomachs were removed and imaged and counted on a gamma camera. The % administered dose in the stomach was calculated. The gastric contents were analyzed for titrable acid and equal volumes of standard and sample were counted for Tc-99m activity and the % administered dose in 5cc of gastric juice computed.

There was a 47% decrease in the cimetidine treated animals with essentially no change or slight increase in acid output for the control group. The difference in the % administered dose between the gastric contents and stomach wall in the cimetidine treated animals is 2.5 times greater than the difference in the controls. The blood clearance data is similar in control and experimental animals indicating no stomach uptake.

Our data suggest that Tc-99m pertechnetate is concentrated by the gastric mucosa but its excretion into the gastric contents is inhibited in cimetidine treated animals. These findings also suggest that the parietal cells secrete both acid and pertechnetate and when one is suppressed, so is the other. It is also possible that cimetidine inhibits the secretion of Tc-99m pertechnetate by its action on the superficial mucosal cells.

ASSESSMENT OF GASTRIC FUNCTION BY i.v. INJECTION OF Tc-99m PERTECHNETATE. F. Fazio, E. Pesciullesi, M. Possa and G. Peri. Ospedale S.Raffaele, Milan, Italy, and Hammersmith Hospital, London, U.K.

As Tc-99m O_4^- is quickly concentrated and secreted by the gastric mucosa, i.v.injection of pertechnetate and external recording has been proposed as a non-invasive test of gastric function (Taylor, T.V., Bone, D., Torrance, B., Br.J. Surg., 64: 702, 1977). We have developed a modified version of this technique in order to improve its accuracy, and we have compared it with acid output data obtained from naso-gastric aspiration. We studied normal subjects, patients with duodenal ulcer (DU), and patients with gastric ulcer (GU). Fifteen minutes following pentagastrin stimulation, 1 mCi of Tc-99m pertechnetate was injected i.v. with the subject supine under the gamma camera. Activity over abdominal region was continuously recorded on a digital computer for 30'. Stomach activity was corrected for background and gastric emptying, normalized and expressed as percentage of the injected dose (as measured from an identical dose placed in a phantom simulating the stomach and abdominal wall). Stomach activities were higher in patients with DU (hypersecretive), intermediate in normal subjects, and lower in patients with GU and gastric carcinoma (hyposecretive). There was no overlap between patients with DU and GU. Corrected stomach activities showed excellent correlation with the acid output (in mEq/h) measured by naso-gastric aspiration on a separate session but at corresponding times after pentagastrin stimulation. I.v. injection of Tc-99m pertechnetate is an accurate and non-invasive technique for the diagnostic screening of DU and GU and for the evaluation of medical and surgical treatments in patients with stomach pathology.

MEASUREMENT OF GASTRIC EMPYTING RATE (GER) AFTER SURGICAL TREATMENT FOR OBESITY: USE OF Tc-99m TAGGED CHOPPED CHICKEN LIVER (TCCL). D.D. Patton, H.V. Villar, L.W. Norton, and S. L. Wangensteen. University of Arizona, Tucson, AZ.

We wished to know whether there was a relationship between GER and satiety, rate of weight loss, and caloric intake in patients with morbid obesity treated with gastric bypass (GBy) or gastric stapling (GSt). Since GER depends on test meal type (liquid, solid, fat, etc.) we selected an intrinsically labeled solid food, TCCL (Meyer et al: Am J Dig Dis 21:296, 1978). Ten mCi Tc-99m sulfur colloid is injected into a live chicken, which is sacrificed after 20 min. The liver is boiled and chopped. The tracer is intrinsically bound to the test substance, which is a real food; the study is physiologically sound. To test tracer binding we boiled the TCCL in 1 N HCl for 20 min. The supernatant contained <0.05% of the liver activity.

Patients fasted for 12 hours and were given 1 mCi TCCL (15 gm), 30 gm chopped fat-free roast beef, and 200 ml water. The stomach was imaged in anterior and posterior views with the patient erect, for 2-3 hours. Geometric mean counts were determined so as to minimize changes in stomach position.

Seven patients had GBy (division of the stomach in a fundic pouch drained by a gastrojejunostomy) and 12 had SGt (transverse stapling of the stomach creating 2 pouches communicating by an 8 mm opening). All studies were done 2 months after surgery. GER was 6.6 ± 5.5 %/min. after GBy and 1.7 ± 1.4 %/min. after GSt ($P<.005$). Feeling of fullness was similar in both groups, as was caloric intake and rate of weight loss. We concluded that although GER is significantly slower after GSt than after GBy, GER does not appear to be a factor determining rate of weight loss, caloric intake, or satiety.

COMPARISON OF GASTRIC EMPTYING RATES OF INTRACELLULAR AND SURFACE-LABELED CHICKEN LIVER IN NORMAL SUBJECTS. R.W.McCallum, T. Saladino, R. Lange. Yale University, New Haven, CT.

It was our aim to evaluate and compare 2 isotope-labeled meal preparations as measurements of gastric emptying of solids in man: 1) intracellular labeling of chicken liver using ^{99m}Tc-sulfur colloid (Meyer, et al, 1976); 2) surface labeling of commercial chicken liver with the same isotope. In the latter method, ^{99m}Tc-sulfur colloid was applied to the surface of 1cm cubes of pre-cooked chicken liver. Both meals were similar in composition: 30grms of chicken liver, 7½oz beef stew, 10oz water, and 2 crackers consisting of 16 grms protein, 26grms carbohydrate, 12grms fat, and contained 274 calories. 7 normal subjects ingested each meal on separate days and lay supine under a gamma camera. Gastric emptying was expressed as percent of isotope remaining in the stomach for 120 minutes after counting began.

Meal	N	% Isotope Remaining in Stomach (X±SEM) 30	60	90	120 MIN
Intracellular	7	90.4±3.5	79.1±6.0	62.4±5.7	50.4±5.8
Surface	7	87.0±4.1	77.1±5.4	60.8±5.7	50.1±7.7

The mean rate of gastric emptying per hour was 24.9% after the intracellularly-labeled meal and 25.0% for the surface-labeled. In vitro studies of adsorption of ^{99m}Tc-sulfur colloid to the chicken liver surface were performed by mixing the surface-labeled chicken liver in 10oz of water at pH 2. Approx. 1/3 of isotope was displaced from the liver within 10-15 mins. Adsorption remained stable after that time. We conclude: 1) gastric emptying rates for intracellurly and surface-labeled chicken liver preparations are similar; 2) in vitro studies indicate stable adsorption of 2/3 of the isotope dose to the liver surface; 3) surface-labeled pre-cooked chicken liver may be acceptable for evaluation of solid food gastric emptying in man.

PERSISTENT RENAL UPTAKE OF GALLIUM IN THE ABSENCE OF RENAL PATHOLOGY IN PATIENTS WITH SEVERE HEPATOCELLULAR DISEASE. B.B. Sterkel, N.P. Alazraki, and A. Taylor. Veterans Administration Medical Center, San Diego, CA.

We have noted persistent renal accumulation of gallium in patients who had no apparent renal pathology, although these patients did have advanced hepatocellular disease. A retrospective study was performed to determine if marked hepatocellular disease could be associated with renal accumulation of gallium in the absence of renal pathology. Scan review of 40 patients who had Tc-99m sulfur colloid liver/spleen scans and gallium-67 citrate scans within one month showed 14 with marked hepatocellular disease on liver/spleen scan.

Of these 14 patients, 9 had renal accumulation of gallium at 48 or 72 hours. Eight of these 9 had advanced alcoholic liver disease while one had hemachromotosis. An autopsy was performed on 5 of these patients within two months of the scans; three had no evidence of renal disease, the fourth had renal calcium and urate deposits, and the fifth had candidiasis involving the kidney although all five patients had normal renal function at the time of their gallium scan. Of the remaining 4 patients, 2 had no evidence of renal disease and 2 had an elevated BUN and creatinine.

In summary, 5 of 9 patients with persistent renal uptake of gallium had no evidence of renal disease and in 2 additional patients, it is unlikely that significant renal pathology existed. Therefore, advanced hepatocellular disease can be associated with persistent renal gallium uptake in the absence of renal pathology. Hepatocellular disease should be excluded in patients with renal uptake of gallium before the scan is interpreted as representing renal disease.

4:00-5:30 Room 3039

RADIOPHARMACEUTICAL CHEMISTRY

BRAIN

Session Chairman: Michael J. Welch
Session Co-Chairman: Linda C. Knight

LOCALIZATION OF I-123 IODOPHENYLALKYL AMINES IN RAT BRAIN. H.S. Winchell, R.M. Baldwin, T.H. Lin. Medi-Physics, Inc., Emeryville, CA.

Localization in rat brain of forty iodophenylalkyl amines labeled with I-123 was evaluated to develop gamma-emitting agents for brain studies. Highest activity in brain and brain-to-blood activity ratios were noted for iodine position on the benzene ring of p>m>o; for alkyl groups, α-methylethyl>ethyl>methyl>none; for N additions, single lipophilic group>H>two lipophilic groups. It is suggested that introduction of a halogen into the ring structure of many amines results in greater concentration of the agent in brain than is seen with the non-halogenated parent. Thirty-four of the forty compounds showed higher rat brain activity, and higher brain-to-blood activity ratios at 5 min than did I-123 4-iodoantipyrine. Ten of the compounds showed a ten-fold or greater brain-to-blood activity ratio at 5 min than did I-123 4-iodoantipyrine. Activity in brain did not correlate solely with the blood concentration of non-ionized base, or lipophilicity of the base, anticipated from consideration of their chemical structure. We propose that the concentration of these agents in brain is a consequence of their affinity for high-capacity, relatively nonspecific binding sites for non-hydroxylated amines located in the brain and/or brain capillary endothelium. The agent N-isopropyl-p-iodoamphetamine was chosen for further study because, in the rat, it showed high brain activity, 1.57%/gram, and brain-blood ratio, 12.6 at 5 min which increased to 2.14%/gram and 20.7, respectively, at 60 min (R isomer) following its intravenous administration. Clinical utility may exist for these agents in scintigraphic measurement of regional cerebral blood flow, regional brain amine transport and/or binding mechanisms, studies of the retina, and localization of tumors of neural origin.

LOCALIZATION OF I-123 N-ISOPROPYL-p-IODO-AMPHETAMINE IN DOG AND MONKEY BRAIN. H. S. Winchell, R. Hattner, H. Parker. Medi-Physics, Inc., Emeryville, CA, University of California at San Francisco, San Francisco, CA.

Previous work demonstrated rapid localization and prolonged retention in rat brain of I-123 N-isopropyl-p-iodoamphetamine. The present work extends the in vivo distribution studies on this agent to the dog and monkey. The agent was administered intravenously to dogs and a capuchin monkey. One dog was sacrificed at 6 min and another at 200 min. Activity was assayed in certain tissues and scintigraphic images of coronal slices of the brain were obtained. Images and digital data were collected following administration of the agent to the monkey and changes in distribution of activity were computer analyzed. In the dog, the ratio of activity in gray-to-white matter decreased from 1.32 at 6 min to 0.93 at 200 min. No specific localization in brain nuclei was seen, but progressive accumulation of activity in eyes was noted. Rapid initial localization of activity in the monkey brain was noted suggesting substantial first-pass clearance. Further slow accumulation of activity in brain occurred during the next 20 minutes. High levels of brain activity were maintained for several hours and good scintigraphic images of the brain were obtained with pinhole collimator/scintillation camera imaging 1½ to 2 hr after administration. At 165 min, of the activity emanating from the body, 18% was in the head, 27% in the upper abdomen (liver/kidney/stomach), and 8% in the pelvis (bladder). The data suggest utility of the agent in imaging regional brain perfusion (early study) and possibly in assessing dynamics of CNS amphetamine binding sites (late studies with and without competitive binding agents).

NEW BRAIN IMAGING AGENTS: RADIOIODINE LABELED TERTIARY DIAMINES. K. Tramposch, H. Kung and M. Blau. State University of New York at Buffalo and VA Medical Center, Buffalo, NY.

Selenium-75 labeled tertiary diamines, MOSE and PIPSE, localize in brain by a regional pH shift mechanism (J.N.M. Feb. 1980). Since the mechanism of uptake and retention of these compounds is related principally to lipid solubility and its change with pH, other radioactive labels can be used. We have prepared and studied a series of I-labeled pH shift agents. To minimize *in vivo* deiodination, the radioiodine was covalently bound to an aromatic ring.

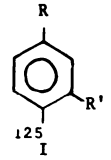

m-IDM, R=R'= $-CH_2-N(CH_3)_2$

m-IPIP, R=R'= $-CH_2-N$ 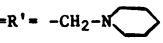

m-IMO, R=R'= $-CH_2-N$ 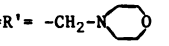

o-IBDM, R=H, R'= $-CH_2-N(CH_3)_2$

The above tertiary diamines were prepared by brominating 4-iodo-m-xylene with N-bromosuccinimide and reacting the product with disubstituted amines. o-IBDM was obtained by reacting o-iodobenzyl chloride with dimethylamine. I-125 labeling was done by exchange at elevated temperatures. Partition coefficient-pH profiles (n-octanol:buffer, pH 6.0-8.0) and biodistribution in rats at various times after i.v. injection were studied.

The brain uptake at 2 min (1.7-2.4% dose/organ) was comparable to the Se-75 pH shift agents. Washout from brain was fast for m-IMO and the monoamine o-IBDM ($T_{\frac{1}{2}}$ <15 min) and very slow for m-IDM and m-IPIP ($T_{\frac{1}{2}}$ >6 hrs). These compounds labeled with I-123 would be useful as brain imaging agents.

THE SYNTHESIS OF [F-18]-4-FLUOROANTIPYRINE FOR THE MEASUREMENT OF REGIONAL CEREBRAL BLOOD FLOW. C.-Y. Shiue, R. S. Kutzman, and A. P. Wolf. Brookhaven National Laboratory, Upton, NY.

[C-14]-antipyrine has been investigated as a tracer for estimating regional cerebral blood flow using autoradiography in animals. Its radioiodinated analogs have been used to study the symmetry of brain perfusion using the gamma camera and single photon tomography. However, it is known that 4-iodoantipyrine is unstable in vivo. Therefore we have explored the possibility of using F-18 labeled 4-fluoroantipyrine as a non-volatile tracer for the measurement of regional cerebral blood flow.

[F-18]-4-fluoroantipyrine is prepared by fluorination of antipyrine (1) with [F-18]-F_2 in acetic acid. Fluorination of 1 with fluorine-18 gives [F-18]-4,4-difluoro-3-hydroxy-2,3-dimethyl-1-phenylpyrazolidin-5-one (2), 4-fluoroantipyrine (3), and 4,4-difluoro-3-methyl-1-phenyl-2-pyrazolin-5-one (4). The product distribution depends on the ratio of 1 and molecular fluorine. The products are purified by silica gel column chromatography or by preparative GLPC. Current production procedures result in radiochemical yields of ∿18% (based on recovered F-18) in a synthesis time of 90 minutes from EOB. [F-18]-

4-fluoroantipyrine can be prepared with a specific activity of $\geq$ 0.27 mCi/mg.

Studies of the biodistribution of 3 at 15,30,60,120 seconds and 10 minutes in Swiss albino mice (BNL strain) indicate that the radioactivity persists in brain tissue for up to 120 sec at a level per unit weight greater than that of bone. [F-18]-4-fluoroantipyrine is being studied as a radiopharmaceutical for measuring brain perfusion and blood flow.

CEREBRAL EXTRACTION OF (N-13) AMMONIA (NH): DEPENDENCE ON CEREBRAL BLOOD FLOW AND CAPILLARY PERMEABILITY-SURFACE AREA PRODUCT (PS). M.E. Phelps, S.C. Huang, D.E. Kuhl, E.J. Hoffman, C. Selin. UCLA School of Medicine, Los Angeles, CA 90024

We have systematically examined mechanisms of transport, metabolism and removal of NH and its uses as a biological tracer in brain. Cerebral extraction and clearance was measured by single pass extraction fraction (E) technique in monkeys, and in dogs by use of μ sphere flow model. E for whole brain was determined at different levels of cerebral blood flow (CBF). Net extraction of NH was measured in gray and white matter, mixed tissue and cerebellum when CBF variations were produced by embolization, local brain compressions and ventilation with carbon dioxide in dogs. E for NH varied from 70 to 20% over a CBF range of 12 to 140cc/min/100gms. Estimates of PS with Renkin/Crone model showed increases with CBF: magnitude and rate of increase was highest in gray matter > mixed tissue > white matter. We have proposed a new unidirectional transport model in which CBF increases by recruitment of capillaries and increases of blood velocity. This saturable-recruitment (SR) model provides a possible explanation for the mechanism of flow changes at capillary level. Local (N-13) tissue concentrations after i.v. injection increased non-linearly with CBF: doubling or halfing basal CBF produced 40 to 50% changes, and further increases in CBF produced smaller changes. NH appears to be a good tracer for detection of cerebral ischemia with positron tomography but exhibits poor response at high CBF. Because NH is specific to capillaries, PS dependent, rapidly incorporated into glutamine in astrocytic pericapillary end feet and has a long retention time, it provides a new method to examine capillary mechanisms

4:00-5:30 Room 2043

INSTRUMENTATION

CARDIAC TOMOGRAPHY

Session Chairman: Patrick Bradley-Moore
Session Co-Chairman: James Carey

7-PINHOLE TOMOGRAPHY. IS IT WORTH IT? R.E. Henkin, D.J. Hale, B.C. Salo, A. Rao, and W. Chang. Loyola Univ. Med. Center, Maywood, IL.

Questions exist as to the specificity (SP) and sensitivity (SE) of 201-Thallium 7 pinhole tomograms (PHT). We evaluated 120 patients with PHT imaging and cardiac cath. Standard thallium images (TI) were made with a high resolution collimator, 1000 ID per image, in four projections at stress and 4-6 hours later. PHT studies were performed on the same device. A commercial collimator and software were employed.

Cath was analyzed for left anterior descending (LAD), posterior descending (PDA) and obtuse marginal-circumflex (OM-CX) disease. Caths, TI and PHT were interpreted independently. 70% or greater stenoses were considered significant. The SE of TI images for detection of patients with coronary artery disease (CAD) was .83, and SP was .88. PHT had an SE of .93 for CAD and an SP of .67.

The SE and SP for PHT and TI were analyzed by vascular distribution. The LAD SE was .71 and SP was .89 for the TI. For PHT, SE was .86 and SP was .7. For the PDA the TI was .43 sensitive and .92 specific. PHT had an SE of .75 and an SP of .96 for the PDA. For the OM-CX the TI was .2 SE and 1.00 SP. The PHT had a .4 SE and 1.00 SP.

This demonstrates increased sensitivity of PHT for CAD with decreased specificity. Data for the PDA and OM-CX shows significant increases in SE with no loss of SP. The majority of false-positive studies were in the LAD septal area. The explanations for this relate to attenuation due to variable patient anatomy. At present we see no way to eliminate this problem and advise interpreting isolated septal lesions with care.

Tc-99m-PYROPHOSPHATE TRANSAXIAL EMISSION COMPUTED TOMOGRAPHY IN PATIENTS WITH ACUTE MYOCARDIAL INFARCTION. B.L. Holman, B.J.Friedman, J.F. Polak, G. Curfman, J.Wynne, C-M. Kirsch, and R.J. English. Peter Bent Brigham Hospital, Boston, MA.

Assessment of acute myocardial infarction with myocardial scintigraphy has been limited by the constraints of two-dimensional imaging. We have investigated the feasibility of transaxial emission computed tomography of the heart using Tc-99m-pyrophosphate. We studied 6 patients with acute myocardial infarction (3 with inferior and 3 with anterior infarcts) and 4 patients without infarction. Imaging was performed with a gamma camera and then with the CLEON 711 radionuclide body function imager 3 hours after injection of Tc-99m-pyrophosphate using a slice interval of 2.5 cm beginning at the base of the heart and progressing towards the apex. Immediately following the imaging with 99m-Tc-pyrophosphate, Tc-99m-pertechnetate was injected, resulting in in vivo RBC labeling. Repeat images of the cardiac blood pool were performed to assist in localizing the pyrophosphate uptake. There was increased uptake in the vertebra and sternum without myocardial wall uptake in the 4 patients without infarction. Patients with anterior infarction had pyrophosphate uptake in the anterior wall of the left ventricle with extension in 2 patients into the intraventricular septum. Patients with inferior infarction had uptake involving the diaphragmatic left ventricular wall with extension in 2 patients to the posterior, postero-septal, posterolateral and posterior right ventricular walls. In all cases the quality of the images was superior with tomography than with the gamma camera. We conclude that emission transaxial emission computed tomography with 99m-Tc-pyrophosphate is feasible in man and may lead to more accurate localization and sizing of acute myocardial infarction.

ASSESSMENT OF REGIONAL MYOCARDIAL FUNCTION BY POSITRON EMISSION TOMOGRAPHY. G. Wisenberg, H. Schelbert, E. Hoffman, S.C. Huang, M. Phelps, and D. Kuhl. UCLA School of Medicine, Los Angeles, CA.

Regional myocardial wall thickening (RM) has been proposed as a sensitive index of regional myocardial function. We have previously shown that regional myocardial indicator concentrations and regional blood flow (MBF) can be accurately and non-invasively quantified by positron emission tomography (PCT). Because of the partial volume effect, concentrations recovered by PCT, however, are a function of object size. Myocardial concentrations measured by PCT, therefore, must be corrected for left ventricular wall thickness (WT). Conversely, PCT may be used to measure RM from the change in recovered indicator concentrations from enddiastole to endsystole. This possibility was examined in 7 open chest dogs imaged after left atrial injections of Ga-68 labeled microspheres (positron emitting) and gamma microspheres (for in vitro determination of MBF). Gated enddiastolic and endsystolic images were acquired for each of two planes per animal. In vivo recovery coefficients (RC) were derived from the relationship: WT to ratios of uncorrected in vivo MBF by PCT to in vitro measured MBF. This relationship described by RC = 0.09 + .04 WT (mm) closely approximated the curve derived from phantom studies for the range of 8-20mm WT. Using the in vivo RC regression equation, percent increases in regional count recovery by PCT were converted to percent RM and compared well to percent RM measured by echocardiography by $y = .05 + .97$ ($r = 0.95$; $n = 20$. SEE = .08). Thus PCT permits measurement of percent RM that can be correlated with simultaneously determined regional myocardial metabolism and blood flow.

CLINICAL APPLICATIONS OF ROTATING SLANT HOLE TOMOGRAPHY TO CARDIOVASCULAR NUCLEAR MEDICINE. R.J. Herfkens, D.W. Shosa, R.S. Hattner, D.B. Faulkner, E. Botvinick, and W. O'Connell
University of California, San Francisco, San Francisco, CA

Reconstruction tomography using a seven pinhole collimator with a large field gamma camera appears to offer advantages over projection images for the heart. A similar concept using a rotating slant hole collimator was described some time ago but never became widely utilized because of limitations intrinsic to then available imaging and display instrumentation, and image reconstruction algorithms. We have developed rotational slant hole tomography (RSHT) using state of the art instrumentation and improved reconstruction algorithms. Three groups of patients were evaluated using imaging times comparable to conventional imaging. TL-201 RSHT in 20 patients with ischemic heart disease was compared to standard images. Tomographic images of TcPYP in 10 patients suspected of having myocardial infarction were compared to conventional images. Multiple gated wall motion studies were obtained tomographically in 9 patients and compared to conventional images. RSHT has been useful in clearly defining ischemia and infarcted areas on TL-201 images. The use of TcPYP RSHT has been useful in defining infarcted areas separating rib uptake, and blood pool activity in the diffuse uptake pattern. Tomographic wall motion studies have been useful in defining chamber size and segmental motion abnormalities despite projection. Besides improvement in image definition using RSHT, RSHT offers other advantages over the seven pinhole approach. Image registration and uniformity standardization are unecessary with RSHT. Positioning is not critical. Adequate tomographic studies can be obtained with a 25 cm gamma camera. RSHT offers the advantages of tomography with few of the disadvantages of the 7 pinhole technique.

A MULTICENTER COMPARISON OF STANDARD AND SEVEN PINHOLE TOMOGRAPHIC TL-201 SCINTIGRAPHY: RESULTS OF QUANTITATIVE INTERPRETATION OF TOMOGRAMS. R. Vogel, P. Alderson, D. Berman, J. Caldwell, J. Thrall, A. van Aswegen, L. Becker, T. Brady, M. Freeman, D. Kirch, M. LeFree, J. Links, N. Pantaleo, J. Ritchie, H. Staniloff, G. Hamilton, B. Pitt, and H. Wagner, Jr. Denver V.A.M.C., Denver, CO, Cedars-Sinai M.C., Los Angeles, CA, Johns Hopkins M.I., Baltimore, MD, Seattle V.A.M.C., Seattle, WA, and University Hospital, Ann Arbor, MI.

Standard scintigraphy and seven pinhole tomography were performed following thallium-201 administration in a total of 110 patients at the above medical centers excluding the Denver V.A.M.C. Studies were initiated 5-10 minutes post treadmill exercise and 2 hours later or at rest. Circumferential activity profiles obtained from the tomograms were analyzed using quantitative criteria of redistribution and lower limits of normal. The latter were derived on institutionally specific, reconstruction computer specific, and total group bases. Of the 23 patients with < 50% coronary artery stenoses by angiography, 21 (91%) were judged normal by these criteria. Using the institutional, computer use, and total group lower limits of normal, 95%, 91%, and 87%, respectively, of the coronary artery disease patients were judged abnormal. Visual interpretation of the tomographic images resulted in specificity and sensitivity values of 79% and 84%, respectively, compared with 88% and 80% values, respectively, for visual interpretation of the standard scintigraphy. These data suggest that thallium-201 tomography interpretation is improved by use of quantitative criteria and that quantitative tomographic diagnosis of coronary artery disease compares favorably with standard technique.

A MULTICENTER COMPARISON OF STANDARD AND 7 PINHOLE TOMOGRAPHIC MYOCARDIAL PERFUSION IMAGING: ROC ANALYSIS OF QUALITATIVE VISUAL INTERPRETATION. A.Green, New England Nuclear Corp.; P.Alderson, Johns Hopkins University; D. Berman, Cedars-Sinai Hospital; J. Caldwell, V.A. Seattle; J. Thrall, University of Michigan, and R. Vogel, V.A. Denver.

To compare the accuracy of visual qualitative interpretation of thallium Tl-201 myocardial perfusion images with routine ("planar") parallel hole collimation and tomographic 7 pinhole collimation. 91 patients (73 abnormal, 18 normal) post-angiography at 3 institutions were evaluated in a randomized crossover study using both techniques. Immediate post-exercise and 2-4 hour "redistribution" images were obtained with both collimators for each patient. Images were interpreted as usual at each institution and again in a forced blinded reading by a panel of 4 experienced and 2-3 inexperienced observers. ROC analysis of the blinded panel readings was performed. Receiver operating curves for qualitative visual interpretation of planar and tomographic images were virtually superimposeable. Inexperienced and experienced observer ROC's were not significantly different for the two techniques. Individual institutional ROC's were not significantly different for the two techniques. Conclusions: i) the accuracy of qualitative visual interpretation of planar and tomographic myocardial perfusion images in this series was comparable; ii) the accuracy of qualitative visual interpretation by experienced and inexperienced observers was comparable in this series for the two techniques; iii) the accuracy of qualitative visual interpretation of 7 pinhole tomographic images in this series with varying accuracy of planar studies was comparable with both techniques; iv) preliminary quantitatjve analysis of tomographic images showed significant increase in accuracy.

CLINICAL COMPARISON OF MULTIPLE PINHOLE TOMOGRAPHY WITH PLANAR IMAGING FOR THALLIUM-201 STRESS MYOCARDIAL SCINTIGRAPHY. D. Berman, M. Freeman, E. Garcia, H. Staniloff, N. Pantaleo, J. Maddahi, J. Forrester, H.J.C. Swan, and A. Waxman. Cedars-Sinai Medical Center, Los Angeles, CA.

In order to evaluate the relative diagnostic potential of multiple pinhole tomography (TOMO) for Tl-201 stress myocardial scintigraphy, TOMO and standard planar imaging (PLANAR) were performed on 39 pts undergoing coronary arteriography. Twenty-six pts had significant coronary artery disease (CAD) (>50% stenosis) and 13 had normal coronary arteriograms. Of the 26 CAD pts, 14 had disease in the anterior (ANT) and posterior (POST) coronary circulations, and 12 had either ANT or POST CAD. Following single injection of Tl-201 at peak exercise, all pts had PLANAR and TOMO studies, with random variation of study sequence. PLANAR was performed with ½ inch crystal mobile camera, and TOMO with large field camera and 7 pinhole collimator. Images were inspected independently by 2 experienced observers, with disagreements solved by consensus. Satisfactory images were obtained by both techniques in all 39 pts. TOMO was positive in 23/26 CAD pts, and PLANAR positive in 22/26. TOMO and PLANAR were negative in 11/13 pts with no CAD. Regarding extent of CAD, TOMO correctly identified 9/14 pts with both ANT and POST CAD, and incorrectly predicted ANT and POST in only 2/12 with single region CAD. PLANAR correctly identified 6/14 pts with both ANT and POST CAD, and incorrectly predicted 2 region CAD in only 2/12 with CAD in a single region. These preliminary results suggest that TOMO and PLANAR Tl-201 techniques have similar accuracy in the detection of CAD, and that TOMO may be slightly more accurate in the assessment of extent of CAD.

TOMOGRAPHIC RADIONUCLIDE ANGIOGRAPHY (TRA). R.W. Myers, R.P. Baile, V.R. Reed, E. Drasin, J.D. Hill, and J.R. Sephir. Herrick Memorial Hospital, Berkeley, CA.

Determination of left ventricular (LV) function with TRA using a seven pinhole collimator was evaluated by comparing results of invasive contrast LV angiography (CVG) and planar multigated blood pool imaging (PBP) in multiple projections to TRA in 15 patients. Left anterior oblique seven pinhole multigated blood pool acquisition of eight segments (50 to 80 msec each) for 70% of the cardiac cycle was reconstructed to produce eight LV slices from apex to base in each segment. A three dimensional reconstruction (depth of slice = third dimension) for each segment allowed viewing as a cyclic angiogram in any projection for evaluation of wall motion abnormalities (WMA). PBP and CVG were graded similarly but independently for WMA. Ejection fraction (EF) was determined for TRA by integration of tomographic slices to produce a noncalibrated volume at end-diastole (ED) and end-systole (ES). EF was determined by standard methods from CVG (volume by area-length) and PBP (count-based). In all modalities, EF = (ED-ES)/ED.

For detection of WMA the sensitivity and specificity for TRA were 77% and 80% and for PBP 91% and 100%. Significant correlation with CVG EF was obtained for each modality—TRA ($r = .78$, $p < .001$, SEE = .08) and PBG ($r = .93$, $p < .001$, SEE = .06). Difficulty with proximal LV WMA and tendency to underestimate LV EF at high EF were notable problems with TRA.

TRA appears to offer no improvement in accuracy over PBP for assessment of LV function. Its advantages relate to multiview display after single view acquisition, visualization of LV without other chamber interference and potentially, estimation of LV volume.

THALLIUM-201 IMAGING FOR DETECTION OF CORONARY ARTERY DISEASE: COMPARISON OF PLANAR AND SEVEN-PINHOLE TOMOGRAPHIC TECHNIQUES. J.H. Thrall, M. Besozzi, R. Kline, T. Brady, L. Rogers, J. Keyes, Jr., B. Pitt, University of Michigan Medical Center, Ann Arbor, MI.

To determine the relative utility of planar (PLAN) and seven-pinhole tomographic (TOMO) imaging for detection of coronary artery disease (CAD) both techniques were performed on 55 patients prior to coronary angiography. Each patient received 1.5 millicuries Tl-201 at peak exercise with PLAN and TOMO performed in random sequence. All images were interpreted in a blinded fashion, and in addition, the TOMO images were analyzed by a quantitative circumferential mapping (CIRC-MAP) program to detect areas of uptake falling below previously determined regional standards for lower limits of normal. Total imaging time was recorded for each type of study.

Arteriographically, 42 patients had significant CAD as defined by $\geq$ 70% stenosis in one or more vessels. 13 patients had either normal coronary arteries on insignificant CAD ($\leq$ 30% stenosis).

Scintigraphic Results:

		PLAN		TOMO		CIRC-MAP	
Sensitivity	1 VSD	9/14		10/14		11/14	
	2 VSD	11/14		14/14		14/14	
	3 VSD	12/14		12/14		13/14	
	Total	32/42	76%	36/42	85%	38/42	91%
Specificity		12/13	92%	12/13	92%	12/13	92%

Imaging time averaged 12 min. for TOMO and 22 min. for PLAN.

These results suggest that TOMO has equal specificity to PLAN a slightly higher sensitivity and affords a 45% reduction in imaging time.

CLINICAL EFFICACY OF MYOCARDIAL PERFUSION TOMOGRAPHY WITH 7-PINHOLE COLLIMATOR. Y. Yonekura, Y. Ishii, K. Yamamoto, T. Mukai, T. Fujita, K. Minato, and K. Torizuka. Kyoto University Medical School, Kyoto, Japan.

The clinical efficacy of tomographic presentation of heart imaging using Kirch collimator (7-pinhole) was evaluated. Twenty-five patients having coronary artery disease (CAD) and hypertrophic cardiomyopathy (HCM) documented by coronary angiography and left ventriculography were selected for this study. Following the conventional Tl-201 myocardial perfusion imaging (MPI), myocardial perfusion tomography (MPT) with 7-pinhole collimator was performed in both LAO and RAO projection. In addition, to examine wall motion abnormalities tomographically, Tl-201 MPI as well as Tc-99m-RBC blood pool images were gated to reconstruct multigated MPT (MGMPT) and multigated cardiac pool tomography (MGCPT).

The MPT in LAO projection revealed superior sensitivity to the conventional MPI in the case of inferior wall infarction, and the MPT in RAO projection revealed superior sensitivity in the case of anterior wall infarction. Combination of the MGMPT and MGCPT succeeded in visualizing a subendocardial infarction as a focal gap between these two images. In the case of a small ischemia ellusive in the conventional MPI, it can be seen as subtle wall motion abnormalities in the tomographic presentation in movie format. An asymmetrical hypertrophy in HCM can readily be localized in tomographic visualization. Tomographic reconstruction with 7-pinhole collimator from the optimal tomographic plane should be attempted, when the conventional display is equivocal.

4:00-5:30 Room 2040

INSTRUMENTATION

COMPUTER SYSTEMS

Session Chairman: Bruce Line
Session Co-Chairman: David Weber

ALL DIGITAL NUCLEAR MEDICINE DEPARTMENT. G.M. Kolodny, H.D. Royal, J.A. Parker, J. Khettry. Division of Nuclear Medicine, Beth Israel Hospital, Boston, MA.

Nuclear medicine images within our department are stored digitally rather than photographed, saving time and eliminating the file room, film processor, and dark room. Studies from each gamma camera are acquired on separate floppy discs and then transferred to a 300 megabyte hard disc for permanent storage. A second 300 megabyte disc drive is used for backup. In list mode, the data is collected directly on to the 300 MB backup disc. Studies are analyzed and interpreted directly from a CRT screen in our reading area, where contrast, gray scale and background subtraction are easily varied. Previous studies can be recalled from the storage disc and the image quality manipulated as desired. Satellite CRT displays within hospital conference areas will be available for remote access to patient studies.

Scan interpretations are dictated into a commercial RTAS reporting system where the voice is digitized, compressed, and stored on 80 MB discs. The referring physician can obtain immediate access to the report via any telephone. He dials the RTAS phone number, and then, after overdialing the patient name, hears the report. The hard copy of the report is typed by a typing service outside the hospital which is connected to the RTAS via telephone. The typed report comes back over the telephone to appear on the RTAS printer. The RTAS also includes a scheduling system and immediate automatic printing of normal reports.

Cost benefit analysis of the all digital department shows considerable savings over photographic storage and conventional dictation arrangements. Other advantages include better service to patients and referring physicians because of the ease of locating images and their interpretations and the ability to readily manipulate and compare studies.

USES OF A MICROPROCESSOR-BASED DATA PROCESSING SYSTEM IN A NUCLEAR MEDICINE DEPARTMENT. S.M. Spies and J.M. Cuevas. Northwestern Memorial Hospital, Chicago, Illinois.

The increasing availability and concurrent decreasing price of microprocessor-based digital computer systems makes these devices very attractive for use in implementing a variety of clerical as well as computational tasks in a nuclear medicine department. To test the practicality of this hypothesis, an inexpensive Z-80 microcomputer system configured from commercially available subsystems was assembled and applications software developed. The basic system hardware consisted of a Z-80 based microcomputer with cathode ray tube terminal, 16K bytes of random access memory and mass data storage using flexible magnetic disks. Total hardware cost was less than $2000. Programs were developed in a high level interpreter language (BASIC), and designed to minimize data entry errors caused by inexperienced users. Two major application areas were addressed: 1) clerical applications including both patient scheduling functions and departmental statistics data base management and 2) routine calculations including thyroid uptake measurements and erythrocyte survival determination. The use of this system has met with great acceptance by departmental personnel. Clerical errors have been reduced and the time required to tabulate monthly departmental statistics greatly diminished. Additional applications now being investigated include the management of a teaching file data base, and computerized instruction for nuclear medicine residents and nuclear medicine technology students. The use of microcomputers in non-real time dependent applications is inexpensive, convenient, and practical in a medium to large sized nuclear medicine department.

DATA BASE SYSTEM FOR NUCLEAR MEDICINE SCANS AND IN-VITRO DATA. A.S. Johnston, D.R. Spelbring, S.M. Pinsky and H. Mermall. Michael Reese Medical Center, Chicago, IL.

A system of codes has been written in BASIC for both storage of scan data and storage of in-vitro data including automatic matching of patient names with lab results and storage of quality control data.

A coding system which uses a 7 digit code number was developed for specifying scan types and the results of readings. The code number has 4 fields, which are: 1) scan type; 2) reading results; 3) follow-up information; 4) project status.

A double data entry system for both initial entry and verify entry is provided.

The in-vitro code includes entry of demographic data and zip ticket number by secretaries. Entry of zip ticket number a second time by the laboratory technologist, with the numbers entered in the order that sample tubes are counted in a well counter, gives an automatic assignment of results to the corresponding patient name. Counter results are transferred to the computer by punched paper tape.

Secretarial and scientific work flow patterns were considered in code design.

Retrieval of all demographic data and each code number field is allowed. Name data is retrieved by letter combinations which occur within a name. AND logic is permitted between different data units.

RAPID AUTOMATIC MEASUREMENT AND REPORTING OF ANTIBIOTIC EFFECT IN MICROBIAL CULTURES MONITORED BY A RADIOMETRIC METHOD. B.G. Yangco, J.A. Madden*, E.A. Eikman, D.A. Solomon, S.C. Deresinski. University of South Florida and James A. Haley VA Hospital, Tampa, FL

Optimal tailoring of antibiotic treatment requires tedious culture methods that are difficult or impossible to apply to slow growing organisms. The sensitive measurements of $C\text{-}14O_2$ evolution in the two compartment culture/counting vial of Buddemeyer provides speed in measuring growth effects. We have designed a computer-assisted approach to the analysis and reporting of the voluminous data generated.

Using a general purpose minicomputer the raw data from the liquid scintillation counter is acquired, sorted by vial number and grouped into time series for each set of replicates. Each time series is filtered, analyzed for replication time and plotted. Sensitivity to antibiotics is expressed as percent inhibition with respect to control samples.

Full analysis of over 150 samples and controls is automatically reported after a few minutes of computation time. Drug susceptibility of Mycobacterium avium/intracellulare is calculable within 4 days, a savings of more than a month compared with current methods. The approach is adaptable to many other culture systems and on-line or off-line computers.

ALL PURPOSE PICTURE ORIENTED COMPUTER PACKAGE: APPLICATION TO THE FIRST FOURIER COEFFICIENT EVALUATION OF HEART STUDIES. J.A. Salomon, U.B.Noelpp, E. Ben Ezra, H.Roesler and H. Atlan. Inselspital, Bern, Switzerland and Hadassah University Hospital, Jerusalem, Israel.

We have developed on a DEC Gamma 11 system a software which allows to interactively manipulate pictures beyond the level found in this currently available nuclear medicine package.

Useful improvements to conventional display features include:

1. The ability to fully monitor a display session from within a user program (i.e. a software interface to the display, which is the base of all subsequent highlights).
2. Manipulation of multiple overlaying pictures on the same screen, including overlaying simultaneous thresholding, masking and contour finding.
3. User command language to pre-program a sequence of displays to be merged with a dedicated application. As an example, a First Coefficient Fourier analysis* of multiple gated pictures which takes advantage of the temporal radioisotope distribution for a refined separation of the heart chambers has been included in this package.

Since the design of display protocols around any new user application is done in the easiest way, we believe that this approach will increase the quality of the analysis of presently available nuclear medicine scans, especially in the hot field of cardiac imaging.

* Bitter, F., Adam, W.E., Geffers, H., Weller, R. and Ellerbruch, H.: Nuclear Medicine, In Press.

AUTOMATED BATCH PROCESSING OF RADIONUCLIDE ANGIOGRAMS. J.P. Wexler, A.M. Rabinowitz, W.I. Ganz, C. Yee, and M.D. Blaufox. Albert Einstein College of Medicine, Bronx, N.Y.

Most automated methods of analyzing radionuclide angiograms require frequent operator-computer interaction. We have developed a method of batch processing multiple patient studies which requires only identification of the studies to be processed and for each study rough delineation of the left ventricular region of interest during end diastole. Once initiated the program finds the ventricular edge in each frame of all studies, performs computations, creates and discretely labels storage and playback buffers, and prepares hard copy. The number of studies which can be processed is limited only by the disc capacity. Processing by this method (A) was compared to processing by subroutines which were initiated manually (M). Linear regression revealed LVEF (A) = 0.95 LVEF (M) + 1.94, n = 97, r = 0.97, $p < 0.001$. Operator processing time was reduced from 30 to 2 minutes per patient study. These results demonstrate that multiple gated radionuclide angiograms can be batch processed without loss of precision and with significant reduction in computer-operator interaction time.

A NUCLEAR MEDICINE DATA PROCESSING SYSTEM EMPLOYING LARGE CAPACITY IMAGE MEMORY AND IMAGE HANDLING UNITS. K.Kume, K.Omura and M.Kiri. Shimadzu Corp., Kyoto, Japan.

A new data processing system has been developed for the high quality RI routine diagnosis that is destined to handle a huge amount of image file. In this system, 16 bits microcomputer and solid state image memory comparable to a magnetic disc and high speed image handling units are utilized. The outline of this system is as follows.

1) The memory unit which consists of 64 K bits/chip RAM is expandable to that of 12 bits 16 megawords, that means 256 frames of 256 x 256 image at its maximum.
It enables high speed data acquisition, such as 100 frames/sec.

2) The data in the image memory is accessed by the DMA unit in several modes as follows; in a mode, square part at designated addresses of X and Y in a frame is accessed, while in another mode, the pixels which have same address of X and Y of the time dependent data frames are transferred between the memory unit and the main memory of CPU.
The latter is suitable for the purpose to make histgram or functional map.
These two modes allow the discrete data file to be accessed with similar speed to that in sequential case.

3) Hardwear image processor for partial array is equipped in as one of the units.

4) An operation unit for arithmetic, logical, and floating point calculation between two images is also provided.

5) Image interpolator for expanding the size of image by interpolation from a 64 x 64 image to a 128 x 128 or 256 x 256 image is provided.
It enables high speed moving image display without buffer memory.

6) Final images are presented on a CRT display whose resolution is 256 x 256 pixels, with 64 gray levels or any combination of color scales.

PHYSICIAN-COMPUTER INTERACTIVE CLINICAL DECISION MAKING. D.D. Patton, M.J. Daly and J.M. Woolfenden. University of Arizona Health Sciences Center, Tucson, AZ.

A physician-computer interactive clinical decision making program (PCICDM) has been developed that finds over-

all utility for a given diagnostic strategy. Diagnostic decision making requires tradeoffs between false negative and false positive penalties. A decision strategy has utility to the extent that it leads the physician to the correct next action. In a test used to distinguish normals from abnormals, the overall utility U of a decision strategy=$\Sigma U(i) \times P(i)$, where U(i)=utility of each of the four possible outcomes TP, TN, FP, FN; and P(i)=probability of each outcome. Values of P(i) depend on the decision criterion line x_c and on the prior probability of disease P_o. Values of U(i) are subjective but can be ranked: -1=worst possible outcome, +1=best possible outcome, and 0=makes no difference. Overlapping Gaussian distributions describe normal and abnormal populations. A criterion x_c divides patients to be called "normal" from those who will be called "abnormal".

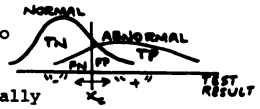

The utility function $U(x_c)$ usually passes through a maximum, and this value of x_c can be used by the physician to establish a personal diagnostic decision criterion. By varying U(i), P(i) and P_o, the physician gains insight into how the "best" criterion x_c might be selected, and into his own personal tradeoff preferences that lead to his selection of U(i) values. Rapid and easy to use, PCICDM requires no expertise in mathematics or computer technology, and uses only standard concepts except for U(i). PCICDM provides personal freedom for the physician to express his own tradeoff preferences. Examples of its clinical applications will be shown.

MUTUAL INFORMATION: AN INFORMATION MEASURE APPLIED TO MEDICAL DIAGNOSIS. D.F. Preston, L.T. Cook, S.J. Dwyer, III, R.G. Robinson, N.L. Martin. Univ. of Ks. Med. Ctr.

The application of the concepts of mutual information permit several valuable determinations to be made, two of which are: the value of a current diagnostic scheme, and resultant value of adding a new disease parameter to an established diagnostic scheme.

Consider liver diagnosis to fall into 3 groups, normal (X1) diffuse disease (X2) and focal disease (X3). If the apriori incidence of disease p(X1), p(X2), p(X3) is known, the information associated with (X1), the normal state is p(X1) x (Log (base 2) p(X1)). If the sensitivity and specificity of each clinical, laboratory and imaging technique is known, mutual information, I(X|Y), could be calculated where I(X|Y) = H(X) - H(X|Y). H(X) is the average amount of information associated with the 3 disease states $H(X)=-\Sigma(pi)$ Log (pi) and $H(X|Y)=-\Sigma\Sigma p(Xi,Yj)$ log p(Xi|Yj) is the average noise.

Disease State	p	SGOT	ALK PTASE	Size	Vascular Spiders	Diffuse	Mottled
N=X1	.5	.05	.05	.05	.1	.3	.05
D=X2	.1	.7	.1	.3	.5	.7	.1
N=X3	.4	.2	.8	.15	.2	.5	.8

Mutual information is calculated first with the first 4 parameters.

	I(X|Y) =	H(X)	- H(X|Y)
4 parameters	.663	1.361	.698
6 parameters	.894	1.361	.467

There is measurable diagnostic value of .231 bits due to the ability to differentiate between focal and mottled inhomogenieties in the liver Mutual information can be used to compare diagnostic systems.

FRIDAY, JUNE 27, 1980

8:30-10:00 Room 2043

CLINICAL

VENTRICULAR FUNCTION

Session Chairman: Salvador Treves
Session Co-Chairman: Thomas Verdon

PHASE ANALYSIS OF RADIONUCLIDE CARDIAC GATED STUDIES IN PATIENTS WITH NORMAL AND ABNORMAL ELECTRICAL ACTIVATION OF THE HEART. D. Pavel, S. Swiryn, E. Byrom, D. Witham, C. Meyer Pavel, K. Rosen. University of Illinois Medical Center, Chicago, IL.

Phase analysis was applied to cardiac gated studies in 17 patients (pts.) without organic heart disease. The procedure is based upon temporal Fourier analysis of 64 images representing a cardiac cycle. A qualitative and quantitative evaluation of phase differences within and between cardiac chambers was performed. Five pts had normal electrical activation (N), 6 had left bundle branch block (LB), 5 had Wolff-Parkinson-White Syndrome (WPW) and 1 had junctional rhythm with retrograde activation of the atria (JR). Patients with N had complete overlap of right and left ventricular phase resulting in a discrete histogram with a single peak. The widest FWHM found was 24°. Pts with LB had the FWHM>30° and a discrete phase histogram within each ventricle. However, left ventricular phase was late, resulting in two discrete peaks in 5/6 pts. The sixth patient did not have two well defined peaks but still had increased FWHM (45°). 4/5 pts with WPW had an area of early phase at the base of the pre-excited ventricle. This area was closer in phase to the atria than was seen in normal ventricles. In each patient the remainder of the pre-excited and the contralateral ventricle was comparable to pts with N. The pt. with JR had overlap of right ventricular and atrial phase, corresponding to nearly simultaneous QRS and P wave on electrocardiogram. Conclusion: Abnormalities of electrical activation are clearly reflected in the phase image. Quantification of these findings has the potential to provide a variety of useful pathophysiologic information.

HEMODYNAMIC EFFECTS OF SITE AND TIME OF INDUCED PREMATURE VENTRICULAR CONTRACTIONS. E.E. Camargo, M.H. Bourguignon, K.S. Harrison, P.R. Reid, R. Wise, W. Ehrlich, H.N. Wagner, Jr. The Johns Hopkins Medical Institutions, Baltimore, MD.

Premature ventricular contractions(PVC) were induced in open chest dogs at 3 different sites in the ventricular myocardium and 4 different times after the R wave. After intravenous injection of 15 mCi of Tc-99m HSA, a cardiac probe(Nuclear Stethoscope™) was positioned over the left ventricle(LV) and a beat-to-beat time-activity curve obtained together with measurement of LV and left atrial (LA) pressure, and aortic flow by electromagnetic flowmeter (Biotronex 610). A stimulator kept a constant heart rate of 500 ms/R-R(120 beats/min.). PVC were induced at 400, 430, 460 and 490 ms after the R wave. For each of these times, at least 5 PVC were obtained, with 9 normal beats between consecutive PVC. Only PVC induced in the right ventricular(RV) base resulted in forward ejection of blood, detected both by the probe and aortic flowmeter. Stimulation at the base or the apex of LV were found both by the probe and LA pressure transducer to result in regurgitant flow back through the mitral valve. Stroke volume(SV) of compensatory beats(CB) occurring immediately after the PVC measured both by the probe and flowmeter showed 2 types of response: (1) for RV stimulation, the forward flow decreased with increasing time of induction of the PVC after the R wave; (2) for LV stimulation, forward ejection fell and then rose with increasing time of induction of the PVC after the R wave. Thus, the cardiac probe permitted continuous monitoring of volume changes within the LV together with pressure changes and makes possible the measurement of the work of LV as a function of the site of origin and time of PVC and CB.

THE END SYSTOLIC P/V INDEX: A NEW PARAMETER FOR THE SCINTIGRAPHIC EVALUATION OF CORONARY ARTERY DISEASE. G.J. Dehmer,* J. Corbett,* L.D. Hillis, F.L. Datz, R.W. Parkey, J.T. Willerson, and S.E. Lewis,* Univ. of Texas Health Science Center, Dallas, TX.

Alterations in the end systolic pressure volume relationship reflect changes in the inotropic state of the left ventricle (LV). To determine the importance of this relationship in detecting the presence and severity of coronary artery disease (CAD), LV end systolic volume (ESV) and ejection fraction (EF) were determined with radionuclide ventriculography (RV) at rest and during peak supine bicycle exercise (PEx) in 13 normals (NL) and 33 patients (pts) with angiographically proven CAD. Cuff determined peak systolic blood pressure was divided by the ESV index yielding the P/V index. EF increased during PEx in NL (.72±.02, SEM to .82±.02, $p<.001$) and in pts with single vessel (SV) CAD (.68±.04 to .78±.02, $p<.02$) but decreased in those with 2 and 3 vessel (2/3V) CAD (.56±.03 to

.52±.03, p<.05). ESV decreased at PEx in NL (34±3 to 28±3, p<.01), did not change with SV CAD and increased with 2/3V CAD (86±12 to 102±12, p<.01). The P/V index increased at PEx in NL (7.6±.73 to 15.0±1.78, p<.05) but did not change in those with 2/3V CAD (4.2±.60 to 4.0±.50). The change in P/V index at PEx distinguished those with 2/3 V CAD. Combining a fall in EF, new wall motion abnormalities and an abnormal EKG response together the sensitivity of RV in detecting CAD was 0.44 with SV, 0.96 with 2/3V disease and 0.82 in all pts with CAD. The addition of the P/V index improved the sensitivity to 0.66 for SV, 1.0 for 2/3V and 0.91 for all pts with CAD. Thus, we conclude that the P/V index: 1) enhances the sensitivity of RV for the detection of significant CAD and 2) allows one to estimate the relative extent of angiographically important CAD.

EVALUATION OF LEFT VENTRICULAR FUNCTION IN ACUTE MYOCARDIAL INFARCTION USING RADIONUCLIDE VENTRICULOGRAPHY: RELATION OF REGIONAL WALL MOTION TO THE PARAMETERS OF GLOBAL LEFT VENTRICULAR FUNCTION. F. Ohsuzu, C.A.Boucher, M.D. Osbakken, J.B. Bingham, J.B. Newell, H.K. Gold, R.C. Leinbach, G.M. Pohost, and H.W. Strauss. Massachusetts General Hospital, Boston, MA.

Radionuclide ventriculography was performed in 127 patients (pts) within 18 hours of acute myocardial infarction (AMI). Infarct size was assessed by evaluating regional wall motion of 5 segments in both the anterior and LAO projections and by scoring each on a scale from 4=normal to 0=Dyskinesis. The sum of the 10 scores (SS) represented an overall index of wall motion (normal=40). Ejection Fraction (EF) was calculated using a variable region of interest counts method. LV end-diastolic volume (EDV) was calculated from the LV outlines in the anterior and LAO views, using the area-length method. LV end-systolic volume (ESV) was calculated from (1 -EF)xEDV. Systolic blood pressure (CSP) was recorded with a cuff during imaging and CSP/ESV calculated as a measure of LV contractile function. EF, ESV, and CSP/ESV correlated well with SS (r=0.83 P<0.00005, -0.69 P<0.00005 and 0.61 P<0.00005, respectively), but EDV correlated less well with SS (r=0.38, P<0.00005). Multiple linear regression analysis revealed that SS is not significantly dependent on CSP/ESV (contractility) directly, but is a function of EF; SS=8.879+36.0xEF. The correlation of EF and SS was significantly higher in normotensive pts than hypertensive patients (Fisher's Z=10.9 and 7.1 respectively). These data indicate that EF is the single most valuable indicator of the extent of damage in the early phase of AMI, especially in normotensive pts.

RADIONUCLIDE AND CONTRAST VENTRICULOGRAPHY IN THE DETECTION OF REGIONAL WALL MOTION ABNORMALITIES CAUSED BY KNOWN QUANTITIES OF ISCHEMIC MYOCARDIUM. M.L.Born, M.W.Kronenberg, C.W.Smith, L.Brorson, J.C.Collins, R.A.Steckley, G.C. Friesinger, F.D.Rollo. Vanderbilt University, Nuclear Medicine, Radiology, and Cardiology, Nashville, TN.

Radionuclide (RVG) and contrast (CVG) ventriculography have been used in the detection of regional myocardial ischemia. The utility of these tests depends not only on their sensitivity and specificity for regional myocardial dysfunction but also on the fundamental relationship between visible regional dysfunction and the quantity of ischemic myocardium. The purpose of this project is to compare the sensitivity and specificity (1.0-false positive fraction) of RVG and CVG for the detection of regional wall motion abnormalities caused by known quantities of ischemic myocardium. The relationship between sensitivity and false positive fraction is compared for different reciever operating characteristics (ROC). Fifty-two events in 14 closed chest dogs were evaluated by near-simultaneous RVG, CVG, and myocardial blood flow measurements (microsphere technique). The weight of ischemic (25% flow deprived) tissue ranged from 0.1 to 38 grams. Conclusion: At low false positive rates (less than 0.2) RVG and CVG are equivalent tests for ischemia with a sensitivity of .89 for ischemia greater than 4% of left ventricular weight (4 grams). The sensitivity for ischemia less than 4% myocardial weight is low, 0.33 for both tests.

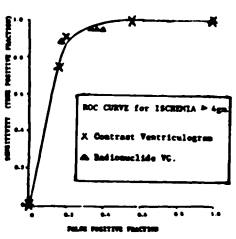

ADRIAMYCIN CARDIOTOXICITY: CORRELATION OF RADIONUCLIDE ANGIOGRAPHY AND PATHOLOGY
D.H. Feiglin, R.Y. Gulenchyn, P.R. McLaughlin, M. Druck, B. Bar-Shlomo, M.P. McEwen, J.E. Morch M. Silver, A. Gottlieb, W.K. Evans. Divisions of Nuclear Medicine, Cardiology, Oncology and Pathology, Toronto General Hospital.

Preliminary data of a prospective study of adriamycin (ADR) cardiotoxicity are reported in 15 patients (pts) who have received 144 to 954 mg/m^2 of ADR. 17 gated radionuclide angiograms (RNA) and endomyocardial biopsies (EMB) including 2 post mortem examinations were performed. Light and electron microscopic changes have been graded according to Billingham's classification.

Of the studies in these pts, 8 showed normal EMB and RNA, 2 showed abnormal EMB but normal RNA and in 7 both studies were abnormal. It is of interest that in one pt with early changes of ADR toxicity on EMB, abnormalities in left ventricular function were detected on exercise RNA when the rest RNA was normal. The minimum dose at which both EMB and RNA were abnormal was 206 mg/m^2; however, both studies have been normal at doses as high as 525 mg/m^2.

These data demonstrate a correlation between pathological and functional changes in the myocardium of pts receiving ADR. Although changes may occur at low doses in some pts careful serial followup with RNA may safely allow extension of effective ADR treatment.

REST AND EXERCISE RADIONUCLIDE VENTRICULOGRAPHY IN ADRIAMYCIN CARDIOTOXICITY: HISTOLOGICAL AND FUNCTIONAL CORRELATIONS. J.H. McKillop, M. Lopez, M.R. Bristow and M.L. Goris, Stanford University School of Medicine, Stanford, CA.

In 21 patients receiving adriamycin, rest and exercise ECG gated nuclide angiocardiography (EGNA) estimation of left ventricular ejection fraction was compared to endomyocardial biopsy and right heart catheterization, which is of value in predicting the risk of congestive cardiac failure (ccf) if given further adriamycin.

Rest EGNA correlated more closely with catheter than biopsy results but this relationship was less clearcut for rest and exercise EGNA, 8/11 patients with moderate or severe biopsy changes having abnormal studies irrespective of catheter findings.

When patients were classified as no, low or high risk of ccf from biopsy/catheter data, the following results were obtained:

	Frequency of Abnormal EGNA	
Risk of ccf	Rest	Rest/Exercise
No risk	3/12	2/11
Low risk	2/6	5/6
High risk	3/3	1/1

Patients with a normal rest/exercise EGNA have no or low risk of ccf and can receive more adriamycin. Abnormal rest and exercise EGNA may occur in some patients with no or low risk of ccf. Therefore, if there is a strong clinical indication for more adriamycin, an abnormal nuclide study should be followed by biopsy and catheterization to define the risk more precisely.

MINIATURIZED CdTe DETECTOR MODULE FOR CONTINUOUS MONITORING OF LEFT VENTRICULAR FUNCTION: PROTOTYPE SYSTEM DESIGN AND INITIAL CLINICAL DATA. H. Berger, P.B. Hoffer, J. Steidley, A. Gottschalk, B. Zaret. Yale University, New Haven, CT.

A miniaturized detector system which allows continuous assessment of left ventricular ejection fraction (LVEF) from the equilibrium cardiac blood pool has been developed. The module includes a cadmium telluride (CdTe) detector (active area 1.5 cm^2; active depth 2 mm) and a single hole straight

bore lead collimator. The unit is 3 cm in length, 3.5 cm in diameter, and weighs 175 grams. The relative efficiency of the detector for 140 keV photons is approximately 50%. The module is placed directly on the patient's (pt) chest in the 45° left anterior oblique position and is interfaced through a miniaturized preamplifier to a multichannel analyzer (MCA) operating in time-sequence mode. Channel intervals are 30 msec for the LV and 60 msec for background (BKG). An ECG R wave is used to trigger the MCA to recycle. After Tc-99m blood pool labeling (20 mCi), the module is first positioned over the LV and then at a BKG region lateral to LV. Following BKG-correction, a summed relative LV volume curve is obtained in 60 secs. LVEF measured with the module was compared to LVEF by multicrystal camera (first-pass) and NaI probe (gated) in 13 pts. By first-pass, LVEF averaged (±SEM) 54±4% (range, 29-70%) and was abnormal (<55%) in 5/13 pts. With the module, LVEF averaged 55±3% (pNS) and correlated well with both camera (r=0.79) and NaI probe (r=.81) data. End-diastolic counts/channel prior to BKG-correction were 32,095±3,402/min.

Thus, LVEF can be assessed rapidly with a miniaturized CdTe detector module affixed directly to the pts chest. This new approach allows continuous monitoring of LV performance in ambulatory and critically ill pts, expanding the application of radionuclide LV performance studies.

8:30-10:00 Room 3040

CLINICAL

GI III

Session Chairman: W. Klingensmith
Session Co-Chairman: Leon S. Malmud

Tc-99m HEPATIC BINDING PROTEIN (HBP) LIGAND LIVER IMAGING, R.C. Stadalnik, D.R. Vera, K.A. Krohn, University of California Davis Medical Center, Sacramento, CA

Various parameters are used in evaluating liver disease. Current radiopharmaceuticals utilize function of hepatic cells (85%), Kupffer cells (15%). Tc-99m sulfur colloid lacks specificity, fails to detect lesions, and often yields false positive or indeterminate results. Tc-99m hepatobiliary agents have short hepatocyte residence times, varying renal excretion, effected by elevated serum bilirubin.

HBP ligands are a family of compounds that bind to receptors found only on hepatocyte membrane. The common structural feature for these ligands is the presence of terminal galactosyl residues exposed upon treatment of plasma glycoprotein with desialylating enzyme neuraminidase, or chemical coupling of galactose to protein backbone. The former produces asialoglycoprotein; the latter galactosyl neoglycoalbumin (NGA). The molecular biology of HBP ligands is well characterized. After binding at hepatocyte membrane the HBP ligand complex is transferred to hepatic lysosomes for catabolism.

We have labeled asialoglycoproteins and NGA with Tc-99m. Uptake by HBP is a high affinity process which peaks at 10 minutes in normal rabbits. Biodynamic studies indicate that labeled metabolic products of Tc-99m-NGA are released by hepatocyte and rapidly removed from the circulation by the kidneys (urinary bladder activity is 15% ID at 30 minutes). No change in liver uptake kinetics or biodistribution were found in rabbits with an elevated serum bilirubin (7 mg%). There is also <0.1% ID total biliary excretion at 2 hours.

The potential application in man will be to visualize and quantitate hepatic cell function. Also, these agents should be useful in jaundiced patients, since the cellular physiology of HBP does not involve hepatic detoxification.

EVALUATION OF LIVER GRAFT HEMODYNAMICS. H.Creutzig Chr.Broelsch, R.Pichlmayr, H.Hundeshagen. Medizinische Hochschule Hannover, West Germany

After liver transplantation (Tx) graft hemodynamics have to be evaluated serially. We investigated the role of simple noninvasive isotope techniques in this evaluation. Liver blood flow was calculated from millimicrospheres clearance rates and compartment analysis, the relation of arterial to portalvenous flow (A/P) from a Pertechnetate first-pass study.

Blood flow (ml/min·kg BW) and A/P (%)

	Hepatic	Splenic	A/P
Normal (14)	27 ± 4.7	4.3 ± 2.9	28 ± 8
Cirrhotic (8)	9 ± 2.1	5.4 ± 2.3	58 ± 6
Prae Tx (6)	<5	6.3 ± 3.2	>80

The variation in LBF estimation was less than 12% in normals and 18% in cirrhotic patients, while 1/4 of normals and 1/2 of cirrhotic patient had a difference in A/P of more than 20% in two different investigations.

Six patients with a terminal cirrhosis received a graft. One week after Tx LBF doubled and A/P declines to 40-50%. In all five episodes of acute rejection and one delete chronic rejection confirmed histologically there was a dramatic fall in LBF to less than 4 ml/min·kg BW and an increase of A/P to near 100%, followed by a normalization after recovery. These noninvasive simple methods seem to be sufficient in the evaluation of liver graft hemodynamics.

A COMPARISON OF IN VIVO LABELED RED BLOOD CELLS WITH TC-SULFUR COLLOID IN THE DETECTION OF ACUTE GASTROINTESTINAL BLEEDING. R. Dann, A. Alavi, R. Baum, and S. Baum. University of Pennsylvania, Philadelphia, PA.

The sensitivity of the two agents was studied using a previously described animal model.

In 21 dogs studied with Tc-99m-sulfur colloid, bleeding sites were detectable at rates as low as 0.05-0.1 ml/min, with a total volume at the site of 0.6-1.2 ml. In 8 dogs studied with RBC's labeled in vivo with Tc-99m, a minimun of 30-60 ml was necessary to detect bleeding.

The sensitivity of the RBC's is therefore at least 50 times less than Tc-Sc, primarily because of the high background activity. Early images (5-10 minutes post injection) will fail to demonstrate bleeding with intravascular indicators unless the bleeding rate is 5-10 ml/min or more, whereas the site of bleeding is detected in this period at very low rates with Tc-SC. If the bleeding is detected only with later imaging, the site of extravasation may be misrepresented. Using Tc-SC we have noted patients bleeding from the hepatic flexure or transverse colon who would have been diagnosed as bleeding from the sigmoid colon had the imaging been delayed 10-15 minutes. Gastric activity from the in vivo labeling process will lead to false positive results, as will vascular lesions, such as varices, or structures with significant blood volume. Finally, the total time required to perform the study using RBC's is unreasonably long, as frequent scans may be required for as long as 24 hours.

The animal data reported here, as well as extensive clinical experience, suggest that Tc-SC is a superior agent to intravascular indicators in general, and in vivo labeled RBC's in particular, in the detection of GI bleeding.

SCINTIGRAPHIC DETECTION OF ACUTE GASTROINTESTINAL BLEEDING WITH Tc-99m LABELED HEAT-DAMAGED RED BLOOD CELLS (HDRBC). P. Som, Z.H. Oster, H.L. Atkins, D.F. Sacker, A.G. Goldman and P. Richards. Brookhaven National Laboratory, Upton, New York and SUNY at Stony Brook, New York.

Early detection of acute GI bleeding is of utmost importance to the clinician. Tc-99m sulphur colloid and Tc-99m Red Blood Cells have been successfully used for scintigraphic detection of acute GI bleeding. Neither of the agents are ideal due to high liver and spleen uptake with the former and high blood background with the latter agent. The purpose of this study was to evaluate Tc-99m-HDRBC for detection of acute GI bleeding, since damaged cells are quickly sequestered by the spleen only. Advantages are: 1) a somewhat slower blood clearance rate permitting a greater accumulation at the bleeding site, 2) better visualization of the right upper quadrant and 3) the possibility of using less radioactivity and thereby lowering the radiation dose.

Studies were carried out in dogs under pentobarbital anesthesia. One end of a catheter was inserted into the femoral artery, the other end was inserted into an infusion pump. Another catheter was led through the infusion pump to the small intestine. Autologous RBC were labeled using the BNL kit and heated for 10 min. at 49.5°C. The bleeding was initiated to prime the system, then 0.06 mCi/Kg Tc-99m-HDRBC was injected I.V. Sequential scintiphotos were taken with good visualization of the bleeding site. The slowest bleeding rate that could be detected (0.12 ml/min.) was comparable to the slowest rates detected with Tc-99m sulphur colloid.

It is concluded that Tc-99m-HDRBC can be used to detect acute GI bleeding with the advantage of significantly lower blood and liver background activity and smaller radiation dose.

LIVER/SPLEEN SCANS IN PATIENTS WITH ACUTE VIRAL HEPATITIS: PROGNOSTIC SIGNIFICANCE. A. Waxman, J. Rakela, and A. Redeker. Liver Unit, University of So. California, and Cedars-Sinai Medical Center, Los Angeles, CA.

The purpose of this study was to determine Tc-sulfur colloid scan characteristics in acute viral hepatitis, and to relate the scan findings to prognosis in patients with severe disease.

Sixty-three patients with acute viral hepatitis were studied; 41 patients with classic acute hepatitis (CH), 14 patients with fulminant hepatitis who survived (FH-S), and 9 patients with fatal fulminant hepatitis (FH-F).

Hepatic size (vertical measurement midway between the lateral border of the liver and midportion of the sternum) in CH was 17.22 cm ± 2.50 (mean ± SD). FH-S was 15.96 cm ± 2.33, and FH-F 12.28 cm ± 2.36. FH-F was statistically lower than FH-S and CH ($p<.001$). The spleen size in CH was 12.76 cm ± 2.32; FH-S 11.0 cm ± 3.46 and FH-F 9.49 cm ± 2.90.

The relative intensity of splenic uptake in the three groups did not show significant differences. However, the proportion of increased bone marrow uptake was higher among FH (57%) compared with CH (24%). In addition, 3 of 9 patients with FH-F showed increased pulmonary uptake, a finding which had not been previously reported.

We conclude that the colloid scan pattern in CH is either normal or demonstrates mild hepatomegaly. FH as a group showed a decrease in liver size proportional to the degree of severity of disease with a tendency toward mild increase in bone marrow activity. Despite massive necrosis evident at autopsy in FH-F, no gross hepatic filling defects were identified on scan. A small liver associated with a small spleen, increased marrow and/or lung uptake was uniformly associated with an unfavorable prognosis.

RIGHT/LEFT (R/L) LIVER LOBE RATIO: A SENSITIVE AND SPECIFIC CRITERION FOR CIRRHOSIS. D.P. Shreiner and M. Barlai-Kovach. VA Medical Center and University of Pittsburgh Medical School, Pittsburgh, PA.

Since scans of cirrhotic livers commonly show a reduction in size and colloid uptake of the R lobe, a quantitative measure of uptake of Tc-99m sulfur colloid was made using a mini-computer to determine total counts in regions of interest defined over R and L lobes, and comparing R/L ratios in 51 patients (pt) with and without liver disease. The mean R/L ratio for normal pt was 2.87 ± .64 (SD); and for pt with known cirrhosis was 1.11 ± .36 ($p<.0005$). The mean R/L ratio for known cirrhotic pt was also significantly different from that in chronic alcoholics and that in hepatomegaly unrelated to alcoholism ($p<.0005$ in each case). Chronic alcoholics without proven cirrhosis had a mean R/L ratio of 2.13 ± .59 ($p<.025$ compared with normals); but pt with nonalcoholic hepatomegaly and pt with hepatic metastases had R/L ratios not different from normal ($p>.20$). No false positive tests occurred in 28 nonalcoholic pt (specificity = 100%), and only 2 false negative tests occurred among 16 known cirrhotic pt (sensitivity = 87.5%). Of the alcoholics without proven cirrhosis, 20% had positive tests and probably had cirrhosis. The R/L ratio was more sensitive for cirrhosis than other criteria, e.g. early hepatic perfusion and splenomegaly; and more specific than extrahepatic colloid uptake, nonhomogeneity, hepatomegaly, liver-spleen ratios, or serum tests of hepatic dysfunction. The results show that pt with alcoholic cirrhosis have relatively less radiocolloid uptake in the R lobe than in the L lobe, and that the R/L ratio can be used as a sensitive and highly specific criterion for alcoholic cirrhosis.

BREATH ANALYSIS AFTER INTRAVENOUS ADMINISTRATION OF C-14-AMINOPYRINE IN LIVER DISEASE. S. Pauwels, A.P. Geubel, and C. Beckers. Dept. Nuclear Medicine & Gastroenterology, Univ. Louvain Medical School, Brussels, Belgium.

The determination of 14-CO_2 in breath after oral administration of C-14-aminopyrine has been proposed as a quantitative liver function test. In order to shorten the procedure and to avoid misinterpretations related to variable rates of intestinal absorption, the aminopyrine breath test (ABT) was performed after intravenous administration of 1.1 µCi of C-14-aminopyrine in 21 normal controls (NC), 33 alcoholic cirrhosis (AC), 15 untreated postnecrotic cirrhosis (PNC), 9 primary biliary cirrhosis (PBC), 12 non cirrhotic alcoholic liver disease (NCALD), 7 chronic persistent hepatitis (CPH), 3 untreated chronic active hepatitis (CAH), 10 miscellanous liver diseases (MISC). The specific activity of the first hr sample corrected for body weight and expressed as % of the injected C-14 (SA1) was the most accurate expression of breath data. In NC, SA1 was 0.86 ± 0.1 (SD) % and significantly reduced ($p < 0.001$) in all patients (0.5 ± 0.3), CAH (0.16 ± 0.13), AC (0.2 ± 0.15) and PNC (0.47 ± 0.17). Normal values were common in CPH (0.86 ± 0.13), NCALD (0.83 ± 0.27) and PBC (0.65 ± 0.19). The results obtained were reproducible and SA1 correlated with other conventional liver function tests, including 45 min BSP retention. ABT was the most sensitive screening test for the presence of cirrhosis and, in evaluating alcoholic patients, allowed a sharp distinction between cirrhotic and non-cirrhotic cases. In untreated chronic hepatitis, ABT provided a reliable index of the activity of the disease. Our data indicated that intravenous ABT, performed over a 1 hr period, is a fast, sensitive and quantitative liver function test.

IN VIVO QUANTITATION OF HEPATIC STEATOSIS WITH XENON-133. F.D. Thomas, S.A. Blumenthal and A. Singh. Upstate Medical Center, Syracuse, NY.

We have correlated hepatic Xenon-133 uptake and washout time with concurrent biopsy measurements of liver fat content. In 26 studies, a 4-minute equilibration period with Xenon-133 followed by a 10-minute washout was recorded in 15-second frames on a Gamma-11 computer system. Both uptake amplitude and washout time were estimated: Uptake was expressed as the ratio of maximum xenon liver counts to soft tissue background; washout was expressed as the time required for liver counts to reach background activity. The patients studied had intra-operative liver biopsies during gastric or intestinal bypass surgery for morbid obesity and post-operative needle biopsies at 6-month intervals. % fat and triglyceride assays were done on these biopsy specimens.

Linear correlation analysis of log transformed xenon data showed good correlation with % fat: Xenon uptake vs % fat, $r = .663$, $p < .001$; xenon washout time vs % fat, $r = .916$, $p < .001$. Xenon washout time also correlated well with triglyceride assays ($r = .826$, $p < .001$). While other clinical studies have shown reasonably good qualitative correlation between liver fat and xenon uptake, we have found an excellent quantitative prediction of liver fat from this non-invasive procedure. The washout time appears to have less variability than uptake measurements.

NEW QUANTITATIVE TESTS FOR MEASURING CONCENTRATION AND CONTRACTION FUNCTIONS OF THE HUMAN GALLBLADDER FOLLOWING INJECTION OF Tc-99m-HIDA. G. T. Krishnamurthy, V. R. Bobba, & E. Kingston. VA Medical Center & UOHSC, Portland, OR.

The primary function of the gallbladder (GB) is to store and concentrate bile during fasting hour and contract and discharge into duodenum upon feeding or injection of cholecystokinin (OP-CCK). The present investigation was under-

taken to measure these two functions as they occur in 12 normal subjects. After an overnight fast, each subject was given 5 mCi of Tc-99m-HIDA intravenously. Ninety min. later the subject was positioned supine under a gamma camera fitted with a 5mm pinhole collimator and the detector was centered over GB. The GB images were obtained at 2 min. intervals for 90 min. and the data were simultaneously acquired on 64x64 computer matrix at 1 frame/min. At 60 min. 40 ng/kg of OP-CCK was infused over 3 min. period.

Two regions of interest, 1 over the GB and the other over the liver (Bkg) were chosen with a light pen. The counts were normalized to 100 pixels and decay corrected using Tc-99m decay factor. The net GB counts were obtained by subtracting Bkg. counts. The first 60 min. data were smoothed (5 points). The 0-1 min. counts were considered to represent total GB counts. The GB showed isovolumic reduction in counts indicating diffusion. The diffusion index was calculated using 59-60 min. counts. The data obtained after OP-CCK were used to calculate the ejection fraction (EF). The mean diffusion index was 16% hr. and the mean EF 32%.

It is concluded that the concentration and contraction functions of the GB can be measured quantitatively & that this new technique may aid in our understanding of the role of GB in the pathogenesis of cholelithiasis.

8:30-10:00 Room 3039

RADIOPHARMACEUTICAL CHEMISTRY

POTPOURRI

Session Chairman: William Eckelman
Session Co-Chairman: Donald M. Wieland

RADIOIODINATED PHOSPHONIC ACID: A NEW AGENT FOR THE STUDY OF BONE RESORPTION. F.P. Castronovo, Jr., H.W. Strauss and K.A. McKusick. Massachusetts General Hospital, Boston, MA.

This investigation was undertaken to develop a skeletal seeking radiopharmaceutical for the study of bone resorption. A phosphonic acid derivative containing a phenyl group[phosphonic acid (phenyl-methylene hydroxy) bis] was synthesized according to the method of Henkel and Cie.After labeling with I-125, studies of whole body retention (n=16 mice) was measured from immediately after injection to 100 days and expressed as % retained dose as a function of time:

COMPONENT	%	$T_{\frac{1}{2}b}$	λ day^{-1}
First	66.5	0.2d	3.465
Second	5.5	9.0d	0.077
Third	33.0	962d	0.00075

The tissue distribution studies (mice, n=9) showed that less than 2% of the dose was in the blood at 1 hour and from 5 days to 100 days, the biological distribution remained essentially unchanged. At 14 days, 44% of the dose was localized in the skeleton and 33% remained in the bone at the termination of the study (100 days). Whole body images in the rat were recorded up to 80 days post administration which demonstrated tracer in the skeleton only.

Eighty days post I-125 tracer administration, a bone fracture was induced. A zone of decreased radioactivity was observed after 48 hours. A concomitant T-99m MDP study showed increased bone metabolism at this site.

These data suggest that I-125 labeled phenyl phosphonic acid can be used to measure chronic bone resorption, and with a concomitant Tc-99m diphosphonate study, acute new bone formation.

EFFECT OF STORAGE ON FIBRINOGEN. S.J. DeNardo, A-L. Jansholt, G.L. DeNardo, K.A. Krohn, K.M. Crawford. Department of Nuclear Medicine, University of California, Davis, CA. (Supported by American Cancer Society Grant PDT-94A)

We have used fibrinogen routinely for clinical studies for 6 years. Purified fibrinogen from 2 donors meets clinical requirements for a year, and the effect of storage has not been previously well evaluated. Fibrinogen (Blömbeck I-2 fraction), purified by conventional methods, was stored as lyophilized powder (LP) and frozen solution (FS) at -70°C. Aliquots of each before and after radioiodination with ICl were tested initially and at 3, 6, 12 and 22 months using isotopic (IC) and spectrophotometric clotability (SC), Sepharose 4B column chromatography, acrylamide gel electrophoresis and blood clearance in patients. Clottability of both storage forms were similar. SC of unlabeled lyophilized (ULP) and frozen (UFS) and IC of labeled lyophilized (LLP) and frozen (LFS) fibrinogen were >90%, but decreased to 85% by 12 mos. IC of LLP and LFS fibrinogen (after Sephadex G-25 chromatography) decreased to 76% by 22 mos. On column chromatography, the Kav and peak contours were similar for ULP, UFS, LLP and LFS through the entire study with Kav approximately 0.48. However, by 22 mos UFS had a shoulder at Kav of 0.65 to 0.8, which was 20% of the total fibrinogen peak. Acrylamide gel electrophoresis demonstrated no changes up to 12 mos. There was no discernible difference in the $T_{\frac{1}{2}}$ of the catabolic phases of the catabolic phases of ULP, UFS, LLP and LFS.

In summary, purified fibrinogen can be stored lyophilized or frozen for at least 6 mos without discernible changes. Subsequent changes in LP are minor, whereas FS develops definite chemical alterations by 22 mos. Either storage form is probably usable in clinical studies for 12 mos and LP for 22 mos after preparation.

ON THE MECHANISM OF ALANINE LOCALIZATION IN THE HEART AND PANCREAS. P.V. Harper, J. Wu, K.A. Lathrop, T. Wickland, and A. Moossa. The University of Chicago, Chicago, IL.

The localization of N-13 in the myocardium and pancreas following injection of N-13 labeled L-alanine has been convincingly demonstrated in human subjects. We have investigated the use of a C-11 label to overcome the difficulties due to the shorter half-life of N-13. C-11-DL-alanine was prepared using a modified one-step Strecker synthesis reacting acetaldehyde with C-11-labeled cyanide and ammonium carbonate in the presence of an excess of ammonium hydroxide. Condensation followed by hydrolysis occurred in a Parr bomb at 255°C in a 13-min run. The alanine was purified on a Rexyn 101 column in acetate buffer at pH 4 with a 35% chemical yield in a total time of 35 min in a volume of 6 ml. Results of chromatography and NMR spectroscopy of the product matched those of authentic alanine. Localization studies in mice appeared rather similar to those of DL-tryptophan. However, human studies showed virtually no localization in the heart or pancreas and substantial decarboxylation was evidenced by exhalation of C-11-carbon dioxide. These findings suggest that the persistent localization described for N-13 alanine in the human really represents only that of the N-13 label. Since the carboxyl C-11 label does not appear to localize in a similar manner, this suggests that alanine loses its amino group to some other molecule rather than the alanine being incorporated as such. The carbon chain of the alanine is presumably converted to lactate or pyruvate and rapidly metabolized as indicated by the conversion to C-11-carbon dioxide. Since localization occurs in the mouse pancreas, the failure of extrapolation of animal data to humans is again illustrated.

LIPOPROTEINS AS CARRIERS FOR RADIOPHARMACEUTICALS. R.E. Counsell, L.W. Schappa, N. Korn, and R.C. Pohland. Department of Pharmacology, The University of Michigan Medical School, Ann Arbor, Mi.

The covalent linkage of radionuclides to carrier molecules has been a successful strategy in radiopharmaceutical design. More recently, the non-covalent incorporation of radiopharmaceuticals into liposomes has introduced another approach for the achievement of target organ specificity. As an extension of this concept, studies were undertaken to examine the potential of lipoprotein complexes as a carriers system for radiopharmaceuticals. Lipoproteins differ from liposomes by having a hydrophobic rather than a hydrophilic central core. 125-I-19-Iodocholesterol (125-IC) was incorporated into the matrix of rat high density lipoportein (125-IC-HDL). Except for much less radioactivity appearing in the thyroid following administration of 125-IC-

HDL, there was little difference between the tissue distribution profiles of these agents in normal rats. However, depletion of the circulating lipoprotein levels by prior treatment with 4-aminopyrazolo-(3,4d)-pyrimidine (4-APP) caused over a fourfold increase in adrenal cortex radioactivity following 125-IC-HDL administration over that observed for 125-IC. This finding is compatable with the current view that the rat adrenal contains specific receptors for HDL. The incorporation of other hydrophobic radiopharmaceuticals into lipoproteins is now under investigation.

TRANSPLANTATION OF MOUSE THYROID IN SYNTHETIC POUCHES: A NEW TECHNIQUE. H. J. Dworkin and S. J. Long. Department of Nuclear Medicine, William Beaumont Hospital, Royal Oak MI.

Currently available information is insufficient to decide whether the development of hypothyroidism following radiation of the thyroid is due principally to vascular damage or impairment of stem cell regeneration. A transplantation (TPX) technique has thus been devised which permits the radiation of thyroid tissue independent of its original vascular supply. Isogenic mouse thyroid TPX was carried out in which the donor thyroid is transplanted into a synthetic pouch, and then implanted in various sites in hypothyroid recipient mice. It is possible to achieve quantitative recovery of the transplanted tissue for cell counting studies. Neo-natal BDF-1 mouse thyroid glands were placed in one of two types of synthetic pouches (millipore or Unipore filter membranes) transplanted under the kidney capsule, in the spleen, I.P., or subcutaneously in hypothyroid, BDF-1 recipients, and allowed to remain for two to four weeks. Histological examination and radioiodine uptake values demonstrated the success of the pouch technique in maintaining functional thyroid tissue showing neo-vascularization, with best results obtained when the pouch transplant was placed under the kidney capsule of the recipient. Uptakes 12 hrs. post-I-131 dose I.P. in pouches with histologically identified thyroid tissue (N = 11) was 1 to 20.9% compared to normal thyroid in situ (N = 24) of 1.3 - 9.3%.

Establishment of this model now permits radiation exposure of mouse thyroid tissue in such pouches to be carried out at various dose levels to examine radiation effects on stem cells free of original vascularity.

DETERMINATION OF MICROGRAM AMOUNTS OF STANNOUS TIN IN TECHNETIUM LABELING KITS.* G.E. Meinken, S.C. Srivastava, and P. Richards, Brookhaven National Laboratory, Upton, NY.

Reliable performance of Tc-labeling kits, most of which contain submilligram amounts of tin as the reducing agent, depends a great deal on the presence of unoxidized Sn(II) in the proper chemical form at the time of addition of $99mTcO_4^-$. A simple method for determining Sn(II) in these kits is highly desirable but not available at the present time. In this study two methods were developed for the micro determination of Sn(II) in the presence of various media of radiopharmaceutical interest: (i)potentiometric titration with iodate in 1N HCl; and (ii)spectrophotometric determination using the Mo-Blue reaction. The titration procedure can be used down to 50 µg Sn(II) in 10 ml, and the spectrophotometric method gives reliable results with as little as 2 µg Sn(II) per ml. Standard Sn(II) solutions were prepared by dissolving 99.999% pure tin wire in conc HCl in an inert atmosphere and diluting with water. Aliquots were titrated with standard Ce(IV). Multiple such determinations indicated 3-6% less Sn(II) than expected based on the weight of the Sn wire. The Sn(II) in acid was added to a stirred solution containing excess citrate and the pH kept to 7 with base. Aliquots of Sn(II) citrate stock solution, in 1N HCl, were titrated in an inert atmosphere with 10^{-4} N iodate at 70°C to a potentiometric end point using a platinum electrode. For the spectrophotometric method, to Sn(II) samples (4-25 µg), 4 ml of the phosphomolybdate reagent were added. The color was extracted with amyl alcohol, and the absorbance measured at 725 nm. The unknowns were treated similarly and the Sn(II) concentration was read from the standard calibration curve. The two methods give precise results and show substantial promise for application to microdetermination of Sn(II) in many currently used Tc-labeling kits.

*Work done under FDA-IAG #224-79-3002 (FDA and DOF).

A STABLE STOCK SOLUTION OF STANNOUS CHLORIDE. B.H. Mock. Indiana University Medical Center, Indianapolis, IN.

Stannous ion is the most commonly used reducing agent for Tc-99m radiopharmaceuticals, however, great care must be taken to minimize the oxidation and/or formation of insoluble hydroxides. Accordingly, most kits are freeze-dried and packaged under nitrogen. This paper reports a simple in-house stock solution of stannous chloride which is easily prepared, has a shelf-life of several months, and is routinely used to prepare Tc-99m RBC's in vitro at labeling efficiencies in excess of 96%. $SnCl_2 \cdot 2H_2O$ is dissolved in 4N HCl, diluted with 3 volumes water, millipored to remove any insoluble tin hydroxides, bubbled with nitrogen gas for 5 min., and autoclaved in a rubber stoppered serum vial. The final sterile solution contains 10 mg tin per ml of 1N HCl. Sn++ concentration is determined by titration with standardized 1mN Iodine using starch T.S.

Long-term stability is affected by the initial tin concentration and the HCl normality. At tin levels less than 5 mg/ml, oxidation was significant even in 4N HCl. At N/2 HCl or less, a yellowish precipitate formed in a few days even at tin levels of 40 mg/ml. Nitrogen bubbling was found unexpectedly to increase the Sn++ concentration by 13% over the first 20 days, whereas the non-bubbled solutions declined by 6%. Over the next 2 weeks, the Sn++ level of both solutions declined by only 0.9-1.2%. A nominal 10 µg of Sn++ ion is easily obtained for labeling RBC's by adding 0.1 ml of the stock solution to a 10 ml vial of saline. If used within 30 minutes, this dilute solution contains 10 µg Sn++ ion in 0.1 ml of 0.01N HCl in saline. Such concentration and acidity does not appear to damage the RBC's when added to 4 ml of heparinized whole blood.

WHOLE BODY AUTORADIOGRAPHY: A PROCEDURE FOR EVALUATION OF RADIOPHARMACEUTICALS. N. Venkatesh, T.F. Budinger, and C-T. Peng. Donner Laboratory and Lawrence Berkeley Laboratory, University of California, Berkeley, CA.

The technique of whole body autoradiography is becoming recognized as an important tool for studying the distribution of drugs. Adaptation of this Ullberg technique has been made to facilitate the selection of new radiopharmaceuticals for single photon and positron annihilation photon imaging studies. The technique involves the use of a large microtome equipped with knives 9 cm or more wide, located in a large top-entry freezer maintained at -20°C. Animals as large as 300 gm rats or individual organs of large animals (e.g., monkey brain) are rapidly frozen in acetone-dry ice (-70°C), and embedded in a 10% solution of carboxymethyl cellulose in a metal mold. The block container with the embedded animal is frozen and while frozen the block is cut into halves. The cut block is mounted on the microtome stage for sectioning and 20 µm sections are picked up by a wide Scotch tape during microtome cutting. Radioactive debris is controlled by suction cleansing in the freezer. After freeze-drying, the section is laid on photographic film. Using an injected dose of 50 µCi of C-14 and Kodak X-Omat film, exposure for 24 to 48 hrs is adequate. Quantitation is done by densitometry or grain counting.

The power of this technique of in vitro tomography is exemplified by studies in rats of the distribution of C-14-β-taurine and H-3 taurine (longer exposure on special film). Remarkably high tissue concentrations were found in the heart, kidneys and gut.

Whole body autoradiography is a flexible method whereby new radiopharmaceuticals can be quantitatively studied for biodistribution with high spatial resolution as well as for kinetics.

8:30-10:00 Room 2048

RADIOPHARMACEUTICAL CHEMISTRY

INORGANIC

Session Chairman: Edward Deutsch
Session Co-Chairman: Charles Russell

AMINO ACID COMPLEXES OF RUTHENIUM-103: SYNTHESIS AND BIODISTRIBUTION. C.D. Meyer, and M.A. Davis. Department of Radiology, Joint Program in Nuclear Medicine, Harvard Medical School and Department of Medicinal Chemistry and Pharmacology, Northeastern University, Boston, MA 02115.

To develop a Ru-97 pancreatic imaging agent, ammineruthenium(III) complexes of carbon and nitrogen-bound L-histidine, β-(4-pyridyl)-α-alanine, and S-β-(4-pyridylethyl)-L-cysteine were synthesized in low specific activity from [Ru-103]chloropentaammineruthenium(III) dichloride by appropriate modification of literature procedures. The identity of the Ru-103 labeled complexes was verified by comparison of ir and uv spectra with cold Ru samples having satisfactory elemental analyses. The biologic distribution of each complex was then determined in normal mice following tail vein injection of acidified saline solutions. All four complexes were rapidly cleared through the kidney with 50% of the injected dose concentrated in the urine within fifteen minutes. Minor differences in distribution were found in lung, heart, spleen, stomach, intestine, bone and soft tissue. None of the complexes accumulated in any major organ, but the 4-pyridylalanine complex exhibited a steadily increasing pancreas to liver concentration ratio during the first hour, reaching a maximum of 17.0. This is considerably higher than commonly reported values of about 2.5 for [Se-75]-selenomethionine, making this agent a promising candidate for further evaluation as a radiopharmaceutical for pancreatic imaging. Rapid blood and urinary clearance in conjunction with low uptake by normal tissue also indicate all four complexes are potentially useful as disease specific radiotracers when labeled with cyclotron-produced Ru-97.

RUTHENIUM-97-DMSA FOR DELAYED RENAL IMAGING. Z.H. Oster, P. Som, M.C. Gil, A.G. Goldman, D.F. Sacker, H.L. Atkins, and P. Richards. Brookhaven National Laboratory, Upton, New York and SUNY at Stony Brook, New York.

Scintigraphic visualization of the decompensated kidneys requires delayed imaging which is difficult to accomplish with Tc-99m-DMSA because of its short physical half-life. Ru-97, a pure gamma emitter with a $T_{\frac{1}{2}}$ of 69.6 hrs and a photon energy of 216 keV is suitable for delayed imaging. The goal of this study was to label DMSA with Ru-97 and evaluate the biological differences of some compounds in the experimental animals.

DMSA is mixed with SnCl2, dissolved in 0.2N sodium hydroxide and Ru-97 is added. For tin-free preparations the same procedure is followed except the addition of SnCl2. The mixture is incubated in boiling water for ½ hr and after cooling the pH is adjusted to 6.5.

The ratio of DMSA/Sn+2 = 1.85 was found to give the highest concentration of Ru-97-DMSA in the kidneys as well as the optimal ratios for imaging. When no tin is added the concentration in the kidneys and blood is lower because of higher urinary excretion. In the animal with normal functioning kidneys the delayed excretion is advantageous but in renal insufficiency this factor may not be important since the clearance may be slower because of the pathological process. Good quality images of the kidneys were obtained in normal dogs and studies are in progress to evaluate these agents in different models of kidney pathology. We conclude that Ru-97-DMSA could facilitate delayed imaging of the kidneys.

RU-97-DTPA: A NEW RADIOPHARMACEUTICAL FOR CISTERNOGRAPHY. Z.H. Oster, P. Som, R.G. Fairchild, A.G. Goldman, M.C. Gil, H.L. Atkins, D.F. Sacker, E.R. Schachner, G.E. Meinken, S. C. Srivastava and P. Richards. Brookhaven National Laboratory, Upton, New York, and SUNY at Stony Brook, New York.

Ru-97-DTPA was evaluated for its possible use as a cerebrospinal fluid imaging agent. Ru-97 has favorable physical properties (decay by electron capture; γ energy = 216 keV, 86%; $T_{\frac{1}{2}}$ = 2.9 d) which are very suitable for imaging. Ru-97-DTPA was prepared by dissolving 9 mg of DTPA in 2 ml of 0.2N NaOH, and adding Ru-97. The pH was adjusted to 3.5 and the solution was heated in a boiling water bath for ½ hr. It was then cooled and pH adjusted to 6.5. Dogs were injected with 0.3 mCi Ru-97-DTPA or In-111-DTPA into the cisterna magna. The movement of the agents was monitored with a camera interfaced to a computer or with a dual-probe system placed over the head and bladder. In addition, blood and urine samples were collected at fixed intervals for 6 hours. At 24 hrs after Ru-97 administration, scintiphotos of the head, kidneys, and bladder were obtained and the animals sacrificed. Residual Ru-97 activity in the brain, gonads, liver, spleen, kidneys, bladder and CSF was determined. The results show that the kinetics and excretion of this compound are similar to In-111-DTPA. Intracisternaly injected Ru-97-DTPA peaked in blood at 5-7 min. and the clearance showed two components ($T_{\frac{1}{2}}$ = 14 min; $T_{\frac{1}{2}}$ = 17 hrs.). Urinary excretion was 18% at 3 hrs. and 30% by 6 hrs. High quality images were obtained both immediately and 24 hrs. after injection. We calculated that the radiation dose for identical activities was twice as high for In-111 because of the low energy electrons emitted. We conclude that Ru-97-DTPA can be used for studies of CSF dynamics with the advantage of a lower radiation dose.

RUTHENIUM LABELED TRANSFERRIN--A POTENTIAL TUMOR-LOCALIZING AGENT.* S.C. Srivastava, G.E. Meinken, P. Richards, Brookhaven National Laboratory, Upton, NY; S.M. Larson, Z. Grunbaum, and J.S. Rasey, VA Hospital, Seattle, WA.

The excellent properties of 2.9d Ru-97 (216 Kev ν, 86%), the chemical reactivity of Ru, the antitumor activity of several Ru coordination compounds, and the BLIP production of Ru-97, provide a unique combination for the application of this isotope in nuclear oncology. Tumor uptake of transferrin (TF) labeled with ruthenium in the EMT-6 sarcoma in BALB/c mice and other animal tumor models has been investigated in the present study. TF was labeled with Ru-103 or Ru-97 as follows. To purified TF in 0.1 M sodium acetate was added the desired amount of Ru activity and the pH adjusted to 7. The mixture was heated at 40°C for 2 hr, and passed over a Sephadex column to separate pure monomeric Ru-TF in ~65% yield. In the EMT-6 sarcoma mice, tumor uptake (% dose per g; 24 hr after i.v. injection) of Ru-103 chloride (5.25) was comparable to that of Ga-67 citrate (7.09); the uptake of Ru-103-TF (12.75) was almost twice as high. Tumor(T) to blood(B), muscle(M), liver(L), and kidney (K) ratios were high enough for imaging at 24-72 hr. At 72 hr, the ratios were as follows: Ru-103-TF: T/B,5.0; T/M,11.8; T/L,2.0; T/K,2.0. Ga-67 citrate: T/B,10.7; T/M,10.8; T/L, 0.6; T/K,0.6. The tumor concentration index (TCI) defined as the ratio of % dose per g in tumor to % dose per g remaining in the whole body at 72 hr for Ru-TF was 4.48 (1.57 for Ga citrate). Preliminary data in several animal tumor models have shown similar results. Efforts to further reduce the blood and normal tissue background of Ru-TF by (i) chemical modification, (ii) administration of chelating agents, and (iii) using computer subtraction techniques are being evaluated. It is concluded that Ru-97-TF is a potential tumor localizing agent that would result in improved diagnostic performance with high information content and reduced patient radiation dose when compared to Ga-67 citrate and other agents presently in use.

*Work done under Contract EY-76-C-02-0016 U.S.D.O.E.

TROPOLONE: A LIPID SOLUBILIZING AGENT FOR CATIONIC METALS. L.R. Hendershott, R.C. Gatson, J.W. Fletcher, and R.M. Donati. VA Medical Center and St. Louis University, St. Louis, MO.

Lipid soluble agents which will chelate radioactive cations have several potential uses in nuclear medicine. These include uses such as brain scanning agents, labeling of blood elements and identifying fatty infiltration of organs (i.e., liver). A tropolone-gallium complex has been characterized by in vitro partition coefficients correlated with in vivo rat distribution studies. Partition coefficients were determined for gallium (Ga-67 citrate), indium (In-114m chloride) and iron (Fe-59 chloride) cations complexed with tropolone in chloroform/water, octanol/water and olive oil/water two phase systems. Tropolone proved to be highly effective in the lipid solubilization of these metal cations. Biodistribution studies of the Ga-67, In-114 and Fe-59 complexed with tropolone demonstrated an alteration of biodistribution when compared to appropriate controls. Tropolone effects biodistribution of Ga-67 by moving this cation into rat tissues containing a high lipid content when compared to the appropriate control (i.e., Ga-67 citrate) at 30 minutes after intravenous injection. The red blood cells of the rats receiving the Ga-67 tro-

polone complex contain 36% of the whole blood activity as compared to 6% for the Ga-67 control. Thus, tropolone appears to form stable complexes with Ga-67, In-114m and Fe-59 in the presence of transferrin in plasma to provide lipid solubility for these radioactive cationic metals.

RADIOPHARMACOKINETICS, A METHOD FOR NUCLEAR MEDICINE TO MEASURE NON-INVASIVELY THE ORGAN PHARMACOKINETICS OF DRUGS. W. Wolf and R.C. Manaka. Radiopharmacy Program, University of Southern California, Los Angeles, CA.

The use of the radioisomer of a drug, chemically and biologically identical to the parent molecule, allows for the non-invasive measure of drug distribution and kinetics at any organ or tissue site. We have developed methods to accomplish such studies and wish to document the methodology and scope of this novel technique with a specific example.

The distribution of Cisplatin, labeled with Pt-195m(Wolf and Manaka, J Clin Hemat Oncol 7, 79(1977)) was determined in control rats; a seven state, single input, five output, linear, time invariant, closed model was formulated using computational programs based on system/identification theory. Four of the five outputs can be readily measured non-invasively in man (whole body, blood, kidney and bladder content + urine), with one output necessitating serial sampling. This seven state model was predictive in rats; i.e. the IV bolus data predicted accurately the blood and organ levels of the drug following various infusion regimens. Moreover, this model based on rat data was predictive of blood levels of Cisplatin in patients. These results suggest that we might predict in a given patient the kinetics of the toxic species (probably free Cisplatin, Cole and Wolf, work in progress) in the kidney, the critical organ. Such information might provide us with the necessary input to develop strategies on how to control the desired toxic or therapeutic levels of the drug at a given organ or tissue site.

Inasmuch as radiopharmacokinetic methods are applicable to the study of most any drug, they might allow us the prediction of the availability of the drug or its active metabolite at a given organ site in a given patient for any dose regimen, and thereby assist in optimization of chemotherapy.

CHELATES OF RADIOMANGANESE TO ASSESS KIDNEY FUNCTION. R.W. Atcher, A.M. Friedman, G.V.S. Rayudu, D.A. Turner, and J.R. Huizenga. Argonne National Laboratory, Argonne, IL, Rush University Medical Center, Chicago, IL, and University of Rochester, Rochester, NY.

Manganese-52m is a positron emitter with a short physical half life, 21.1 minutes, that is produced in a generator system from Fe-52. Carrier-free manganous chloride concentrates in organs of high metabolic activity, especially in the kidney, enabling one to assess perfusion. There is little redistribution in the first few hours after i.v. administration and the major excretory route is through the intestines. Thus it would be advantageous to use Mn-52m to assess kidney function since the physical half life is on the order of the biological half time of excretion through the kidneys. Three chelates were used to bind the manganese to increase kidney excretion: sodium ethylenediaminetetraacetate (EDTA), calcium sodium diethylenetriaminepentaacetate (DTPA) and sodium cyclohexylenedinitriloacetate (CDTA). The biodistribution curves show similar shape peaking at approximately 10 minutes in the kidney. Three mice were injected for each data point at 5, 10, 20 and 30 minutes. The maximum dose percent per gram of tissue for the kidneys is: EDTA -- 20 percent; DTPA -- 32 percent; and CDTA -- 42 percent. The stability of the complex is directly proportional to the excretion through the kidneys. The increasing stability of the chelate-metal complex can be explained by the increasing steric hindrance in the progressively larger molecule.

TIN-117m-LABELED 23-(TRIMETHYLSTANNA)-24-NOR-5α-CHOLAN-3β-OL (*Sn-23-TSC) SHOWS SIGNIFICANT ADRENAL UPTAKE IN RATS. F. F. Knapp, Jr., T. A. Butler, A. P. Callahan and K. R. Ambrose. Nuclear Medicine Technology Group, Oak Ridge National Laboratory (ORNL), Oak Ridge, TN.

The attractive properties of *Sn (159 keV γ in 86% abundance; 14 day physical half-life) have prompted us to explore the synthesis of *Sn-labeled tissue-specific agents. In a model synthesis, 23-TSC was prepared in 49% yield by reaction of Me_3Sn-Li with 3β-acetoxy-23-bromo-24-nor-5α-cholane (23-Br-ANC) at 27°C in THF. The IR, MS and NMR properties of 23-TSC were consistent with the proposed structure. *Sn-labeled 23-TSC was synthesized as follows from reactor produced *Sn: *Sn → *$SnCl_4$ + Me_4Sn → Me_3*Sn-Cl + Li → Me_3*Sn-Li + 23-Br-ANC → *Sn-23-TSC. Tissue distribution studies indicated pronounced adrenal uptake of *Sn-23-TSC in female Fisher rats.

Days after injection	Range of three animals - % dose/gm			
	Adrenals	Liver	Blood	Ovaries
1	37.1-53.5	4.7-5.7	1.3-1.5	11.9-21.7
3	45.8-59.5	1.8-2.5	0.8-0.8	10.2-11.7
7	17.5-21.3	0.3-0.6	0.2-0.3	3.8-6.7
14	21.4-22.8	0.5-0.6	0.2-0.3	4.7-7.1

Approximately 50% of the injected activity was excreted within 5 days, primarily in the feces. These data indicate that *Sn-23-TSC may represent an attractive new agent for adrenal visualization in humans.

ORNL is operated by Union Carbide Corporation under contract W-7405-eng-26 with the U.S. Department of Energy.

SIGNIFICANT ALTERATION OF THE BIODISTRIBUTION OF PERTECHNETATE WITH A CLEARING AGENT. W.A. Pettit, R.M. Beihn, and F.H. DeLand. Veterans Administration and University of Kentucky Medical Centers, Lexington, KY.

The biodistribution of $^{99m}TcO_4^-$ has been significantly altered in rats following the intravenous administration of a nonradioactive agent, stannous tartrate. The femoral veins of rats were canulated to permit the administration of $^{99m}TcO_4^-$, followed by the clearing agent at preselected times that ranged from 5-20 min. Whole body distribution data was collected for 90 min with a LFOV gamma camera interfaced to a minicomputer. From the stored data activity vs time curves were generated and static sequential images obtained. The animals were sacrificed for determining the organ distribution of radioactivity. Immediately after injection of stannous tartrate, stomach and thyroid deposition of activity ceased while blood concentration increased, suggesting extraction of activity from the extravascular space. By 70 min, however, blood levels of activity were lower in animals injected with stannous tartrate than in the controls and urinary excretion was enhanced 5-fold. This data demonstrates that a clearing agent offers the potential advantages of enhanced target to background ratios while reducing total body radiation exposure.

8:30-10:00 Room 3038

INSTRUMENTATION

INSTRUMENT PERFORMANCE AND EVALUATION

Session Chairman: C. Craig Harris
Session Co-Chairman: Raleigh Johnson

A COMPARISON OF UNIFORMITY CORRECTION SYSTEMS. T. K. Lewellen, H. Karimi, R. Murano. University of Washington, Seattle, WA.

A comparison of the uniformity correction systems offered by several gamma camera manufacturers has been performed. The comparison involved five cameras: A General Electric Porta IIC, an Ohio Nuclear Sigma 410, a Picker DC4/15, a 37 PMT Searle ZLC, and a 75 PMT Searle ZLC. Basic intrinsic and extrinsic performance parameters (including energy resolution, uniformity, linearity, photopeak map, and line spread function) were measured and submitted to

the area service organizations for review. If the camera was not within specification, it was serviced. The comparison centered on contrasting individual camera performance with and without the respective correction system in operation. Particular attention was paid to the changes in resolution, point source count density, and low contrast detectability. Some of the cameras were also studied under non-standard conditions such as asymmetric PHA windows and gain shifted PM tubes.

The results indicate that the systems with both photopeak map and linearity corrections are preferred over the renormalization systems. The preference is primarily due to the ability to see asymmetric windows in order to improve scatter rejection. The renormalization systems cause some data distortion but also improve the low contrast detectability as compared to the uncorrected image. The renormalization systems did not operate identically and produced some interesting differences, both in low contrast performance and the ability to tolerate asymmetric energy windows.

AN EVALUATION OF A LINEARITY CORRECTION SYSTEM FOR GAMMA CAMERAS. T.K. Lewellen, H.Karimi, R.Murano, University of Washington, Seattle, Washington

A uniformity correction system using photopeak map and linearity corrections has been designed by Dr. Glen Knoll, Dept. of Nuclear Engineering, Univ. of Michigan and Medical Data Systems. Several prototype systems were built and one was installed on a MDS Simul computer system at the Univ. of Washington Hospital for evaluation. The system replaces the normal ADC boards and digitizes the energy as well as the position signals. The photopeak map and linearity corrections are performed real time using a fast table look up scheme. The tables are created during a morning calibration run on each camera using a software package which runs under the MDS MDOS operating system. The system selects the energy window and allows asymmetric windows to be used. At this time, only single window operation is supported. Currently, the system is being used with an older Picker DC4/15 and a Picker DC4/11.

The system provides uniform flood fields without the data distortion produced by renormalization correction methods. The most impressive result has been the improvement in low contrast detectability, particularly in the DC4/15. This improvement demonstrates the importance of photopeak map corrections. The correction system also corrects for regional differences in energy resolution which proved to be an important parameter for the older DC4/15 used in the evaluation. The system improved the DC4/15 energy resolution by 30% and the integral uniformity by a factor of 3.

COUNTRATE LIMITATIONS OF ANGER SCINTILLATION CAMERAS. J.G. Colsher and G. Muehllehner. University of Pennsylvania, Philadelphia, PA.

The countrate capability of the Anger scintillation camera is limited both by the decay time of the light emitted from NaI(Tl) scintillation crystals and by the data processing capability of analog and digital processing electronics. Significant improvements are possible through more sophisticated processing schemes.

Limitations due to the decay time of light can be partially overcome by electronic pulse shortening techniques. A delay line method has been used to shorten pulses to less than 200 nsec duration. During this time about 50% of the total light is emitted and some statistical information is lost. This results in decreased spatial resolution but the countrate capability of the camera is more than double.

Limitations due to the processing electronics can be partially overcome by the use of serial buffers. To avoid counting losses due to long deadtimes in the ratio correction (energy normalization) circuit and display or digital conversion circuits, it is desirable to buffer the position information. Analysis of this problem indicates that the use of 3 serial buffers preceeding the ratio circuit increases the rate at which 10% count losses occur by a factor of 7.

With the introduction of these techniques the camera no longer behaves as a simple paralyzable system. Hence characterizing deadtimes by methods such as the two-source technique are becoming increasingly inaccurate.

ENERGY AND ANGULAR DEPENDENT DISTORTIONS IN ANGER CAMERA IMAGES. L. Shabason, M.T. LeFree, D.L. Kirch and B.H. Hasegawa. University of Colorado Health Sciences Center and Veterans Administration Medical Center, Denver, CO.

It is generally assumed that events recorded by Anger camera imaging systems are strictly a function of the gamma ray interaction site. Two different conditions were found to yield relative translational shifts. The first of these is that images acquired with radionuclides whose photon energies differed by 80 KeV shows a translational shift of as much as 4 mm. This discrepancy between the images acquired at two energies may cause resolution loss in dual isotope subtraction studies and in multipeak Ga-67 scintigraphs. Since uniformity correction methods are applied on a pixel by pixel basis, the use of a data matrix acquired at one energy may be applicable for images at other energies. These energy dependent shifts are most likely caused by electronic artifacts and the camera may be adjusted to minimize these effects.

The second effect is a positional shifting as a function of incident photon angle. In varying the photon incident angle from 0 to 70 degrees the imaged peak location was found to shift by more than 1 cm. This effect was found to be strongly dependent on the choice of energy window width. This effect would have its strongest impact on imaging techniques where photons of varying incident angles are simultaneously acquired such as reconstructed images from coded apertures and seven pinhole tomography. In this case, the distortions appear to be dependent on geometric effects and cannot be significantly altered by tuning.

MISALIGNMENT OF MULTIPLE PHOTOPEAK ANALYZER OUTPUTS: EFFECTS ON IMAGING PERFORMANCE. D. Chapman, E. Garcia, A. Waxman. Cedars-Sinai Medical Center, Los Angeles, CA

The purpose of this study was to demonstrate the effects of multiple misaligned images on spatial distortion, resolution, and image contrast. In particular we studied misaligned images generated from simultaneous outputs of cameras with multiple pulse height analyzers.

Two of three cameras in our institution demonstrated multiple misaligned edge packing on intrinsic Ga-67 point source floods. This indicates the camera response is spatially distorted when using multiple photopeak analyzers.

One of these cameras was used to image a Hine-Duley bar pattern, a Rollo phantom, and to measure the FWHM and FWTM at different crystal locations. We compared images from multiple pulse height analyzers vs. simulated images of perfect alignment obtained by summing the outputs from the three major photopeaks of Ga-67 one at a time using the same analyzer. The results are as follows: 1) loss of resolution indicated by degradation of the FWHM and the Hine-Duley bar pattern images, 2) loss of contrast indicated by degradation of the FWTM, Hine-Duley bar patterns and the Rollo phantom images, 3) the degree of resolution and contrast degradation is spatially variant (x-y dependent).

With the increased use of multiple pulse height analyzer cameras to image multiple photopeak radionuclides such as In-111, Tl-201, and Ga-67, it is important to check the image alignment of multiple analyzer outputs periodically. It is not acceptable to pay for increased count densities with degradation of image quality.

THE NOISE-EQUIVALENT BANDPASS AS A MEASURE OF SPATIAL RESOLUTION FOR GAMMA CAMERAS. D.W. Shosa and L. Kaufman. University of California, San Francisco, San Francisco, CA

The noise-equivalent bandpass is related to integrals of the squares of the system spread function and modulation transfer function. For components of a system spread function which can be characterized by a single parameter, an effective width can be extracted from the bandpass. This width can be used to characterize the spatial resolution of

the system in a manner similar to the use of FWHM. Results of this investigation have shown that bandpass measurements can be used to accurately predict the contrast modulation of small signals. This approach has the advantage of being applicable to distinctly non-Gaussian spread functions. It is also an advantage that bandpass measurements can be accurately obtained from sparsely sampled noisy data. The measurements are thus obtained quickly and without sophisticated sampling equipment.

RELATIVE AND ABSOLUTE UPTAKE MEASUREMENTS WITH THE GAMMA CAMERA: AN ASSESSMENT OF ERRORS. L.P. Clarke and A. Serafini. University of Miami, Fla.

The important response parameters for gamma cameras for most measurements, are their sensitivity, uniformity and spatial resolution. Standard methods are used to verify them. Cameras are also used to make relative or absolute uptake measurements in nuclear cardiology, nephrology, gastric emptying and adrenal studies. The important response parameter is the ability to faithfully relate the integrated count within a region of interest (ROI) over the organ to its activity. The problems associated with photon attenuation and selection of background areas have been assessed. However, the systematic errors associated with selecting small ROI that enclose the image of an organ have not been studied in detail. Calibration measurements that specifically include both large and small ROI's were performed to determine the cameras response to cylindrical sources of varying size (3-60ml) and source depth in scattering medium (5-20cm). Data were taken with standard collimators for photon energies of 140 and 364 KeV. Assumptions usually made in estimating source size was evaluated. Data were compared to that of the rectilinear scanner designed for absolute measurements.

Results demonstrated that larger systematic errors are encountered with small ROI's. Greater corrections for source size and depth were required. These were interdependent and not unique. Thus, for example, errors in absolute measurements were greater than ± 40% for small sources of 364 KeV photons. Much larger ROI's, not feasible for clinical studies, were required to reduce this error range. Data has equal significance for tomographic imaging systems.

INTERNAL MAMMARY LYMPHOSCINTIGRAPHY USING BILATERAL COLLIMATOR: MEASUREMENT OF THE DEPTH OF THE LYMPH NODE. E. Ohtake, M. Iio, H. Toyama, M. Noguchi, S. Kawaguchi, H. Murata, K. Chiba, and H. Yamada. Tokyo Metropolitan Geriatric Hospital, Tokyo, Japan.

The purpose of this study is to evaluate the method to measure the depth of internal mammary lymph nodes using the bilateral collimator originally designed for cardiac study.

The lymphoscintigram was obtained 4 hours after bilateral subcostal injection of Tc-99m sulfur colloid and the image was made by Searle Pho/Gamma LFOV scintillation camera with a bilateral collimator consisting of two arrays slanting ± 30 degrees. At that time, the collimator was set to image the lymph node in the dual fields and Co-57 markers with 5 cm interval were placed along the centerline of the two slant arrays at the surface of the body to measure the ratio of minification.

The distance (D) from the image (crystal) plane to the lymph node can be expressed by the equation:

$$D = \frac{1}{2} \cdot L \cdot \cot 30^\circ = 0.866 \cdot L$$

where L is the interval of dual images of the same lymph node calibrated into the real length by using the minification factor. The real depth from the surface of the collimator to the lymph node is obtained by subtracting the distance (T) between the image plane and the surface of the collimator from D. For the calculation of T, the same equation was applied by placing Co-57 markers on the surface of the collimator.

By this method, we could easily estimate the depth of the internal mammary lymph node with satisfactory accuracy. This method may facilitate the effective postoperative irradiation of the internal mammary lymph nodes for the patients with breast cancer.

10:30-12:00 Room 2043

CLINICAL

THALLIUM-201 IMAGING

Session Chairman: Denny D. Watson
Session Co-Chairman: James C. Ehrhardt

A KINETIC MODEL OF ^{201}Tl-TRANSPORT IN THE MYOCARDIUM. N.M. Alpert, J. Newell, J. Ingwall, R. Okada, H.W. Strauss and G.M. Pohost. Massachusetts General Hospital, Boston, MA.

To understand the factors controlling the rate of uptake and loss of thallium in the myocardium, a model of Tl kinetics has been developed. The parameters of the model are the cellular input and output rates (K_I and K_O), the ratio of interstitial (V_1) to extravascular volume (V_1+V_2) and the blood Tl concentration (C_B). The myocardial Tl concentration is given by $C(t) = K_I V_1 (V_1+V_2)^{-1}$ EXP $(-K_O t)$ $\int_0^t C_B(S)\text{EXP}(K_O S)dS$. The model was tested in (1) a cultured fetal mouse heart preparation (CFMP) and (2) an open chest canine preparation (OCCP). Figure 1 compares the measured Tl uptake and the model prediction in CFMP; while, Figure 2 shows the measured count rate and model prediction for an OCCP. Studies in the CFMP have shown that K_O varies linearly with % LDH lost in ischemic-like insults (K_O=-0.05+0.05X % LDH LOST, R=0.95), whereas, K_I remains constant.

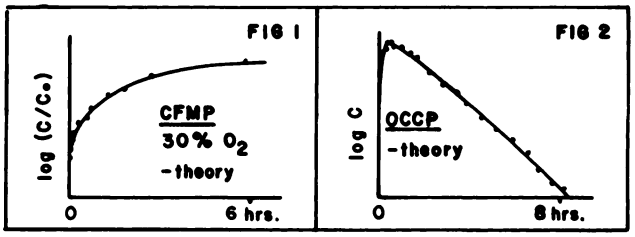

This model rigorously takes into account Tl-redistribution on the basis of blood-tissue concentration gradients and differing clearance rates and thus may be useful in the study of Tl transport in normal and insulted myocardium.

INCREASED SENSITIVITY OF Tl-201 KINETIC IMAGING FOR DETECTING ACUTE PERFUSION DEFECTS IN MYOCARDIUM. **R.M. Beihn, M.R. Jones, M.W. Vannier, J.D. Slack, H.G. Hanley, and F.H. DeLand. Veterans Administration and University of Kentucky Medical Centers, Lexington, KY.**

Since redistribution of Thallium-201 may limit the sensitivity of myocardial perfusion scintigraphy in detecting transient myocardial perfusion abnormalities, a new technique to analyze the immediate deposition kinetics of Tl-201 was developed. By means of computer processing separate rate constants (k) for myocardial deposition of Tl-201 are determined following the Tl-201 injection. The k values are derived for each pixel of a 64x64 computer matrix by exponential least squares analysis. Ten dogs were chronically instrumented with circumflex artery occluders and flow probes, LV pressure transducers, and ultrasonic segment length crystals. While graded occlusions were imposed and blood flow was reduced, Tl-201 was injected followed by one min of kinetic data accumulation. The occlusions were then discontinued and one additional minute of data was collected. Serial static images were performed from 0.5 to 30 minutes. In 15/16 studies k values for Tl-201 accumulation in the distribution of the circumflex artery were reduced during partial occlusion (-15.75 ± 8.7 $\times10^{-4}$sec^{-1} to -70.31 ± 19.34 $\times10^{-4}$sec^{-1}) and in 16/16 studies k values increased when the occlusion was released (to 43.13 ± 13.30 $\times10^{-4}$sec^{-1}). An abnormal static image occurred in only 1 of 16 studies. Analysis of kinetic data from Tl-201 imaging appears more sensitive for the detection of acute alterations in myocardial perfusion than routine static scintigraphy.

ARE CORONARY COLLATERALS PROTECTIVE?
D.D. Watson, B.C. Berger, G.A. Beller, C.D. Teates.
University of VA, Charlottesville, VA.

The ability of collateral vessels to restore adequate coronary reserve capacity in patients with coronary artery disease is a continuing question. Sequential thallium-201 (Tl) myocardial imaging was employed to evaluate the effect of collaterals on regional myocardial blood flow at rest and following exercise stress. Sixty-two patients with significant coronary artery disease had post-exercise Tl studies and 35 other patients were studied during rest. Delayed redistribution images were obtained in all cases and the images divided into 6 segments and interpreted using computer assisted quantitative analysis. All patients had coronary angiograms. A total of 464 segments were in regions perfused by stenotic vessels of which 172 segments were supplied partially or totally by collateral flow. In the resting studies, Tl perfusion defects were observed somewhat less frequently (40%) when collaterals were present than when they were absent (56%). During exercise stress, Tl defects were observed far more frequently (78%) in myocardial segments supplied by collateral vessels than in those without collateral flow (45%). These data excluded all segments with corresponding Q waves where Tl defects were presumed to indicate myocardial scars. We conclude that the collateral vessels may have offered some augmentation of blood flow during the resting state but failed to restore the coronary reserve capacity as indicated by the high prevalence of stress-induced perfusion defects observed in myocardial segments which were viable but to which collateral blood flow was observed. In fact, the presence of collateral flow appears to be an indicator that there is a significant pressure gradient across the lesion in the native vessel.

THALLIUM STRESS TEST RESULTS AND VENTRICULAR ARRHYTHMIAS.
P.C. Voukydis, K.A. McKusick, M. Moore, S.A. Forwand, L.M. Zir, M. Johnson and H.W. Strauss. Mount Auburn and Massachusetts General Hospitals, Cambridge and Boston, MA

To determine the relationship between ventricular ectopic activity (VEA) and findings from Tl-201 stress testing (TlST) 95 patients (pt) undergoing TlST had continuous recording of their electrocardiogram during exercise and then a Holter monitor between the stress and redistribution image. The Tl scintiscans were recorded for 400 K on triple lens Polaroid film and on transparency film at two intensity levels. The images were examined for presence of myocardial scar (S), myocardial "ischemia" (I), left ventricular dysfunction (F) and rapid relative regional Thallium washout (R^3WO), the latter defined as a normal area on the stress scan which demonstrates a definite decrease or thinning of Tl-201 concentration in the delayed image, relative to adjacent areas. The findings were correlated to various exercise parameters and occurrence of VEA. Pt with normal scans were less likely to have VEA and pt with F more likely to have VEA than the entire group. Pt with S in combination with other abnormal findings, i.e., I, F or R^3WO (but not with S alone) were more likely to have VEA during Holter monitoring than the entire group. Similarly, pt with R^3WO in combination with other abnormal findings, i.e., S, I or F (but not with R^3WO alone) were more likely to have VEA during Holter monitoring than the entire group. Pt with I had more VEA during exercise compared to the entire group. Occurrence of ST-segment depression or angina during exercise and failure to achieve 85% of expected maximal heart rate did not predict the presence of VEA during exercise or Holter monitoring. Thus, attributes of Tl scanning correlated with VEA, but attributes of the exercise electrocardiogram did not.

NONINVASIVE ASSESSMENT OF EXTENT AND LOCATION OF CORONARY ARTERY STENOSIS BY COMBINED EXERCISE THALLIUM-201 AND EXERCISE GATED EQUILIBRIUM CARDIAC BLOOD POOL SCINTIGRAPHY.
M. Weinstein, U. Elkayam, D. Berman, J. Maddahi, H. Staniloff, M. Freeman, H.J.C. Swan, J. Forrester, and A. Waxman, Cedars-Sinai Medical Center, Los Angeles, CA.

Although exercise (Ex) Tl-201 (Tl) and Ex multiple gated equilibrium scintigraphy with Tc-99m-RBC's (Tc) are useful for detection of coronary artery (CA) disease (D), little is known about the combination (Tl+Tc) in evaluation of the extent and location of CAD. Ex Tl and Ex Tc were performed in 54 pts with CAD (>50% stenosis). Left anterior descending (LAD) D was present in 44 pts, circumflex (Cx)D in 33, and right coronary (RCA)D in 22. Forty-two pts had multiple vessel (+)D and 9 had single vessel (SV)D. On Tl, anterior (ANT) and septal (SEP) defects were considered positive (+) for LAD, posterolateral (PL) defects + for Cx, and inferior (Inf) defects + for RCA D. On LAO Tc, performed during sitting ergometry, SEP abnormality (abnl) was + for LAD, PL abnl + for Cx and RCA was not evaluated. In addition, the ability of Tl+Tc to detect inferoposterior CAD was assessed by considering the Cx and RCA as one major vascular distribution.

		LAD	Cx	RCA	Cx and/or RCA
	Tl	80(90)	37(100)	63(58)	65(100)
Sens (Spec)	Tc	82(70)	61(84)		50(83)
Percent	Tl+Tc	89(70)	66(84)	63(58)	83(83)

sens=sensitivity; spec=specificity

MVD was correctly predicted by Tl+Tc in 74% and SVD by Tl+Tc in 67%. Thus, the combination of Ex Tl + Ex Tc appears to improve sensitivity in localizing CAD with mild reduction in specificity. In addition, combined Tl + Tc may improve the evaluation of the extent of CAD.

CARDIOVASCULAR ABNORMALITIES IN PATIENTS WITH STRESS THALLIUM PERFUSION DEFECTS AND NORMAL CORONARY ARTERIES.
L.S. Goodenday, R.F. Leighton, A.D. Nelson, L.T. Andrews, N.E. Wheeler. Medical College of Ohio, Toledo, OH.

Determinations of the sensitivity and specificity of stress thallium scintigraphy (STS) are usually based on the findings of coronary angiography. We examined other cardiovascular characteristics of 14 patients who had abnormal STS and angiographically normal coronary arteries compared to 15 patients who had normal STS with angiographically normal coronary arteries and normal left ventricular function. STS were analyzed by a quantitative computer technique previously found to have a diagnostic accuracy of 95.5% for coronary artery disease. Significant differences were found in resting systolic pressure (BP-R), maximum exercise systolic pressure (BP-Max) and left ventricular ejection fraction (EF) between the two patient groups:

	Abnormal STS	Normal STS	p <
BP-R	135	122	0.025
BP-Max	195	170	0.001
EF	0.62	0.69	0.025

Ischemic electrocardiographic responses occurred in 4 patients with abnormal STS and no patients with normal STS. Subsequent resting thallium scintigrams obtained in 13 patients with abnormal STS were normal in 6, but 7 had persistent defects in the same location as the defects on STS.

Patients with abnormal STS and angiographically normal coronary arteries tend to be more hypertensive and have relatively diminished left ventricular function compared to patients with normal STS. Thus the abnormal STS in such patients should not be considered "false positives".

DETECTION AND FOLLOW-UP OF MYOCARDIAL SARCOID INVOLVEMENT BY TL-201: PRELIMINARY REPORT.
S.L. Gottlieb, M.E. Siegel J. Caldwell, O.P. Sharma, J.K. Siemsen, and L.J. Haywood. LAC-USC Medical Center, Los Angeles, CA

The purpose of this study is to evaluate the feasibility of using Tl-201 myocardial scanning to detect myocardial sarcoid granulomas, evaluate their response to therapy and correlate right ventricular abnormalities with pulmonary involvement.

Thirty patients with histologic diagnosis of sarcoid had resting Tl-201 scans performed in 3 projections. Patients with focal defects also had stress thallium scans. Multiple follow-up scans, up to 1.5 years were performed on patients with focal disease. Right ventricular Tl-201 uptake, pulmonary function tests, chest x-ray and ECG were also evaluated.

Of 30 patients with systemic sarcoid, 4 (13%) had focal defects at rest; 3 were exercised and the defects decreased in size. Nine patients had increased right ventricular uptake of the tracer at rest. Thus 11 of 30 or 47% of

the patients had abnormal resting scans. One patient with multiple follow-up scans showed resolution after initial therapy with subsequent recurrence, while the other demonstrated no effect from the steroidal therapy. Approximately 90% of patients with abnormal right ventricular uptake had stage II or III chest x-rays and all patients with focal defects had severe restrictive or obstructive and restrictive pulmonary disease.

This preliminary data suggests focal LV defects with non-ischemic stress responses, can be demonstrated and probably represent myocardial sarcoid; that RV uptake appears to correlate with severity of pulmonary disease and that serial thallium scans may be useful in monitoring lesion progression or response.

10:30-12:00 Room 3040

CLINICAL

IMAGE CORRELATION II

Session Chairman: Heidi S. Weissman
Session Co-Chairman: Daniel R. Biello

A COMPARISON OF RADIONUCLIDE LIVER/SPLEEN SCANS AND ULTRASOUND FOR SPLENIC TRAUMA: A PROSPECTIVE STUDY. J.W. Froelich, G.W. Winzelberg, J. Simeone, H.W. Strauss, J.B. Bingham and K.A. McKusick, Massachusetts General Hospital, Boston, MA.

To compare radionuclide liver/spleen scans with ultrasound for the evaluation of splenic trauma a prospective investigation was undertaken in 20 sequential patients with abdominal and chest trauma. The studies were analyzed by a staff ultrasonographer and a staff nuclear medicine physician without benefit of clinical information or results of other studies. Ultrasound studies were inadequate in 6 (30%) cases of injury to the left upper quadrant (i.e., chest tube, subcutaneous hematoma and rib fractures). Four studies were abnormal, 10 were normal with 100% agreement between the radionuclide studies and ultrasound. In the 4 patients with abnormal studies, 1 had a lacerated spleen removed; 2 had repeat radionuclide studies with resolution of the abnormalities; and one had no follow-up studies but was clinically stable 1 month later. Of the 6 patients who had technically inadequate studies could not have ultrasound, all were normal on radionuclide scan. The 16 patients who did not undergo further radionuclide evaluation were followed for 2-8 weeks and remained clinically stable. One patient had a normal radionuclide spleen scan, but the liver showed a subcapsular hematoma. Ultrasound of the spleen was normal. However, subsequent ultrasound of the liver also demonstrated a hematoma.

This study suggests that when ultrasound of the spleen can be performed, it is a sensitive method of detecting splenic trauma; however, 30% of patients trauma may not be evaluated by ultrasound, and therefore, radionuclide scanning remains the single procedure of choice for evaluation of spleen and liver trauma.

COMPUTERIZED TOMOGRAPHY, ULTRASOUND, TECHNETIUM-99m PYROPHOSPHATE AND SULFUR COLLOID SCANS AFTER EMBOLIZING THE SPLEEN AND LIVER. J.A. Harolds, F. Correa-Paz, C.M. Coulam, G.R. Novak, and R.B. Grove, Vanderbilt University Hospital, Nashville, TN.

Multiple modalities were used to image the liver and spleen of dogs after embolization.

Mongrel dogs had normal baseline scans after administering technetium-99m pyrophosphate (PYP) and sulfur colloid (SC). Using selective catheterization, a gelfoam embolus was used to create a small (s), medium (m) or large (l) sized-infarct in the spleen of each of three dogs. Periodic images with PYP up to three weeks after the embolization showed no increased uptake in the spleen. The SC scans showed the infarcts as defects. Ultrasound images were normal. The s infarct was seen on computerized tomography (CT) as a low density area both before and after contrast administration. The m infarct was seen on CT only after contrast enhancement. The l infarct was not seen on CT.

A gelfoam embolus was introduced into the liver of two dogs. The SC scan of each animal showed a corresponding defect. Ultrasound and CT did not show any abnormality. The PYP scans done 48-72 hours after angiography showed areas of increased uptake corresponding to the area of each embolus. It is hypothesized that the success of PYP imaging in the liver, but not in the spleen during the time frame of this experiment is due to the dual blood supply of the liver.

Non-invasive infarct imaging of the spleen of dogs shortly after embolization is best done with SC scans. Confirmation of the nature of a liver defect may be done with a PYP scan.

COMPARATIVE STUDY OF NPH BY RN CISTERNOGRAPHY AND CT SCAN IN THE AGED. Shinichiro Kawaguchi, Masahiro Iio, Hajime Murata, Kazuo Chiba, Hideo Yamada, Masahiro Noguchi, Eiji Ohtake. Tokyo Metropolitan Geriatric Hospital, Tokyo, Japan

In the aged cases, RN cisternography revealed with high incidence the existence of continuous ventricular reflux(VR) of the label, suggesting normal pressure hydrocephalus (NPH). On the other hand brain CT scan of the geriatric cases frequently show periventricular lucency(PVL) with & without ventricular dilatation(VD). Since PVL is sometimes referred as the evidence of hydrocephalus, in this study, RN cisternography & CT scan were simultaneously performed on the geriatric cases with & without NPH and relationship between VR, VD and PVL were examined. Materials were 67 clinically suspected NPH cases, with 31 males & 36 females. Ages were 13 to 86 with average of 68.5 years old. In RN scan, presence of VR, CSF pressure & C_{24}/C_6 ratio as index of CSF circulation were evaluated. CT scan was performed by GE CT/T scanner, with 5 mm slices along the OM line. In CT scan, ventricle/cerebrum ratio was measured as an index of ventricular size. Presence of PVL was diagnosed in the slice involving pineal body. The results were as follows: RN study revealed VR(+) in 36(group 1), (±) in 7(group 2) and (-) in24 cases(group 3). Then, results of CT scan were analysed according to the RN study. V/C index were 0.30±0.05 in group 1 and 0.29±0.06 in group 3. PVL was found in 54% in group 1, 38% in group 3. C_{24}/C_6 ratio was 1.28±0.61 in group 1, 1.58±0.89 in group 3.CSF pressure was 108±38 mmH_2O in group 1, 116±67 mmH_2O in group 3.

To conclude, NPH diagnosed with ventricular reflux of RN study is not specifically represented by static CT study . Neither periventricular lucency nor ventricular dilatation relate with ventricular reflux in NPH cases of the aged.

COMPARISON OF BRAIN IMAGING UTILIZING Tc-99m PHOSPHATES, Tc-99m PERTECHNETATE, AND COMPUTED TOMOGRAPHY. D.S. SCHAUWECKER, R.W. BURT, AND B.D. RICHMOND. VAMC-Indiana University School of Medicine, Indianapolis, IN.

Computed tomography (CT), Tc-99m Phosphates (PHOS), and Tc-99m Pertechnetate (Tc04) brain scans in the evaluation of stroke (CVA) and other disease processes and the relative uptake of PHOS and Tc04 were compared.

A retrospective review was made of 110 consecutive patients. Of these, 78 had a clinical diagnosis of CVA; while 15 had no known intracranial lesions. There was no significant difference between CT, PHOS and Tc04 in detecting CVA. (p=.49)

In CVA, the Tc04 and PHOS images have a definite time course. Before 6 days 47% of the Tc04 scans were positive but rose to 82% between 6 days to 4 months, and fell to 29% afterwards. PHOS scans within 1 week after the CVA visualized 67%. Between 1 week and 1 month, 81% were better visualized with PHOS. After 2 months, only 8% were better visualized, but 45% were seen. After 5 months none were visible.

Ten patients had a diagnosis of tumor and all were as well or better visualized with Tc04. Seven patients had other diagnoses. The hypothesis that if a lesion is seen with greater intensity on PHOS than on Tc04 it is a CVA and not a tumor was true ($p < .001$) if evaluated within 4 weeks. After 6 weeks, the difference is no longer statistically significant. (p=.19)

CONCLUSIONS: 1.) There was no statistical difference in CVA visualization by CT, PHOS or TcO4. 2.) CVA can be differentiated from tumor by increased uptake of PHOS if done before 4 weeks.

INVITED SPEAKER
Aldo N. Serafini, University of Miami School of Medicine, Miami, FL
IMPACT OF REAL TIME ECHOCARDIOGRAPHY ON CARDIOVASCULAR NUCLEAR MEDICINE.
Invited by the Council of Correlated Imaging Modalities

10:30-12:00 Room 3039

RADIOPHARMACEUTICAL CHEMISTRY

RADIONUCLIDE PRODUCTION AND AND GENERATORS

Session Chairman: Harold A. O'Brien
Session Co-Chairman: Roy S. Tilbury

A NEW TARGET FOR THE PREPARATION OF F-18 HF WITH NO ADDED CARRIER. J.R. Dahl, R.E. Bigler, B. Schmall, R. Lee, Memorial Sloan-Kettering Cancer Center, New York, NY.

Ni is the material usually selected for construction of targets to contain neon for irradiation with deuterons to produce F-18 for subsequent use in anhydrous labelling procedures. The choice of Ni is based on available data regarding safe handling of fluorine and protection of apparatus against corrosion by passivation through reaction with fluorine to form a nickel fluoride coat. Passivation with fluorine of a target for producing no carrier added F-18 is unacceptable because the millimolar amounts of F-19 may cause isotope dilution. The extreme reactivity makes it difficult to recover fluorine from the target. A study was performed to determine which metal allows the easiest recovery of the F-18 with a given purge gas. Preliminary experiments showed that Cu readily released F-18 to a 10% hydrogen in helium purge gas. A target chamber was constructed entirely of Cu. Reproducible yields of 3 mCi F-18 (End of Bombardment) per microamp after a 1 hr. bombardment were obtained by collecting the F-18 from the purge gas on dry KOH in a Cu vessel. The target was heated to 310 degrees C. during purge. This is 75% of the total activity in the target chamber and target gas after bombardment.

PRECISION FLOW-CONTROLLED Rb-82 GENERATOR FOR BOLUS AND CONSTANT INFUSION. Y. Yano, J. Cahoon, and T. F. Budinger. Donner Laboratory and Lawrence Berkeley Laboratory, University of California, Berkeley, CA.

When Rb-82 is infused intravenously under precise flow control at rates of 2 ml/min for constant infusion (CI), 75 ml/min for bolus infusion (BI), or at exponential infusion rates (ET), organ flow x extraction can be ascertained.

We have developed a unique flow rate controller and large volume (150 ml) reservoir pumping system for delivery of a sterile solution of 75 sec Rb-82 in saline from an alumina column Sr-82 generator under extremes of either slow or fast elution rates and operating pressures of 100 p.s.i. or more.

A stepping motor drive with a wide speed range is interfaced to a microprocessor which reads flow rate and quantity of eluant injected. Thumb-wheel switches on the control panel are set to predetermined values for CI, BI, or EI studies. The flow rate is a function of pulse rate sent to the stepping motor. A belt drive connects the motor drive to a recirculating ball nut and screw which moves the piston inside of a machined Lexan barrel. A Bellofram rolling diaphragm around the piston allows extremely low friction. The entire pumping system is mounted on FR-4 glass-epoxy for electrical isolation from the patient.

The primary and secondary lead shielding arrangement allows reloading with fresh Sr-82 by transporting only the column with its primary shielding. The pumping system, electronic controls and secondary shielding remain at the clinical site.

Electrocardiogram gated myocardial studies have been done with this new system containing 150 mCi Sr-82.

DEVELOPMENT OF A GALLIUM-68 GENERATOR ON ALUMINA. W.W. Layne, and M.A. Davis. Department of Radiology, Joint Program in Nuclear Medicine, Harvard Medical School, Boston, MA.

The availability of annihilation coincidence detection devices has increased interest in the production of short-lived positron emitting radioisotopes. Most biological positron emitters (C-11, N-13, O-15, F-18) are cyclotron-produced, and because of their short half-lives, available only to large hospitals and research centers in the proximity of the producing cyclotrons. If more widespread use is to occur, generator systems must be developed to furnish sources of such radionuclides. To this end we have developed a generator system which produces Ga-68 in a more versatile form than the generator currently available from which Ga-68 is eluted as the EDTA complex.

Chemical separation of Ga-68 from Ge-68 using adsorption chromatography on Woelm basic super 1 alumina has been achieved using 0.1N NaOH as eluent. Typical elution yields are 50-65%. Ge-68 breakthrough varies from an initial value of 2.7×10^{-5} decreasing to a constant value of $2.5 \pm 0.4 \times 10^{-6}$ after the first 100 elutions. (Four hundred elutions with 0.1N NaOH were performed.)

After the first three elutions the aluminum breakthrough averages 130-150 µg/ml. Storage of the alumina columns in 0.1N $NaHCO_3$ between elutions decreases the aluminum breakthrough by 40-50%.

LEAD-211: A SHORT-LIVED, GENERATOR-PRODUCED ALPHA AND BETA EMITTING RADIONUCLIDE SUITABLE FOR THERAPEUTIC USE. R.W. Atcher, A.M. Friedman, R.P. Spencer, J.R. Huizenga. Argonne National Laboratory, Argonne, IL, University of Connecticut Health Center, Farmington, CT, and University of Rochester, Rochester, NY.

A generator system has been developed to separate Pb-211 which has a 36.1 minute half life from its grandparent Ra-223 which has an 11.3 day half life and is naturally occuring. Pb-211 decays through two short-lived daughters to stable Pb-207 by the emission of two beta particles (1.36 and 1.43 MeV maximum) and an alpha particle (6.62 MeV). Photon emission is principally a 351 keV gamma ray (13 % abundance) which is suitable for imaging but is in low enough abundance to avoid excessive dose far from the target. Ra-223 is co-precipitated with barium stearate and is placed in a vacuum manifold. The system is pumped to a vacuum of 50 microns (Hg) or less and a collection tube is cooled to liquid nitrogen temperatures. The intermediate radon daughter which has a 4 second half life is distilled from the radium stearate and the Pb-211 allowed to grow in. The stability of the vacuum is good if the collection tube is kept cold. An acetate buffer (pH 5) is frozen into the tube to prevent Pb-211 from reacting with the vessel walls. Breakthrough is very low, typically less than one part per million, and is easily detected by gamma ray spectroscopy. Yield is 10 percent and is linear in the range of 0.5 to 10 mCi. Thus millicuries of Pb-211 could be obtained from a generator containing tens of millicuries of Ra-223. Integrated dose for Pb-211 and daughters is 1.4×10^4 Rads/gram/mCi. A number of compounds can be used to insure that the lead and daughters are chemically unreactive and unlikely to leave the treatment site.

USE OF ELECTRON LINEAR ACCELERATOR FOR PRODUCTION OF CLINICALLY-USEFUL AMOUNTS OF POSITRON EMITTING RADIO-

NUCLIDES. H.V. Piltingsrud. FDA, Nuclear Medicine Laboratory & Eugene L. Saenger Radioisotope Laboratory, University of Cincinnati, Cincinnati, OH.

To date, the availability of the very short-lived positron emitting radionuclides C-11, O-15 and N-13 has been primarily confined to those facilities that are fortunate enough to have cyclotrons. This paper describes our experience in the use of an electron linear accelerator, similar to some commercial radiotherapy accelerators, for the production of C-11 and O-15 by use of γ,n reactions using high energy, high intensity Bremsstrahlung radiation produced by the accelerator. Equipment used consists of a 30-MeV electron linear accelerator having a maximum beam current of approximately 200 μA and both primary and secondary target systems designed specifically for nuclear medicine applications. Continuous-flow production rates of O-15 experienced to date have been approximately 250 μCi/L Helium/μA beam current at flow rates of approximately 1 L/min helium using a 20-cm H_2O target path length. Use of this material for laboratory imaging experiments will be described. Plans for further target development will be presented. At this time, it appears that a practical production means exists for producing clinically-useful amounts of certain positron-emitting radionuclides using electron linear accelerators.

SMALL ACCELERATOR SYNTHESIS OF MN-51 FOR MYOCARDIAL IMAGING. M.E. Daube, R.D. Hichwa and R.J. Nickles, Radiology Dept., University of Wisconsin, Madison, WI.

The mitochondrial concentration of manganese results in marked myocardial uptake of such radiotracers as Mn-54 and Mn-52m, eluted from an 8-hour Fe-52 generator. The latter invites positron imaging, in spite of the contamination by the 1433 keV gamma in single photon and even coincidence devices. The pure positron decay of the 46-min Mn-51 avoids this problem, but must be made *de novo* on a nearby accelerator. Only the deuteron irradiation of Cr-50 proves suitable for the UW EN tandem Van de Graaf, with the low yield at 10 MeV dictating 95% enrichment of the chromium sesquioxide target material. The cost of the separated isotope is offset by scaling down the target (2 mm) and beam (1 mm) diameters, while maintaining a thick target to the beam. The few milligrams of irradiated oxide are dissolved in fused sodium hydroxide:sodium peroxide. This melt is then dissolved in water, acidified with HCl, and the supernatent passed through an AG1x10 anion exchange column. The dichromate is trapped for subsequent recovery, while the divalent (no-carrier-added) Mn-51 is eluted with water. Millipore filtration, pH adjustment and dilution to isotonicity follow. Half-life and Ge(Li) analysis confirm the Mn-51 radionuclidic purity>99.9% at the time of injection. Synthetic runs with Mn-carrier verify the radiochemical form. The forty minute synthesis results in 2 mCi/uA at injection, with a decay-corrected yield in excess of 90%.

Four plane laminographic imaging of normal subjects shows encouraging myocardial delineation. Sequential studies confirm the rapid uptake and stability of the Mn-localization. Basic work into the subcellular mechanism of manganese uptake will identify the proper role for Mn-51 in the study of regional myocardial metabolism.

10:30-12:00 Room 2048

RADIOPHARMACEUTICAL CHEMISTRY

DOSIMETRY

Session Chairman: Katherine Lathrop
Session Co-Chairman: Dennis Swanson

HUMAN DOSIMETRY OF IN-111 GRANULOCYTES. L.E. Williams, L. Forstrom, B.J. Weiblen, J. McCullough and M.K. Loken. University of Minnesota Hospitals, Minneapolis, MN.

The study was undertaken to determine the normal human dosimetry of granulocytes labeled with In-111. Six adults were given 0.1mCi of the radiopharmaceutical and followed serially with blood sampling and posterior projection gamma camera imaging for 20h. A human liver phantom was used to correct for tissue attenuation of liver and spleen emissions. Mean fractional uptakes at 20h post-injection were 34, 25, 27, 8 and 6 percent for blood, spleen, liver, lungs and bone. The blood half-time was 5.0 ± 1.6h. No biological clearance was seen in organs other than blood. Using the above 5 organs as sources, the radiation doses were as follows:

TARGET ORGAN	DOSE/mCi of In-111-Granulocytes
Stomach Wall	1.0 rad
Liver	3.8
Lungs	1.5
Red Marrow	0.65
Ovaries	0.14
Spleen	23.4
Testes	0.029
Whole Body	0.45

We conclude that the spleen is the critical organ in normal humans receiving their own granulocytes labeled with In-111. Splenic and hepatic uptake are, however, approximately 25% each.

RADIATION DOSIMETRY OF Sn-117m LABELED 23-(TRIMETHYLSTANNA)-24-NOR-5α-CHOLAN-3β-OL(Sn-117m-23-TSC): A POTENTIAL ADRENAL IMAGING AGENT. J.L. Coffey and F.F. Knapp, Jr. Oak Ridge Associated Universities (ORAU) and Nuclear Medicine Technology Group, Oak Ridge National Laboratory (ORNL), Oak Ridge, TN.

Tissue distribution studies in rats with Sn-117m-23-TSC indicate that this agent has potential as an adrenal imaging agent. Tin-117m decays by isomeric transition to stable Sn-117 with a half-life of 14 days. The 159-keV gamma (86% abundance) and the stability of 23-TSC are desirable properties for a radiopharmaceutical. Using the MIRD technique and data from studies in rats, we have estimated the radiation dose in humans from the Sn-117m 23-TSC. A total body retention study in rats indicated a single exponential elimination component with a 4.2 day half-time. Maximum adrenal uptake in rats was about 50% dose/g and occurred between 1 and 3 days after injection. This would correspond to an uptake of approximately 2.2% of the injected dose in the human adrenals. The critical organ for dosimetry is the adrenals which would receive a dose of about 83 rad/mCi (2.2 cGy/MBq). The ovaries would receive a dose of about 4.4 rad/mCi (0.12 cGy/MBq). These doses are less than those calculated from rat data for NP-59 which is currently being used for adrenal studies (140 rad/mCi to the adrenals). The dose per detectable photon is also much less for Sn-117m-23-TSC, 2.9 rad/million detectable photons as opposed to 18 rad per million detectable photons for I-131-NP-59.
(Research at ORAU sponsored by DOE contract EY-76-C-05-0033 and also by Interagency Agreement No. FDA 224-75-3016, DOE 40-286-71. ORNL is operated by Union Carbide Corporation under contract W-740S-eng-26 with the U.S. Department of Energy.)

HUMAN RADIATION DOSIMETRY OF F-18-2-FLUORO-2-DEOXYGLUCOSE TO THE CRITICAL ORGAN. S.C. Jones, A. Alavi, D. Christman, I. Montanez, J. Fowler, A. Wolf, and M. Reivich. University of Pennsylvania, Philadelphia, PA and Brookhaven National Laboratory, Upton, NY.

In the measurement of the local cerebral metabolic rate for glucose (LCMRglu) with F-18-2-fluoro-2-deoxyglucose (FDG) and positron emission tomography the critical organ is the bladder wall. When the human bladder wall dose is calculated using the animal biodistribution data of Gallagher et al (J Nucl Med 18:990, 1977) and the MIRD 'S' tables, an overestimate is obtained.

To provide a more realistic estimate of the human bladder wall dose, bladder uptake of F-18 was monitored for two hours with an external probe in ten humans during LCMRglu determinations with the FDG technique of Reivich et al (Circ Res 44:127, 1979). This time course, together with the urine volume and activity, was used to calculate the cumulated activity for each of the ten subjects. Additional F-18 bladder uptake was monitored between two and four hours in two subjects. The mean dose ± S.E. was

435 ± 76 mrad/mCi.

The amount of activity needed to provide a statistically meaningful reconstruction for LCMRglu determinations with the PETT III results in a critical organ dose of 2 rads. This measurement sets a limit on the amount of activity that can be injected in the quest for increased spatial resolution and eliminates any assumptions in using animal biodistribution data for human dosimetry calculations.

Supported by NIH 14867-01.

Tc-99m HIDA DOSIMETRY IN PATIENTS WITH VARIOUS HEPATIC DISORDERS. R.K. Wu, J. Reilley, G. Applegate, L.S. Malmud. Temple University Hospital, Philadelphia, PA.

The purpose of this study was to estimate the radiation burden from Tc-99m HIDA in patients with a variety of hepatocystic disorders. The pharmacodynamics of the HIDA agents indicates that HIDA competes with bilirubin, and that the dosimetry to various organs, especially the gallbladder, will depend upon 2 factors: 1, the percent of the administered dose that enters the liver, and 2, the degree of cystic duct or common duct obstruction. A variety of patients was studied using a gamma camera on line to a digital computer. Areas of interest were outlined over the liver, gallbladder, kidney, small intestine, head (eyes), and a patch of known activity on the skin surface.

Timed activity curves were generated and the rate of uptake and clearance used as the basis for dosimetry calculations using the nonfeedback catenary compartment model of Bernard and Hayes.

In conclusion, the target organ for Tc-99m HIDA in normal subjects is the gallbladder which receives 0.3 rad per millicuries administered. In complete obstruction of the common duct, the target organ is the urinary bladder which receives 0.23 rads per millicurie administered. In acute cystic duct obstruction, the target organ is the upper large intestine which receives 0.3 rad per millicuries administered. Our results indicate that the radiation dose to the gallbladder is considerably less than that previously reported.

DOSIMETRY OF Tc-99m-HIDA BASED ON QUANTITATIVE DATA IN NORMAL SUBJECTS. P. H. Brown, G. T. Krishnamurthy, V.R. Bobba, E. Kingston. VAMC & UOHSC, Portland, OR.

Radiation dose has been calculated in 10 normal human subjects. After an overnight fast, 3 mCi of Tc-99m HIDA (Medi-Physics) was injected and serial gamma camera and computer images were obtained at 1 min. intervals for 60 min. with additional images at 3 & 24 hrs. Periodic blood and urine samples were obtained for 24 hours. The radiation source organs are blood, kidney, bladder, liver, gallbladder (GB), small intestine (SI), upper and lower large intestine (ULI & LLI). The blood data were analyzed by a 3 component exponential fit. Urinary bladder excretion biological half-life ($t_{\frac{1}{2}}$) was 2 hr. with activity in the bladder extrapolated to 7% at time zero. Kidney cumulated activity is taken equal to that of the bladder. By placing a computer region of interest over the liver, GB, and SI, the remaining 93% of activity was found to leave the liver at $t_{\frac{1}{2}}$ of 43 min. with 52% going to GB while 41% goes directly to SI. The GB $t_{\frac{1}{2}}$ was measured as 4 hr. based on a pinhole collimator determination of GB ejection fraction of 65% following a fatty meal (8 oz/70kg) and an assumed 6 hr. meal schedule. The SI, ULI, LLI $t_{\frac{1}{2}}$ were 2.8,9.0, 17 hr. from published data. The GB is a 50 ml ellipsoid, 10 gm. wall.

The Rad/mCi are: GB-1,1, ULI-0.35, LLI-0.24, SI-0.19, liver-0.09, ovaries-0.07, kidney-0.06, bladder-0.05,testes-0.005, marrow-0.03, total body -0.02. The GB critical organ dose is lower than manufacturer's calculated dose based on animal data, but higher than other published data (SNM Ann. Mtg. 1979) which assumed that the GB was not a source organ. Human dosimetry should be based on quantitative human data with proper biological modeling.

10:30-12:00 Room 3038

INSTRUMENTATION

CLINICAL EMISSION TOMOGRAPHY

Session Chairman: Michael Flynn
Session Co-Chairman: James Carlson

TOMOGRAPHIC THYROID SCINTIGRAPHY: COMPARISON WITH STANDARD PINHOLE IMAGING. W.W. Resinger, E.A. Rose, J.W. Keyes Jr., K.F. Koral, W.L. Rogers, T.J. Brady, R.C. Kline, J.C. Sisson, J.H. Thrall, University of Michigan Medical Center, Ann Arbor, MI.

A prospective study was undertaken to evaluate the hypothesis that coded aperture tomography of the thyroid offers significant advantages over conventional pinhole imaging.

Following 10 mCi of Tc-99m pertechnetate, 200,000 count pinhole images were obtained in the anterior, RAO and LAO projections in 136 consecutive patients. Immediately after this, coded aperture imaging was carried out in the anterior projection using the same camera. Total coded aperture acquisition time was twice the time required for the anterior pinhole image. Four coronal sections through the thyroid were then reconstructed by computer. All images were redisplayed and photographed on transparency film from a high quality video display under uniform conditions. Pinhole and coded aperture images were then read separately by five observers.

Final analysis was based on readings from 113 pairs of studies. ROC analysis revealed that three readers performed better with the tomograms. There was virtually no difference for the other two. The tomograms were also noted to offer additional advantages including accurate size representation of the gland at all depths and reduced total imaging time. The major disadvantage to tomography was the two hour processing time required for computer reconstruction of the data.

If the computer processing times for coded aperture tomograms can be reduced, the technique offers sufficient advantage over conventional pinhole imaging to warrant its routine use.

APPLICATION OF MULTIPLE PINHOLE EMISSION RADIONUCLIDE TOMOGRAPHY TO IMAGING OF THE BRAIN AND THYROID. R.B. GROVE*, A. RODEWALD, R.L. BELL, H.J. DeBLANC, JR., PARK VIEW HOSPITAL, NASHVILLE, TN. --Multiple pinhole emission tomographic imaging techniques are currently being applied to cardiac imaging and show promise for improvement of myocardial perfusion and equilibrium gated blood pool studies. The purpose of this study was to evaluate the feasibility and utility of this technique in brain and thyroid imaging. A 7 pinhole collimator having 5.5 mm pinhole apertures and a 13 cm field of view at 12 cm from the collimator surface was used in conjunction with a widefield camera. Axial full-width-half-maximum (FWHM) resolution was approximately 1.0 cm in a parallel plane 12 cm from the collimator face. Z-axis FWHM resolution was approximately 1.5 cm at this distance. After definition of the appropriate procedures for use of this system for cerebral and thyroid studies in normals, patients with cerebral and thyroid lesions were successfully imaged. Using 20 mCi Tc-99m DTPA for brain scans and 5 mCi Tc-99m pertechnetate for thyroid studies, images of 750K were obtained in 2-5 min. Tomographic reconstruction time is currently 90-120 sec. Small cerebral metastatic lesions were clearly delineated. The presence or absence of recurrent intracerebral tumor in patients with activity in skull flaps was more readily apparent on tomographic studies than on standard brain scans. Tomograms definitely demonstrated cold thyroid lesions of 1 cm which were poorly seen on standard pinhole images. Results suggest that for certain clinical problems, pinhole tomography has advantages over standard techniques for brain and thyroid imaging.

THE USE OF SEVEN-PINHOLE TOMOGRAPHY IN LIVER IMAGING — A PHANTOM AND CLINICAL EVALUATION. V.A. Brookeman, A.J.W.

Hilson, M.N. Maisey. Guy's Hospital, London, UK.

Seven-pinhole emission tomography has been applied to liver phantoms and patient studies to determine its feasibility and possible role in clinical liver scintigraphy. A set of 3 anthropomorphic liver phantoms, 1 normal and 2 abnormal containing lesions of 1, 2, and 3 cm diameter (1), surrounded by scattering material (rubber torso) was employed. Only part of the liver may be imaged at one time and each phantom was imaged anteriorly with the tomocollimator placed in turn over the right and left lobes and porta hepatis at different distances from the torso surface from 0 to 6 cm at 1 cm intervals. With tomographic reconstruction, the 2 and 3 cm lesions were clearly resolved, and possibly the 1 cm lesion, more clearly than with planar emission imaging. However the software did not reconstruct a normal right lobe to a uniform distribution but produced a central dip. Tomographic imaging was performed on 34 patients also having routine planar emission liver studies. The tomocollimator was positioned anteriorly over the equivocal area where possible and 10 sections were reconstructed. Lesions not visible on the planar emission study were seen and we were able also to distinguish between the normal and abnormal porta hepatis. We conclude that seven-hole tomographic imaging is of value in liver scintigraphy particularly as an adjunct to planar emission imaging in equivocal studies.

1. MOULD RF: A liver phantom for evaluating camera and scanner performance in clinical practice. Br J Radiol 44: 810-811, 1971.

CONTRIBUTIONS OF THE SEVEN PIN HOLE COLLIMATOR TO CISTERNOGRAPHY. **F.H. DeLand, E.E. Kim, P.A. Domstad, S.L. Magoun. Veterans Administration and University of Kentucky Medical Centers. Lexington, KY.**

A series of patients with clinical diagnosis of cerebral atrophy were examined by routine imaging, tomographic radionuclide imaging with a 7 pin hole collimator, and transmission computerized tomography. To enter the study routine imaging had to show: (1) evidence of transient ventricular penetration by the radiotracer in the 6 hr examination, (2) no ventricular retention at 24 hr, and (3) delayed flow of the radiotracer over the cerebral convexities at 24 hr. Comparative analysis of the data was limited to the 24 hr examination. Images were obtained in routine standard projections (2-D) and in 1 cm tomographic slices with the 7 pin hole collimator. A number of differences were observed between the 2-D and the tomographic images. Although in cerebral atrophy, routine anterior, posterior, and vertex projections are usually relatively symmetrical, tomography demonstrated frequent asymmetries. Major differences observed were asymmetry of flow beneath the frontal lobes and asymmetrical and fractionated flow through the sylvian cisterns. Although ventricular penetration was not present on the routine images, ventricular radioactivity was observed in the tomographic images and again was asymmetrical and fractionated. These results indicate that: (1) the collection of data by routine camera imaging of cisternograms masks relatively marked asymmetries and fractionations of flow in the cisterns and lateral ventricles, (2) obscures mid-line structures such as dilated 3rd ventricles, and (3) tomography provides a more accurate and sensitive depiction of CSF flow.

A NEW QUALITY CONTROL PHANTOM FOR GATED ACQUISITION SYSTEMS R.R. Price, F.D. Rollo, R. Steckley, M. Born, J.A. Patton, J.J. Erickson, and J.J. Touya, Vanderbilt Medical Center and VA Medical Center, Nashville, TN 37232.

The traditional validation of a multiple gated acquisition system requires complex correlation of radionuclide and contrast ventriculography. A simple dynamic cardiac phantom has been constructed which provides the capability of performing quality control testing of system hardware and software for ejection fraction and wall motion. The phantom consists of two chambers shaped as ellipsiods of revolution stacked vertically to simulate the left ventricle and atrium. When rotated, the chambers exhibit wall motion in phase with the rotational (cardiac) cycle. The chambers are rotated by means of a variable speed D.C. motor capable of providing an adjustable heart rate ranging from approximately 20-200 beats per minute. An ECG trigger pulse is generated for each rotation. The actual amount of wall motion for each ellipsoid at any phase of the cycle is determined by the heart rate and image framing rate. Ejection fraction is controlled by a series of calibrated attenuators on the systolic surfaces of the chambers. A flood source with paraffin attenuators provides a realistic representation of pericardiac background activity.

This phantom is mechanically simple and easy to use, yet provides an assessment of the three major parameters of gated acquisition: heart rate, ejection fraction, and wall motion. Thus, it is ideally suited for quality control and comparative evaluation of gated acquisition systems.

THE NUCLEAR STETHOSCOPE - EXPERIENCE WITH A COMMERCIAL VERSION. J.J. Steinbach. Veterans Administration Medical Center, Buffalo, NY.

Ejection fraction (EF) was determined using a commercial version of the nuclear stethoscope and compared with scintillation camera and angiographic EF studies. Thirty-five patients with suspected coronary artery disease on whom gated camera EF was done were subsequently examined by the nuclear stethoscope. EF values were obtained using the beat by beat (BB) and gated modes. Each patient was studied by one or more investigators (1-6). One hundred ten investigator-patient measurements (each = mean of 20 values) were obtained for the BB mode and 87 for the gated mode. Nineteen of the 35 patients had recent angiographic studies.

Analysis of variance of within observer and between observer variability showed that between observer variability was significantly greater ($p<0.001$) from that of within observer. The estimated observer variance was 102 (SD=10.1, CV of mean=22%) for the BB mode and 209 (SD=14.4, CV of mean=24%) for the gated mode.

Comparison of gated camera EF with angiographic values revealed a correlation coefficient of 0.83 (y-intercept -5). Comparison of the gated camera studies with the nuclear stethoscope studies revealed a correlation coefficient of 0.61 for the BB mode and 0.59 for the gated mode. Comparison of the angiographic EF with the nuclear stethoscope revealed a correlation coefficient of 0.59 for the BB mode and 0.52 for the gated mode.

Observer variance might be experience related. In our hand, this instrument did not lend itself for immediate clinical application.

MONITORING LEFT VENTRICULAR FUNCTION WITH INDIUM-113m AND A CARDIAC PROBE. S.C. Liu, H.N. Wagner, Jr., Z.J. Chen, and S.H. Wang. Chinese Academy of Medical Sciences, Fu Wei Hospital, Peking, China, and Johns Hopkins Medical Institutions, Baltimore, MD.

Left ventricular ejection fraction was monitored with a cardiac probe (nuclear stethoscope) in 68 studies of 22 normal subjects and 24 patients with heart disease (7 with CHD; 13 with congestive cardiomyopathy; 4 other). In 20 normal persons, technetium-99m RBC's were compared with indium-113m (pH 3.0) which binds to transferrin after intravenous injection. With Tc-99m, average EF was 0.57 $\pm$ 0.07 (1 s.d.); with In-113m, average EF was 0.55 $\pm$ 0.08 (no significant difference). Sequential measurements on different days revealed good reproducibility (coefficients of variation were between 1.4 and 7.5% with Tc-99m and between 3.4 and 5.4% with In-113m; average difference 4.8%). The average LVEF in normal persons was 0.60 $\pm$ 0.10; in CHD 0.34 $\pm$ 0.13; in congestive cardiomyopathy, 0.37 $\pm$ 0.11. With isometric hand grip exercise, there was no significant difference in the response of EF between normal persons and patients with cardiac disease. We conclude: (1) that In-113m bound to transferrin can be used to monitor left ventricular function with the cardiac probe; (2) EF can be measured with good reproducibility; (3) isometric handgrip exercise may be inadequate stress for detection of cardiac disease; (4) the cardiac probe and In-113m transferrin can be used to evaluate the left ventricular response to various drugs, including known beta adrenergic stimulating and

blocking agents as well as Chinese traditional herbal medicines. The use of In-113m with the cardiac probe is important because this agent is more available than Tc-99m in developing countries.

DETERMINATION OF LEFT VENTRICULAR EJECTION FRACTION EMPLOYING A NON-COMPUTERIZED CARDIAC MODULE. F.S. Prato, K. Wilkins, L. Reese, St. Joseph's Hospital and University of Western Ontario, London, Ontario, Canada.

The cardiac module (CM), an inexpensive non-computerized Anger camera accessory, was evaluated for its determination of left ventricular ejection fraction (LVEF) and left ventricular wall motion (WM). Twenty-nine subjects were compared to established first pass (FP) and gated blood pool techniques (GBP).

For assessment of WM, gated images of the heart in both left and right anterior oblique projections were produced by the CM. As tested these were not found to be useful.

Two gated modes of operation of the CM were used in the determination of LVEF. In the automatic mode (CMA), left ventricular background is automatically sampled within an anulus around the left ventricle. In the manual mode (CMM), background is sampled over the left lung. Each determination took about 5 minutes. The CMM was superior to the CMA in reproducibility ($r = 0.92$ compared to $r = 0.85$) and intertechnique comparisons to GBP ($r = 0.85$ compared to $r = 0.78$) even though it was expected, because of design, that the CMA would have been superior.

Computer simulation indicated that the reproducibility and hence the intertechnique comparisons could not be improved for the CMA unless repeat determinations of LVEF were averaged, and/or background selection was altered so that background counts were increased. Preliminary experiments indicated that results can be improved in this way.

For acceptable results from the CM multiple determinations of LVEF must be averaged, and the background critically selected.

2:00-3:30 Room 2043

CLINICAL

ADVANCES IN CARDIAC RADIOPHARMACEUTICALS

Session Chairman: Leonard B. Holman
Session Co-Chairman: Bertram Pitt

IN-111 LABELED AUTOLOGOUS LEUKOCYTES (IN-WBC) FOR IMAGING INFLAMMATORY RESPONSE TO ACUTE MYOCARDIAL INFARCTION (MI) IN MAN. R.A. Davies, M.L. Thakur, H.J. Berger, F. Wackers, A. Gottschalk and B. Zaret. Yale University, New Haven, CT

The feasibility of imaging the inflammatory response to transmural MI using In-WBC was studied in 36 patients (pts). Six of these received 500 μCi In-WBC at 0-24 hrs, 12 at 24-48 hrs, 12 at 49-72 hrs, 4 at 73-96 hrs and 2 at 92-112 hrs after onset of MI. Cardiac imaging was performed 24 hrs later. Positive images (+) were obtained in 6/6, 8/12, 6/12, 1/4 and 0/2 in the respective temporally defined patient groups (21 (+) and 15 (-)). Six pts with MI receiving free In-111 oxine and 6 with stable coronary artery disease receiving In-WBC served as controls and gave negative (-) images. The in vitro In-WBC adherence and phagocytosis studied in 8 and 10 pts respectively was similar in pts with (+) or (-) images. Peak serum creatine kinase averaged 1030 + 121 i.u./l in pts with (+) images vs 725 ± 87 i.u./l in (-) images (insignificant difference). In pts with (+) images 14 had anterior and 7 had inferior MI compared to 5 anterior and 10 inferior in pts with (-) images. 15/21 (+) vs 7/15 (-) received lidocaine or procainamide and 14/21 (+) vs 4/15 (-) received indomethacin or aspirin. Pts with (+) images were younger (53 ± 2 yr vs 65 ± 3 yr, $P < 0.05$) and received In-WBC earlier (43 ± 4 vs 63 ± 7 hr, $P < 0.05$) following MI than those with (-) images.

The data indicate that In-WBC has potential for imaging the inflammatory response to MI. The presence of a (+) image correlated with both the age of the MI and the age of the patient. Factors resulting in (-) images are not completely understood at this time.

INDIUM-111-PLATELETS FOR THE INVESTIGATION OF STERILE ENDOCARDITIS ASSOCIATED WITH FOREIGN INTRACARDIAC SURFACES: WORK-IN-PROGRESS. S.D. Sarkar, J.B. Parra-Campos, R. Bower. Wayne County General Hospital, Westland, MI.

Platelets are involved in the formation of non-bacterial thrombotic vegetations associated with substitute heart valves or with indwelling cardiac catheters. We investigated the use of In-111-platelets for imaging these vegetations and for platelet survival studies in a dog model. Cardiac vegetations were produced by placing a polypropylene catheter under sterile conditions in the left or right side of the heart through an incision in the left carotid or jugular vessels, respectively. Autologous platelets labeled with 200-350 microcuries of In-111-oxine by the "button-plasma" method, were injected IV at 3 or 24 hr after catheterization. Scintiphotos, obtained at 24-48 hr after tracer, were compared with autopsy findings. Heart lesions from 2 randomly selected dogs were sent for histopathology and bacterial culture, respectively. Platelet survival was studied in 4 normal dogs, 4 with left heart catheter and 3 controls with ligated left carotid.

All endocardial and/or valvular lesions were imaged in 7/7 dogs. Mean radioactivity concentration in vegetations from 2 dogs, 24 hr after tracer and 27 hr after catheterization, was 79 and 406 times greater than in blood and myocardium, respectively. Microscopic examination showed bland thrombus and culture at 1 day after catheterization showed no growth. Mean half life of platelets in normals, 1.15±0.28(1SD), was similar to that in controls(1.19±0.15), but longer(p less than 0.01) than that in dogs with left heart catheters(0.78±0.14). The results suggest that this approach may provide a suitable means of studying the pathogenesis of heart vegetations due to foreign surfaces.

NONINVASIVE RADIOISOTOPIC TECHNIQUE FOR DETECTION OF PLATELET DEPOSITION IN BJÖRK-SHILEY MITRAL PROSTHESIS AND RENAL EMBOLISM IN DOGS. M. K. Dewanjee, M. P. Kaye, V. Fuster, Mayo Clinic and Mayo Foundation, Rochester, MN.

At 24 hours after implantation of Björk-Shiley mitral prosthesis in five dogs, in vivo images were obtained with a gamma camera after intravenous administration (0.5-0.6 mCi) one hour postoperatively of autologous Indium-111-labeled platelets. The site of platelet deposition in the Dacron (D) ring and peripheral damaged tissue (Per Tis) is clearly delineated in the scintiphoto. In vitro biodistribution (% injected dose) of the five implanted and seven normal dogs performed with a gamma counter was tabulated below:

	Blood (%)	Kidneys(%)	D Ring(%)	Per Tis(%)
Normal (n=7)	45.1 ± 10.6	0.7 ± 0.4	---	---
Implanted (n=5)	28.5 ± 6.8	1.6 ± 0.6	0.3 ± 0.1	0.2 ± 0.1

The strut and pyrolytic carbon-coated disc retained only (.0033 ± .0004)% and (.0031 ± .0003)% respectively.

There was a 2.3-fold increase of labeled platelets in kidneys of implanted dogs due to renal trapping of microembolism. Also, three- to fivefold increase in ratios of lung, brain, cardiac, and skeletal muscle to blood indicates that internal organs and whole body work as filter for microembolism generated by cardiovascular surgery and use of heart-lung machine. Twenty percent of the administered platelets are consumed in surgical repair of damaged tissue. Indium-111-labeled platelets thus provide a sensitive marker for noninvasive imaging of Björk-Shiley mitral prosthesis, thromboembolism after implantation of prosthetic device, and in vitro quantitation of surgical consumption.

N-13 AMMONIA AS AN INDICATOR OF FLOW: FACTORS INFLUENCING ITS UPTAKE AND RETENTION IN MYOCARDIUM. H. Schelbert, M. Phelps, H. Huang, E. Hoffman, C. Selin, H. Hansen, D. Kuhl. UCLA School of Medicine, Los Angeles, CA.

Previously we characterized N-13 ammonia (NA) as an indicator of myocardial blood flow (F) suitable for positron tomography. In this study we examined the effects of changes in F, the cardiac hemodynamic and metabolic state and in plasma pH on the extraction fraction (E) and clearance-time (T) of NA in myocardium. In 155 studies in 35 dogs NA was injected into the circumflex coronary artery. E and T were determined from the peak and slope of the residue function of the myocardial time-activity curve recorded with a scintillation probe. During its initial capillary transit NA was nearly 100% extracted followed by F related back diffusion that competed with metabolic trapping. E is the ratio of NA retained in myocardium to total injected NA. At F of 0.8ml/min/gm, E averaged 0.87± 0.05 SD and T 4.8±0.6 hrs. Both were inversely related to F by $E = -0.607 \exp(-125/F)$ and $T = 358 \exp(-0.00027 \times F)$. Cardiac work, heart rate, propranolol, isoproterenol and changes in glucose uptake had no effect on E and T. High plasma pH (7.46 - 7.66) did not affect E and T but E fell by 16% ($p<0.01$) at low plasma pH (7.03 to 7.12). Glutamine synthetase inhibition by methionine sulfoximine depressed E indicating that NA is fixed in myocardium by amination of glutamate to glutamine. Thus, metabolic trapping is important for fixation of NA in myocardium but over a wide range of conditions it is not affected by changes in cardiac metabolism and function. We conclude that T and E of NA are mainly related to F. The near linear relationship between E x F and F at physiologic F's confirms the suitability of NA as a flow indicator.

METABOLIC CHANGES IN ACUTE REGIONAL MYOCARDIAL ISCHEMIA DETERMINED BY F-18 DEOXYGLUCOSE (FDG) AND C-11 PALMITATE (CPA) AND POSITRON EMISSION TOMOGRAPHY. H. Schelbert, M. Phelps, E. Hoffman, G. Robinson, H. Hansen, C. Selin, and D. Kuhl. UCLA School of Medicine, Los Angeles, CA.

In acute myocardial ischemia glycolysis is known to increase while β-oxidation of free fatty acids (FFA) declines. The potential of positron emission tomography (PCT) to noninvasively demonstrate these changes was studied in 9 dogs. Ischemia was induced by stenosing the anterior descending coronary (LAD) and atrial pacing. Oxygen (O), glucose (GLU) and FFA consumption and lactic extraction in LAD myocardium were determined from the A-V differences and blood flow (MBF) measured by microspheres. To compare MBF to metabolism by PCT, ischemia was induced twice: For PCT imaging of 1) MBF with N-13 ammonia; and 2) local GLU or FFA uptake with FDG or CPA. With pacing, MBF in LAD myocardium fell by 20.3% (ns), consumption of O by 30.2% (ns), and of FFA by 62.8% ($p<.01$). GLU uptake increased by 63.8% ($p<0.05$). Lactic acid extraction fell by 88.3% ($p<0.01$). On the PCT images, MBF and FDG or CPA concentrations fell in LAD myocardium; CPA concentrations matched MBF while FDG concentrations were in excess of MBF. Using in vitro tissue counting, FDG and CPA concentrations were linearly related to MBF. However, at MBF < 3 to 6ml/min/gm the linear relationship was maintained for CPA while FDG concentrations were in excess of MBF. Thus, FFA uptake in ischemia is proportional to MBF, while GLU uptake increases above MBF. PCT clearly delineated these regional changes in FFA and GLU metabolism. We conclude that PCT may permit noninvasive characterization of metabolic changes associated with acute myocardial ischemia.

THE METABOLISM OF ω-I-123-HEPTADECANOIC ACID IN PATIENTS WITH HEART DISEASE. A. Höck, Ch. Freundlieb, K. Vyska, B. Lösse, R. Erbel, L.E. Feinendegen. Institute of Medicine, Nuclear Research Center Jülich, FR Germany.

Previous studies have demonstrated the suitability of ω-I-123-heptadecanoic acid (IHA) for myocardial metabolic studies [1]. The present paper reports data obtained in patients with congestive cardiomyopathy (COCM) and coronary artery disease (CAD). In 35 patients suffering from CAD examined at rest the ischemic areas could be recognized in IHA scintigrams as activity accumulation defects. According to the observed rate of fatty acid turnover determined in dynamic studies with IHA, these patients could be subdivided in two groups. In the first group in ischemic areas prolonged half times of IHA elimination (30-70 min) were detected. In the second group in the ischemic areas normal or slightly shortened half times of IHA elimination (18-29 min) were observed. During exercise, in ischemic regions, accumulation defects were accentuated and half times of IHA elimination significantly prolonged. In normal areas no changes of half times of IHA elimination were detected. Following coronary dilatation in patients with normal or slightly shortened half times of IHA elimination, the accumulation defects disappeared. In patients with COCM there were areas with diminished IHA accumulation as well as areas with significantly shortened half times of IHA elimination (7-11 min). No correlation between the localization of accumulation defects and areas of shortened half times of IHA elimination was observed in the case of COCM.

IHA seems to provide clinically valuable information about myocardial metabolism.

[1] K. Vyska et al. J. Nucl. Med. 20: 650 (1979) (abstr.)

LOCALIZATION OF ANTIMITOCHONDRIAL ANTIBODY IN EXPERIMENTAL CANINE MYOCARDIAL INFARCTS. P.V. Kulkarni, R.W. Parkey, L.M. Buja, S.E. Lewis, E. Eigenbrodt, M.J. Stone, F.J. Bonte, and J.T. Willerson. U. Texas Health Science Center at Dallas, Texas.

Alterations in cell and subcellular membrane integrity occur during evolving ischemic myocardial injury. We tested the hypothesis that an antibody against human liver mitochondria [antimitochondrial antibody (AMA) developing in a patient with primary biliary cirrhosis (PBC)] could identify altered cell membrane integrity in experimental canine myocardial infarcts (MI). Twelve dogs had proximal LAD coronary artery ligations for 1 hour followed by IV injection of 2 mg of I-131$(Fab')_2$ fragments from either a control human IgG (6 dogs) or an AMA IgG (6 dogs). The animals were sacrificed 5 days later and tissue obtained from ischemic (I) and nonischemic LV for analysis. The I-131 $(Fab')_2$ AMA IgG concentrated maximally in the central I endocardium (endo) [mean value above normal tissue levels of 9.2±3.5, (S.D) vs. 4.6±3.3 for control $(Fab')_2$ IgG, ($p<0.05$)]. There was also twofold greater AMA $(Fab')_2$ in the central I epicardium (epi) and the I periphery endo and epi. Immunofluorescence microscopy using intact IgG demonstrated granular subcellular localization of AMA in both normal and I canine myocardium; control IgG failed to localize in either. Thus, an AMA concentrates in irreversibly damaged myocardium after experimental canine MI. Presumably, this occurs because of altered cell membrane integrity and exposure of mitochondrial membranes to the AMA.

HEART IMAGING WITH AN ^{123}I-NORADRENALINE STORAGE ANALOG. D.M. Wieland, L.E. Brown, K.C. Worthington, W.L. Rogers, D.P. Swanson, W.H. Beierwaltes and D.D. Marsh. University of Michigan Hospital, Ann Arbor, MI.

Despite the physiological importance of noradrenaline as an adrenergic transmitter, no radiopharmaceutical exists that can assess catecholamine hormone accumulation and turnover in peripheral tissue. We report the evaluation of a "non-metabolizeable" radioiodinated aralkylguanidine that shares the same uptake and storage mechanism as noradrenaline in adrenergic nerves.

Tissue-distribution studies of I-125-meta-iodobenzylguanidine (m-IBG) reveal high and selective uptake in the heart of the rat, dog and rhesus monkey. Peak heart concentrations and heart-to-blood ratios are similar to those obtained with thallium-201. Other organs with rich adrenergic innervation, such as spleen and adrenal medulla, also show high uptake and retention. The compound does not significantly penetrate the blood-brain barrier.

The mechanism of heart localization of I-125-m-IBG was probed pharmacologically. Pretreatment of rats with d-amphetamine, a compound known to both release and inhibit the uptake of noradrenaline by nerve cells, lowers the heart concentration of I-125-m-IBG by 35-50%. Similar treatment with reserpine, a drug that selectively blocks vesicular uptake in the neurons, lowers the heart accumulation by 30-50%. These blocking studies suggest that the heart retention is mainly due to specific uptake in the adrenergic neurons where it is partially trapped in the noradrenaline storage vesicles.

Two dogs, each injected with 5 mCi of I-123-m-IBG, gave

excellent tomographic heart images from 5 min. to 4 Hr. using a wide field-of-view gamma camera with a 7 pinhole collimator.

2:00-3:30 Room 3038

INSTRUMENTATION

GENERAL I

Session Chairman: Paul Murphy
Session Co-Chairman: Thomas Lewellen

EXTENDED AREA EMISSION TOMOGRAPHY USING A CONVENTIONAL CAMERA SYSTEM. K.W. Logan, K.A. Hickey, and R.R. Hurst. Veterans Administration Hospital and University of Missouri, Columbia, MO.

With the introduction of the 7 pin-hole collimator near practical emission tomography (ET) became a clinical reality for many laboratories. Although its cost is not excessive its present usefulness has been limited to small organs and it requires a computer for image reconstruction. A method to further extend the practical use of ET employing conventional standard field of view camera systems that will image any size organ and not require computer reconstruction of the ET image is under development in our laboratory. The approach requires the adaptation of several small and inexpensive accessories to a standard scintillation camera with whole body imaging table, multi-imager and a commercial converging collimator (Nise, Inc., Cerritos, CA). Conversion from the ET to the conventional imaging mode only requires changing of the collimator. The tomographic effect is created by changing relative source and camera positions from the movement of the table. A series of phantom studies have shown excellent tomographic plane separation to depths of 10 centimeters. Image contrast and in-plane resolution has been shown to exceed that of 7 pin-hole tomographics in several instances. These results lead us to conclude that this method of ET may be the most practical yet to image any body organ or the whole body.

RECENT IMPROVEMENTS IN LONGITUDINAL SECTION TOMOGRAPHY. J.A. Patton, R.R. Price, D.R. Pickens, and F.D. Rollo, Vanderbilt University Medical Center, Nashville, TN.

A new improved version of the Searle Pho/Con tomographic scanner has recently been announced. This new system (model 192) has more photomulitplier tubes (19 vs. 7), larger crystal diameter (9.3" vs. 8.5"), thinner crystal (½" vs. 1"), improved electronics (LFOV vs. Pho/Gamma IV),better intrinsic resolution (6.5mm vs. 15mm FWHM), and improved collimation. Line spread functions and modulation transfer functions demonstrate the superior imaging capabilities of the new system. The spatial resolution vs. distance characteristics of the new scanner are slightly superior to that of a state-of-the-art LFOV camera with a high resolution collimator. The old model Pho/Con had the depth response characteristics of a rectilinear scanner with a focussed collimator due to the coupling of a high resolution collimator with a poor intrinsic resolution camera. The new model has the depth response characteristics of a camera with a converging collimator due to the improvement in intrinsic resolution of the camera to match that of the collimator. Plane source sensitivity measurements show the new Pho/Con with the high resolution collimator to have approximately the same sensitivity as the old version with all-purpose collimator; however, the camera is still 2.4 times as sensitive as the scammer. Clinical images demonstrate significant improvement in image quality over the previous model and provide spatial resolution comparable to that of the large field camera with the added benefits of tomography. A specific improvement in our department has been achieved in the areas of total body bone and tumor imaging, where we have been able to maintain resolution and obtain tomographic information while reducing study times.

LONGITUDINAL AND TRANSVERSE SECTION SCANNING WITH THE SEARLE PHO/CON-192. D.R. Pickens, R.R. Price, J.J. Erickson, J.A. Patton, and F.D. Rollo, Vanderbilt Medical Center, Nashville, TN.

A Searle PHO/CON-192 Multiplane Imager has been interfaced to a PDP-11/34 minicomputer in our laboratory. Programs have been developed to collect and process scan data with this system. Computer reconstruction by backprojection of the list mode data collected during the scans produces longitudinal planes at any level and separation. Transverse planes are also produced by backprojection. Images can be produced in the following formats: 64 X 64, 128 X 128, and 400 X 256 pixels. Several images can be formed simultaneously. Post-reconstruction image processing is used to decrease background noise and increase contrast. Multiplane simultaneous deconvolution methods for removal of off-plane contributions on longitudinal planes are being investigated. Preliminary results are encouraging.

Both phantom and patient studies have been performed. Longitudinal and transverse sections are presented for Tc-99m phantom studies and Tl-201 myocardial scans. Longitudinal images are shown for Tc-99m bone scans and Ga-67 whole body scans.

These computer processed images demonstrate the capabilities of the digital data collection and processing system. We believe that the advantages of this system are: 1) any plane can be reconstructed at any time following data collection; 2) transverse images can be produced--a reconstruction mode not possible otherwise; 3) post-reconstruction deblurring and filtering can be performed.

HIGH PRESSURE, MULTIWIRE PROPORTIONAL CHAMBER FOR CARDIAC IMAGING. R.E. Zimmerman, F.H. Fahey, R.E. Burns. Harvard Medical School and Xentronics, Inc., Boston, MA.

A 10 Atm. Xenon-filled multiwire proportional chamber has been constructed for use in cardiac imaging for the energy range 50-100 keV. The chamber consists of an anode with two cathode wire planes and a drift region. Position signals are obtained from the cathode planes using the integral delay line method. The drift region extends 2.2 cm either side of the anode-cathode plane resulting in a total chamber thickness of 5 cm. Passive getters are used to purify the gas in the sealed chamber. Energy signals can be obtained from the anode or from the summed cathode signals. The total outside dimensions are 40 cm diameter by 25 cm thick. The field of view is 17 cm.

The intrinsic spatial resolution is < 2 mm (FWHM) over the energy range of interest. Energy resolution is at present 30-40% FWHM at 60 keV and will improve with the addition of more purifiers. Sensitivity was measured relative to an Anger camera with a 6 mm thick crystal over the energy range of 60-81 keV and was consistent with calculated values which took into account the 2.5 mm thick entrance window and the 5 cm thick interaction region, i.e., approximately 70% of the Anger camera sensitivity. Sensitivity and resolution are very dependent on pulse height analyzer settings since escape peaks are very prominent.

It is expected that this camera will prove very useful in the performance of cardiac imaging studies with present and new low energy isotopes such as Ta-178, Xe-133, Ir-191m and Tl-201.

A GERMANIUM EMISSION CAMERA WITH PARALLEL PLATE COLLIMATION. M.M. Urie, W. Mauderli, L.T. Fitzgerald, C.M. Williams. University of Florida, Gainesville, FL.

A unique collimator-detector geometry has been employed to obtain better spatial and energy resolution than existing gamma cameras. A high purity germanium detector is divided into 30 parallel independent channels (1.5 mm wide) which are positioned behind parallel collimating plates (40 mm high). Activity distributions are mathematically reconstructed from data measured at various angular orientations. Both hot spot resolution and cold lesion detection capabilities of this device are superior to that of present gamma cameras with high resolution collimators. Bar phantom resolution at the face is 3 mm and 6 mm at 10 cm depth. Cold lesions at least 0.5 cm smaller in diameter are imaged with excel-

lent size correlation. Both the geometry and the energy resolution (3.5 keV FWHM for Tc-99m) contribute to these improvements, the clinical significance of which is demonstrated in rat images. Imaging times are comparable, indicating satisfactory sensitivity.

A DISCONTINUOUS MOSAIC CADMIUM TELLURIDE ARRAY DETECTOR
J. Lazewatsky, R. Moore, N. Alpert, G. Entine*, H.W. Strauss
Mass. General Hospital, Boston, MA, *R.M.D. Corporation, Watertown, MA.

The determination of cardiac function with radionuclides requires that the left ventricle be adequately sampled, and that there be little change in sensitivity as the heart moves toward or away from the detector. The measurement can be made either with a small detector and a single long bore collimator to achieve the required field size and to limit the effects of change in cardiac position, or with a parallel hole collimator with a field size comparable to that of the heart.

For patient safety and convenience the nuclear detector to measure cardiac function during normal daily activities should employ low voltage, have a high degree of reliability, and should be of small size and minimal weight. A multicrystal discontinuous mosaic detector was made of 7-16mm diameter CdTe crystals packaged in a 10cm diameter can lined with 2mm lead for side and back shielding, and containing a 3.5mm long triangular hole parallel hole collimator which weighs 220 grams.
The detector uniformity for a point source at 10cm is ±50%, but is less than 10% but when a 2cm source is sampled. By connecting the CdTe crystals in parallel, there was a 7-fold increase in noise, with a 3-fold increase in signal (total-noise), compared to the value expected by summing the results of individual array elements. These data suggest that the signals from each detector must be sampled and processed prior to summation. A preliminary study utilizing a beating heart phantom indicate that the array response is linear with changes in volume. We expect this array will be useful in ambulatory cardiac function tests.

THE EFFICACY OF HIGH CONTRAST FILM COPYING FOR Tl-201 MYOCARDIAL IMAGE PROCESSING. H.M. Park, B.E. Oppenheim, R.W. Burt, A.R. Siddiqui, H.N. Wellman, C.R. Appledorn, and S. Lewis. Indiana University School of Medicine, Indianapolis, IN.

Various methods for enhancing Tl-201 myocardial images have been described in the literature. Most of them use some sort of computer processing which may not be available to many hospitals. This investigation was undertaken to evaluate the efficacy of high contrast film copying for enhancing contrast in analog Tl-201 myocardial images.

Stress and rest images of 47 patients with coronary artery disease and 19 patients with normal coronary arteries as determined by coronary angiography were studied. Five blinded observers interpreted each patient's study presented in 4 different displays: (1) original analog (unprocessed) images, (2) computer processed images, (3) high contrast copies of analog images and (4) analog plus computer images. Computer processing involved background cut-off at 5 standard deviations below the maximum value in the image. Results were analyzed by constructing ROC curves.

Results disclosed (1) a higher rate of correct diagnosis was realized with copy films than with analog images alone by 4 out of 5 observers, and (2) the average score for the computer processed images was slightly better than for the copy films although 2 out of 5 readers did better with copy films. For a false positive rate of 25% the average true positive rates were 56% for the analog images, 67% for the copy films, 68% for the computer processed images and 72% for the combination of analog computer images.

Thus Tl-201 image processing, either by computer or by high contrast film copying, gave essentially equivalent results surpassing results obtained with unprocessed images.

SPATIAL RESOLUTION FOR Tl-201 AS A FUNCTION OF WINDOW WIDTH, H.H. Hines, E.C. Glass, G.L. DeNardo, University of California, Davis Medical Center, Sacramento, CA

The K x-rays (70, 80 keV) of Tl-201 are used to image the myocardium. If a wide window is used, spatial resolution may decrease because scattered photons from the higher energy photons from Tl or from radiocontaminates. We studied the relationship between spatial resolution and imaging time for different window widths. FWHM and FWM-10% were determined from line spread functions acquired from a 37 PM camera (0.25" crystal, LEAP collimator). The line source, a 1 mm ID tube filled with Tl-201, was placed at mid depth in a water bath 10 cm deep. The results are:

Window (%)	Time (min)	FWHM (mm)	FWM-10% (mm)
10	10.0	8.0	16.3
15	7.4	8.5	17.4
20	5.7	8.9	18.1
25	5.1	9.6	20.7
30	4.6	10.0	24.0
35	4.3	10.3	26.5
40	3.9	10.7	27.3

To assess observer response to effects of window widths on resolution, observers ranked 300K images of a Rollo phantom containing Tl-201 and separated from the collimator by 2.5 cm of water. 11/12 observers ranked the 20% window image (WI) first, 11/12 the 25% WI second, 8/12 the 30% WI third and 8/12 the 40% WI fourth.

In conclusion, window widths of 15-20% provide an optimal compromise between imaging time and spatial resolution for conventional Tl imaging. Wider windows noticably decrease resolution while yielding only modest decreases in imaging times.

4:00-5:30 Room 2048

SCIENTIFIC MEETING HIGHLIGHTS

Session Chairman: Henry N. Wagner, Jr.

4:00-5:30 Room 3038

INSTRUMENTATION

GENERAL II

Session Chairman: Audry Wegst
Session Co-Chairman: Guy Simmons

REMOTE SYSTEMS FOR CHEMISTRY USING LARGE AMOUNTS OF CYCLOTRON PRODUCED RADIONUCLIDES. J.R. Barrio, G.D. Robinson, and A. Najafi. UCLA School of Medicine, Los Angeles, CA.

A reliable approach to designing systems for chemical processing of cyclotron targets and for the synthesis of organic compounds with short-lived radionuclides has been developed.

The processes, although some times complex, are broken down into the required number of unit operations (e.g., adding reagents, removing solvent, extraction, chromatography, etc). These simple unit operations are performed on a remote, semiautomated basis where standard laboratory glassware and equipment are normally used in conjunction with solenoid valves.

Chemist interaction is entirely remote and involves addition of reagents, transfer of fluids by application of pressure or vacuum, and the initiation of each operation by actuating the appropriate switch or combination of switches.

This approach has been applied to designing systems which are now being used for target processing and preparation of the Zn-62/Cu-62 generator (20 mCi), synthesis of F-18 labeled 2-deoxy-2-fluoro-D-glucose (two runs/day, yield = 20-25 mCi/run), and synthesis of C-11 labeled palmitic acid (multiple runs/day, 25-30 mCi/run).

Advantages of this approach include: very low cost, rapid reconfiguration to accomodate new or revised syntheses, reduced radiation exposure to the chemist ($\leq$ 1 mR/run), and highly reliable, routine production of large mCi amounts of clinically useful radiopharmaceuticals.

INSTRUMENTAL SPECIFICATIONS FOR HIGH-RESOLUTION POSITRON TOMOGRAPHS. J. A. McIntyre. Texas A&M University, College Station, TX.

The spacing, d, and width, w, of the gamma ray detectors in a positron tomograph determine the spatial resolution of the reconstructed image produced by the tomograph. With the positron range data of Derenzo now available, a calculation has been made of the effect of d and w on the image of a point source of positrons. In addition to the source spread introduced by the positron range, the effect of the misalignment of the two annihilation gamma rays was also incorporated into the point-spread-function f(r) of the positron source. A Ga-68 source was used for the analysis since the positron range for Ga-68 is greater than that for the important isotopes, C-11, N-13, O-15, and F-18. The FWHM of the point-spread-function f(r) was found to be 3.1 mm.

Reasonably acceptable reconstructions of f(r) were obtained for d and w equal to 2 mm. If d was increased to 4 mm, the FWHM of f(r) increased by 60% and a 10% "aliasing" negative intensity was generated in the tail of the reconstructed distribution. The sampling distance d should thus not be larger than 2 mm for sources with intensity variations occurring in distances of less than about 3 mm.

While a width w of 2 mm is also preferable, a width of 4 mm introduces only an additional 20% in the FWHM of f(r). However, 8 mm wide detectors increase the FWHM by 80%. Since detectors wider than 4 mm should therefore not be used, the introduction of a "wobble" is not required to obtain the necessary 2 mm sampling distance.

EFFICIENCY CONSIDERATIONS FOR Xe-133 CHARCOAL TRAPS. L.W. Grossman, R.J. Van Tuinen and J.G. Kereiakes. FDA, Nuclear Medicine Laboratory and Eugene L. Saenger Radioisotope Laboratory, University of Cincinnati College of Medicine, Cincinnati, OH.

Adsorption into activated charcoal beds has become the preferred method for disposal of Xe-133. The kinetics of these devices have been poorly understood. Consequently, there has been a great deal of confusion about expected efficiencies, as well as optimal use. An expression has been developed for calculating trapping efficiency for any given trap using information about caseload, air volume per study, charcoal mass and charcoal dynamic adsorption coefficient. Substantial deviation of an observed efficiency from the calculated value provides an indication that corrective maintenance, such as charcoal replacement, is required. An effective dynamic adsorption coefficient can be calculated from the observed trap efficiency. A decline in the value of this coefficient with age is a sign of inadequate protection of the charcoal from moisture or other contaminants.

A survey of efficiency and maintenance of activated charcoal traps in fourteen hospitals underlined the need for a clear understanding of trapping kinetics. Seven of the fourteen routinely monitored trap exhaust. Of the seven that performed no monitoring, two used traps that were found to be defective. Of the monitored units, one had a measured efficiency of about 85%. This had been tolerated under the assumption that the trap was working at its design limit until, the calculated efficiency was found to be much higher. Additionally, eight of the fourteen hospitals failed to maintain dessicant material needed to protect the charcoal from moisture.

NUCLEAR MEDICINE INSTRUMENTS: LABORATORY TRAINING OF RESIDENT PHYSICIANS. R.J. Van Tuinen, L.W. Grossman and J.G. Kereiakes. FDA, Nuclear Medicine Laboratory and Eugene L. Saenger Radioisotope Laboratory, University of Cincinnati College of Medicine, Cincinnati, OH.

The application of radiologic physics concepts should provide a bridge between the interpretation of data furnished by equipment and the nuclear medicine physician's understanding and control of the process by which the data are obtained. While the topical scope of radiologic physics training in the nuclear medicine residency program is well defined, didactic programs often fail to highlight the clinical significance of physical concepts. Accordingly, for nuclear medicine instruments, we propose the use of instructional modules which provide hands-on familiarization of instrument performance characteristics and quality control. Through a series of laboratory sessions, the resident is provided an in-sight into each instrument, its capabilities and limitations, and the value of quality control testing. Each experiment is written to challenge the resident in clinical significance of his observations and measurements.

CHILLING— AN EFFECTIVE WAY OF REDUCING VOLATILITY OF THERAPEUTIC IODINE SOLUTIONS. L.W. Grossman, FDA, Nuclear Medicine Laboratory, and C.C. Williams, University of Cincinnati, Cincinnati, OH.

Refrigeration is a well-known way to reduce the vapor pressure of volatile substances. A lead pig has been developed for I-131 therapy administrations which not only provides shielding, but cools the solution to just above 0°C and maintains it there for several minutes. Recent reformulations have greatly reduced therapeutic I-131 volatility. Even so, measurements of a 90-mCi bottle of therapy solution found 5 μCi volatilized in the first 5 min after opening and another 5 μCi in the next 15 min. These measurements were obtained using a specially built low-volume air sampler which collected all the radioiodine emitted in a TEDA (1,4 diazabicyclo octane) impregnated charcoal cartridge. A recent NRC guideline uses thyroid burdens of .04 μCi and .14 μCi as action points, the latter being an absolute upper limit beyond which immediate corrective action is required. These action limits are a small fraction of the total radioiodine that might be volatilized during preparation and administration of a therapy dose. Measurements made at room temperature (25°C) and near 0°C indicate that volatility was reduced a factor of 5 by the cooling. A special lead pig, the size of a 12-oz. beverage can, was built to perform the same function as an ice bath. The inside diameter of the pig was chosen to provide a squeeze fit to plastic bottles for thermal coupling. For glass bottles, a small amount of mineral oil provides good coupling. The pig requires no special preparation before use, other than storage in a freezer. It has the added advantages of being easy to clean in the event of a spill, and it serves as an effective radiation shield.

GAMMA CAMERA ACCEPTANCE TESTING, RECOMMENDATIONS OF THE AAPM. A. V. Wegst. University of Kansas Medical Center, Kansas City, KS.

The Nuclear Medicine Committee of the American Association of Physicists in Medicine has developed a protocol for acceptance testing of gamma cameras. The protocol is published as a report by the Association, written for analog gamma camera-imaging systems, and can be performed with a minimum of test phantoms and sources.

The protocol details methods for physical inspection, uniformity testing, spatial resolution and distortion, energy resolution (optional), temporal resolution, multiple window spatial registration, point source sensitivity over the field of view, collimator testing and integrity of camera head shielding. Each test which provides a numerical value comparible to, but not identical to, the specifications outlined by the National Electrical Manufacturer's Association document on performance measurements standards for scintillation cameras, is clearly indicated. The exact NEMA specifications cannot be duplicated because of specialized equipment requirements.

Acceptance testing of gamma cameras should be performed immediately upon clinical readiness of a new system and should establish whether or not the camera is performing according to manufacturer's specifications, provide an optimum baseline for quality control measurements and inform the user of the operating limitations of the system.

The protocol will be briefly described.

ROC REVIEW: WHICH CURVE IS BETTER? A.B. Ashare. St. Elizabeth's Hospital, Boston, MA.

After ROC (receiver operating characteristic) curves are

obtained for two different procedures or two image processing techniques, the investigator is then beset with the problem of determining which curve describes the better performance. If there are differences between the curves, how can one determine that these differences are meaningful? No fully satisfactory statistical technique has been developed as yet to test the significance of apparent differences between measured ROC curves. However, several techniques have been used in an attempt to compare ROC curves from two different procedures. One approach is to select a specific value of the false positive fraction (FPF) in the "useable" portion of the curves, and to compare the values for the true positive fraction at that FPF for each of the ROC curves. Another approach is to examine the difference in the areas under each ROC curve; this has the advantage of using the entire curve rather than a selected point. A third technique is to use the d' measure; this is obtained by replotting the ROC data on double probability graph paper and then measuring the difference between the curves along the negative diagonal. None of these techniques are totally satisfactory, but they can provide some insight into the question: which ROC curve, and therefore which imaging technique, is better?